Investigating the Generation and Reaction of Organoaluminiums in Marine Container Refrigeration Systems

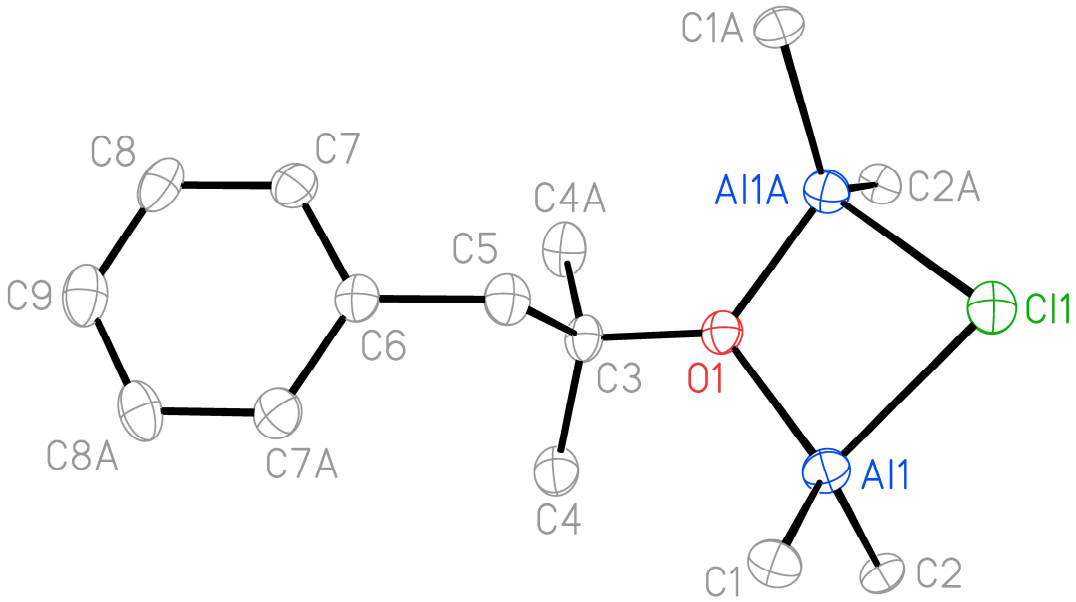

Jonathan Slaughter

Churchill College

Department of Chemistry

University of Cambridge

February 2019

This dissertation is submitted for the degree of Doctor of Philosophy

Declaration

This dissertation is submitted to the Board of Graduate Studies in partial fulfilment of the requirements for the qualification of Doctor of Philosophy at the University of Cambridge. Research presented herein was carried out by the author at the University Chemical Laboratories between January 2015 and December 2018. Except where specific reference is made to the contrary, it is original work and contains nothing that is the outcome of work done in collaboration. Neither the whole nor any part of the work has been submitted before for a degree in any other institution. This thesis does not exceed 60,000 words.

_____

Jonathan Slaughter

18th February 2019

Abstract

Investigating the Generation and Reaction of Organoaluminiums in Marine Container Refrigeration Systems

Jonathan Slaughter

The unexpected presence of chloromethane in marine container refrigeration systems has led to multiple explosions reported around the world. This is thought to occur due to the generation of methylaluminium chlorides, from the reaction of aluminium with chloromethane, which can then react with the refrigeration oil. This work investigated the generation of organoaluminiums and their subsequent reaction with refrigeration oils.

Initial work focused on determining the composition of two industrial refrigeration oils. They analysed as a polyolester (POE) and a polyvinyl ether (PVE). To investigate the reaction of these oils with organoaluminiums, reactions were attempted using simple models of the oils, based on esters and ethers.

The reaction of monoesters with organoaluminiums resulted in ester cleavage when reacted with TMA, Me_2AlCl or $Me_{1.5}AlCl_{1.5}$. The products of these reactions revealed that the ester had undergone addition of two methyl groups to form organoaluminium alkoxides. In addition, reactions involving Me_2AlCl or $Me_{1.5}AlCl_{1.5}$ both revealed elimination from the dimethylated species above 60 °C, producing alkenes and methane.

To further model the POE oil, two tetraesters were synthesised. Reactions of these tetraesters with organoaluminiums revealed similar reactivity to that seen with monoesters, with ester cleavage observed with TMA, Me_2AlCl or $Me_{1.5}AlCl_{1.5}$. This ester cleavage was also demonstrated with the POE refrigeration oil.

Reactions between ethers, models for the PVE oil, and organoaluminiums were then attempted. Whilst most ether-organoaluminium combinations revealed only adduct formation, some led to elimination of the ether to give an organoaluminium alkoxide, an alkene and methane. The PVE oil underwent elimination when reacted with Me_2AlCl or $MeAlCl_2$ at elevated temperatures.

The reaction of the refrigeration oils with *in situ* formed organoaluminiums was achieved by combining aluminium, chloromethane and the refrigeration oil in a sealed vessel. Both

oils revealed decomposition, with similar reactivity to that seen for the model systems. This oil decomposition is clearly a concern when applied to marine container refrigeration systems as the reaction products cannot provide the same lubrication as the refrigeration oil. Also, the production of alkenes and methane is potentially hazardous due to their flammable nature.

Acknowledgements

I would like to start by thanking Dr. Andrew Wheatley for his support and guidance throughout my PhD. He has allowed me to freely explore many aspects of the project but was always there to offer advice when needed. I will always be grateful for the opportunity that he has provided for me.

This project would not have been possible without the funding provided by Cambridge Refrigeration Technology and Maersk. I appreciate the insight provided by Richard Lawton and Paul Clarke on the practical working of refrigeration units and how my work was applied to real-world systems.

I am indebted to Dr. Andy Peel, who has been a constant source of help. This has included offering insight into my research, structure refinement of particularly tricky X-ray data and for constant encouragement. I would like to thank the Wheatley, Wright and Boss-Barker groups for making my time spent in the laboratory and office such an enjoyable experience. I would also like to thank Sam Molyneux for his hard work and enthusiasm during his part III project.

During my studies, numerous members of the technical support staff have proved invaluable in helping me undertake my research. I would like to thank Steve Wilkinson for setting up and maintaining a high-pressure reaction vessel. Thanks are also owed to Dr. Andrew Bond for assistance in collecting X-ray data, to the NMR staff for running samples and to Paul Skelton for running LC-MS. Lastly, I would like to thank the microanalysis staff, particularly Alan Dickerson, for analysing my sensitive samples.

Outside of my research, ultimate frisbee has been important to me during my time in Cambridge. I would like to thank all of the teammates that I have played with over the years.

Finally, I would like to thank my family and friends for supporting me throughout my PhD. Without them none of this would have been possible.

Abbreviations

acac	acetylacetonate ($C_5H_7O_2$)
BHT	2,6-di-^{t}butyl-4-methylphenolate ($OC_6H_2Me^tBu_2$)
Bn	benzyl (CH_2Ph)
CFC	chlorofluorocarbon
COSHH	Control of Substances Hazardous to Health
COSY	correlation spectroscopy
Cp	cyclopentadienyl (C_5H_5)
Cp*	1,2,3,4,5-pentamethylcyclopentadienyl (C_5Me_5)
C_{quat}	quaternary carbon
CRT	Cambridge Refrigeration Technology
DEPT	distortionless enhancement by polarisation transfer
Et	ethyl (CH_2CH_3)
FTIR	fourier transform infrared
GWP	global warming potential
HCFC	hydrochlorofluorocarbon
HFC	hydrofluorocarbon
HFO	hydrofluoroolefin
HMBC	heteronuclear multiple-bond correlation
HSQC	heteronuclear single-quantum correlation
i-	*ipso-*
I	nuclear spin
^{i}Pr	isopropyl ($CH(CH_3)_2$)
LC-MS	liquid chromatography-mass spectrometry
LUMO	lowest unoccupied molecular orbital

m-	*meta*-
MAO	methylaluminoxane $\{Al(Me)O\}_n$
Me	methyl (CH_3)
Me_b	bridging methyl
Mes	mesityl ($C_6H_2Me_3$)
Me_t	terminal methyl
2-MeTHF	2-methyltetrahydrofuran (MeC_4H_7O)
MTBE	methyl *tert*-butyl ether (MeO^tBu)
NMR	nuclear magnetic resonance
NOESY	nuclear Overhauser effect spectroscopy
^{n}Pr	normal propyl ($(CH_2)_2CH_3$)
o-	*ortho*-
p-	*para*-
PAG	polyalkylene glycol
PAO	polyalphaolefin
Pent	pentyl ($(CH_2)_4CH_3$)
Ph	phenyl (C_6H_5)
POE	polyolester
PVE	polyvinyl ether
py	pyridine (C_5H_5N)
R	general organic group
R-22	chlorodifluoromethane ($CHClF_2$)
R-40	chloromethane (CH_3Cl)
R-134a	1,1,1,2-tetrafluoroethane (CH_2FCF_3)
R-1234yf	2,3,3,3-tetrafluoropropene ($CH_2=CFCF_3$)
^{t}Bu	tertiary butyl ($C(CH_3)_3$)

THF	tetrahydrofuran (C_4H_8O)
TMA	trimethylaluminium ($AlMe_3$)
UVB	Ultraviolet B

δ	chemical shift (ppm)
J	scalar coupling constant (Hz)
ppm	parts per million
s	singlet
d	doublet
t	triplet
q	quartet
quint	quintet
sept	septet
m	multiplet
br	broad
sh	shoulder

M	molecular weight
a, *b*, *c*	unit cell lengths
α, β, γ	unit cell angles
V	unit cell volume
Z	number of formula units per unit cell
ρ_{calcd}	calculated density
λ	X-ray wavelength
μ	linear absorption coefficient
T	temperature

θ	Bragg angle
R_{int}	merging R-factor
$R1$	R-factor (unweighted)
$wR2$	R-factor (weighted)
S	goodness of fit
e	electron

Definition of Numbered Compounds

1^{R} 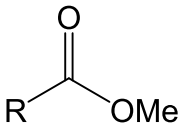 R = Et, Bn

2^{R} 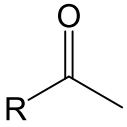 R = Et, Bn

3 Me_2AlOMe

4^{R} 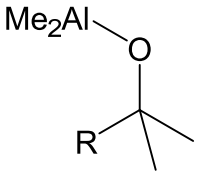 R = Et, Bn, C_5H_{11}

5 $MeAl(OMe)Cl$

6 $Al(OMe)Cl_2$

7a 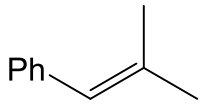

7b 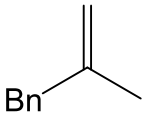

8 $Me_3Al_2(OH)Cl_2$

9 $Me_2Al_2OCl_2$

10 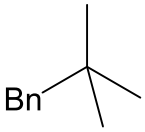

11a 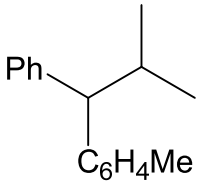

11b

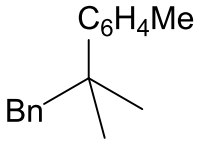

12

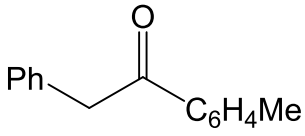

13^{R}

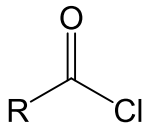

R = Bn, C_5H_{11}

14^{R}

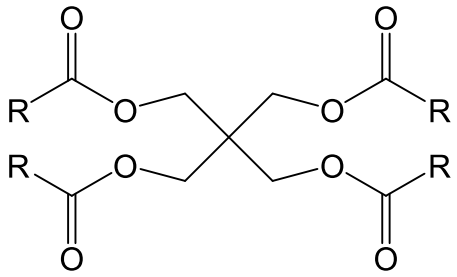

R = C_5H_{11}, Bn

15

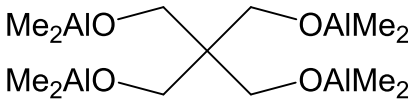

16^{Bn}

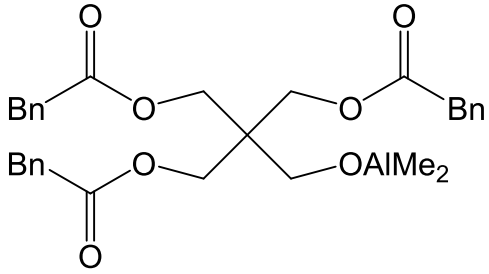

17^{Bn}

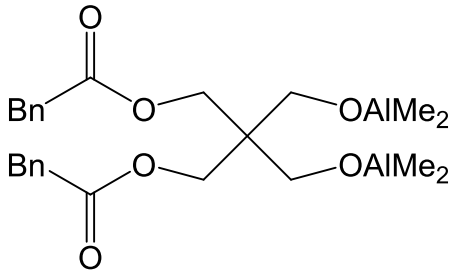

18^{Bn}

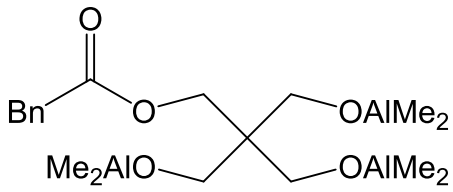

19

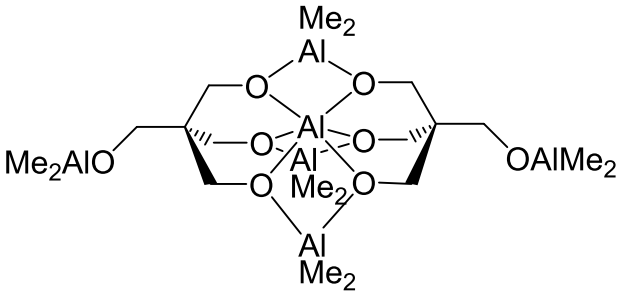

20

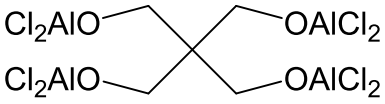

21

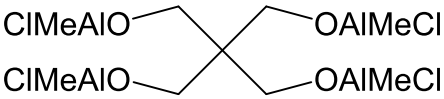

22

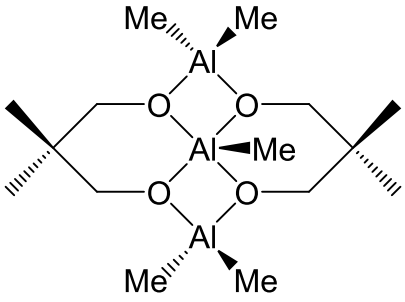

23

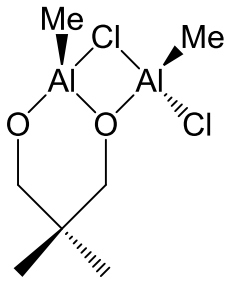

24

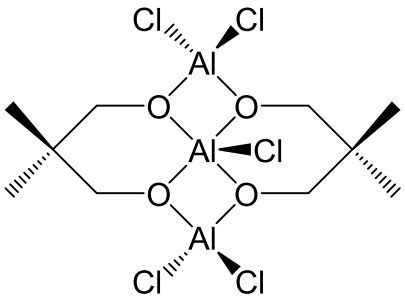

25

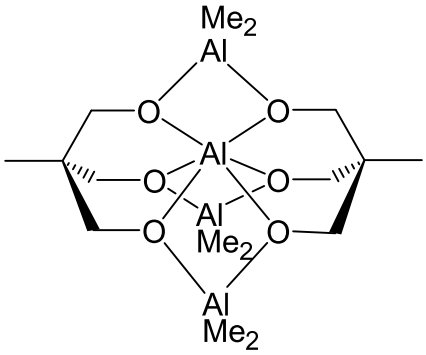

26

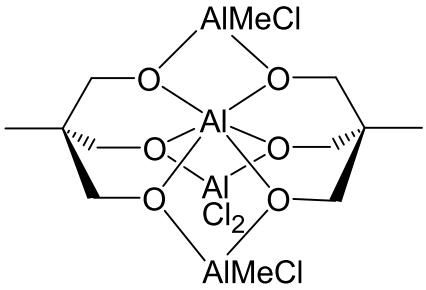

27

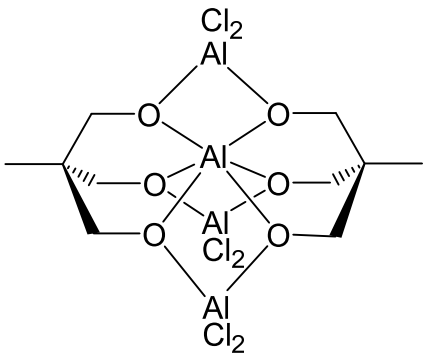

28

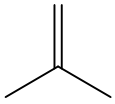

29a

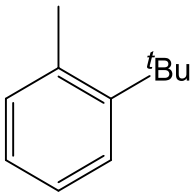

29b

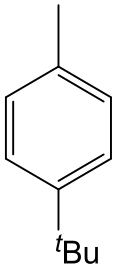

30

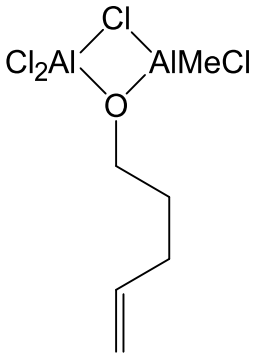

31

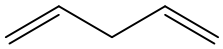

32 $MeAl_2(OH)Cl_4$

33 Al_2OCl_4

34

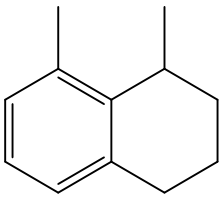

35

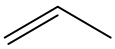

36

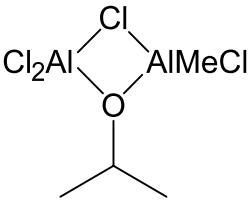

37a

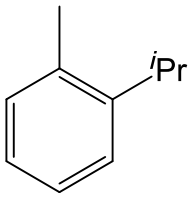

37b

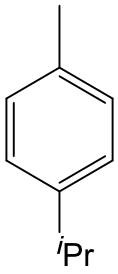

38 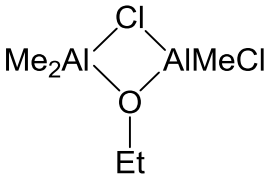

39 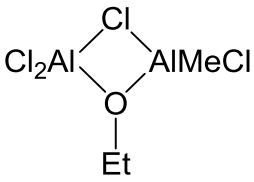

40a 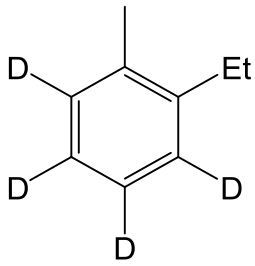

40b 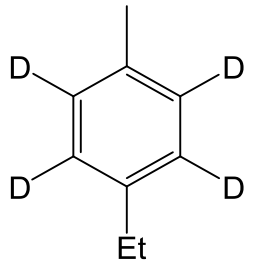

Contents

List of Schemes

List of Figures

List of Tables

Chapter 1

Introduction

1.1 Overview

This chapter begins by examining aspects of marine container refrigeration units design and operation that are important to the study of potential chemical reactions occurring within them. These reactions have been found to depend crucially on the formation of organoaluminium compounds and their derivatives. Hence, an introduction to organoaluminium chemistry is then presented, with a particular focus on the production and reactivity of methylaluminium chlorides, as these compounds are expected to be formed within industrial refrigeration units. The production of methylaluminium chlorides is thought to be due to the reaction of aluminium with chloromethane within these refrigeration systems.

1.2 Project Background

The international transportation of foodstuffs is a multibillion-dollar industry. As global transportation of these products can take days or weeks, reduced temperatures are often required to prevent any spoilage of goods. This is achieved through the use of refrigerated shipping containers. These are shipping containers fitted with a refrigeration cooling system to maintain a constant temperature throughout the transportation process.

In 2011 three separate refrigeration container compressors exploded in Itajai (Brazil), Cat Lai (Vietnam) and Qingdao (China). These incidents resulted in the deaths of three workers and led to the quarantine of over 1000 refrigeration units worldwide. The cause of these explosions was thought to be the introduction of contaminated or counterfeit refrigerant gas during servicing.[1] Economic and environmental considerations mean that recycling of refrigerants is common practice during servicing. This reclaimed refrigerant can then be used to refill other refrigeration units, meaning that the contamination of only one unit can easily lead to multiple contaminated units.

The refrigerant in industrial refrigeration units should be 1,1,1,2-tetrafluoroethane (R-134a; this R-terminology is commonly used by refrigeration companies to identify refrigerants). However, qualitative tests showed, unexpectedly, the presence of chloromethane (R-40) and chlorodifluoromethane (R-22) in a large number of quarantined containers, with a smaller number containing other chlorinated gases.[2] It was subsequently hypothesised that R-40 might undergo reaction with aluminium components in the refrigeration systems to produce organoaluminium compounds.[1] Consultative work done by the Wheatley group at Cambridge prior to the start of this PhD project suggested trimethylaluminium (TMA) to be present in aliquots obtained from industrial units.[3] However, the majority of units found to contain R-40 have not undergone explosions; implying that there must be at least one additional factor or set of conditions that must be fulfilled to explain the three catastrophic failures seen in the field.

1.3 Aspects of Modern Refrigeration Systems

1.3.1 Refrigerants

Most refrigerated shipping containers use a vapour-compression refrigeration cycle. In this type of cycle, a refrigerant is used to transfer heat from the inside of the container to the outside of the container, maintaining a stable internal temperature within the unit. This is accomplished by using the phase change between a liquid and a gas to absorb and release heat. To achieve this a compressor is used, which condenses the refrigerant and results in an increase in temperature. The hot compressed vapour then passes through a condenser, undergoing a phase change to a liquid and releasing heat outside of the unit. The refrigerant then goes through an expander, which results in a reduction in pressure, before it enters an evaporator, with evaporation resulting in heat being absorbed by the refrigerant and internal cooling of the unit taking place (Figure 1.1).[4]

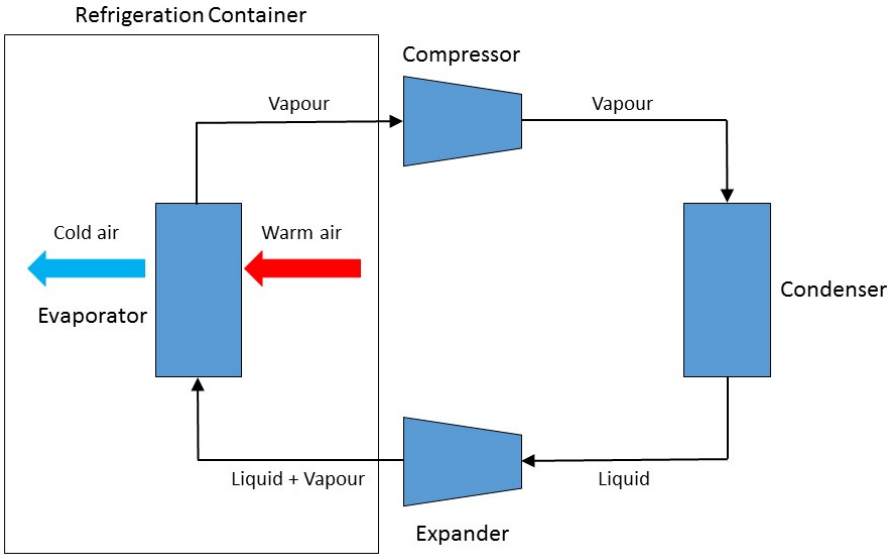

Figure 1.1: Schematic showing a vapour-compression cycle.

A good refrigerant should have a large enthalpy of vaporisation to maximise the heat being transferred, whilst its boiling point at operating pressure should be below the desired temperature of the unit, to allow for the phase change between a liquid and a gas. The refrigerant should also be inert with respect to any of the mechanical and chemical components in the system. Aside from those properties essential for the smooth operation of the refrigeration unit, consideration must also be given to the hazards that refrigerants present in the event of human exposure and upon release into the environment. It is therefore desirable for the refrigerant to also be safe with respect to human exposure, by not being toxic or flammable, and to minimise climate change and ozone depletion. In the 1970s it was discovered that chlorofluorocarbons (CFCs), the most commonly used refrigerant at that time, and hydrochlorofluorocarbons (HCFCs) were present in the stratosphere. There are no significant natural sources, so their presence was concluded to be due to human manufacture for refrigeration. CFCs and HCFCs are relatively inert, but when exposed to ultraviolet light they undergo homolytic cleavage to release chlorine atoms. These chlorine atoms are able to catalyse the breakdown of ozone, a chemical crucial in the absorption of harmful UVB wavelengths of light.[5] The result was that legislation was implemented to eliminate the use of chemicals with a high ozone depletion potential such as CFCs and HCFCs. These chemicals were therefore replaced in industrial applications by hydrofluorocarbons (HFCs).[6,7]

Generally speaking, HFCs have become widely used as refrigerants due to their good thermal stability and chemical inertness, which results from the high C–F bond strength.[8]

Furthermore, the high electronegativity of fluorine results in low polarisability, which in turn gives rise to weak intermolecular cohesion forces, ensuring good lubricity.[8] As a result of these properties, modern refrigeration units have generally come to be operated using a refrigerant that is normally a HFC. A common example is R-134a, which has a boiling point of −26.6 °C at atmospheric pressure,[9] is non-toxic, does not appear to react with the components of refrigeration units and has a zero ozone depletion potential.[10]

As the use of HFCs has become more prevalent, their environmental impact has been further investigated. It was found that HFCs contribute significantly to global warming, hence regulations have been implemented to reduce their usage. These regulations have spearheaded global efforts to phase out refrigeration gases with a global warming potential (GWP = 100 year warming potential of one kg of a gas relative to one kg CO_2) greater than 150.[11,12] HFCs generally have high GWPs (R-134a GWP = 1430).[13] Current efforts are therefore focused on achieving a global HFC reduction in consumption and production of at least 85% by 2047.[14] This has resulted in HFCs being replaced by hydrofluoroolefins (HFOs) such as 2,3,3,3-tetrafluoropropene (R-1234yf).[15] These refrigerants have similar physical properties to HFCs, but much lower GWPs (R-1234yf GWP = 4) and an atmospheric lifetime of only 11 days.[13,16] However, R-1234yf is a flammable gas and there have been some reports of it decomposing at high temperature to produce HF and trifluoroacetic acid.[17] This could cause significant problems as HF and trifluoroacetic acid are both corrosive substances, which could lead to complete failure of the refrigeration systems. Mixtures of R-134a and R-1234yf are also being supplied for use as refrigerants as these demonstrate lower levels of flammability, by virtue of the properties of R-134a.

Concurrent with the introduction of the above regulatory frameworks aimed at reducing the use of HFCs, reports emerged of explosions having occurred in a number of industrial refrigeration systems. Tests conducted on samples of refrigerant obtained from multiple units revealed the unexpected presence of R-40.[2] In the past (up to the 1960s) R-40 was used as a refrigerant, but this was phased out due to concerns over its toxicity and flammability.[18] The detection of R-40 in isolated units raised substantial concerns over the potential extent of contamination within operational containers. R-40 has a boiling point of −23.7 °C,[18] so when it is in the sealed refrigeration system or mixed with R-134a it is hard to distinguish from pure R-134a (boiling point of −26.6 °C). This raises the possibility that a large number of refrigeration systems globally may have unknown amounts of R-40 in them.

The difficulty in identifying the presence of counterfeit refrigerant on the basis of physical properties is only added to by the limited (and rather primitive) chemical assays available for R-40 that can be deployed in the field. Currently, one method of detection involves using a flame halide detector, the so-called Beilstein test.[19,20] The flame detector uses a copper plate heated up in a flame, which produces a copper(II) oxide surface layer. The refrigerant gas is then passed through the flame. If there are only fluorinated compounds in the gas, the flame retains its characteristic blue colour. However, if there are any compounds containing chlorine, bromine or iodine present, the flame will turn green (Figure 1.2). This is due to the formation of copper(II) chloride, $CuCl_2$, or the corresponding bromide or iodide. This does not occur with fluorides as copper(II) fluoride is not volatile. This test has a R-40 detection limit of 300 ppm and therefore allows for the rapid identification and decommissioning of units with the potential for explosive failure.[21] However, the presence of R-40 plainly does not necessarily result in the explosion of the refrigeration units, suggesting that additional conditions must be met before a unit becomes explosive. Also, it was not known how the presence of R-40 affected other components in the refrigeration system.

Figure 1.2: A flame halide detector is used to determine if chlorine, bromine or iodine compounds are present in refrigerant gas. On the left is a blue flame from 100% R-134a and on the right is a green flame due to a chlorinated compound.[21]

1.3.2 Refrigeration Oil

In refrigeration systems, oil is required to lubricate the system in order to reduce mechanical wear. If the oil is miscible with the refrigerant it also helps to uniformly distribute the chemical throughout the system. R-134a is miscible with certain oils, including polyalkylene glycols (PAGs), polyolesters (POEs) and polyvinyl ethers (PVEs). However, PAGs are very hygroscopic; they have the potential to introduce damaging levels of water into the refrigeration system and so their use is discouraged.[22] Therefore, in R-134a systems, POEs and PVEs are usually used.[23,24] This is in spite of the fact that, while POEs are less hygroscopic than PAGs and show good hydrolytic stability, if exposed to air they can degrade.[25] Many POEs are based on the neopentane structure ($C(CH_3)_4$). They are produced through the reaction of monobasic aliphatic acids with a neopentyl polyol such as neopentyl glycol ($C(CH_3)_2(CH_2OH)_2$), trimethylolethane ($CH_3C(CH_2OH)_3$) or pentaerythritol ($C(CH_2OH)_4$) (Figure 1.3).[26–28]

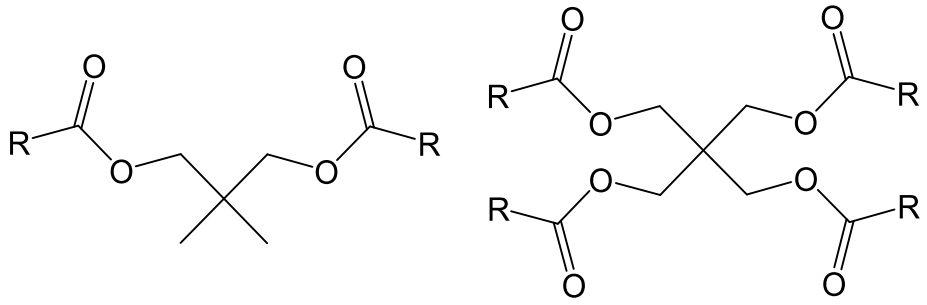

Figure 1.3: Examples of POEs derived from neopentyl glycol (left) and pentaerythritol (right). The R groups are aliphatic chains.

Due to the number of different combinations of polyol core and acid, the properties of POEs can easily be tuned. By increasing the number of alcohol groups on the neopentyl polyol a greater number of ester groups can be introduced to the POE, resulting in increased polarity. This can also affect miscibility, lubricity and viscosity. Alternatively, these properties can also be varied by changing the length and branching of the acid groups. Consequently, lubricants with the optimal combination of properties can readily be obtained by blending mixtures of different polyols and acids.[22]

The neopentyl core of POEs serves not only to provide a node from which extensive branching may be introduced into the molecule, but is also responsible for its thermal robustness. The absence of β-hydrogens in the neopentyl core prevents thermal decomposition and the production of an alkane and a carboxylic acid (Scheme 1.1) that is otherwise common in esters and which normally occurs at raised temperatures (*ca*. 350

°C).[29] This means that neopentyl chemistry has underpinned the significant enhancement of thermal stability, which is favourable in refrigeration systems where localised high temperatures can be reached in piston housings.

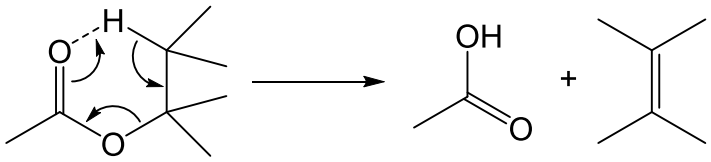

Scheme 1.1: Thermal decomposition of an ester by β-hydrogen elimination to give a carboxylic acid and an alkene.

In comparison to POEs, PVEs are less hygroscopic and they cannot undergo hydrolysis. Their polymeric structures (Figure 1.4) mean that PVE viscosity can be changed by altering the molecular weight. However, this altering of the molecular weight does not necessarily significantly change other basic characteristics of the oil, such as polarity or miscibility. The viscosity and miscibility can be altered by changing the branching alkoxy group.[30]

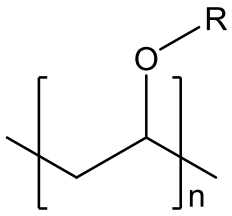

Figure 1.4: General structure for PVEs. The R groups are aliphatic chains.

1.3.3 Other Refrigeration Components

In addition to the refrigerant and the oil, the choice of materials used in the construction of mechanical parts is important to the normal functioning of refrigeration units. The main types of compressor used in refrigeration systems are piston or scroll type. Piston type compressors work by vapour entering a compression cylinder, where it is compressed (by a piston moving in a reciprocating motion) before being discharged. Scroll type compressors are composed of two interleaving scrolls. While one of the scrolls is fixed, the other orbits eccentrically without rotating, resulting in a compression of the refrigerant. Compressors are primarily made from aluminium alloyed with copper, zinc or magnesium. Typically, these alloys have a high silicon content (3-25%) that improves corrosion resistance through the presence of silicon precipitates.[31] Aluminium alloys also have good thermal conductivity, and so can dissipate heat from the compressor effectively.

The refrigeration cycle also contains a dryer column to remove any water that is present. The removal of water is essential, as at operating temperatures and pressures the water would freeze and block the system. Filter dryers are therefore employed to remove water using 3 Å molecular sieves or activated alumina.

As discussed earlier, the refrigeration oil can be a PAG, POE or PVE, though the actual composition of these oils is not generally disclosed by vendors. Moreover, commercial oils usually also contain a number of additives that are included in order to further improve the performance. For example, phosphate esters are frequently incorporated as antiwear additives, whilst amines or alcohols are employed as antioxidants.[27,28,32–34] Whilst these additives are typically present in only small quantities, the possibility that they play a role in initiating the reaction between chloromethane and aluminium cannot be discounted. The fact that the composition of the oil and additives is proprietary knowledge has hampered investigations into the contamination and explosion of refrigeration units.

1.3.4 Reactions in Refrigeration System

The mechanical and chemical components of refrigeration systems are carefully selected to ensure compatibility. It has been shown that mixtures of POE oil and R-134a provide fairly low wear media that work well in conjunction with aluminium components in refrigeration units compared to other oils and refrigerants. However, it has also been shown that at pressures above 0.69 MPa and at a temperature of 80 °C, R-134a can undergo reactions with AlSi alloy, which results in surface fatigue.[35] This could potentially lead to the exposure of oxide-free aluminium. Additionally, some methods of R-134a manufacture give hydrochloric acid as a by-product,[36] which if not carefully removed from the product may react with aluminium components or destroy the protective oxide layer. Without a passivating oxide layer aluminium is much more reactive.

Whilst aluminium is inert to HFCs, such as R-134a, it is known to react with chlorinated compounds, such as R-40, to produce organoaluminium compounds. As described above, the presence of R-40 has been confirmed in industrial units, therefore potentially leading to unwanted reactivity. To ascertain the potential for hazardous reaction within R-40 contaminated refrigeration units, the project sponsors (CRT) have performed simple tests in which aluminium pistons, R-40, R-134a, POE oil and dryer were combined in a sealed pressurised vessel and heated to 50 °C for one month. These reactions consistently resulted

in a significant increase in the viscosity of the oil, concomitant with the production of pyrophoric materials (Figure 1.5). The extent of these observations was closely linked to the initial amount of R-40 present in the test, with greater amounts of R-40 resulting in a more violent reaction when exposed to air (when the vessel was vented), as well as more viscous oil (or a solid at high R-40 concentrations). The increased viscosity has been taken to indicate that the POE oil is undergoing reaction with *in situ* formed organoaluminiums. However, while these straightforward tests gave a broad indication of the gross effects of R-40 contamination, they did little to provide an exact knowledge of the actual reactions taking place, the conditions which bring them about and how likely it is that R-40 contamination will result in catastrophic failure of a refrigeration unit.

Figure 1.5: Preliminary tests performed by CRT using pressurised reaction vessels containing aluminium pistons, R-40, R-134a, POE oil and dryer. The production of pyrophoric material was observed when the vessel was opened (left), along with a substantial change in the refrigeration oil to form a solid (right).

In addition to tests performed by CRT, McCampbell Analytical also investigated the possible reaction of R-40 with refrigeration system materials using a pressurised vessel. The authors suggested that the main causal factor in the explosive failure of refrigeration units was structural weakening of the compressor through aluminium loss. The report indicated that the major products from the reaction of aluminium alloy, R-40, R-134a, POE oil and dryer were AlF_3, 1,1,1-trifluoro-2-chloroethane and an unknown POE derivative. However, in none of the experiments discussed therein was pyrophoric behaviour reported.[37] This is in contrast to the findings of similar investigations by CRT and analysis by the Wheatley group of samples from industrial units. The different results from similar tests could not be explained, partially due to a lack of fundamental understanding of the chemistry involved. Hence, further investigation into the possible reactions occurring is crucial and will be carried out in this work.

1.4 Organoaluminiums

As described in the previous sections, it is thought that chloromethane and aluminium may be undergoing reactions within industrial refrigeration systems, and that these processes are producing organoaluminiums. These organoaluminiums can then react with other species, such as the refrigeration oil, and that in some currently unknown manner this potentially leads to catastrophic failure of the system. This behaviour was suggested by preliminary experiments carried out by CRT. In these tests, lubricant oil had clearly undergone reaction and a pyrophoric material had been produced. These data made it desirable for the production and reactivity of organoaluminium species to be investigated in a more systematic fashion. Initially, this will require the understanding of organoaluminiums, which will be explained in the following sections.

1.4.1 Organoaluminium Production

Organoaluminium compounds are used extensively in industry and can be produced via a number of methods. A convenient route is the reaction of aluminium metal with alkyl halides to produce alkylaluminium sesquihalides. For example, aluminium reacts with alkyl chlorides to produce alkylaluminium sesquichloride (an equimolar mixture of R_2AlCl and $RAlCl_2$). The sesquichloride is an equilibrium mixture of the heterodimer ($R_2AlCl{\cdot}RAlCl_2$) and the homodimers ($(R_2AlCl)_2$ and $(RAlCl_2)_2$).[38] The reaction can be initiated with a small amount of aluminium chloride or iodine,[39,40] but has also been shown to proceed in the absence of a detectable catalyst.[41] Alkylaluminium sesquihalides can undergo reduction with an alkali metal, such as sodium, to produce dialkylaluminium halides or trialkylaluminiums (Scheme 1.2). These organoaluminium species can then be purified through distillation.[42,43]

$$2\ Al + 3\ RCl \longrightarrow R_3Al_2Cl_3$$
$$2\ R_3Al_2Cl_3 + 3\ Na \longrightarrow 3\ R_2AlCl + Al + 3\ NaCl$$
$$3\ R_2AlCl + 3\ Na \longrightarrow 2\ R_3Al + Al + 3\ NaCl$$

Scheme 1.2: The production of alkylaluminium sesquichloride and reduction to dialkylaluminium chloride and trialkylaluminium with sodium.[44]

Trialkylaluminiums, alkylaluminium chlorides and aluminium chloride can be combined to produce the desired alkyl and chloride stoichiometry through reproportionation reactions (Scheme 1.3).[38]

$$2\ AlR_3 + AlCl_3 \longrightarrow 3\ R_2AlCl$$
$$AlR_3 + 2\ AlCl_3 \longrightarrow 3\ RAlCl_2$$

Scheme 1.3: The reproportionation reactions of trialkylaluminium and aluminium chloride.[38]

Another common synthesis of trialkylaluminiums involves the reaction of aluminium with terminal alkenes in the presence of hydrogen. These reactions are activated by trialkylaluminium reagents, producing dialkylaluminium hydrides, which then undergo hydroalumination with terminal alkenes to produce trialkylaluminiums (Scheme 1.4).[45] The method results in no side products, but does require the use of hydrogen gas.

$$4\ AlR_3 + 2\ Al + 3\ H_2 \longrightarrow 6\ R_2AlH$$
$$6\ R_2AlH + 6\ CH_2{=}CHR' \longrightarrow 6\ R_2Al(CH_2CHR')$$

Scheme 1.4: The formation of trialkylaluminiums from the reaction between aluminium, hydrogen and terminal alkenes.[45]

Organoaluminiums can also be synthesised by the metathesis of aluminium chloride with organolithiums, or from the transmetallation of aluminium with diorganyl mercury (Scheme 1.5).[46] Beyond requiring the use of pyrophoric or toxic organometallic reagents, these methods also require separation of the desired organoaluminium from side products.

$$AlCl_3 + RLi \longrightarrow AlR_3 + 3\ LiCl$$
$$2\ Al + 3\ HgR_2 \longrightarrow 2\ AlR_3 + 3\ Hg$$

Scheme 1.5: The synthesis of organoaluminiums from metathesis and transmetallation reactions.[46]

1.4.2 Structure and Bonding

By definition, an organoaluminium compound is any compound containing an Al–C bond. However, this definition can be expanded to include any aluminium-heteroatom bond. Aluminium can be found in a number of different valencies, which can be stabilised by the use of certain ligands. Low-valent organoaluminium compounds can form Al–Al bonds. Aluminium(I) compounds such as $(AlCp^*)_4$ form a tetrahedral Al_4 core (Figure 1.6,

left) with delocalised bonding of 8 electrons in the Al_4 core.[47] Aluminium(II) compounds can form dimeric species, such as $(Al\{CH(SiMe_3)_2\}_2)_2$ (Figure 1.6, right) with electron precise bonding.[48] These low-valent aluminium compounds can be generated by reduction of dialkylaluminium chlorides with potassium. Low-valent aluminium species are currently of interest as they show reactivity with usually inert species, such as oxidative addition of C–F bonds of fluoroalkenes.[49]

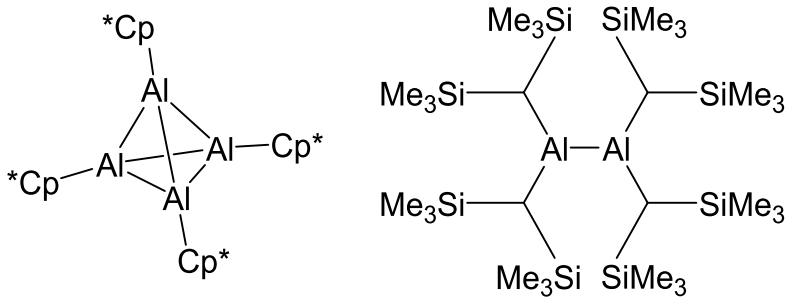

Figure 1.6: The structures of $(AlCp^*)_4$ (left) and $(Al\{CH(SiMe_3)_2\}_2)_2$ (right).[47,48]

Whilst low-valent aluminium species have garnered increasing interest in recent decades, the majority of known organoaluminiums are based on aluminium(III). Formation of three polar Al–C bonds requires participation of only three of the four available valence orbitals on aluminium. The polar Al–C bonds result in the aluminium centre being positively charged. Organoaluminium compounds are therefore Lewis acidic, as they can accept a pair of electrons into the empty valence orbital to form a dative covalent bond with a Lewis base, for example in $AlPh_3(THF)$.[50] Adduct formation with a Lewis base reduces the positive charge on the aluminium and prevents further oligomerisation. If there is no Lewis base present, organoaluminiums often aggregate to form dimers (Al_2R_6), resulting in 4-coordinate aluminium. For trialkylaluminiums, the bonding in these dimers can be described by two bridging alkyl ligands forming 3-centre 2-electron bonds and four terminal alkyl ligands forming 2-centre 2-electron bonds (Figure 1.7). The X-ray crystal structure of $(TMA)_2$ confirmed formation of a dimer and the weaker bonding within the Al–C–Al bridge therein, suggested by an Al–C bridge distance of 2.14(1) Å, compared to 1.97(1) Å for the terminal Al–C bonds.[51]

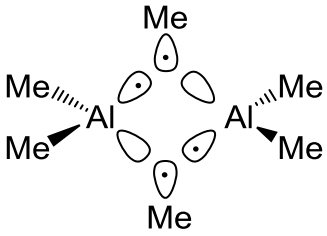

Figure 1.7: Orbital interaction diagram for the Al–Me–Al bridging units in $(TMA)_2$, showing 3-centre 2-electron bonding.

The weak Al–C–Al bridges in $(TMA)_2$ results in fluxionality in solution, as the bridging and terminal ligands can easily interchange via an intermolecular exchange mechanism that features an equilibrium between monomeric and dimeric forms (Scheme 1.6). This equilibrium has been measured using ^{27}Al NMR spectroscopy, with the dimer and monomer exhibiting signals at δ 155 and 265 ppm, respectively.[52] The extent of dissociation to monomer increased with decreasing concentration and increasing temperature.[53] At room temperature, the ^{1}H NMR spectrum revealed one signal due to rapid exchange of the bridging and terminal methyl groups of the dimer. However, cooling the sample to −75 °C resulted in the replacement of this signal by two others, with a 1:2 integral ratio, corresponding to the bridging and terminal methyl protons.[54] This has important implications for organoaluminium reactivity, as the monomer is the more reactive species.

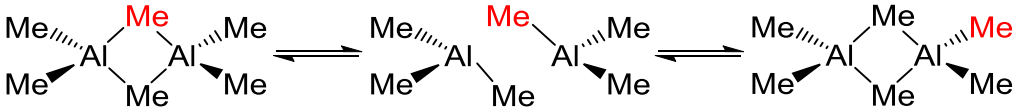

Scheme 1.6: The intermolecular exchange of bridging and terminal methyl groups in trimethylaluminium.[52]

The incorporation of aryl groups can result in bonding similar to that seen for alkyl groups. For example, in the solid-state, triphenylaluminium is dimeric, with bridging occurring via the phenyl groups. The X-ray structure revealed the bridging phenyl rings to be perpendicular to the core Al_2C_2 ring. These bridging phenyls showed significant distortion. The C–C–C bond angle at the bridging carbon had decreased from the expected value of 120° to 114° and the C–C bond lengths involving the bridging carbon were also longer than in benzene.[55] This was interpreted as being caused by a partial loss of aromaticity by the bridging phenyl groups, with these now being able to donate two sp^3 orbitals to bonding with metal centres (Figure 1.8). This type of coordination could logically lead to stronger 2-centre 2-electron bridging than the 3-centre 2-electron bridging seen for alkylaluminium dimers. This expected stronger bridge bonding was indeed observed for

dimethylphenylaluminium dimers, where the phenyl groups were found to occupy the bridging positions by X-ray crystallography.[56,57]

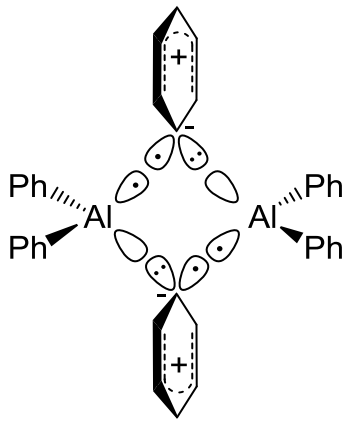

Figure 1.8: Orbital interaction diagram for the Al–Ph–Al bridging units in $(AlPh_3)_2$, showing the 2-centre 2-electron bonding enabled by partial dearomatisation of the bridging ligands.

Many organoaluminium species contain ligands other than organyl groups, leading to alternative bonding possibilities. Organoaluminiums containing alkoxide, amide or chloride ligands show a preference for these ligands to be in the bridging positions. This can be observed, for example, in the crystal structures of $(MeAlCl_2)_2$ and $(Me_2AlOMe)_3$ (Figure 1.9).[58,59] This arrangement is favoured as the available lone pairs can form dative 2-centre 2-electron bonds to aluminium. This leads to stronger bridge bonding and much slower intermolecular exchange.[53,60] An investigation into dimethylaluminium alkoxides showed they exist as dimeric or trimeric species, with the equilibrium dependent on the sterics of the alkoxide. The slow intermolecular exchange was demonstrated by isolating dimeric dimethylaluminium ^{n}propoxide, $(Me_2AlO^{n}Pr)_2$, which slowly converted to the trimer, $(Me_2AlO^{n}Pr)_3$, over a period of weeks at 25 °C.[59]

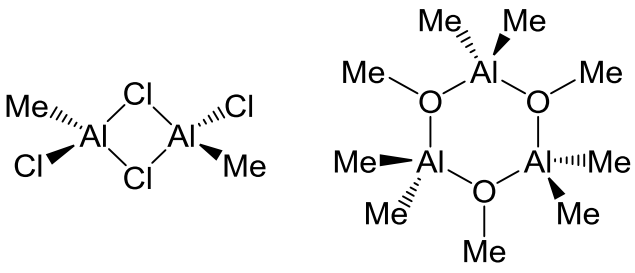

Figure 1.9: The structures of $(MeAlCl_2)_2$ (left) and $(Me_2AlOMe)_3$ (right), showing the preference for chloride and alkoxide bridging over alkyl ligands.[58,59]

While aluminium often has a coordination number of 4, other coordination numbers are not unusual. With extremely bulky ligands, organoaluminiums can also be found as monomers with 3-coordinate aluminium, for example $Al(Mes)_3$.[61] The lower coordination

number of aluminium in these species often leads to high reactivity.[62] If a 3-coordinate aluminium associates with a heteroatom-based ligand, there is the possibility of π-interactions occurring. Hence, for example, the monomeric species $Me_2Al(BHT)$ has the potential for stabilisation of the aluminium centre through donation of a lone pair from the oxygen (Figure 1.10).[63]

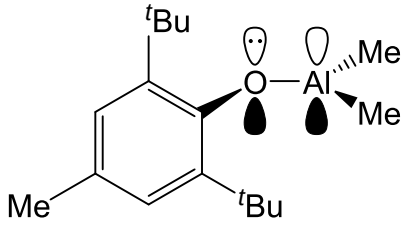

Figure 1.10: The structure of $Me_2Al(BHT)$, showing the potential stabilisation of the 3-coordinate aluminium by a π-interaction with the oxygen.[63]

A metal coordination number of 5 or 6 is also common in organoaluminium chemistry. These higher coordination numbers are usually stabilised by bonding to electronegative elements such as oxygen, resulting in a greater ionic contribution to bonding. The higher coordination number can occur intramolecularly, such as in $(Me_2Al\{\mu_2\text{-}O(CH_2)_3OMe\})_2$ (Figure 1.11, left)[64] and in $Al(acac)_3$ (Figure 1.11, right).[65] The aluminium centres have a trigonal bipyramidal and octahedral geometry, respectively.

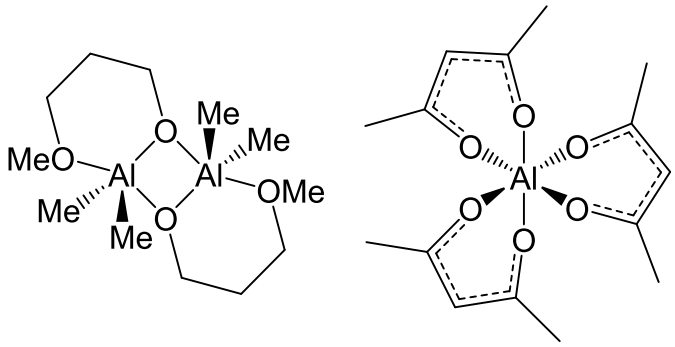

Figure 1.11: The structures of $(Me_2Al\{\mu_2\text{-}O(CH_2)_3OMe\})_2$ (left) and $Al(acac)_3$ (right), showing 5- and 6-coordinate aluminium, respectively.

Intramolecular coordination of aluminium by a neutral Lewis base is a dynamic process in solution. As such, it can lead to multiple potential structures being formed. The organoaluminium may form a monomeric or dimeric species, with the dimeric species showing either 4- or 5-coordinate aluminium (Scheme 1.7).[66]

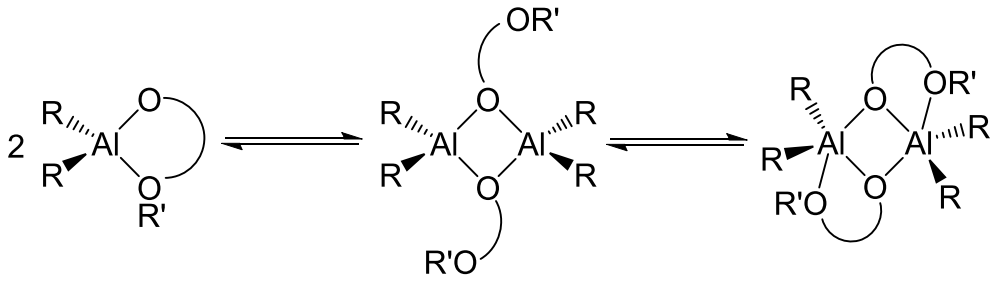

Scheme 1.7: The potential equilibria available to chelating dialkylaluminium alkoxides.[66]

For a coordination number higher than 4, a hypervalent bonding model can be used to explain the bonding. For the 5-coordinate case a trigonal bipyramidal geometry can be explained with sp^2-hybridisation of the aluminium. The equatorial ligands form 2-centre 2-electron bonds to the aluminium through the sp^2 orbitals, leaving a single *p* orbital available to bond to the axial ligands. This results in a linear 3-centre 4-electron bonding system and longer axial bonds.[67] In 6-coordinate aluminium the *p* orbitals can interact with oxygen-based ligands trans to each other, forming three 3-centre 4-electron bonding interactions.[68]

By using ^{27}Al NMR spectroscopy, it is possible to distinguish between different aluminium coordination numbers from observation of the chemical shift (Figure 1.12). The general trend is for higher-coordinate aluminium resulting in higher field resonances. More electronegative ligands also result in higher field resonances.[69]

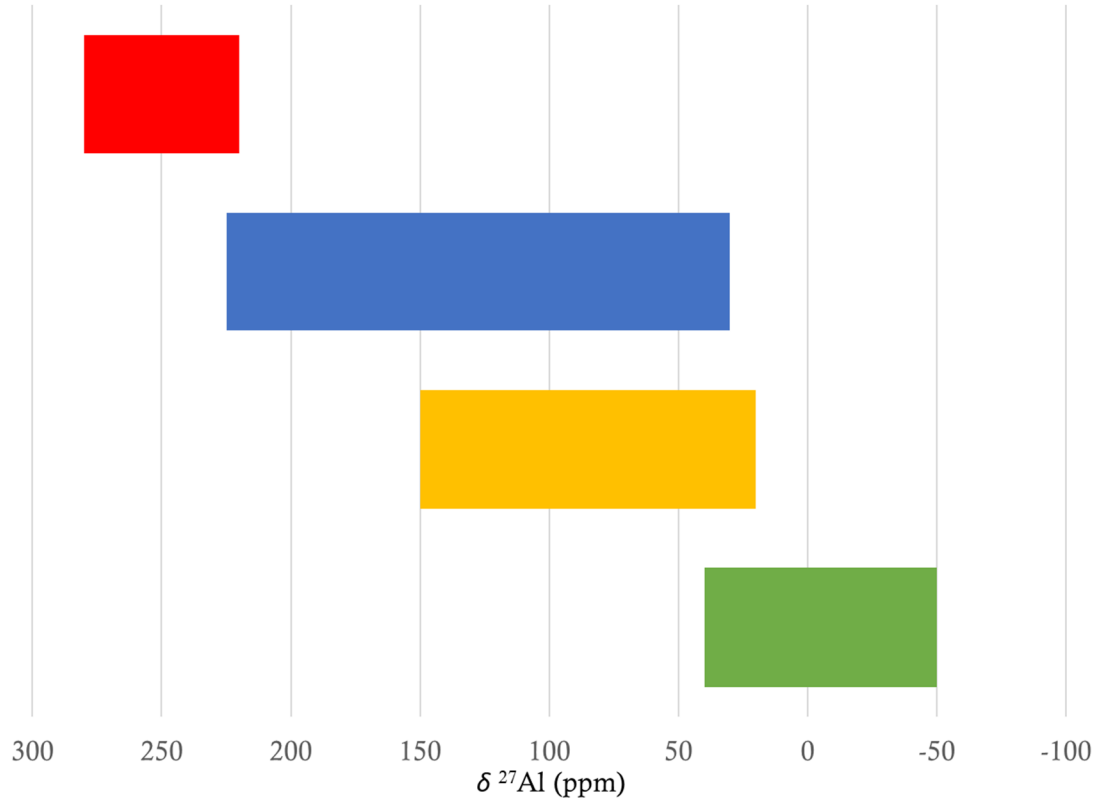

Figure 1.12: The ^{27}Al NMR chemical shift range as a function of coordination number (three in red, four in blue, five in yellow, and six in green).[69]

^{27}Al is a quadrupolar nucleus (I = 5/2), hence it has a non-spherical (oblate or prolate) charge distribution. The quadrupolar nucleus interacts with the external magnetic field and the electric field gradient generated by the surrounding environment. Consequently, the main relaxation pathway is the interaction between the nuclear quadrupole moment and changes in the electric field gradient. This can occur by tumbling of the molecule in solution, leading to a change in the direction of the charge distribution. Dipole-dipole and solvent interactions can then lead to a quick relaxation of the spin states, resulting in broad signals. In contrast, aluminium with tetrahedral or octahedral symmetry demonstrates a much sharper signal. This is because the electric field gradient is closer to zero, so the nucleus now behaves more like a I = 1/2 nucleus and undergoes slower relaxation. The signal breadth can be reduced by increasing the temperature.[69–71]

1.4.3 Reactivity of Organoaluminiums

Organoaluminium compounds are used extensively in organic synthesis, with their ability to act as a Lewis acid and a nucleophile key to their reactivity. These combined properties

often lead to carbon–carbon bond formation. Thus, they feature in numerous reactions with organic species, such as deprotonation, reaction with unsaturated species and multiple possible reactions with carbonyl groups.[72]

1.4.3.1 Organoaluminiums as bases

The Al–C bonds in organoaluminiums are polarised due to the electronegativity difference between aluminium and carbon. This polarity underpins their reactivity as the alkyl groups can act as Brønsted bases. For example, reaction with one equivalent of an alcohol or a primary or secondary amine produces a dialkylaluminium alkoxide or dialkylaluminium amide. Addition of further equivalents of alcohol or amine results in further deprotonation, until all the Al–C bonds have undergone reaction (Scheme 1.8).[59,73,74] These products tend to oligomerise to form dimers or trimers, with bridging occurring via oxygen or nitrogen. These deprotonative reactions are highly exothermic due to the release of alkanes, which is entropically favoured, and the formation of strong Al–O or Al–N bonds, so are often carried out slowly at low temperatures to prevent thermal runaway.

$$AlR_3 + n\ R'OH \longrightarrow R_{3-n}Al(OR')_n + n\ RH$$

$$AlR_3 + n\ R'NH_2 \longrightarrow R_{3-n}Al(NHR')_n + n\ RH$$

$$AlR_3 + n\ R'_2NH \longrightarrow R_{3-n}Al(NR'_2)_n + n\ RH$$

Scheme 1.8: The reaction of trialkylaluminium compounds with alcohols, primary amines and secondary amines.

The deprotonative reactions described in this section proceed via the initial formation of a Lewis acid-Lewis base complex, e.g. $AlR_3(R'OH)$. Though the isolation of these pre-reaction adducts has proved difficult due to their highly reactive nature, the reaction of Al^tBu_3 with $HO(CH_2)_3NMe_2$ resulted in the formation of $^tBu_3Al\{O(H)(CH_2)_3NMe_2\}$, which could be characterised. This species was found to be stabilised by intramolecular hydrogen bonding between the amine and the hydroxyl proton. However, heating to above 45 °C resulted in the elimination of ^{t}BuH and the formation of dimeric $^tBu_2Al\{O(CH_2)_3NMe_2\}$ (Scheme 1.9).[75]

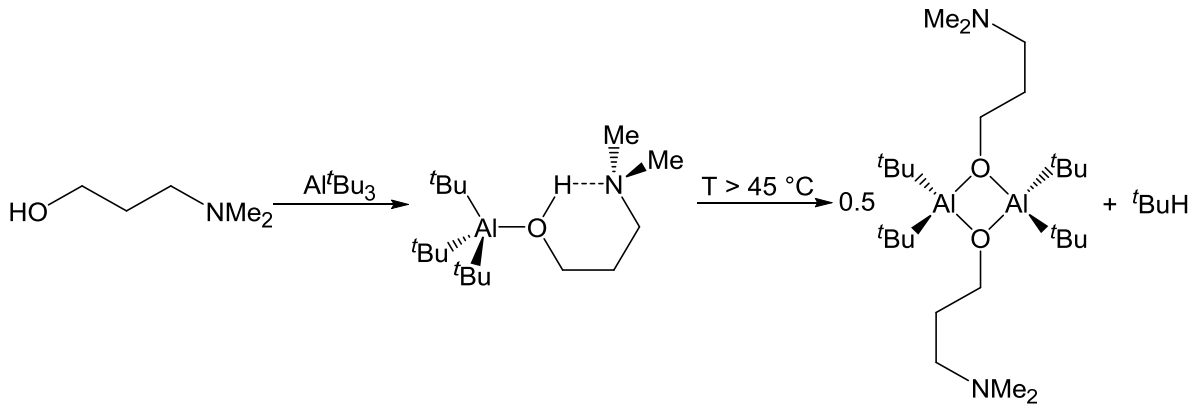

Scheme 1.9: The reaction of $HO(CH_2)_3NMe_2$ with Al^tBu_3 showing initial adduct formation, with elimination of ^{t}BuH occurring above 45 °C.[75]

The reactivity between organoaluminium compounds and water has been extensively studied. Initially, an adduct is formed between the water and organoaluminium (as seen above for alcohols), which is followed by elimination of RH. With controlled addition of water, partial hydrolysis of organoaluminiums can be achieved, leading to the formation of aluminoxanes. These are characterised by the presence of at least one oxo-group bridging two or more aluminiums (Scheme 1.10). Methylaluminoxane (MAO) is the most common such aluminoxane and has the general formula $\{Al(Me)O\}_n$, where n can range from 2 to 20. The structure of MAO is not well defined and a number of possible structures have been proposed based on chains, rings and cages (Figure 1.13).[76–78]

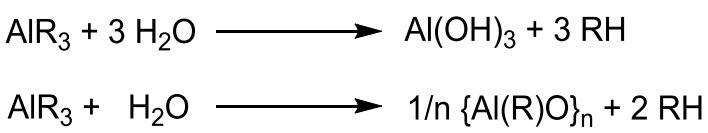

Scheme 1.10: The reactions between an organoaluminium and water can lead to the formation of aluminium hydroxide or aluminoxanes, depending on the stoichiometry.

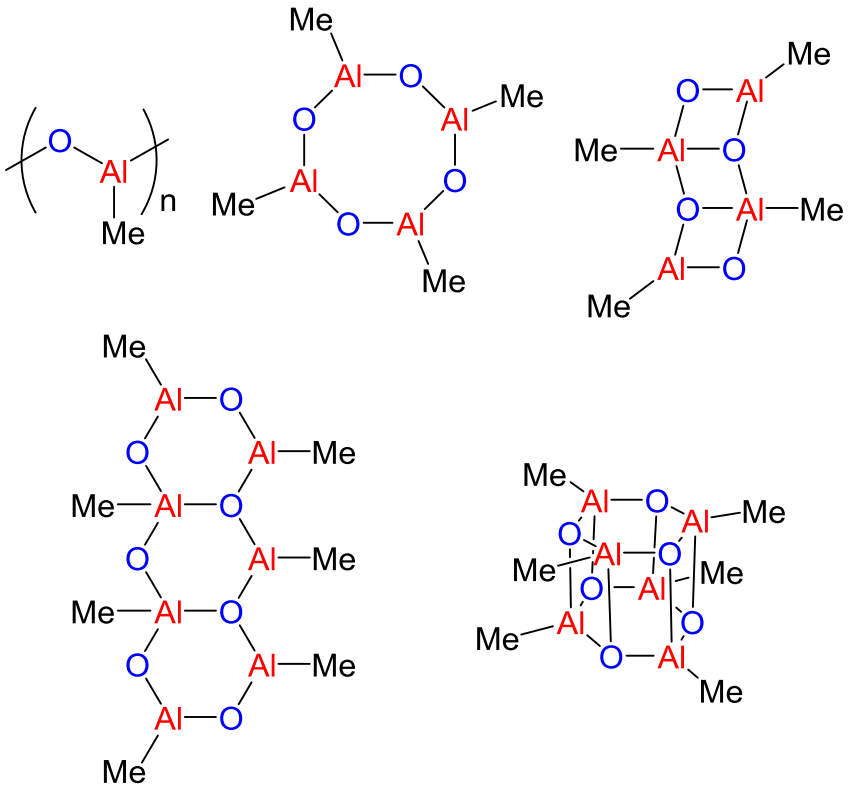

Figure 1.13: Some proposed structures for MAO, including chains, rings and cages.[76]

To further understand the structural features of MAO, the 2:1 reaction of alkylaluminiums with water was undertaken in order to produce the more tractable species $R_2AlOAlR_2$. The low-temperature hydrolysis of Al^tBu_3 initially yielded the trimeric hydroxide $\{^tBu_2Al(\mu_2\text{-}OH)\}_3$, with heating of this resulting in the formation of the dimeric aluminoxane $\{^tBu_2Al(\mu_2\text{-}OAl^tBu_2)\}_2$ (Figure 1.14, left). In the solid-state this compound exhibits two 3-coordinate aluminium centres and two 4-coordinate aluminium centres. The addition of pyridine to this species resulted in the formation of a monomeric aluminoxane, $\{^tBu_2Al(py)\}_2(\mu_2\text{-}O)$ (Figure 1.14, right), which X-ray diffraction showed to have a linear Al–O–Al bridge.[79]

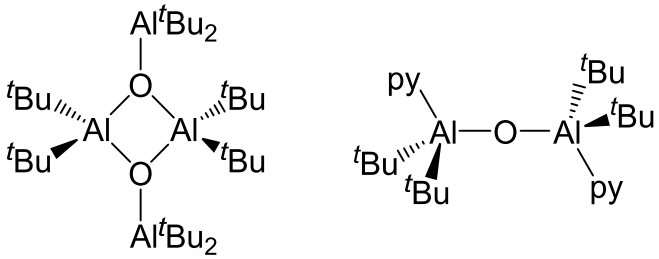

Figure 1.14: The structures of $\{^tBu_2Al(\mu_2\text{-}OAl^tBu_2)\}_2$ (left) and $\{^tBu_2Al(py)\}_2(\mu_2\text{-}O)$ (right).[79]

1.4.3.2 Ziegler-Natta chemistry

A very important industrial reaction involving organoaluminium compounds is the Ziegler-Natta process, which is used extensively for the polymerisation of α-alkenes. Trialkylaluminium compounds can undergo carboalumination reactions with alkenes and alkynes, with addition of the Al–C bond occurring across a C=C or C≡C bond (Scheme 1.11).[80] This can proceed thermally, as seen during ethylene polymerisation,[81] or in the presence of a transition metal catalyst, such as Cp_2ZrCl_2.[82] A similar reaction, hydroalumination, can occur with Al–H bonds (Scheme 1.11).[83] Both of these transformations are useful in organic synthesis as the resulting alkyl- and alkenylaluminium compounds can then be reacted with electrophiles to obtain a number of different functional groups. The Al–C and Al–H bonds can react with different regioselectivity, with the major product having the aluminium on the least hindered position (as this carbon is better able to stabilise a negative charge).[80] Addition of the Al–C and Al–H bond occurs via a *syn* mechanism that involves a 4-membered transition state. This can clearly be seen for the case of addition to alkynes as the groups added are cis to each other.[84]

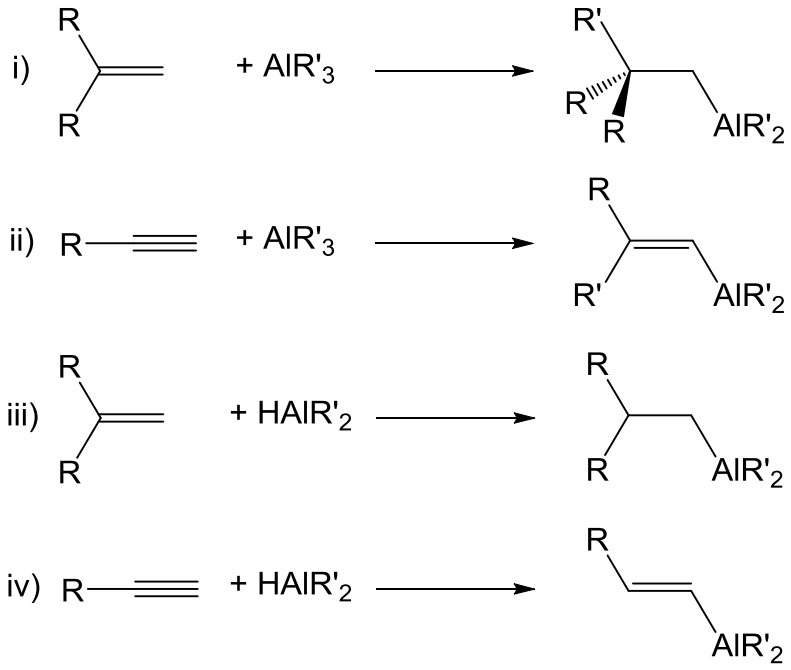

Scheme 1.11: The carboalumination of i) alkenes and ii) alkynes, and the hydroalumination of iii) alkenes and iv) alkynes.

The thermal polymerisation of α-alkenes by organoaluminiums was studied extensively by Ziegler in the 1950s.[81,85] The polymerisation of ethylene with triethylaluminium was

shown to proceed via a carboalumination reaction, forming linear alkyl chains. This occurred by a chain growth addition mechanism, with the addition of two carbon atoms for each equivalent of ethylene. The organoaluminium then underwent a β-hydride elimination, producing an α-alkene and a dialkylaluminium hydride. The dialkylaluminium hydride was then shown to react with further ethylene to regenerate triethylaluminium and undergo further insertion reactions (Scheme 1.12).[81,85]

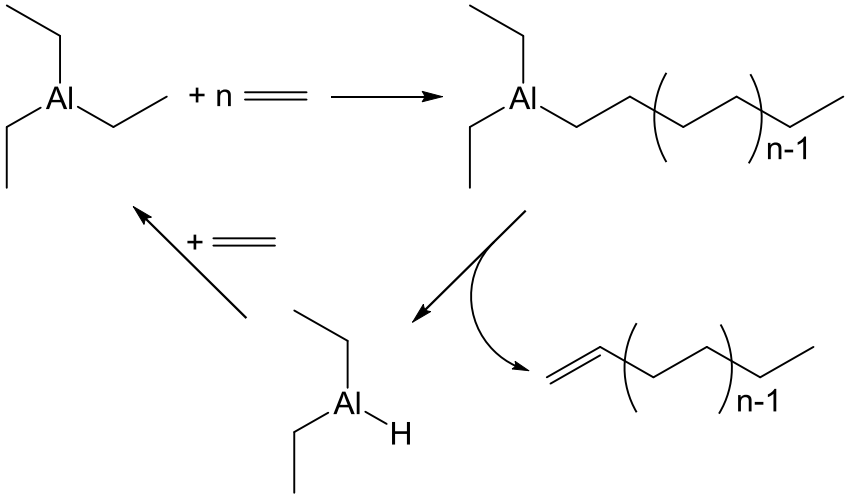

Scheme 1.12: The thermal polymerisation of ethylene by triethylaluminium.[81]

The addition of a transition metal complex co-catalyst, such as $TiCl_4$ or Cp_2TiCl_2, resulted in an enhancement in the polymerisation activity. This occurred due to the formation of a bimetallic species, with bridging ligands between the aluminium and the transition metal (Scheme 1.13).[85–87]

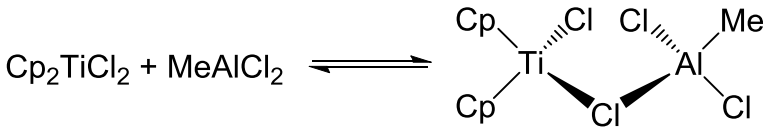

Scheme 1.13: The formation of a bimetallic species, with a bridging chloride, for Ziegler-Natta polymerisation.[87]

In the 1970s it was reported that the addition of small amounts of water led to an increase in the yield and polymerisation activity.[88,89] This was found to be due to the formation of MAO (see above), which can act as a co-catalyst with group 4 metallocenes in alkene polymerisation reactions (this catalytic system is known as a Kaminsky catalyst). The increase in activity compared to pure organoaluminium co-catalysts is due to MAOs enhanced Lewis acidity.[90,91] MAO is able to methylate the metallocene chloride, followed by abstraction of the chloride ligands. This produces an ion-pair consisting of the activated

metallocene catalyst and the MAO-derived anion (Scheme 1.14). MAO can also act as a scavenger for any impurities in the reaction, such as oxygen, water or carbon dioxide.[88,92]

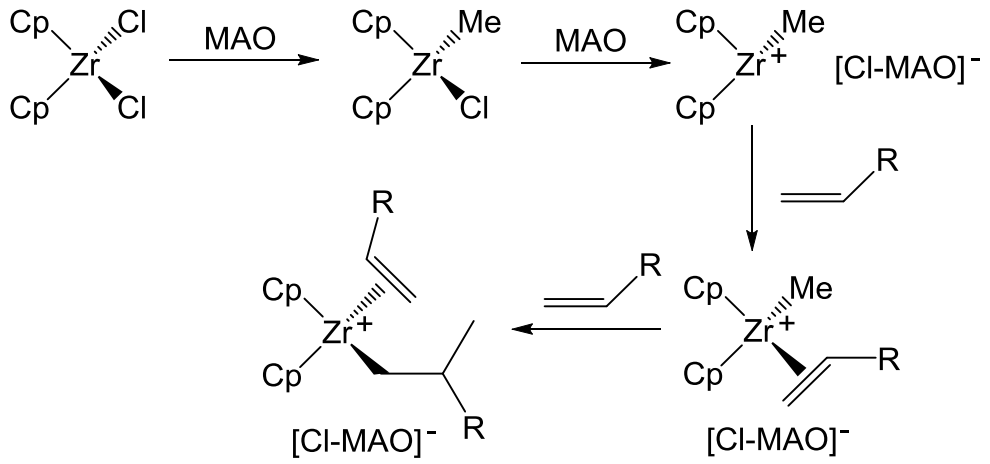

Scheme 1.14: A simplified scheme showing the role of MAO in Ziegler-Natta alkene polymerisation.[76]

Organoaluminiums readily react with oxygen, which inserts into the Al–C bond to form aluminium alkoxides (Scheme 1.15).[93] This oxidation reaction is highly exothermic and it is believed that the process proceeds by a radical chain mechanism, initially through the formation of an organoaluminium peroxide.[93] Aluminium alkoxides can be hydrolysed to form alcohols and this is a common way to produce long chain alcohols (known as the Ziegler process) (Scheme 1.15).[94]

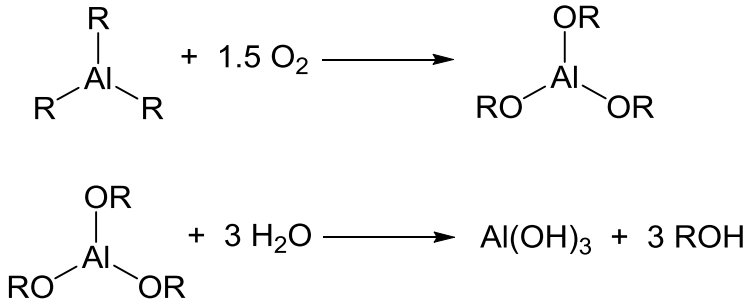

Scheme 1.15: The oxidation of alkylaluminium compounds to produce aluminium alkoxides. The addition of water to aluminium alkoxides results in the production of alcohols.

1.4.3.3 Organoaluminiums as nucleophiles

Due to the polarity of their Al–C bonds, organoaluminiums can act as nucleophiles. This nucleophilicity can often be enhanced by organoaluminiums also acting as Lewis acids, increasing the reactivity of the electrophile. The addition of organoaluminium compounds to carbonyl species is relatively common, but several different types of reaction can occur

(Scheme 1.16),[95] which are dependent on the organoaluminium and carbonyl compounds. Initially, adduct formation occurs with the oxygen donating a pair of electrons to the Lewis acidic aluminium centre.[96–99] With alkylaluminiums, alkylation can occur with the alkyl group acting as a nucleophile, producing an aluminium tertiary alkoxide.[100] Under forcing conditions exhaustive alkylation can occur, resulting in replacement of the alkoxide group with another alkyl group.[101,102] Enolisation of carbonyl compounds is favoured by sterically hindered carbonyls, with alkylation being disfavoured.[103,104] Reduction of the carbonyl to an alcohol can only occur if the alkyl groups of the organoaluminium contain a β-hydrogen. This is because the β-hydrogen of the alkyl group adds to the carbonyl and undergoes an elimination to produce an alkene. The result is that methyl ligands cannot undergo reduction reactions.[38] This is important to the current project as it is expected that methyl groups will be the only aluminium-bound alkyl groups present in experimental systems (as methylaluminium chlorides resulting from the reaction between chloromethane and aluminium).

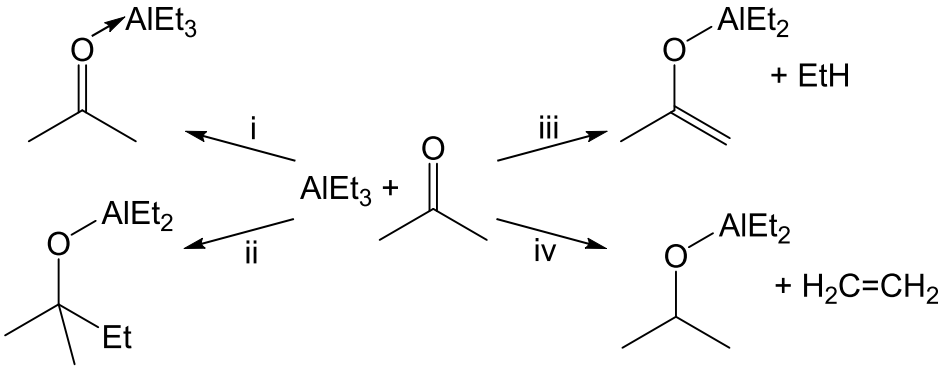

Scheme 1.16: Possible reactions between $AlEt_3$ and acetone: i) adduct formation, ii) alkylation, iii) enolisation and iv) reduction.[95]

The formation of hemialkoxides from addition reactions has been evidenced from the 1:2 reaction of ketones with alkylaluminiums. The reaction of acetone with TMA resulted in alkylation, to form dimethylaluminium *tert*-butoxide. The second equivalent of TMA then stabilised this alkoxide by forming an adduct, based upon a 4-membered Al_2CO ring (Scheme 1.17).[100]

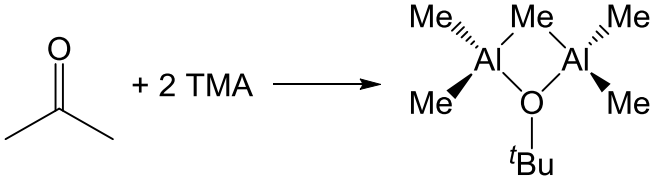

Scheme 1.17: The reaction between acetone and 2 equivalents of TMA, producing a hemialkoxide with bridging *tert*-butoxide and methyl groups.[100]

The symmetry of the hemialkoxide was observed by ^{1}H NMR spectroscopy, as at −30 °C the AlMe region contained two sharp signals with a 1:4 integral ratio, corresponding to the bridging and terminal methyl ligands. Increasing the temperature resulted in coalescence of the two AlMe signals at 110 °C. This exchange of the methyl groups occurred through the breaking of one of the bridging Al−Me bonds, followed by replacement of the bridging methyl group with one of the terminal methyl groups (Scheme 1.18). This exchange is much slower than that seen for TMA (see 1.4.2). Furthermore, the strength of the Al−O bond meant that disproportionation of the hemialkoxide to Me_2AlO^tBu and TMA dimers (which proceeds via a fully dissociative mechanism) occurred very slowly, requiring weeks at 110 °C.[100]

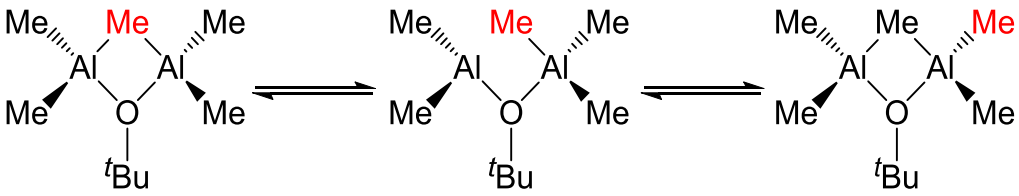

Scheme 1.18: The intramolecular exchange of aluminium-bound methyl groups in a hemialkoxide.[100]

The addition of alkylaluminiums to carbonyl compounds has been proposed to occur by either a 4-membered or a 6-membered transition state (Figure 1.15). For the 4-membered transition state, monomeric AlR_3 initially forms an adduct with the carbonyl group, which then allows for addition of an alkyl group. In contrast, the 6-membered transition state results from dimeric Al_2R_6 forming an adduct with the carbonyl group, with one of the alkyl groups bridging the aluminium atoms. Addition of an alkyl group results in the Al_2R_5 moiety coordinating to the alkoxide and the formation of the hemialkoxide, as shown above (Scheme 1.17).[100,105,106]

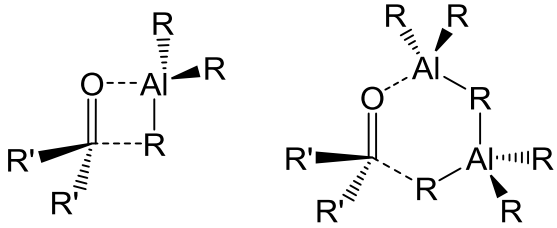

Figure 1.15: Proposed 4-membered (left) and 6-membered (right) transition states for the addition to carbonyls from alkylaluminiums.[100,105,106]

1.4.3.4 Lewis acidic behaviour

The Lewis acidity of organoaluminium compounds is due to the electrophilic nature of the aluminium centre and the energetic accessibility of the aluminium-based LUMO. This Lewis acidity (particularly of alkylaluminium halides) makes them extremely useful as catalysts in a number of reactions. Increasing the number of chloride ligands leads to an increase in Lewis acidity, so the choice of organoaluminium can be tailored to provide the Lewis acidity required. The use of TMA, Me_2AlCl, $MeAlCl_2$ or $AlCl_3$ (and the analogous Et compounds) as catalysts in Diels-Alder reactions is well documented and is particularly useful as many dienophiles are sensitive to protic acids.[107,108] The use of methylaluminium chlorides is also advantageous as they act as proton scavengers through cleavage of the Al–C bond. Organoaluminiums have also been used as Lewis acid catalysts in ene reactions and in Claisen rearrangements.[109,110]

The Lewis acidic nature of organoaluminiums makes them suitable for Friedel-Crafts reactions. Alkylaluminium chlorides, such as Et_2AlCl, are able to act as chloride acceptors from chloroalkanes to form a negatively charged aluminium species, e.g. $Et_2AlCl_2^-$, and the electrophilic alkyl species, R^+. The latter can then initiate electrophilic aromatic substitution, while the Brønsted basicity of $Et_2AlCl_2^-$ results in gradual loss of ethane by reaction with the resulting putative arenium system, yielding $EtAlCl_2$ (Scheme 1.19). Repetition of this process then gives $AlCl_3$.[111] Ethylaluminium dichloride has also been used as a catalyst for Friedel-Crafts reactions with alkenes.[112]

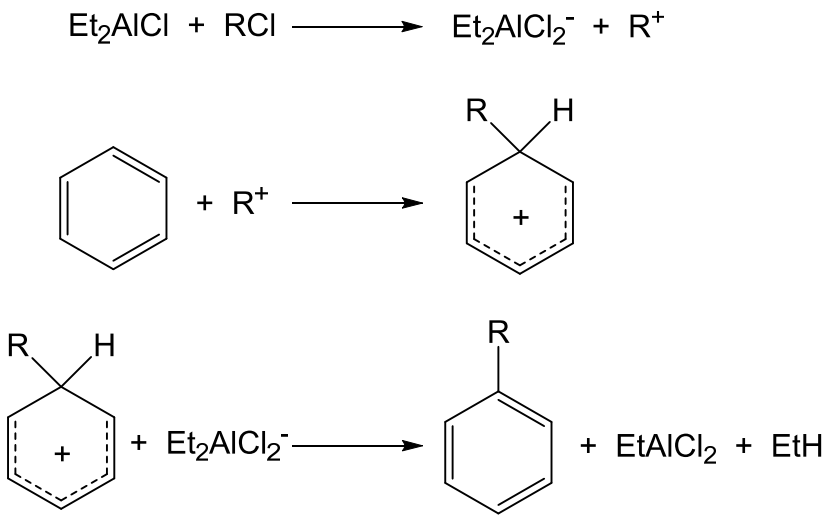

Scheme 1.19: The mechanism proposed for Friedel-Crafts alkylation with Et_2AlCl.[111]

This chapter has introduced the issues present in real-world refrigeration systems, many of which are thought to be caused by chloromethane contamination. The chloromethane is expected to react with aluminium components in the refrigeration systems, resulting the in the production of methylaluminium chlorides. Tests undertaken by CRT suggested that these organoaluminium species are reacting with lubricating oils, resulting in system failure. To better understand the potential processes taking place, the reactions of organoaluminium species with various organic compounds have been explored. In the next chapter the aims of the current project will be presented.

Chapter 2

Aims

The overall aim of this project is to understand the causes of corrosion in, and in some cases the explosion of, marine container refrigeration systems observed around the world. The concurrent discovery in 2011 of multiple refrigeration units contaminated by chloromethane suggested that the presence of chloromethane was in some way related to these incidents. Initial tests carried out by CRT suggested that reaction between aluminium (present in a range of components in these systems) and chloromethane was producing organoaluminium compounds, which could then react with refrigeration oil.

Initial investigations in the current project will be focused on determining the composition of industrial refrigeration oils, provided by CRT; using multiple spectroscopic methods to establish their chemical structures. Once the compositions of the oils used industrially have been determined, simple models for these refrigeration oils will be reacted with organoaluminiums at different stoichiometries and temperatures. These model reactions will help to understand possible reactions that may take place in industrial refrigeration systems between the refrigeration oil and organoaluminiums generated by the reaction between aluminium and chloromethane. In particular, the formation of flammable species, which can explain the explosive behaviour seen in real-world systems, will be investigated. Once the general reactivity has been understood, work will move towards performing reactions that more closely imitate industrial refrigeration units. This will require the use of pressurised reaction vessels to allow for the reactions between aluminium and chloromethane to produce methylaluminium chlorides. These reactions will be carried out in the presence and absence of refrigeration oils, to mimic real-world contaminated refrigeration units.

Chapter 3

General Experimental Techniques

3.1 COSHH

For all the experiments undertaken a full risk assessment was produced for the substances and techniques used. The control measures used included fume hoods to remove toxic and flammable vapours and using goggles, laboratory coats and gloves to protect against toxic and corrosive substances. The controls used for the experiments were recorded in a laboratory book to COSHH standards.

3.2 Inert Atmosphere Techniques

Many of the reagents and products obtained were air and moisture sensitive; therefore the exclusion of oxygen and air from reaction mixtures and products was essential. A number of inert atmosphere techniques were employed in the synthetic procedures and in analysis of the products to prevent significant degradation by oxygen or moisture. Standard Schlenk techniques were used during the synthesis and manipulation of the compounds throughout the project and unless specified reactions were carried out in Schlenk flasks.[113] A vacuum and nitrogen double manifold was used to produce an inert atmosphere within the reaction vessels by exposing the flask to a vacuum followed by flushing with nitrogen and then repeating the procedure twice more. Liquid reagents and solvents were added through a rubber Suba-Seal® with a dry syringe and the Schlenk flask under a positive pressure of nitrogen. Solid reagents were added to the flask in an inert atmosphere glove box before it had been attached to the vacuum line. There was continual recirculation of the inert atmosphere through the glove box by four columns, one containing molecular sieves (BDH 3 Å, 16") and three containing an oxygen scavenging copper catalyst (BASF Cu catalyst R11), maintaining low levels of oxygen and moisture.

Crystals were isolated by attaching the Schlenk flask to the N_2 line and then the solution from which they had crystallised was removed with a dry syringe. The crystals were then dried under vacuum and analysed in a glove box. Air sensitive filtration was employed

with the use of a filter stick. The filter stick was attached to a second Schlenk flask and the whole arrangement was purged as described above. The flask containing the solution to be filtered was directly attached to the filter by quickly removing the cap from the filter stick and the stopper from the original Schlenk. The apparatus was inverted, and the receiving flask was partially evacuated to produce a pressure gradient to force the filtrate through the filter.

3.3 High Pressure Reactions

Reactions using gaseous species (such as chloromethane) were conducted using a Parr reactor. Gaseous species were added to the reactor via Swagelok® piping and connecting joints. The reaction mixtures could be heated using a heating mantle and thermocouple couple to reach the desired temperature. After reactions were complete, excess pressure was slowly released in a vented fume cupboard.

3.4 Thermal Control

Reactions carried out at −78 °C were achieved by combining acetone and dry ice in a bath, with the Schlenk flask placed in the bath during addition of the reagents. For reactions carried out at raised temperatures, a silicon oil bath was used and if required a condenser was fitted to the top of the Schlenk flask. Solutions were left to crystallise at room temperature, 4 °C, −20 °C or −27 °C.

3.5 Reagents and Solvents

All reagents were purchased from Sigma-Aldrich apart from RL 32H and FVC 46D refrigeration oils (provided by CRT), neopentyl glycol and pentaerythritol (Alfa Aesar), phenylacetyl chloride and hexanoyl chloride (Fisher Scientific) and chloromethane (BOC). The monoesters and ethers were stored over molecular sieves (4 Å). TMA (2.0 M in toluene, 1.0 M in hexane and 2.0 M in heptane), Me_2AlCl (1.0 M in hexanes), phenylacetyl chloride and hexanoyl chloride were stored at 4 °C. Aluminium, $AlCl_3$ and the polyols were stored in a glove box.

Solvents were obtained from communal stills where they were continually distilled over sodium (hexane and pentane), sodium-potassium amalgam (toluene) or sodium-benzophenone (THF and Et_2O). The solvents were transferred to the reaction vessel *via* a dry, purged syringe.

3.6 Melting Point Determination

The melting point of the sample was determined using a sealed capillary tube and Griffin melting point equipment and repeated to ensure accuracy.

3.7 Elemental Analysis

The samples were analysed to determine the mass percent of carbon, hydrogen and chlorine for comparison against the predicted values for the compound. Air-sensitive samples were placed in aluminium capsules in the glove box and sealed using a press. Mass analysis was carried out on a Perkin-Elmer 240 elemental analyser.

3.8 Multinuclear Nuclear Magnetic Resonance (NMR) Spectroscopy

About 20 mg of the sample was dissolved in 0.7 ml of benzene-d_6, toluene-d_8 or chloroform-*d*. The solution was then transferred to a thin-walled glass J Young NMR tube (Wilmad, 528-PP). ^{1}H, ^{13}C and ^{27}Al NMR Spectroscopy was carried out using either a Bruker Avance 500 FT-NMR spectrometer or a Bruker Avance 400 FT-NMR spectrometer. All NMR spectroscopy was performed at 298 K. The chemical shifts for ^{1}H and ^{13}C NMR were internally referenced to tetramethylsilane. For ^{27}Al NMR, shifts were measured relative to $AlCl_3 \cdot 6H_2O$. All ^{13}C NMR is ^{1}H decoupled. The same spectrometers were used to carry out DEPT, HSQC, HMBC, COSY and NOESY experiments.

3.9 X-ray Diffractometry

For crystals of the correct size (less than 0.5 mm x 0.5 mm x 0.5 mm) and quality single crystal X-ray diffraction data were collected. The "oil drop mounting technique"[114] was implemented to ensure that the crystals could be selected under a microscope and loaded onto the diffractometer without significant degradation by oxidation or hydrolysis. This was done by coating the crystal in inert perfluorinated polyether oil immediately upon removal from the nitrogen atmosphere. The crystals were then placed under a cold nitrogen stream and a single crystal of suitable quality was selected for analysis. The selected crystal was then mounted on a MicroLoop™ attached to the diffractometer goniometer head and placed onto the machine. The crystal was cooled to 180 K to prevent chemical alteration of the crystal and to secure any labile solvent molecules. The cooling also minimises vibrations within the lattice that would add uncertainty to the resulting pattern. Data were collected on either a Nonius Kappa CCD diffractometer (Mo-Kα, λ = 0.71073 Å) or a Bruker D8 Quest diffractometer (Cu-Kα, λ = 1.54184 Å), both equipped with an Oxford Cryostream low temperature device. Structures were solved using SHELXT,[115] with refinement, based on F^2, by full-matrix least squares.[116] Non-hydrogen atoms were refined anisotropically (for disorder, standard restraints and constraints were employed as appropriate) and a riding model with idealised geometry was employed for the refinement of hydrogen atoms.

3.10 Fourier Transform Infrared (FTIR) Spectroscopy

A PerkinElmer Spectrum One FTIR Spectrometer fitted with a PerkinElmer ATR Sampling Accessory was used to record spectra. A background spectrum was run prior to measuring a sample.

3.11 Liquid Chromatography-Mass Spectrometry (LC-MS)

Samples were analysed using a Waters LCT Premier spectrometer, with electrospray ionisation used to produce a charge on the sample.

Chapter 4

Experimental

4.1 Reactivity of Monoesters with Methylaluminium Reagents

4.1.1 Reactivity of Monoesters with TMA

4.1.1.1 Spectroscopic characterisation of $\mathbf{1}^{Et}$ + TMA reaction mixtures

TMA (1.5, 3.0 or 4.5 ml, 3, 6 or 9 mmol, 2.0 M in toluene) was added dropwise to methyl propionate $\mathbf{1}^{Et}$ (0.29 ml, 3 mmol) under a N_2 atmosphere at −78 °C before being allowed to reach room temperature. The resulting solution was stirred for 2 hours at this temperature. An aliquot of the solution was analysed by NMR spectroscopy.

1:1 $\mathbf{1}^{Et}$:TMA

^{1}H NMR spectroscopy (400 MHz, benzene-d_6): δ 3.08 (s, 0.2H, **3** OMe), 2.98 (m, 3H, $\mathbf{1}^{Et}$(TMA) OMe), 1.97 (m, 2H, $\mathbf{1}^{Et}$(TMA) CH_2), 1.42 (q, J = 7.5 Hz, 0.1H, $\mathbf{4}^{Et}$(TMA) CH_2), 1.07 (s, 0.3H, $\mathbf{4}^{Et}$(TMA) Me), 0.65 (m, 3.2H, $\mathbf{1}^{Et}$(TMA) + $\mathbf{4}^{Et}$(TMA) Me), 0.16 (s, 0.1H, $\mathbf{4}^{Et}$(TMA) $AlMe_b$), −0.33 (m, 9H, $\mathbf{1}^{Et}$(TMA) AlMe), −0.49 (s, 0.3H, $\mathbf{4}^{Et}$(TMA) $AlMe_t$), −0.60 (s, 0.4H, **3** AlMe)

^{13}C NMR spectroscopy (100 MHz, benzene-d_6): δ 181.4 ($\mathbf{1}^{Et}$(TMA) C=O), 79.5 ($\mathbf{4}^{Et}$(TMA) CO), 53.8 ($\mathbf{1}^{Et}$(TMA) OMe), 50.4 (**3** OMe), 36.6 ($\mathbf{4}^{Et}$(TMA) CH_2), 27.7 ($\mathbf{1}^{Et}$(TMA) CH_2 + $\mathbf{4}^{Et}$(TMA) Me), 8.8 ($\mathbf{4}^{Et}$(TMA) Me), 8.2 ($\mathbf{1}^{Et}$(TMA) Me), −7.7 ($\mathbf{1}^{Et}$(TMA) AlMe)

^{27}Al NMR spectroscopy (104 MHz, benzene-d_6): δ 185.0 ($\mathbf{1}^{Et}$(TMA)), 157.7 (**3** + $\mathbf{4}^{Et}$(TMA))

1:2 $\mathbf{1}^{Et}$:TMA

^{1}H NMR spectroscopy (400 MHz, benzene-d_6): δ 3.08 (s, 3H, **3** OMe), 2.94 (s, 2.4H, $\mathbf{1}^{Et}$(TMA) OMe), 1.95 (q, J = 7.5 Hz, 1.6H, $\mathbf{1}^{Et}$(TMA) CH_2), 1.42 (q, J = 7.5 Hz, 2H, $\mathbf{4}^{Et}$(TMA) CH_2), 1.07 (s, 6H, $\mathbf{4}^{Et}$(TMA) Me), 0.63 (t, J = 7.5 Hz, 5.4H, $\mathbf{1}^{Et}$(TMA) +

4^{Et}(TMA) Me), 0.09 (br, s, 3H, **4**^{Et}(TMA) $AlMe_b$), −0.32 (s, 7.1H, **1**^{Et}(TMA) AlMe), −0.49 (s, br, 12H, **4**^{Et}(TMA) $AlMe_t$), −0.60 (s, 6H, **3** AlMe)

^{13}C NMR spectroscopy (100 MHz, benzene-d_6): δ 181.8 (**1**^{Et}(TMA) C=O), 79.5 (**4**^{Et}(TMA) CO), 54.0 (**1**^{Et}(TMA) OMe), 50.4 (**3** OMe), 36.6 (**4**^{Et}(TMA) CH_2), 27.7 (**1**^{Et}(TMA) CH_2 + **4**^{Et}(TMA) Me), 8.8 (**4**^{Et}(TMA) Me), 8.2 (**1**^{Et}(TMA) Me), −4.6 (**4**^{Et}(TMA) $AlMe_b$), −7.7 (br, **1**^{Et}(TMA) + **4**^{Et}(TMA) $AlMe_t$), −11.1 (**3** AlMe)

^{27}Al NMR spectroscopy (104 MHz, benzene-d_6): δ 179.7 (sh, **1**^{Et}(TMA)), 153.9 (**3** + **4**^{Et}(TMA))

1:3 **1**^{Et}:TMA

^{1}H NMR spectroscopy (400 MHz, benzene-d_6): δ 3.06 (s, 3H, **3** OMe), 1.41 (q, J = 7.5 Hz, 2H, **4**^{Et}(TMA) CH_2), 1.05 (s, 6H, **4**^{Et}(TMA) Me), 0.61 (t, J = 7.5 Hz, 3H, **4**^{Et}(TMA) Me), 0.09 (s, 3H, **4**^{Et}(TMA) $AlMe_b$), −0.36 (s, 3.5H, TMA), −0.47 (s, 12H, **4**^{Et}(TMA) $AlMe_t$), −0.59 (s, 6H, **3** AlMe)

^{13}C NMR spectroscopy (100 MHz, benzene-d_6): δ 79.9 (**4**^{Et}(TMA) CO), 50.8 (**3** OMe), 37.0 (**4**^{Et}(TMA) CH_2), 28.1 (**4**^{Et}(TMA) Me), 9.2 (**4**^{Et}(TMA) Me), −4.1 (**4**^{Et}(TMA) $AlMe_b$), −6.7 (br, **4**^{Et}(TMA) $AlMe_t$), −10.7 (br, **3** Me)

^{27}Al NMR spectroscopy (104 MHz, benzene-d_6): δ 156.2 (**3** + **4**^{Et}(TMA))

4.1.1.2 Thermal stability of 1:3 1^{Et}:TMA reaction mixture

The reaction mixture at the end of the 1:3 reaction of **1**^{Et} with TMA in toluene (to give **4**^{Et}(TMA) and **3**; see above) was heated to reflux for 4 hours. An aliquot of the solution was analysed by NMR spectroscopy after time, t, = 0 (before heating), 1, 2, 3 and 4 hours.

t = 0 hr

^{1}H NMR spectroscopy (400 MHz, benzene-d_6): δ 3.07 (s, 3H, **3** OMe), 1.41 (q, J = 7.5 Hz, 2H, **4**^{Et}(TMA) CH_2), 1.06 (s, 6H, **4**^{Et}(TMA) Me), 0.62 (t, J = 7.5 Hz, 3H, **4**^{Et}(TMA) Me), 0.10 (s, 3H, **4**^{Et}(TMA) $AlMe_b$), −0.36 (s, br, 1.5H, TMA), −0.48 (s, 12H, **4**^{Et}(TMA) $AlMe_t$), −0.60 (s, 6H, **3** AlMe)

^{13}C NMR spectroscopy (100 MHz, benzene-d_6): δ 79.5 (**4**^{Et}(TMA) CO), 50.4 (**3** OMe), 36.6 (**4**^{Et}(TMA) CH_2), 27.7 (**4**^{Et}(TMA) Me), 8.8 (**4**^{Et}(TMA) Me), −4.5 (**4**^{Et}(TMA) $AlMe_b$), −7.4 (br, **4**^{Et}(TMA) $AlMe_t$), −10.9 (br, **3** AlMe)

t = 1 hr

^{1}H NMR spectroscopy (400 MHz, benzene-d_6): δ 3.06 (s, 2H, **3** OMe), 3.00 (s, 1H, **4**^{Et}(**3**) OMe), 1.44 (q, J = 7.5 Hz, 0.7H, **4**^{Et}(**3**) CH_2), 1.41 (q, J = 7.5 Hz, 1.3H, **4**^{Et}(TMA) CH_2), 1.09 (s, 2H, **4**^{Et}(**3**) Me), 1.05 (s, 4H, **4**^{Et}(TMA) Me), 0.65 (t, J = 7.5 Hz, 1H, **4**^{Et}(**3**) Me), 0.61 (t, J = 7.5 Hz, 2H, **4**^{Et}(TMA) Me), 0.09 (s, 2H, **4**^{Et}(TMA) $AlMe_b$), −0.36 (s, br, 3H, TMA), −0.47 (s, 8H, **4**^{Et}(TMA) $AlMe_t$), −0.48 (s, 4H, **4**^{Et}(**3**) AlMe), −0.59 (s, 4H, **3** AlMe)

^{13}C NMR spectroscopy (100 MHz, benzene-d_6): δ 79.5 (**4**^{Et}(TMA) CO), 77.0 (**4**^{Et}(**3**) CO), 50.4 (**3** OMe), 48.4 (**4**^{Et}(**3**) OMe), 37.1 (**4**^{Et}(**3**) CH_2), 36.6 (**4**^{Et}(TMA) CH_2), 28.1 (**4**^{Et}(**3**) Me), 27.7 (**4**^{Et}(TMA) Me), 8.9 (**4**^{Et}(**3**) Me), 8.8 (**4**^{Et}(TMA) Me), −4.5 (**4**^{Et}(TMA) $AlMe_b$), −7.3 (**4**^{Et}(**3**) AlMe), −7.5 (**4**^{Et}(TMA) $AlMe_t$), −9.5 (**3** AlMe)

t = 2 hr

^{1}H NMR spectroscopy (400 MHz, benzene-d_6): δ 3.07 (s, 1.7H, **3** OMe), 3.01 (s, 1.3H, **4**^{Et}(**3**) OMe), 1.43 (q, J = 7.5 Hz, 0.8H, **4**^{Et}(**3**) CH_2), 1.41 (q, J = 7.5 Hz, 1.2H, **4**^{Et}(TMA) CH_2), 1.09 (s, 2.5H, **4**^{Et}(**3**) Me), 1.06 (s, 3.5H, **4**^{Et}(TMA) Me), 0.66 (t, J = 7.5 Hz, 1.3H, **4**^{Et}(**3**) Me), 0.62 (t, J = 7.5 Hz, 1.7H, **4**^{Et}(TMA) Me), 0.10 (s, 1.5H, **4**^{Et}(TMA) $AlMe_b$), −0.36 (s, br, 4.5H, TMA), −0.48 (s, 7H, **4**^{Et}(TMA) $AlMe_t$), −0.49 (s, 5H, **4**^{Et}(**3**) AlMe), −0.60 (s, 3.5H, **3** AlMe)

^{13}C NMR spectroscopy (100 MHz, benzene-d_6): δ 79.5 (**4**^{Et}(TMA) CO), 77.0 (**4**^{Et}(**3**) CO), 50.4 (**3** OMe), 48.3 (**4**^{Et}(**3**) OMe), 37.1 (**4**^{Et}(**3**) CH_2), 36.6 (**4**^{Et}(TMA) CH_2), 28.1 (**4**^{Et}(**3**) Me), 27.7 (**4**^{Et}(TMA) Me), 8.9 (**4**^{Et}(**3**) Me), 8.8 (**4**^{Et}(TMA) Me), −4.5 (**4**^{Et}(TMA) $AlMe_b$), −7.4 (br, **4**^{Et}(**3**) AlMe + **4**^{Et}(TMA) $AlMe_t$), −9.5 (**3** AlMe)

t = 3 hr

^{1}H NMR spectroscopy (400 MHz, benzene-d_6): δ 3.07 (s, 1.5H, **3** OMe), 3.01 (s, 1.5H, **4**^{Et}(**3**) OMe), 1.44 (q, J = 7.5 Hz, 1H, **4**^{Et}(**3**) CH_2), 1.41 (q, J = 7.5 Hz, 1H, **4**^{Et}(TMA) CH_2),

1.10 (s, 3H, $\mathbf{4}^{Et}$(**3**) Me), 1.06 (s, 3H, $\mathbf{4}^{Et}$(TMA) Me), 0.66 (t, *J* = 7.5 Hz, 1.5H, $\mathbf{4}^{Et}$(**3**) Me), 0.62 (t, *J* = 7.5 Hz, 1.5H, $\mathbf{4}^{Et}$(TMA) Me), 0.10 (s, 1.5H, $\mathbf{4}^{Et}$(TMA) $AlMe_b$), −0.35 (s, br, 4.5H, TMA), −0.47 (s, 6H, $\mathbf{4}^{Et}$(TMA) $AlMe_t$), −0.48 (s, 6H, $\mathbf{4}^{Et}$(**3**) AlMe), −0.59 (s, 3H, **3** AlMe)

^{13}C NMR spectroscopy (100 MHz, benzene-d_6): δ 79.5 ($\mathbf{4}^{Et}$(TMA) CO), 77.0 ($\mathbf{4}^{Et}$(**3**) CO), 50.4 (**3** OMe), 48.3 ($\mathbf{4}^{Et}$(**3**) OMe), 37.1 ($\mathbf{4}^{Et}$(**3**) CH_2), 36.6 ($\mathbf{4}^{Et}$(TMA) CH_2), 28.1 ($\mathbf{4}^{Et}$(**3**) Me), 27.7 ($\mathbf{4}^{Et}$(TMA) Me), 8.9 ($\mathbf{4}^{Et}$(**3**) Me), 8.8 ($\mathbf{4}^{Et}$(TMA) Me), −4.5 ($\mathbf{4}^{Et}$(TMA) $AlMe_b$), −7.5 (br, $\mathbf{4}^{Et}$(**3**) AlMe + $\mathbf{4}^{Et}$(TMA) $AlMe_t$), −9.5 (**3** AlMe)

t = 4 hr

^{1}H NMR spectroscopy (400 MHz, benzene-d_6): δ 3.07 (s, 1.4H, **3** OMe), 3.02 (s, 1.6H, $\mathbf{4}^{Et}$(**3**) OMe), 1.43 (q, *J* = 7.5 Hz, 1.1H, $\mathbf{4}^{Et}$(**3**) CH_2), 1.41 (q, *J* = 7.5 Hz, 0.9H, $\mathbf{4}^{Et}$(TMA) CH_2), 1.10 (s, 3.3H, $\mathbf{4}^{Et}$(**3**) Me), 1.06 (s, 2.7H, $\mathbf{4}^{Et}$(TMA) Me), 0.66 (t, *J* = 7.5 Hz, 1.6H, $\mathbf{4}^{Et}$(**3**) Me), 0.62 (t, *J* = 7.5 Hz, 1.4H, $\mathbf{4}^{Et}$(TMA) Me), 0.10 (s, 1.4H, $\mathbf{4}^{Et}$(TMA) $AlMe_b$), −0.36 (s, br, 5H, TMA), −0.47 (s, 5.5H, $\mathbf{4}^{Et}$(TMA) $AlMe_t$), −0.48 (s, 6.5H, $\mathbf{4}^{Et}$(**3**) AlMe), −0.59 (s, 2.8H, **3** AlMe)

^{13}C NMR spectroscopy (100 MHz, benzene-d_6): δ 79.5 ($\mathbf{4}^{Et}$(TMA) CO), 77.0 ($\mathbf{4}^{Et}$(**3**) CO), 50.4 (**3** OMe), 48.3 ($\mathbf{4}^{Et}$(**3**) OMe), 37.1 ($\mathbf{4}^{Et}$(**3**) CH_2), 36.6 ($\mathbf{4}^{Et}$(TMA) CH_2), 28.1 ($\mathbf{4}^{Et}$(**3**) Me), 27.7 ($\mathbf{4}^{Et}$(TMA) Me), 8.9 ($\mathbf{4}^{Et}$(**3**) Me), 8.8 ($\mathbf{4}^{Et}$(TMA) Me), −4.5 ($\mathbf{4}^{Et}$(TMA) $AlMe_b$), −7.5 ($\mathbf{4}^{Et}$(**3**) AlMe + $\mathbf{4}^{Et}$(TMA) $AlMe_t$), −9.5 (**3** AlMe)

Time (hours)	$\mathbf{4}^{Et}$(TMA)	$\mathbf{4}^{Et}$(**3**)
0	100	0
1	70	30
2	56	44
3	49	51
4	46	54

Table 4.1: The proportion (%) of $\mathbf{4}^{Et}$(TMA) and $\mathbf{4}^{Et}$(**3**) from the heating of a 1:1 mixture of $\mathbf{4}^{Et}$(TMA) and **3** to reflux in toluene, after time 0-4 hours. The proportions are calculated by integration of the ^{1}H NMR spectra.

4.1.1.3 Thermal stability of 1:1 and 1:2 1^{Et}:TMA reaction mixtures

The reaction mixtures at the end of the 1:1 and 1:2 reactions of $\mathbf{1}^{Et}$ with TMA in toluene (see above) were heated to reflux for 2 hours. An aliquot of the solution was analysed by NMR spectroscopy.

1:1 $\mathbf{1}^{Et}$:TMA

^{1}H NMR spectroscopy (400 MHz, benzene-d_6): δ 3.32 (s, 2.4H, $\mathbf{1}^{Et}$ OMe), 3.08 (s, 0.8H, **3** OMe), 3.02 (s, 3H, $\mathbf{4}^{Et}$(**3**) OMe), 1.99 (q, J = 7.6 Hz, 1.6H, $\mathbf{1}^{Et}$ CH_2), 1.50 (q, J = 7.5 Hz, 0.4H, $(\mathbf{4}^{Et})_2$ CH_2), 1.44 (q, J = 7.5 Hz, 2H, $\mathbf{4}^{Et}$(**3**) CH_2), 1.15 (s, 1H, $(\mathbf{4}^{Et})_2$ Me), 1.10 (s, 6H, $\mathbf{4}^{Et}$(**3**) Me), 0.93 (t, J = 7.6 Hz, 2.4H, $\mathbf{1}^{Et}$ Me), 0.69 (t, J = 7.5 Hz, 0.5H, $(\mathbf{4}^{Et})_2$ Me), 0.66 (t, J = 7.5 Hz, 3H, $\mathbf{4}^{Et}$(**3**) Me), −0.42 (s, 1H, $(\mathbf{4}^{Et})_2$ AlMe), −0.50 (s, 12H, $\mathbf{4}^{Et}$(**3**) AlMe), −0.61 (s, 1.6H, **3** AlMe)

^{13}C NMR spectroscopy (100 MHz, benzene-d_6): δ 173.4 ($\mathbf{1}^{Et}$ C=O), 77.3 ($(\mathbf{4}^{Et})_2$ CO), 77.0 ($\mathbf{4}^{Et}$(**3**) CO), 50.5 ($\mathbf{1}^{Et}$ OMe), 50.3 (**3** OMe), 48.3 ($\mathbf{4}^{Et}$(**3**) OMe), 37.1 ($\mathbf{4}^{Et}$(**3**) CH_2), 37.0 ($(\mathbf{4}^{Et})_2$ CH_2), 28.1 ($\mathbf{4}^{Et}$(**3**) + $(\mathbf{4}^{Et})_2$ Me), 26.9 ($\mathbf{1}^{Et}$ CH_2), 9.0 ($(\mathbf{4}^{Et})_2$ Me), 8.8 ($\mathbf{1}^{Et}$ + $\mathbf{4}^{Et}$(**3**) Me), −9.5 (br, **3** + $\mathbf{4}^{Et}$(**3**) AlMe)

^{27}Al NMR spectroscopy (104 MHz, benzene-d_6): δ 156.7 (**3** + $\mathbf{4}^{Et}$(**3**) + $(\mathbf{4}^{Et})_2$), 8.1 (trace)

1:2 $\mathbf{1}^{Et}$:TMA

^{1}H NMR spectroscopy (400 MHz, benzene-d_6): δ 3.06 (s, 0.5H, **3** OMe), 3.01 (s, 3H, $\mathbf{4}^{Et}$(**3**) OMe), 1.50 (q, J = 7.5 Hz, 0.3H, $(\mathbf{4}^{Et})_2$ CH_2), 1.43 (q, J = 7.5 Hz, 2H, $\mathbf{4}^{Et}$(**3**) CH_2), 1.15 (s, 0.9H, $(\mathbf{4}^{Et})_2$ Me), 1.09 (s, 6H, $\mathbf{4}^{Et}$(**3**) Me), 0.68 (t, J = 7.5 Hz, 0.4H, $(\mathbf{4}^{Et})_2$ Me), 0.66 (t, J = 7.5 Hz, 3H, $\mathbf{4}^{Et}$(**3**) Me), −0.40 (s, 0.9H, $(\mathbf{4}^{Et})_2$ AlMe), −0.48 (s, 12H, $\mathbf{4}^{Et}$(**3**) AlMe), −0.59 (s, 0.9H, **3** AlMe)

^{13}C NMR spectroscopy (100 MHz, benzene-d_6): δ 77.3 ($(\mathbf{4}^{Et})_2$ CO), 77.0 ($\mathbf{4}^{Et}$(**3**) CO), 50.4 (**3** OMe), 48.3 ($\mathbf{4}^{Et}$(**3**) OMe), 37.1 ($\mathbf{4}^{Et}$(**3**) CH_2), 37.1 ($(\mathbf{4}^{Et})_2$ CH_2), 28.1 ($\mathbf{4}^{Et}$(**3**) + $(\mathbf{4}^{Et})_2$ Me), 9.0 ($(\mathbf{4}^{Et})_2$ Me), 8.9 ($\mathbf{4}^{Et}$(**3**) Me), −6.1 (br, $(\mathbf{4}^{Et})_2$ AlMe), −9.5 (br, **3** + $\mathbf{4}^{Et}$(**3**) AlMe)

^{27}Al NMR spectroscopy (104 MHz, benzene-d_6): δ 155.1 (**3** + $\mathbf{4}^{Et}$(**3**) + $(\mathbf{4}^{Et})_2$)

4.1.1.4 Spectroscopic characterisation of 1^{Bn} + TMA reaction mixtures

As for $\mathbf{1}^{Et}$ + TMA but using methyl phenylacetate $\mathbf{1}^{Bn}$ (0.42 ml, 3 mmol). An aliquot of the solution was analysed by NMR spectroscopy.

1:1 $\mathbf{1}^{Bn}$:TMA

^{1}H NMR spectroscopy (400 MHz, benzene-d_6): δ 7.13-6.86 (m, 5.5H, $\mathbf{1}^{Bn}$(TMA) + $\mathbf{4}^{Bn}$(TMA) Ph), 3.34 (s, 2H, $\mathbf{1}^{Bn}$(TMA) CH_2), 3.07 (s, 0.4H, **3** OMe), 2.89 (s, 3H, $\mathbf{1}^{Bn}$(TMA) OMe), 2.86 (s, 0.2H, $\mathbf{4}^{Bn}$(TMA) CH_2), 1.12 (s, 0.6H, $\mathbf{4}^{Bn}$(TMA) Me), −0.24 (m, 9H, $\mathbf{1}^{Bn}$(TMA), AlMe), −0.43 (s, 1.2H, $\mathbf{4}^{Bn}$(TMA) $AlMe_t$), −0.59 (s, 0.8H, **3** AlMe)

^{13}C NMR spectroscopy (100 MHz, benzene-d_6): δ 178.1 ($\mathbf{1}^{Bn}$(TMA) C=O), 136.6, 131.7, 130.3, 128.1, 127.6 ($\mathbf{1}^{Bn}$(TMA) + $\mathbf{4}^{Bn}$(TMA) Ph), 79.5 ($\mathbf{4}^{Bn}$(TMA) CO), 54.0 ($\mathbf{1}^{Bn}$(TMA) OMe), 50.7 ($\mathbf{4}^{Bn}$(TMA) CH_2), 50.4 (**3** OMe), 40.7 ($\mathbf{1}^{Bn}$(TMA) CH_2), 28.1 ($\mathbf{4}^{Bn}$(TMA) Me), −7.5 ($\mathbf{4}^{Bn}$(TMA) $AlMe_t$), −9.3 ($\mathbf{1}^{Bn}$(TMA) AlMe), −11.0 (**3** AlMe)

^{27}Al NMR spectroscopy (104 MHz, benzene-d_6): δ 186.3 ($\mathbf{1}^{Bn}$(TMA)), 157.8 (**3** + $\mathbf{4}^{Bn}$(TMA))

1:2 $\mathbf{1}^{Bn}$:TMA

^{1}H NMR spectroscopy (400 MHz, benzene-d_6): δ 7.13-6.86 (m, 12.5H, $\mathbf{1}^{Bn}$(TMA) + $\mathbf{4}^{Bn}$(TMA) Ph), 3.36 (s, 2H, $\mathbf{1}^{Bn}$(TMA) CH_2), 3.09 (s, 4.5H, **3** OMe), 2.89 (s, 3H, $\mathbf{1}^{Bn}$(TMA) OMe), 2.88 (s, 3H, $\mathbf{4}^{Bn}$(TMA) CH_2), 1.13 (s, 9H, $\mathbf{4}^{Bn}$(TMA) Me), 0.14 (s, br, 4.5H, $\mathbf{4}^{Bn}$(TMA) $AlMe_b$), −0.30 (m, 9H, $\mathbf{1}^{Bn}$(TMA), AlMe), −0.44 (s, br, 18H, $\mathbf{4}^{Bn}$(TMA) $AlMe_t$), −0.61 (s, 9H, **3** AlMe)

^{13}C NMR spectroscopy (100 MHz, benzene-d_6): δ 178.8 ($\mathbf{1}^{Bn}$(TMA) CO), 136.6, 131.4, 130.3, 129.2, 128.6, 128.0, 126.7 ($\mathbf{1}^{Bn}$(TMA) + $\mathbf{4}^{Bn}$(TMA) Ph), 79.5 ($\mathbf{4}^{Bn}$(TMA) CO), 54.3 ($\mathbf{1}^{Bn}$(TMA) OMe), 50.7 ($\mathbf{4}^{Bn}$(TMA) CH_2), 50.4 (**3** OMe), 40.7 ($\mathbf{1}^{Bn}$(TMA) CH_2), 28.0 ($\mathbf{4}^{Bn}$(TMA) Me), −4.5 ($\mathbf{4}^{Bn}$(TMA) $AlMe_b$), −7.0 ($\mathbf{4}^{Bn}$(TMA) $AlMe_t$), −7.5 ($\mathbf{1}^{Bn}$(TMA) AlMe), −11.2 (**3** AlMe)

^{27}Al NMR spectroscopy (104 MHz, benzene-d_6): δ 180.5 (sh, $\mathbf{1}^{Bn}$(TMA)), 153.6 (**3** + $\mathbf{4}^{Bn}$(TMA))

1:3 **1**^{Bn}:TMA

^{1}H NMR spectroscopy (400 MHz, benzene-d_6): δ 7.15-6.84 (m, 5H, **4**^{Bn}(TMA) Ph), 3.06 (s, 3H, **3** OMe), 2.86 (s, 2H, **4**^{Bn}(TMA) CH_2), 1.11 (s, 6H, **4**^{Bn}(TMA) Me), 0.13 (s, 3H, **4**^{Bn}(TMA) $AlMe_b$), −0.42 (s, 12H, **4**^{Bn}(TMA) $AlMe_t$), −0.59 (s, 6H, **3** AlMe)

^{13}C NMR spectroscopy (100 MHz, benzene-d_6): δ 136.7 (**4**^{Bn}(TMA) *i*-Ph), 130.3 (**4**^{Bn}(TMA) *o*-Ph), 128.0 (**4**^{Bn}(TMA) *m*-Ph), 126.7 (**4**^{Bn}(TMA) *p*-Ph), 79.5 (**4**^{Bn}(TMA) CO), 50.7 (**4**^{Bn}(TMA) CH_2), 50.4 **(3** OMe), 28.0 (**4**^{Bn}(TMA) Me), −4.5 (**4**^{Bn}(TMA) $AlMe_b$), −7.0 (**4**^{Bn}(TMA) $AlMe_t$), −11.1 (**3** AlMe)

^{27}Al NMR spectroscopy (104 MHz, benzene-d_6): δ 154.0 (**3** + **4**^{Bn}(TMA))

4.1.1.5 Co-synthesis and characterisation of Me_2AlOMe 3 and $BnMe_2COAlMe_2$(TMA) 4^{Bn}(TMA)

TMA (4.5 ml, 9 mmol, 2.0 M in toluene) was added dropwise to **1**^{Bn} (0.42 ml, 3 mmol) under a N_2 atmosphere at −78 °C and allowed to reach room temperature. The resulting solution was stirred and generated heat. After 2 hours the toluene was removed *in vacuo*. The remaining liquid was stored at 4 °C for 1 day, producing colourless crystals of **4**^{Bn}(TMA) and **3**.

Yield 910 mg (83% wrt **1**^{Bn})

Melting point <30 °C

Elemental analysis satisfactory analysis could not be achieved

^{1}H NMR spectroscopy (400 MHz, benzene-d_6): δ 7.05-6.84 (m, 5H, **4**^{Bn}(TMA) Ph), 3.06 (s, 3H, **3** OMe), 2.86 (s, 2H, **4**^{Bn}(TMA) CH_2), 1.11 (s, 6H, **4**^{Bn}(TMA) Me), 0.13 (s, 3H, **4**^{Bn}(TMA) $AlMe_b$), −0.43 (s, 12H, **4**^{Bn}(TMA) $AlMe_t$), −0.60 (s, 6H, **3** AlMe)

^{13}C NMR spectroscopy (100 MHz, benzene-d_6): δ 136.7 (**4**^{Bn}(TMA) *i*-Ph), 130.3 (**4**^{Bn}(TMA) *o*-Ph), 128.0 (**4**^{Bn}(TMA) *m*-Ph), 126.7 (**4**^{Bn}(TMA) *p*-Ph), 79.5 (**4**^{Bn}(TMA)) CO), 50.7 (**4**^{Bn}(TMA) CH_2), 50.4 **(3** OMe), 28.0 (**4**^{Bn}(TMA) Me), −4.5 (**4**^{Bn}(TMA) $AlMe_b$), −7.0 (**4**^{Bn}(TMA) $AlMe_t$), −11.1 (**3** AlMe)

^{27}Al NMR spectroscopy (104 MHz, benzene-d_6): δ 153.8 (**3** + **4**^{Bn}(TMA))

X-ray crystallography $C_{15}H_{28}Al_2O$, M = 278.33, Orthorhombic, *Pbcm*, a = 7.3370(4), b = 17.3975(8), c = 13.8976(6) Å, α = 90, β = 90, γ = 90°, V = 1773.97(15) Å^3, Z = 4, ρ_{calcd} = 1.042 g cm^{-3}, λ = 1.54184 Å, μ = 1.378 mm^{-1}, T = 180(2) K, 6976 reflections collected, 1327 unique, θ_{max} = 59.031°, R_{int} = 0.0377, $R1$ = 0.0412 (F_{obs} > 4σ(F_{obs})), $wR2$ = 0.1024, S = 1.072, 94 parameters, peak/hole 0.228/−0.282 e Å^{-3}

The above liquid was treated with hexane (1 ml) and the resulting solution stored at −20 °C for 1 day, producing a small quantity of colourless crystals.

Yield 240 mg (22% wrt **1**^{Bn})

Melting point 68-70 °C

Elemental analysis satisfactory analysis could not be achieved

^{1}H NMR spectroscopy (400 MHz, benzene-d_6): δ 7.05-6.84 (m, 5H, **4**^{Bn}(TMA) Ph), 3.05 (s, 0.3H, **3** OMe), 2.86 (s, 2H, **4**^{Bn}(TMA) CH_2), 1.11 (s, 6H, **4**^{Bn}(TMA) Me), 0.12 (s, 3H, **4**^{Bn}(TMA) $AlMe_b$), −0.42 (s, 12H, **4**^{Bn}(TMA) $AlMe_t$), −0.58 (s, 0.6H, **3** AlMe)

^{13}C NMR spectroscopy (100 MHz, benzene-d_6): δ 136.7 (**4**^{Bn}(TMA) *i*-Ph), 130.3 (**4**^{Bn}(TMA) *o*-Ph), 128.1 (**4**^{Bn}(TMA) *m*-Ph), 126.7 (**4**^{Bn}(TMA) *p*-Ph), 79.5 (**4**^{Bn}(TMA) CO), 50.7 (**4**^{Bn}(TMA) CH_2), 28.0 (**4**^{Bn}(TMA) Me), −4.5 (**4**^{Bn}(TMA) $AlMe_b$), −7.0 (**4**^{Bn}(TMA) $AlMe_t$)

^{27}Al NMR spectroscopy (104 MHz, benzene-d_6): δ 155.4 (**3** + **4**^{Bn}(TMA))

4.1.1.6 Synthesis and characterisation of $(BnMe_2COAlMe_2)_2$ $(\mathbf{4}^{Bn})_2$

TMA (4.5 ml, 9 mmol, 2.0 M in toluene) was added dropwise to **1**^{Bn} (0.42 ml, 3 mmol) under a N_2 atmosphere at −78 °C before being allowed to warm to room temperature. The resulting solution was stirred and generated heat. After 2 hours the toluene was removed *in vacuo*. The remaining liquid was treated with Et_2O (3 ml) to give a white precipitate that dissolved upon gentle heating. Colourless prismatic crystals formed as the mixture cooled to room temperature and over a period of 1 day produced a large crop of $(\mathbf{4}^{Bn})_2$.

Yield 417 mg (67% wrt **1**^{Bn})

Melting point 124-126 °C

Elemental analysis calculated for $C_{24}H_{38}Al_2O_2$ (%): C 69.88, H 9.29; found (%): C 68.73, H 9.70

^{1}H NMR spectroscopy (400 MHz, benzene-d_6): δ 7.07-6.92 (m, 5H, Ph), 3.00 (s, 2H, CH_2), 1.22 (s, 6H, Me), −0.28 (s, 6H, AlMe)

^{13}C NMR spectroscopy (100 MHz, benzene-d_6): δ 137.1 (*i*-Ph), 130.4 (*o*-Ph), 128.3 (*m*-Ph), 126.6 (*p*-Ph), 77.6 (CO), 51.2 (CH_2), 28.5 (Me), −5.7 (AlMe)

^{27}Al NMR spectroscopy (194 MHz, benzene-d_6): Only see background signal

X-ray crystallography $C_{24}H_{38}Al_2O_2$, M = 412.50, Monoclinic, $P2_1/n$, a = 11.9568(5), b = 8.7121(4), c = 23.7485(10) Å, α = 90, β = 98.577(2), γ = 90°, V = 2446.19(18) Å^3, Z = 4, ρ_{calcd} = 1.120 g cm^{-3}, λ = 1.54184 Å, μ = 1.182 mm^{-1}, T = 180(2) K, 34306 reflections collected, 4334 unique, θ_{max} = 66.728°, R_{int} = 0.0301, $R1$ = 0.0340 ($F_{obs} > 4\sigma(F_{obs})$), $wR2$ = 0.0944, S = 1.063, 285 parameters, peak/hole 0.281/−0.234 e Å^{-3}

4.1.2 Reactivity of Monoesters with Me_2AlCl

4.1.2.1 Spectroscopic characterisation of 1^{Bn} + Me_2AlCl reaction mixtures

Me_2AlCl (6 ml, 6 mmol, 1.0 M in hexane) was added dropwise under a N_2 atmosphere at −78 °C to methyl phenylacetate **1**^{Bn} (0.28 ml, 2 mmol) and the mixture allowed to warm to room temperature. After stirring for 2 hours the solvent was removed *in vacuo* to give a clear residue which was analysed by NMR spectroscopy.

^{1}H NMR spectroscopy (400 MHz, benzene-d_6): δ 7.09-6.76 (m, 4.5H, **1**^{Bn}(Me_2AlCl) + **4**^{Bn}(Me_2AlCl) Ph), 3.54 (s, 2H, **1**^{Bn}(Me_2AlCl) CH_2), 2.85 (s, 0.08H, **4**^{Bn}(Me_2AlCl) CH_2), 2.78 (s, br, 3H, **1**^{Bn}(Me_2AlCl) OMe), 1.08 (s, 0.22H, **4**^{Bn}(Me_2AlCl) Me), −0.21 (s, 7.9H, **1**^{Bn}(Me_2AlCl) AlMe), −0.27 (s, 0.45H, **4**^{Bn}(Me_2AlCl) AlMe)

^{13}C NMR spectroscopy (100 MHz, benzene-d_6): δ 182.3 (**1**^{Bn}(Me_2AlCl) C=O), 130.2, 129.4, 128.8, 128.1 (**1**^{Bn}(Me_2AlCl) + **4**^{Bn}(Me_2AlCl) Ph), 56.1 (**1**^{Bn}(Me_2AlCl) OMe), 50.4 (**4**^{Bn}(Me_2AlCl) CH_2), 41.1 (**1**^{Bn}(Me_2AlCl) CH_2), 28.0 (**4**^{Bn}(Me_2AlCl) Me), −7.2 (**1**^{Bn}(Me_2AlCl) + **4**^{Bn}(Me_2AlCl) AlMe)

^{27}Al NMR spectroscopy (104 MHz, benzene-d_6): δ 170.5 (**1**^{Bn}(Me_2AlCl)), 127.7 (sh, **4**^{Bn}(Me_2AlCl))

The above method was repeated, but after warming to room temperature the reaction was heated to reflux for 24 hours and then solvent was removed *in vacuo* to give a clear residue which was analysed by NMR spectroscopy.

^{1}H NMR spectroscopy (400 MHz, benzene-d_6): δ 7.09-6.76 (m, 9.7H, **1**^{Bn}(Me_2AlCl) + **4**^{Bn}(Me_2AlCl) + **4**^{Bn}($MeAlCl_2$) Ph), 6.28 (s, 0.01H, **7a** CH=C), 4.80 (s, 0.03H, **7b** C=CH_2), 4.75 (s, 0.03H, **7b** C=CH_2), 3.90-3.48 (m, 2.3H, **1**^{Bn}(Me_2AlCl) CH_2), 3.30-2.96 (m, 4.7H, unassigned), 2.92 (s, 0.8H, **4**^{Bn}($MeAlCl_2$) CH_2), 2.85 (s, 0.8H, **4**^{Bn}(Me_2AlCl) CH_2), 2.66 (s, br, 2.5H, **1**^{Bn}(Me_2AlCl) OMe), 1.71 (s, 0.04H, **7a** Me), 1.68 (s, 0.03H, **7a** Me), 1.40-1.16 (m, 1.7H, unassigned), 1.12 (s, 2.1H, **4**^{Bn}($MeAlCl_2$) Me), 1.08 (s, 2H, **4**^{Bn}(Me_2AlCl) Me), 0.22-−0.20 (m, 3.5H, unassigned AlMe), −0.22 (s, 1.4H, **4**^{Bn}($MeAlCl_2$) AlMe), −0.27 (s, 5.4H, **4**^{Bn}(Me_2AlCl) AlMe), −0.29 (s, 1H, **4**^{Bn}($MeAlCl_2$) AlMe), −0.30-−0.70 (m, 8.9H, unassigned AlMe)

^{13}C NMR spectroscopy (100 MHz, benzene-d_6): δ 183.4 (**1**^{Bn}(Me_2AlCl) C=O), 135.9, 135.4, 130.3, 130.2, 129.5, 128.8, 128.2 (**1**^{Bn}(Me_2AlCl) + **4**^{Bn}(Me_2AlCl) + **4**^{Bn}($MeAlCl_2$) Ph), 83.7 (**4**^{Bn}($MeAlCl_2$) CO), 81.1 (**4**^{Bn}(Me_2AlCl) CO), 56.7 (**1**^{Bn}(Me_2AlCl) OMe), 53.0-51.8 (unassigned OMe), 50.4 (**4**^{Bn}(Me_2AlCl) CH_2), 50.1 (**4**^{Bn}($MeAlCl_2$) CH_2), 41.1 (**1**^{Bn}(Me_2AlCl) CH_2), 28.0 (**4**^{Bn}(Me_2AlCl) + **4**^{Bn}($MeAlCl_2$) Me), −6.1, −6.4, −8.5 (**1**^{Bn}(Me_2AlCl) + **4**^{Bn}(Me_2AlCl) + **4**^{Bn}($MeAlCl_2$) AlMe)

^{27}Al NMR spectroscopy (104 MHz, benzene-d_6): δ 164.8 (**1**^{Bn}(Me_2AlCl)), 124.4 (**4**^{Bn}(Me_2AlCl) + **4**^{Bn}($MeAlCl_2$))

$AlCl_3$ (267 mg, 2 mmol), toluene (1 ml) and TMA (2 ml, 4 mmol, 2.0 M in toluene) were heated to form Me_2AlCl (6 mmol, 2.0 M in toluene). **1**^{Bn} (0.28 ml, 2 mmol) was added dropwise under a N_2 atmosphere at −78 °C and the mixture allowed to warm to room temperature to give a colourless solution. After stirring for 24 hours at the desired temperature an aliquot of the solution was analysed by NMR spectroscopy.

Room temperature reaction

^{1}H NMR spectroscopy (400 MHz, benzene-d_6): δ 7.09-6.76 (m, 5H, **1**^{Bn}(Me_2AlCl) + **4**^{Bn}(Me_2AlCl) Ph), 3.53 (s, br, 2H, **1**^{Bn}(Me_2AlCl) CH_2), 2.86 (s, 0.24H, **4**^{Bn}(Me_2AlCl) CH_2), 2.82 (s, br, 3H, **1**^{Bn}(Me_2AlCl) OMe), 1.08 (s, 0.6H, **4**^{Bn}(Me_2AlCl) Me), 0.01-−0.25 (m, 1.2H,

unassigned AlMe), −0.27 (s, 13.5H, **1**^{Bn}(Me_2AlCl) + **4**^{Bn}(Me_2AlCl) AlMe), −0.34-−0.49 (m, 2.5H, unassigned AlMe)

^{13}C NMR spectroscopy (100 MHz, benzene-d_6): δ 181.5 (**1**^{Bn}(Me_2AlCl) C=O), 130.2, 129.4, 128.8, 128.1 (**1**^{Bn}(Me_2AlCl) + **4**^{Bn}(Me_2AlCl) Ph), 56.2 (**1**^{Bn}(Me_2AlCl) OMe), 50.4 (**4**^{Bn}(Me_2AlCl) CH_2), 41.1 (**1**^{Bn}(Me_2AlCl) CH_2), 27.9 (**4**^{Bn}(Me_2AlCl) Me), −7.0 (**1**^{Bn}(Me_2AlCl) + **4**^{Bn}(Me_2AlCl) AlMe)

^{27}Al NMR spectroscopy (104 MHz, benzene-d_6): δ 174.1 (**1**^{Bn}(Me_2AlCl)), 126.7 (**4**^{Bn}(Me_2AlCl))

50 °C reaction

^{1}H NMR spectroscopy (400 MHz, benzene-d_6): δ 7.09-6.76 (m, 5H, **1**^{Bn}(Me_2AlCl) + **4**^{Bn}(Me_2AlCl) + **4**^{Bn}($MeAlCl_2$) Ph), 3.57 (m, br, 2H, **1**^{Bn}(Me_2AlCl) CH_2), 3.30-2.96 (m, 0.64H, unassigned), 2.93 (s, 0.26H, **4**^{Bn}($MeAlCl_2$) CH_2), 2.86 (s, 0.48H, **4**^{Bn}(Me_2AlCl) CH_2), 2.85-2.62 (m, br, 3H, **1**^{Bn}(Me_2AlCl) OMe), 1.13 (s, 0.49H, **4**^{Bn}($MeAlCl_2$) Me), 1.08 (s, 1.4H, **4**^{Bn}(Me_2AlCl) Me), 0.01-−0.20 (m, 2.2H, unassigned AlMe), −0.22 (s, 0.4H, **4**^{Bn}($MeAlCl_2$) AlMe), −0.27 (s, 9.5H, **4**^{Bn}(Me_2AlCl) + **4**^{Bn}($MeAlCl_2$) AlMe), −0.36 (s, 0.4H, **4**^{Bn}($MeAlCl_2$) AlMe), −0.45 (s, 2.2H, unassigned AlMe)

^{13}C NMR spectroscopy (100 MHz, benzene-d_6): δ 182.5 (**1**^{Bn}(Me_2AlCl) C=O), 135.9, 130.2, 129.5, 128.8, 128.1 (**1**^{Bn}(Me_2AlCl) + **4**^{Bn}(Me_2AlCl) Ph + **4**^{Bn}($MeAlCl_2$) Ph), 83.7 (**4**^{Bn}($MeAlCl_2$) CO), 81.1 (**4**^{Bn}(Me_2AlCl) CO), 56.7, 56.5 (**1**^{Bn}(Me_2AlCl) OMe), 50.4 (**4**^{Bn}(Me_2AlCl) CH_2), 50.1 (**4**^{Bn}($MeAlCl_2$) CH_2), 41.1 (**1**^{Bn}(Me_2AlCl) CH_2), 27.9 (**4**^{Bn}(Me_2AlCl) + **4**^{Bn}($MeAlCl_2$) Me), −6.7 (**1**^{Bn}(Me_2AlCl) + **4**^{Bn}(Me_2AlCl) + **4**^{Bn}($MeAlCl_2$) AlMe)

^{27}Al NMR spectroscopy (104 MHz, benzene-d_6): δ 176.6 (**1**^{Bn}(Me_2AlCl)), 127.2 (**4**^{Bn}(Me_2AlCl) + **4**^{Bn}($MeAlCl_2$))

60 °C reaction

^{1}H NMR spectroscopy (400 MHz, benzene-d_6): δ 7.34-6.76 (m, **1**^{Bn}(Me_2AlCl) + **4**^{Bn}(Me_2AlCl) + **4**^{Bn}($MeAlCl_2$) + **7a** + **7b** Ph), 6.28 (s, 0.01H, **7a** CH=C), 4.80 (m, 0.02H, **7b** C=CH_2), 4.75 (m, 0.02H, **7b** C=CH_2), 3.59 (m, br, 2H, **1**^{Bn}(Me_2AlCl) CH_2), 3.32-2.97

(m, 1.67H, unassigned), 2.93 (s, 0.57H, **4**^{Bn}($MeAlCl_2$) CH_2), 2.86 (s, 0.73H, **4**^{Bn}(Me_2AlCl) CH_2), 2.83-2.58 (m, br, 2.6H, **1**^{Bn}(Me_2AlCl) OMe), 1.72 (s, 0.02H, **7a** Me), 1.70 (s, 0.02H, **7a** Me), 1.55 (s, 0.06H, **7b** Me), 1.38-1.17 (m, 0.75H, unassigned), 1.13 (s, 1.2H, **4**^{Bn}($MeAlCl_2$) Me), 1.08 (s, 1.9H, **4**^{Bn}(Me_2AlCl) Me), 0.01-−0.20 (m, 2.9H, unassigned AlMe), −0.22 (s, 0.55H, **4**^{Bn}($MeAlCl_2$) AlMe), −0.27 (s, 4.1H, **4**^{Bn}(Me_2AlCl) AlMe), −0.30 (s, 9.1H, **1**^{Bn}(Me_2AlCl) + **4**^{Bn}($MeAlCl_2$) AlMe), −0.37 (s, 0.68H, **4**^{Bn}($MeAlCl_2$) AlMe), −0.45 (s, 2.8H, unassigned AlMe)

^{13}C NMR spectroscopy (100 MHz, benzene-d_6): δ 183.5 (**1**^{Bn}(Me_2AlCl) C=O), 135.9, 135.4, 130.2, 129.5, 128.8, (**1**^{Bn}(Me_2AlCl) + **4**^{Bn}(Me_2AlCl) Ph + **4**^{Bn}($MeAlCl_2$) Ph), 83.7 (**4**^{Bn}($MeAlCl_2$) CO), 81.1 (**4**^{Bn}(Me_2AlCl) CO), 56.7 (**1**^{Bn}(Me_2AlCl) OMe), 50.4 (**4**^{Bn}(Me_2AlCl) CH_2), 50.1 (**4**^{Bn}($MeAlCl_2$) CH_2), 41.1 (**1**^{Bn}(Me_2AlCl) CH_2), 27.9 (**4**^{Bn}(Me_2AlCl) + **4**^{Bn}($MeAlCl_2$) Me), −6.1, −6.7 (**1**^{Bn}(Me_2AlCl) + **4**^{Bn}(Me_2AlCl) + **4**^{Bn}($MeAlCl_2$) AlMe)

^{27}Al NMR spectroscopy (104 MHz, benzene-d_6): δ 171.7 (**1**^{Bn}(Me_2AlCl)), 124.2 (**4**^{Bn}(Me_2AlCl) + **4**^{Bn}($MeAlCl_2$))

70 °C reaction

^{1}H NMR spectroscopy (400 MHz, benzene-d_6): δ 7.34-6.76 (m, **1**^{Bn}(Me_2AlCl) + **4**^{Bn}(Me_2AlCl) + **4**^{Bn}($MeAlCl_2$) + **7a** + **7b** Ph), 6.28 (s, 0.02H, **7a** CH=C), 4.80 (m, 0.15H, **7b** C=CH_2), 4.75 (m, 0.15H, **7b** C=CH_2), 3.59 (m, br, 2H, **1**^{Bn}(Me_2AlCl) CH_2), 3.32-2.97 (m, 4H, unassigned), 2.93 (s, 0.81H, **4**^{Bn}($MeAlCl_2$) CH_2), 2.86 (s, 0.91H, **4**^{Bn}(Me_2AlCl) CH_2), 2.83-2.58 (m, br, 2.4H, **1**^{Bn}(Me_2AlCl) OMe), 1.72 (s, 0.12H, **7a** Me), 1.69 (s, 0.11H, **7a** Me), 1.55 (s, 0.51H, **7b** Me), 1.38-1.17 (m, 1.9H, unassigned), 1.13 (s, 1.9H, **4**^{Bn}($MeAlCl_2$) Me), 1.08 (s, 2H, **4**^{Bn}(Me_2AlCl) Me), 0.01-−0.20 (m, 5H, unassigned AlMe), −0.22 (s, 1.3H, **4**^{Bn}($MeAlCl_2$) AlMe), −0.28 (s, 4.1H, **4**^{Bn}(Me_2AlCl) AlMe), −0.32 (s, 10.8H, **1**^{Bn}(Me_2AlCl) + **4**^{Bn}($MeAlCl_2$) AlMe), −0.37 (s, 1.4H, **4**^{Bn}($MeAlCl_2$) AlMe), −0.45 (s, 3.1H, unassigned AlMe)

^{13}C NMR spectroscopy (100 MHz, benzene-d_6): δ 135.9, 135.4, 130.2, 129.5, 128.8, (**1**^{Bn}(Me_2AlCl) + **4**^{Bn}(Me_2AlCl) Ph + **4**^{Bn}($MeAlCl_2$) Ph), 83.7 (**4**^{Bn}($MeAlCl_2$) CO), 81.1 (**4**^{Bn}(Me_2AlCl) CO), 56.7 (**1**^{Bn}(Me_2AlCl) OMe), 50.4 (**4**^{Bn}(Me_2AlCl) CH_2), 50.1

(**4**^{Bn}($MeAlCl_2$) CH_2), 44.6 (**7b** CH_2), 41.1 (**1**^{Bn}(Me_2AlCl) CH_2), 27.9 (**4**^{Bn}(Me_2AlCl) + **4**^{Bn}($MeAlCl_2$) Me), −6.6 (**1**^{Bn}(Me_2AlCl) + **4**^{Bn}(Me_2AlCl) + **4**^{Bn}($MeAlCl_2$) AlMe)

^{27}Al NMR spectroscopy (104 MHz, benzene-d_6): δ 174.2 (**1**^{Bn}(Me_2AlCl)), 124.5 (**4**^{Bn}(Me_2AlCl) + **4**^{Bn}($MeAlCl_2$))

80 °C reaction

^{1}H NMR spectroscopy (400 MHz, benzene-d_6): δ 7.34-6.76 (m, **1**^{Bn}(Me_2AlCl) + **7a** + **7b** Ph), 6.28 (s, 0.21H, **7a** CH=C), 4.80 (m, 0.93H, **7b** C=CH_2), 4.75 (m, 0.93H, **7b** C=CH_2), 3.59, 3.54 (m, br, 2H, **1**^{Bn}(Me_2AlCl) CH_2), 3.32-2.97 (m, 4.7H, unassigned OMe), 3.15 (s, 2.3H, **7b** CH_2), 2.83-2.62 (m, br, 1.8H, **1**^{Bn}(Me_2AlCl) OMe), 2.37 (s, 0.04H, **10** CH_2), 1.72 (s, 0.78H, **7a** Me), 1.69 (s, 0.78H, **7a** Me), 1.55 (s, 0.51H, **7b** Me), 0.84 (s, 0.26H, **10** Me), 0.01-−0.60 (m, 20H, unassigned AlMe), −0.34 (s, 12.7H, **1**^{Bn}(Me_2AlCl) AlMe)

^{13}C NMR spectroscopy (100 MHz, benzene-d_6): δ 144.8, 139.6 (**7b** C), 129.5, 129.4 (**1**^{Bn}(Me_2AlCl) Ph), 128.9 (**7b** Ph), 125.6 (**7a** =CH), 111.8 (**7b** =CH_2), 57.9 (**1**^{Bn}(Me_2AlCl) OMe), 44.6 (**7b** CH_2), 41.5, 41.1 (**1**^{Bn}(Me_2AlCl) CH_2), 26.4 (**7a** Me), 21.6 (**7b** Me), 18.9 (**7a** Me), −6.8 (**1**^{Bn}(Me_2AlCl) AlMe)

^{27}Al NMR spectroscopy (104 MHz, benzene-d_6): δ 177.1 (**1**^{Bn}(Me_2AlCl)), 124.3

Reaction heated to reflux

^{1}H NMR spectroscopy (400 MHz, benzene-d_6): δ 7.34-6.76 (m, **1**^{Bn}(Me_2AlCl) + **7a** + **7b** Ph), 6.28 (s, 0.39H, **7a** CH=C), 4.80 (m, 1H, **7b** C=CH_2), 4.75 (m, 1H, **7b** C=CH_2), 3.58 (s, 0.39H, **1**^{Bn}(Me_2AlCl) CH_2), 3.32-2.97 (m, 3H, unassigned OMe), 3.15 (s, 3.2H, **7b** CH_2), 2.99 (s, 1.1H, unassigned OMe), 2.81-2.72 (m, br, 1.2H, unassigned OMe), 2.37 (s, 0.16H, **10** CH_2), 1.72 (s, 1.5H, **7a** Me), 1.69 (s, 1.5H, **7a** Me), 1.55 (s, 3.2H, **7b** Me), 1.33 (s, 0.44H, **11b** Me), 1.22 (s, 0.56, **11b** Me), 0.91-0.78 (m, 2.2H, **11a** Me), 0.84 (s, 0.82H, **10** Me), 0.11-−0.60 (m, 21H, unassigned AlMe), −0.36 (s, 12.7H, **1**^{Bn}(Me_2AlCl) AlMe)

^{13}C NMR spectroscopy (100 MHz, benzene-d_6): δ 144.8, 139.6 (**7b** C), 134.7, 130.8, 129.4 (**1**^{Bn}(Me_2AlCl) Ph), 128.9 (**7b** Ph), 125.3 (**7a** =CH), 111.9 (**7b** =CH_2), 44.6 (**7b** CH_2), 29.1 (**15** Me), 26.4 (**7a** Me), 21.6 (**7b** Me), 18.9 (**7a** Me)

^{27}Al NMR spectroscopy (104 MHz, benzene-d_6): δ 190.6 (**1**^{Bn}(Me_2AlCl)), 136.1, 94.9, 93.5

Temperature (°C)	**1**^{Bn}(Me_2AlCl)	**4**^{Bn}(Me_2AlCl)	**4**^{Bn}($MeAlCl_2$)	**7a** + **7b**	**10**	**11a** + **11b**
20	90	9	1	0	0	0
50	74	19	7	0	0	0
60	65	21	13	1	0	0
70	54	18	17	11	0	0
80	46	0	0	53	1	0
111	11	0	0	79	4	6

Table 4.2: The proportions (%) of products from the reaction of Me_2AlCl and methyl phenylacetate **1**^{Bn} in a 3:1 ratio in toluene, heated at the stated temperature for 24 hours. The proportions are calculated by integration of the ^{1}H NMR spectra.

0.1 ml of the 3:1 Me_2AlCl:**1**^{Bn} toluene solution was placed in a sealed J Young NMR tube with 0.6 ml of toluene-d_8 and heated to 100 °C for 24 hours.

^{1}H NMR spectroscopy (400 MHz, toluene-d_8): δ 7.34-6.76 (m, **1**^{Bn}(Me_2AlCl) + **7a** + **7b** Ph), 6.22 (m, 1H, **7a** CH=C), 4.77 (m, 4.2H, **7b** C=CH_2), 4.72 (m, 4.2H, **7b** C=CH_2), 3.60, 3.56 (s, 4.5H, **1**^{Bn}(Me_2AlCl) CH_2), 3.27, 3.16, 2.79 (s, 5.9H, **1**^{Bn}(Me_2AlCl) OMe) 3.20, 2.86 (m, 6.6H, unassigned OMe), 3.13 (s, 9H, **7b** CH_2), 2.99 (s, 1.1H, unassigned OMe), 2.81-2.72 (m, br, 1.2H, unassigned OMe), 1.72 (d, J = 1.4 Hz, 3.7H, **7a** Me), 1.68 (d, J = 1.4 Hz, 3.7H, **7a** Me), 1.54 (s, 13.4H, **7b** Me), 0.17 (s, 4.1H, MeH), 0.11-−0.64 (m, 52H, unassigned AlMe), −0.35 (s, 37H, Me_2AlCl AlMe)

^{13}C NMR spectroscopy (100 MHz, toluene-d_8): δ 184.5 (**1**^{Bn}(Me_2AlCl) C=O), 145.1, 139.9 (**7b** C), 134.9 (**7b** C), 129.8 (**1**^{Bn}(Me_2AlCl) Ph), 128.9 (**7b** Ph), 125.6 (**7a** =CH), 112.2 (**7b** =CH_2), 58.9, 57.2 (**1**^{Bn}(Me_2AlCl) OMe), 44.9 (**7b** CH_2), 41.8, 41.5 (**1**^{Bn}(Me_2AlCl) CH_2), 26.8 (**7a** Me), 22.0 (**7b** Me), 19.3 (**7a** Me), −4.3 (MeH), −6.3 (**1**^{Bn}(Me_2AlCl) AlMe)

^{27}Al NMR spectroscopy (104 MHz, toluene-d_8): δ 183.0 (**1**^{Bn}(Me_2AlCl)), 129.9, 99.8, 97.8

4.1.2.2 Synthesis and characterisation of $BnMe_2COAlMe_2(Me_2AlCl)$ $4^{Bn}(Me_2AlCl)$

$AlCl_3$ (267 mg, 2 mmol), toluene (1 ml) and TMA (2 ml, 4 mmol, 2.0 M in toluene) were heated to form Me_2AlCl (6 mmol, 2.0 M in toluene). $\mathbf{1}^{Bn}$ (0.28 ml, 2 mmol) was added dropwise at −78 °C and the mixture allowed to warm to room temperature to give a colourless solution. The solution was heated to 60 °C for 24 hours. Then the toluene was removed *in vacuo* and the solution stored at −27 °C to produce a white solid. The solid was melted by heating to 40 °C and then left at room temperature to produce crystalline blocks.

Yield 40 mg (7% wrt $\mathbf{1}^{Bn}$)

Melting point decomposed to a yellow solid at 120 °C

Elemental analysis satisfactory analysis could not be achieved

^{1}H NMR spectroscopy (400 MHz, benzene-d_6): δ 7.10-6.74 (m, $\mathbf{1}^{Bn}(Me_2AlCl)$ + $\mathbf{4}^{Bn}(Me_2AlCl)$ + $\mathbf{4}^{Bn}(MeAlCl_2)$ Ph), 6.28 (s, 0.01H, **7a** CH=C), 4.80 (m, 0.02H, **7b** C=CH_2), 4.75 (m, 0.02H, **7b** C=CH_2), 3.57 (s, br, 2.8H, $\mathbf{1}^{Bn}(Me_2AlCl)$ CH_2), 2.92 (s, 0.83H, $\mathbf{4}^{Bn}(MeAlCl_2)$ CH_2), 2.85 (s, 2H, $\mathbf{4}^{Bn}(Me_2AlCl)$ CH_2), 2.74-2.60 (m, br, 3.5H, $\mathbf{1}^{Bn}(Me_2AlCl)$ OMe), 1.38-1.17 (m, 2.2H, unassigned), 1.12 (s, 2.6H, $\mathbf{4}^{Bn}(MeAlCl_2)$ Me), 1.07 (s, 6H, $\mathbf{4}^{Bn}(Me_2AlCl)$ Me), −0.22 (s, 1.4H, $\mathbf{4}^{Bn}(MeAlCl_2)$ AlMe), −0.27 (s, 12H, $\mathbf{4}^{Bn}(Me_2AlCl)$ AlMe), −0.28 (s, 1.4H, $\mathbf{4}^{Bn}(MeAlCl_2)$ AlMe), −0.38 (s, 1.4H, $\mathbf{4}^{Bn}(MeAlCl_2)$ AlMe)

^{13}C NMR spectroscopy (100 MHz, benzene-d_6): δ 135.9, 130.2, 129.5, 128.8, 128.2, 127.0($\mathbf{1}^{Bn}(Me_2AlCl)$ + $\mathbf{4}^{Bn}(Me_2AlCl)$ + $\mathbf{4}^{Bn}(MeAlCl_2)$ Ph), 81.1 ($\mathbf{4}^{Bn}(Me_2AlCl)$ CO), 50.4 ($\mathbf{4}^{Bn}(Me_2AlCl)$ CH_2), 50.1 ($\mathbf{4}^{Bn}(MeAlCl_2)$ CH_2), 41.1 ($\mathbf{1}^{Bn}(Me_2AlCl)$ CH_2), 27.9 ($\mathbf{4}^{Bn}(Me_2AlCl)$ + $\mathbf{4}^{Bn}(MeAlCl_2)$ Me), −6.1 ($\mathbf{1}^{Bn}(Me_2AlCl)$ + $\mathbf{4}^{Bn}(Me_2AlCl)$ + $\mathbf{4}^{Bn}(MeAlCl_2)$ AlMe)

^{27}Al NMR spectroscopy (104 MHz, benzene-d_6): δ 163.6 ($\mathbf{4}^{Bn}(Me_2AlCl)$), 126.0 ($\mathbf{4}^{Bn}(MeAlCl_2)$)

X-ray crystallography $C_{14}H_{25}Al_2ClO$, M = 298.75, Orthorhombic, *Pnma*, a = 7.4160(5), b = 14.3329(10) c = 16.3610(11) Å, α = 90, β = 90, γ = 90°, V = 1739.1(2) Å^3, Z = 4, ρ_{calcd} = 1.141 g cm^{-3}, λ = 1.54184 Å, μ = 2.820 mm^{-1}, T = 180(2) K, 9242 reflections collected, 1590 unique, θ_{max} = 66.789°, R_{int} = 0.0955, $R1$ = 0.0725 ($F_{obs} > 4\sigma(F_{obs})$), $wR2$ = 0.2071, S = 1.042, 91 parameters, peak/hole 0.497/−0.390 e Å^{-3}

4.1.3 Reactivity of Monoesters with $MeAlCl_2$

4.1.3.1 Spectroscopic characterisation of 1^{Bn} + $MeAlCl_2$ reaction mixtures

$AlCl_3$ (533 mg, 4 mmol), toluene (2 ml) and TMA (1 ml, 2 mmol, 2.0 M in toluene) were heated to form $MeAlCl_2$ (6 mmol, 2.0 M in toluene). $\mathbf{1}^{Bn}$ (0.28 ml, 2 mmol) was added dropwise at −78 °C to give an orange solution and the resulting mixture allowed to warm to room temperature to give a clear solution. After stirring for 2 hours an aliquot of the solution was analysed by NMR spectroscopy.

^{1}H NMR spectroscopy (400 MHz, benzene-d_6): δ 7.35-6.78 (m, 5H, $\mathbf{1}^{Bn}$($MeAlCl_2$) Ph), 3.62-3.47 (m, br, 2H, $\mathbf{1}^{Bn}$($MeAlCl_2$) CH_2), 3.24-2.59 (m, br, 3H, $\mathbf{1}^{Bn}$($MeAlCl_2$) OMe), −0.02-−0.51 (m, br, 9H, $\mathbf{1}^{Bn}$($MeAlCl_2$) AlMe)

^{13}C NMR spectroscopy (100 MHz, benzene-d_6): δ 184.2 ($\mathbf{1}^{Bn}$($MeAlCl_2$) C=O), 129.5, 128.9, 128.4 ($\mathbf{1}^{Bn}$($MeAlCl_2$) Ph), 57.9, 57.8 ($\mathbf{1}^{Bn}$($MeAlCl_2$) OMe), 41.5, 41.2 ($\mathbf{1}^{Bn}$($MeAlCl_2$) CH_2), −6.7 ($\mathbf{1}^{Bn}$($MeAlCl_2$) + $MeAlCl_2$ AlMe)

^{27}Al NMR spectroscopy (104 MHz, benzene-d_6): δ 178.9, 135.0, 95.8

The above solution was heated to reflux for 24 hours, resulting in a dark brown solution.

^{1}H NMR spectroscopy (400 MHz, benzene-d_6): δ 7.87-6.30 (m, 9H, Ph), 3.94-3.76 (m, 2H, CH_2), 2.50-1.84 (m, 3H, Me)

^{13}C NMR spectroscopy (100 MHz, benzene-d_6): δ 214.8 (C=O), 155.7, 135.0, 134.2, 130.6, 130.2 (Ph), 44.6, 44.5 (CH_2), 22.2, 22.0, 20.9, 19.3 (Me)

The above brown solution was hydrolysed by addition of water. A brown oil was extracted with toluene.

^{1}H NMR spectroscopy (400 MHz, benzene-d_6): δ 7.87-6.30 (m, 9H, Ph), 4.31-3. 07 (m, br, 2H, CH_2), 2.50-1.55 (m, 3H, Me)

^{13}C NMR spectroscopy (100 MHz, benzene-d_6): δ 195.8 (C=O), 143.0, 135.4, 134.5, 132.8, 129.4, 129.0, 128.7, 128.4, 126.5 (Ph), 48.0, 45.2 (CH_2), 21.4, 21.0, 19.3 (Me)

$AlCl_3$ (533 mg, 4 mmol), heptane (2 ml) and TMA (1 ml, 2 mmol, 2.0 M in heptane) were heated to form $MeAlCl_2$ (6 mmol, 2.0 M in heptane). **1**^{Bn} (0.28 ml, 2 mmol) was added dropwise at −78 °C to give an orange solution and the resulting mixture allowed to warm to room temperature to give a yellow solution. The solution was heated to reflux for 24 hours. The solvent was removed *in vacuo* and the liquid was analysed by NMR spectroscopy.

^{1}H NMR spectroscopy (400 MHz, benzene-d_6): δ 7.15-6.70 (m, 5H, **1**^{Bn}($MeAlCl_2$) Ph), 3.72-3.47 (m, br, 2H, **1**^{Bn}($MeAlCl_2$) CH_2), 3.24-2.64 (m, br, 3H, **1**^{Bn}($MeAlCl_2$) OMe), −0.02-−0.55 (m, br, 9H, **1**^{Bn}($MeAlCl_2$) AlMe)

^{13}C NMR spectroscopy (100 MHz, benzene-d_6): δ 184.5 (**1**^{Bn}($MeAlCl_2$) C=O), 129.7, 128.6, 128.3 (**1**^{Bn}($MeAlCl_2$) Ph), 57.6 (**1**^{Bn}($MeAlCl_2$) OMe), 41.4 (**1**^{Bn}($MeAlCl_2$) CH_2), −6.4 (**1**^{Bn}($MeAlCl_2$) + $MeAlCl_2$ AlMe)

^{27}Al NMR spectroscopy (104 MHz, benzene-d_6): δ 134.5, 95.6

4.1.4 Reactivity of Monoesters with $Me_{1.5}AlCl_{1.5}$

4.1.4.1 Spectroscopic characterisation of **1**^{Bn} + $Me_{1.5}AlCl_{1.5}$ reaction mixtures

$AlCl_3$ (400 mg, 3 mmol), toluene (1.5 ml) and TMA (1.5 ml, 3 mmol, 2.0 M in toluene) were heated to form $Me_{1.5}AlCl_{1.5}$ (6 mmol, 2.0 M in toluene). **1**^{Bn} (0.28 ml, 2 mmol) was added dropwise at −78 °C to give an orange solution and the resulting mixture allowed to warm to room temperature to give a clear solution. After stirring for 24 hours at the desired temperature an aliquot of the solution was analysed by NMR spectroscopy.

Room temperature reaction

^{1}H NMR spectroscopy (400 MHz, benzene-d_6): δ 7.35-6.79 (m, **1**^{Bn}($Me_{1.5}AlCl_{1.5}$) Ph), 3.60, 3.51 (m, br, 2H, **1**^{Bn}($Me_{1.5}AlCl_{1.5}$) CH_2), 3.20, 2.80, 2.74, 2.65 (m, br, 3H, **1**^{Bn}($Me_{1.5}AlCl_{1.5}$) Me), −0.09-−0.49 (m, br, 13.5H, **1**^{Bn}($Me_{1.5}AlCl_{1.5}$) AlMe)

^{13}C NMR spectroscopy (100 MHz, benzene-d_6): δ 183.6 (**1**^{Bn}($Me_{1.5}AlCl_{1.5}$) C=O), 129.5, 128.8, 128.2 (**1**^{Bn}($Me_{1.5}AlCl_{1.5}$) Ph), 57.0 (**1**^{Bn}($Me_{1.5}AlCl_{1.5}$) Me), 41.2 (**1**^{Bn}($Me_{1.5}AlCl_{1.5}$) CH_2), −6.4 (**1**^{Bn}($Me_{1.5}AlCl_{1.5}$) + $Me_{1.5}AlCl_{1.5}$ AlMe)

^{27}Al NMR spectroscopy (104 MHz, benzene-d_6): δ 179.1 (**1**^{Bn}($Me_{1.5}AlCl_{1.5}$)), 128.1, 101.2, 95.8

60 °C reaction

^{1}H NMR spectroscopy (400 MHz, benzene-d_6): δ 7.35-6.79 (m, **1**^{Bn}($Me_{1.5}AlCl_{1.5}$) Ph), 3.62, 3.53 (m, br, 2H, **1**^{Bn}($Me_{1.5}AlCl_{1.5}$) CH_2), 3.22, 2.79, 2.68 (m, br, 3H, **1**^{Bn}($Me_{1.5}AlCl_{1.5}$) Me), 0.10-−0.49 (m, br, 13.5H, **1**^{Bn}($Me_{1.5}AlCl_{1.5}$) AlMe)

^{13}C NMR spectroscopy (100 MHz, benzene-d_6): δ 183.6 (**1**^{Bn}($Me_{1.5}AlCl_{1.5}$) C=O), 129.5, 128.9, 128.3 (**1**^{Bn}($Me_{1.5}AlCl_{1.5}$) Ph), 57.1 (**1**^{Bn}($Me_{1.5}AlCl_{1.5}$) Me), 41.3 (**1**^{Bn}($Me_{1.5}AlCl_{1.5}$) CH_2), −6.7 (**1**^{Bn}($Me_{1.5}AlCl_{1.5}$) + $Me_{1.5}AlCl_{1.5}$ AlMe)

^{27}Al NMR spectroscopy (104 MHz, benzene-d_6): δ 176.8 (**1**^{Bn}($Me_{1.5}AlCl_{1.5}$)), 127.6, 101.2, 95.2

70 °C reaction

^{1}H NMR spectroscopy (400 MHz, benzene-d_6): δ 7.35-6.79 (m, **1**^{Bn}($Me_{1.5}AlCl_{1.5}$) + **7b** Ph), 4.80 (s, 0.02H, **7b** C=CH_2), 4.75 (s, 0.02H, **7b** C=CH_2), 3.60, 3.50 (m, br, 2H, **1**^{Bn}($Me_{1.5}AlCl_{1.5}$) CH_2), 3.19, 3.15, 2.74, 2.62 (m, br, 3H, **1**^{Bn}($Me_{1.5}AlCl_{1.5}$) Me), 1.55 (s, 0.06H, **7b** Me), 0.10-−0.49 (m, br, 13.5H, **1**^{Bn}($Me_{1.5}AlCl_{1.5}$) + unassigned AlMe)

^{13}C NMR spectroscopy (100 MHz, benzene-d_6): δ 183.6 (**1**^{Bn}($Me_{1.5}AlCl_{1.5}$) C=O), 129.5, 128.8, 128.2 (**1**^{Bn}($Me_{1.5}AlCl_{1.5}$) Ph), 57.1 (**1**^{Bn}($Me_{1.5}AlCl_{1.5}$) Me), 41.3 (**1**^{Bn}($Me_{1.5}AlCl_{1.5}$) CH_2), −6.9 (**1**^{Bn}($Me_{1.5}AlCl_{1.5}$) + $Me_{1.5}AlCl_{1.5}$ AlMe)

^{27}Al NMR spectroscopy (104 MHz, benzene-d_6): δ 174.7 (**1**^{Bn}($Me_{1.5}AlCl_{1.5}$)), 127.4, 101.1, 95.5

80 °C reaction

^{1}H NMR spectroscopy (400 MHz, benzene-d_6): δ 7.35-6.79 (m, **1**^{Bn}($Me_{1.5}AlCl_{1.5}$) + **7a** + **7b** Ph), 6.27 (s, 0.01H, **7a** CH=C), 4.80 (s, 0.04H, **7b** C=CH_2), 4.75 (s, 0.04H, **7b** C=CH_2), 3.60, 3.52 (m, br, 2H, **1**^{Bn}($Me_{1.5}AlCl_{1.5}$) CH_2), 3.19, 2.76, 2.66 (m, br, 3H, **1**^{Bn}($Me_{1.5}AlCl_{1.5}$) Me), 3.15 (s, 0.09H, **7b** CH_2), 1.72 (s, 0.05H, **7a** Me), 1.69 (s, 0.05H, **7a** Me), 1.55 (s, 0.14H, **7b** Me), 1.22 (s, 0.07H, **11b** Me), 0.87 (m, 0.09H, **11a** Me), 0.84 (s, 0.05H, **10** Me), 0.10-−0.49 (m, br, 12.5H, **1**^{Bn}($Me_{1.5}AlCl_{1.5}$) + unassigned AlMe)

^{13}C NMR spectroscopy (100 MHz, benzene-d_6): δ 183.7 (**1**^{Bn}($Me_{1.5}AlCl_{1.5}$) C=O), 129.5, 128.8, 128.2 (**1**^{Bn}($Me_{1.5}AlCl_{1.5}$) Ph), 58.5, 57.1 (**1**^{Bn}($Me_{1.5}AlCl_{1.5}$) Me), 44.6 (**7b** CH_2), 41.5, 41.3, 41.2 (**1**^{Bn}($Me_{1.5}AlCl_{1.5}$) CH_2), −6.6 (**1**^{Bn}($Me_{1.5}AlCl_{1.5}$) + $Me_{1.5}AlCl_{1.5}$ AlMe)

^{27}Al NMR spectroscopy (104 MHz, benzene-d_6): δ 177.5 (**1**^{Bn}($Me_{1.5}AlCl_{1.5}$)), 129.9, 101.1, 94.9

100 °C reaction

^{1}H NMR spectroscopy (400 MHz, benzene-d_6): δ 7.35-6.79 (m, **1**^{Bn}($Me_{1.5}AlCl_{1.5}$) + **7a** + **7b** Ph), 6.28 (s, 0.03H, **7a** CH=C), 4.80 (s, 0.02H, **7b** C=CH_2), 4.75 (s, 0.02H, **7b** C=CH_2), 3.59, 3.49 (m, br, 2H, **1**^{Bn}($Me_{1.5}AlCl_{1.5}$) CH_2), 3.28 (d, J = 10.8 Hz, 0.11H, **11a** CH), 3.19, 2.79, 2.76, 2.62 (m, br, 3H, **1**^{Bn}($Me_{1.5}AlCl_{1.5}$) Me), 3.14 (s, 0.07H, **7b** CH_2), 2.37 (s, 0.07H, **10** CH_2), 2.33 (m, 0.09H, **11a** CH), 1.72 (s, 0.12H, **7a** Me), 1.69 (s, 0.12H, **7a** Me), 1.55 (s, 0.11H, **7b** Me), 1.22 (s, 0.53H, **11b** Me), 0.87 (m, 0.68H, **11a** Me), 0.84 (s, 0.27H, **10** Me), 0.10-−0.49 (m, br, 15H, **1**^{Bn}($Me_{1.5}AlCl_{1.5}$) + unassigned AlMe)

^{13}C NMR spectroscopy (100 MHz, benzene-d_6): δ 183.8 (**1**^{Bn}($Me_{1.5}AlCl_{1.5}$) C=O), 129.5, 128.8, 128.3 (**1**^{Bn}($Me_{1.5}AlCl_{1.5}$) Ph), 60.5 (**11a** CH), 58.5, 57.4 (**1**^{Bn}($Me_{1.5}AlCl_{1.5}$) Me), 41.5, 41.4 (**1**^{Bn}($Me_{1.5}AlCl_{1.5}$) CH_2), −6.7 (**1**^{Bn}($Me_{1.5}AlCl_{1.5}$) + $Me_{1.5}AlCl_{1.5}$ AlMe)

^{27}Al NMR spectroscopy (104 MHz, benzene-d_6): δ 176.8 (**1**^{Bn}($Me_{1.5}AlCl_{1.5}$)), 129.9, 101.1, 94.7

Reaction heated to reflux

^{1}H NMR spectroscopy (400 MHz, benzene-d_6): δ 7.35-6.79 (m, **1**^{Bn}($Me_{1.5}AlCl_{1.5}$) + **11a** + **11b** Ph), 3.59, 3.49 (m, br, 2H, **1**^{Bn}($Me_{1.5}AlCl_{1.5}$) CH_2), 3.28 (d, J = 10.6 Hz, 0.77H, **11a** CH), 3.18, 3.12, 3.07 (m, br, 3H, **1**^{Bn}($Me_{1.5}AlCl_{1.5}$) Me), 2.76 (s, 1H, **11b** CH_2) 2.36 (s, 0.29H, **10** CH_2), 2.33 (m, 0.6H, **11a** CH), 1.22 (s, 3.1H, **11b** Me), 0.87 (m, 3.4H, **11a** Me), 0.84 (s, 1H, **10** Me), 0.10-−0.49 (m, br, 22H, **1**^{Bn}($Me_{1.5}AlCl_{1.5}$) + unassigned AlMe)

^{13}C NMR spectroscopy (100 MHz, benzene-d_6): δ 145.8, 145.3, 142.0, 138.9, 130.4, 126.1, 125.8 (**11a** + **11b** Ph),129.5, 128.8, 128.3 (**1**^{Bn}($Me_{1.5}AlCl_{1.5}$) Ph), 60.5 (**11a** CH), 59.3 (**1**^{Bn}($Me_{1.5}AlCl_{1.5}$) Me), 51.0 (**11b** CH_2), 41.6 (**1**^{Bn}($Me_{1.5}AlCl_{1.5}$) CH_2), 38.2 (**11b** C_{quat}), 31.7

(**11a** CH), 29.1 (**15** Me), 28.2, 21.7, 20.6, 19.3(**11a** Me), −8.4 (**1**^{Bn}($Me_{1.5}AlCl_{1.5}$) + $Me_{1.5}AlCl_{1.5}$ AlMe)

^{27}Al NMR spectroscopy (104 MHz, benzene-d_6): δ 177.6 (**1**^{Bn}($Me_{1.5}AlCl_{1.5}$)), 132.5, 93.2, 79.9

Temperature (°C)	**1**^{Bn}(Me_2AlCl)	**4**^{Bn}(Me_2AlCl)	**4**^{Bn}($MeAlCl_2$)	**7a** + **7b**	**10**	**11a** + **11b**
20	100	0	0	0	0	0
60	100	0	0	0	0	0
70	96	0	0	3	0	1
80	91	0	0	5	0	4
100	76	0	0	6	2	16
111	44	0	0	0	5	51

Table 4.3: The proportions (%) of products from the reaction of $Me_{1.5}AlCl_{1.5}$ and methyl phenylacetate **1**^{Bn} in a 3:1 ratio in toluene, heated at the stated temperature for 24 hours. The proportions are calculated by integration of the ^{1}H NMR spectra.

4.1.5 Reactions of Phenylacetyl chloride with TMA and Me_2AlCl

4.1.5.1 Spectroscopic characterisation of 13^{Bn} + TMA reaction mixtures

TMA (2 ml, 4 mmol, 2.0 M in toluene) was added dropwise to phenylacetyl chloride **13**^{Bn} (0.26 ml, 2 mmol) under a N_2 atmosphere at −78 °C and allowed to reach room temperature. After stirring for 2 hours at the desired temperature an aliquot of the solution was analysed by NMR spectroscopy.

Room temperature reaction

^{1}H NMR spectroscopy (400 MHz, benzene-d_6): δ 7.14-6.77 (m, 5H, **4**^{Bn}(Me_2AlCl) Ph), 2.85 (s, 2H, **4**^{Bn}(Me_2AlCl) CH_2), 1.08 (s, 6H, **4**^{Bn}(Me_2AlCl) Me), −0.28 (s, 12H, **4**^{Bn}(Me_2AlCl) AlMe)

^{13}C NMR spectroscopy (100 MHz, benzene-d_6): δ 135.9 (**4**^{Bn}(Me_2AlCl) *i*-Ph), 130.2 (**4**^{Bn}(Me_2AlCl) *o*-Ph), 128.2 (**4**^{Bn}(Me_2AlCl) *m*-Ph), 126.9 (**4**^{Bn}(Me_2AlCl) *p*-Ph), 81.1 (**4**^{Bn}(Me_2AlCl) CO), 50.4 (**4**^{Bn}(Me_2AlCl) CH_2), 27.9 (**4**^{Bn}(Me_2AlCl) Me), −6.1 (**4**^{Bn}(Me_2AlCl) AlMe)

^{27}Al NMR spectroscopy (104 MHz, benzene-d_6): δ 169.4 (**4**^{Bn}(Me_2AlCl))

Reaction heated to reflux

^{1}H NMR spectroscopy (400 MHz, benzene-d_6): δ 7.15-6.77 (m, 5H, **4**^{Bn}(Me_2AlCl) Ph), 2.99 (s, 0.2H, (**4**^{Bn})$_2$ CH_2), 2.85 (s, 2H, **4**^{Bn}(Me_2AlCl) CH_2), 1.22 (s, 0.6H, (**4**^{Bn})$_2$ Me), 1.08 (s, 6H, **4**^{Bn}(Me_2AlCl) Me), −0.28 (s, 12.6H, **4**^{Bn}(Me_2AlCl) + (**4**^{Bn})$_2$ AlMe)

^{13}C NMR spectroscopy (100 MHz, benzene-d_6): δ 135.9 (**4**^{Bn}(Me_2AlCl) *i*-Ph), 130.2 (**4**^{Bn}(Me_2AlCl) *o*-Ph), 128.2 (**4**^{Bn}(Me_2AlCl) *m*-Ph), 126.9 (**4**^{Bn}(Me_2AlCl) *p*-Ph), 81.1 (**4**^{Bn}(Me_2AlCl) CO), 77.6 ((**4**^{Bn})$_2$ CO), 51.2 ((**4**^{Bn})$_2$ CH_2), 50.4 (**4**^{Bn}(Me_2AlCl) CH_2), 28.5 ((**4**^{Bn})$_2$ Me), 27.9 (**4**^{Bn}(Me_2AlCl) Me), −6.1 (**4**^{Bn}(Me_2AlCl) AlMe)

^{27}Al NMR spectroscopy (104 MHz, benzene-d_6): δ 173.6 (**4**^{Bn}(Me_2AlCl))

4.1.5.2 Synthesis and characterisation of BnMe$_2$COAlMe$_2$(Me_2AlCl) 4^{Bn}(Me_2AlCl)

TMA (2 ml, 4 mmol, 2.0 M in toluene) was added dropwise to **13**^{Bn} (0.26 ml, 2 mmol) under a N_2 atmosphere at −78 °C and allowed to reach room temperature. After stirring for 2 hours the solution was concentrated *in vacuo* and stored at −27 °C to produce crystalline blocks.

Yield 140 mg (23% wrt **13**^{Bn})

Melting Point 64-66 °C

Elemental analysis calculated for $C_{14}H_{25}Al_2ClO$ (%):C 56.28, H 8.43, Cl 11.87; found (%): C 56.21, H 8.41, Cl 11.82

^{1}H NMR spectroscopy (400 MHz, benzene-d_6): δ 7.08-6.75 (m, 5H, Ph), 2.85 (s, 2H, CH_2), 1.07 (s, 6H, Me), −0.27 (s, 12H, AlMe)

^{13}C NMR spectroscopy (100 MHz, benzene-d_6): δ 135.9 (*i*-Ph), 130.2 (*o*-Ph), 128.2 (*m*-Ph), 126.9 (*p*-Ph), 81.1 (CO), 50.5 (CH_2), 27.9 (Me), −6.1 (br, AlMe)

^{27}Al NMR spectroscopy (104 MHz, benzene-d_6): δ 171.2

X-ray crystallography verified to be **4**^{Bn}(Me_2AlCl) by crystallographic cell check

4.1.5.3 Spectroscopic characterisation of 13^{Bn} + TMA + Me_2AlCl reaction mixtures

$AlCl_3$ (89 mg, 0.67 mmol), toluene (0.33 ml) and TMA (1.67 ml, 3.33 mmol, 2.0 M in toluene) were heated to form $Me_{2.5}AlCl_{0.5}$ (4 mmol, 2.0 M in toluene). **13**^{Bn} (0.26 ml, 2 mmol) was added dropwise under a N_2 atmosphere at −78 °C and allowed to reach room temperature. After stirring for 2 hours at the desired temperature an aliquot of the solution was analysed by NMR spectroscopy.

Room temperature reaction

^{1}H NMR spectroscopy (400 MHz, benzene-d_6): δ 7.15-6.61 (m, **2**^{Bn}($MeAlCl_2$) + **4**^{Bn}(Me_2AlCl) + **4**^{Bn}($MeAlCl_2$) Ph), 3.09 (s, 2H, **2**^{Bn}($MeAlCl_2$) CH_2), 2.93 (s, 0.8H, **4**^{Bn}($MeAlCl_2$) CH_2), 2.86 (s, 1.4H, **4**^{Bn}(Me_2AlCl) CH_2), 1.64 (s, 3H, **2**^{Bn}($MeAlCl_2$) Me), 1.13 (s, 2.3H, **4**^{Bn}($MeAlCl_2$) Me), 1.08 (s, 4.2H, **4**^{Bn}(Me_2AlCl) Me), −0.05 (s, 2H, **2**^{Bn}($MeAlCl_2$) AlMe), −0.22 (s, 1.3H, **4**^{Bn}($MeAlCl_2$) AlMe), −0.28 (s, 16.5H, **4**^{Bn}(Me_2AlCl) + **4**^{Bn}($MeAlCl_2$) AlMe), −0.38 (s, 1.1H, **4**^{Bn}($MeAlCl_2$) AlMe)

^{13}C NMR spectroscopy (100 MHz, benzene-d_6): δ 233.2 (**2**^{Bn}($MeAlCl_2$) C=O), 135.9, 135.4, 130.2, 129.2, 129.1, 128.2, 127.1, 127.0 (**4**^{Bn}(Me_2AlCl) + **4**^{Bn}($MeAlCl_2$) + **2**^{Bn}($MeAlCl_2$) Ph), 83.7 (**4**^{Bn}($MeAlCl_2$) CO), 81.1 (**4**^{Bn}(Me_2AlCl) CO), 51.0 (**2**^{Bn}($MeAlCl_2$) CH_2), 50.4 (**4**^{Bn}(Me_2AlCl) CH_2), 50.1 (**4**^{Bn}($MeAlCl_2$) CH_2), 29.6 (**2**^{Bn}($MeAlCl_2$) Me), 28.0 (**4**^{Bn}(Me_2AlCl) + **4**^{Bn}($MeAlCl_2$) Me), −6.1 (**4**^{Bn}(Me_2AlCl) + **4**^{Bn}($MeAlCl_2$) AlMe)

^{27}Al NMR spectroscopy (104 MHz, benzene-d_6): δ 173.7 (**4**^{Bn}(Me_2AlCl) + **4**^{Bn}($MeAlCl_2$)), 127.6 (**4**^{Bn}($MeAlCl_2$))

50 °C reaction

^{1}H NMR spectroscopy (400 MHz, benzene-d_6): δ 7.15-6.61 (m, **2**^{Bn}($MeAlCl_2$) + **4**^{Bn}(Me_2AlCl) + **4**^{Bn}($MeAlCl_2$) Ph), 3.06 (s, 2H, **2**^{Bn}($MeAlCl_2$) CH_2), 2.93 (s, 5.4H, **4**^{Bn}($MeAlCl_2$) CH_2), 2.86 (s, 3.1H, **4**^{Bn}(Me_2AlCl) CH_2), 1.63 (s, 3H, **2**^{Bn}($MeAlCl_2$) Me), 1.13 (s, 16H, **4**^{Bn}($MeAlCl_2$) Me), 1.08 (s, 10H, **4**^{Bn}(Me_2AlCl) Me), −0.05 (s, 2.8H, **2**^{Bn}($MeAlCl_2$)

AlMe), −0.22 (s, 8H, **4**^{Bn}($MeAlCl_2$) AlMe), −0.28 (s, 20H, **4**^{Bn}(Me_2AlCl) AlMe) −0.29 (s, 7H, **4**^{Bn}($MeAlCl_2$) AlMe), −0.38 (s, 7H, **4**^{Bn}($MeAlCl_2$) AlMe)

^{13}C NMR spectroscopy (100 MHz, benzene-d_6): δ 233.2 (**2**^{Bn}($MeAlCl_2$) C=O), 135.9, 135.4, 130.2, 129.2, 129.1, 128.2, 127.1, 127.0 (**4**^{Bn}(Me_2AlCl) + **4**^{Bn}($MeAlCl_2$) + **2**^{Bn}($MeAlCl_2$) Ph), 83.7 (**4**^{Bn}($MeAlCl_2$) CO), 81.1 (**4**^{Bn}(Me_2AlCl) CO), 51.0 (**2**^{Bn}($MeAlCl_2$) CH_2), 50.4 (**4**^{Bn}(Me_2AlCl) CH_2), 50.1 (**4**^{Bn}($MeAlCl_2$) CH_2), 29.6 (**2**^{Bn}($MeAlCl_2$) Me), 27.9 (**4**^{Bn}(Me_2AlCl) + **4**^{Bn}($MeAlCl_2$) Me), −6.3 (**4**^{Bn}(Me_2AlCl) + **4**^{Bn}($MeAlCl_2$) AlMe)

^{27}Al NMR spectroscopy (104 MHz, benzene-d_6): δ 174.7 (**4**^{Bn}(Me_2AlCl) + **4**^{Bn}($MeAlCl_2$)), 128.2 (**4**^{Bn}($MeAlCl_2$))

60 °C reaction

^{1}H NMR spectroscopy (400 MHz, benzene-d_6): δ 7.15-6.61 (m, **2**^{Bn}($MeAlCl_2$) + **4**^{Bn}(Me_2AlCl) + **4**^{Bn}($MeAlCl_2$) Ph), 3.04 (s, 0.3H, **2**^{Bn}($MeAlCl_2$) CH_2), 2.92 (s, 2H, **4**^{Bn}($MeAlCl_2$) CH_2), 2.85 (s, 1H, **4**^{Bn}(Me_2AlCl) CH_2), 1.61 (s, 0.4H, **2**^{Bn}($MeAlCl_2$) Me), 1.13 (s, 6H, **4**^{Bn}($MeAlCl_2$) Me), 1.08 (s, 3H, **4**^{Bn}(Me_2AlCl) Me), −0.04 (s, 0.4H, **2**^{Bn}($MeAlCl_2$) AlMe), −0.22 (s, 3H, **4**^{Bn}($MeAlCl_2$) AlMe), −0.28 (s, 6H, **4**^{Bn}(Me_2AlCl) AlMe) −0.29 (s, 3H, **4**^{Bn}($MeAlCl_2$) AlMe), −0.38 (s, 3H, **4**^{Bn}($MeAlCl_2$) AlMe)

^{13}C NMR spectroscopy (100 MHz, benzene-d_6): δ 233.2 (**2**^{Bn}($MeAlCl_2$) C=O), 135.9, 135.4, 130.2, 129.2, 129.1, 128.2, 127.1, 127.0 (**4**^{Bn}(Me_2AlCl) + **4**^{Bn}($MeAlCl_2$) + **2**^{Bn}($MeAlCl_2$) Ph), 83.7 (**4**^{Bn}($MeAlCl_2$) CO), 81.1 (**4**^{Bn}(Me_2AlCl) CO), 51.0 (**2**^{Bn}($MeAlCl_2$) CH_2), 50.4 (**4**^{Bn}(Me_2AlCl) CH_2), 50.1 (**4**^{Bn}($MeAlCl_2$) CH_2), 29.6 (**2**^{Bn}($MeAlCl_2$) Me), 27.9 (**4**^{Bn}(Me_2AlCl) + **4**^{Bn}($MeAlCl_2$) Me), −6.4 (**4**^{Bn}(Me_2AlCl) + **4**^{Bn}($MeAlCl_2$) AlMe)

^{27}Al NMR spectroscopy (104 MHz, benzene-d_6): δ 175.5 (**4**^{Bn}(Me_2AlCl) + **4**^{Bn}($MeAlCl_2$)), 129.4 (**4**^{Bn}($MeAlCl_2$))

70 °C reaction

^{1}H NMR spectroscopy (400 MHz, benzene-d_6): δ 7.15-6.61 (m, **4**^{Bn}(Me_2AlCl) + **4**^{Bn}($MeAlCl_2$) + **7b** Ph), 4.80 (s, 0.03H, **7b** C=CH_2), 4.75 (s, 0.03H, **7b** C=CH_2), 2.92 (s, 2H, **4**^{Bn}($MeAlCl_2$) CH_2), 2.85 (s, 0.7H, **4**^{Bn}(Me_2AlCl) CH_2), 1.55 (s, 0.1H, **7b** Me), 1.13 (s, 6H, **4**^{Bn}($MeAlCl_2$) Me), 1.08 (s, 2.1H, **4**^{Bn}(Me_2AlCl) Me), −0.23 (s, 3H, **4**^{Bn}($MeAlCl_2$)

AlMe), −0.28 (s, 5H, **4**^{Bn}(Me_2AlCl) AlMe) −0.29 (s, 3H, **4**^{Bn}($MeAlCl_2$) AlMe), −0.38 (s, 3H, **4**^{Bn}($MeAlCl_2$) AlMe)

^{13}C NMR spectroscopy (100 MHz, benzene-d_6): δ 135.9, 135.4, 135.0, 130.2, 128.2, 127.1, 127.0, 111.8 (**4**^{Bn}(Me_2AlCl) + **4**^{Bn}($MeAlCl_2$) + **7b** Ph), 111.8 (**7b** =CH_2), 83.7 (**4**^{Bn}($MeAlCl_2$) CO), 81.1 (**4**^{Bn}(Me_2AlCl) CO), 50.4 (**4**^{Bn}(Me_2AlCl) CH_2), 50.1 (**4**^{Bn}($MeAlCl_2$) CH_2), 44.6 (**7b** CH_2), 27.9 (**4**^{Bn}(Me_2AlCl) + **4**^{Bn}($MeAlCl_2$) Me), −6.4 (**4**^{Bn}(Me_2AlCl) + **4**^{Bn}($MeAlCl_2$) AlMe)

^{27}Al NMR spectroscopy (104 MHz, benzene-d_6): δ 174.1 (**4**^{Bn}(Me_2AlCl) + **4**^{Bn}($MeAlCl_2$)), 131.0 (**4**^{Bn}($MeAlCl_2$))

80 °C reaction

^{1}H NMR spectroscopy (400 MHz, benzene-d_6): δ 7.15-6.61 (m, **4**^{Bn}($MeAlCl_2$) + **7a** + **7b** Ph), 6.27 (s, 0.1H, **7a**), 4.80 (s, 0.5H, **7b** C=CH_2), 4.75 (s, 0.5H, **7b** C=CH_2), 3.15 (s, 1.2H, **7b** CH_2), 2.92 (s, 2H, **4**^{Bn}($MeAlCl_2$) CH_2), 1.71 (s, 0.4H, **7a** Me), 1.69 (s, 0.4H, **7a** Me), 1.55 (s, 1.5H, **7b** Me), 1.13 (s, 6H, **4**^{Bn}($MeAlCl_2$) Me), −0.22 (s, 3H, **4**^{Bn}($MeAlCl_2$) AlMe), −0.27 (s, 3H, **4**^{Bn}($MeAlCl_2$) AlMe), −0.35 (s, 3H, **4**^{Bn}($MeAlCl_2$) AlMe)

^{13}C NMR spectroscopy (100 MHz, benzene-d_6): δ 135.9, 135.4, 135.0, 130.2, 128.2, 127.1, 127.0 (**4**^{Bn}($MeAlCl_2$) + **7a** + **7b** Ph), 111.8 (**7b** =CH_2), 83.7 (**4**^{Bn}($MeAlCl_2$) CO), 50.1 (**4**^{Bn}($MeAlCl_2$) CH_2), 44.6 (**7b** CH_2), 27.9 (**4**^{Bn}($MeAlCl_2$) Me), −6.4 (**4**^{Bn}(Me_2AlCl) + **4**^{Bn}($MeAlCl_2$) AlMe)

^{27}Al NMR spectroscopy (104 MHz, benzene-d_6): δ 180.0 (**4**^{Bn}(Me_2AlCl) + **4**^{Bn}($MeAlCl_2$)), 133.3 (**4**^{Bn}($MeAlCl_2$))

Reaction heated to reflux

^{1}H NMR spectroscopy (400 MHz, benzene-d_6): δ 7.15-6.61 (m, **7a** + **7b** + **11a** + **11b** Ph), 6.27 (s, 0.2H, **7a**), 4.80 (s, 0.2H, **7b** C=CH_2), 4.75 (s, 0.2H, **7b** C=CH_2), 3.46 (d, J = 8.5 Hz, 1H, **11a** CH), 3.28 (d, J = 10.8 Hz, 1.8H, **11a** CH), 3.15 (s, 0.4H, **7b** CH_2), 2.96-2.70 (m, 11H, **11b** CH_2), 1.71 (s, 0.8H, **7a** Me), 1.69 (s, 0.8H, **7a** Me), 1.55 (s, 1H, **7b** Me), 1.33 (s, 5.5H, **11b** Me), 1.22 (s, 12H, **11b** Me), 0.95-0.60 (m, 38H, **11a** Me), −0.10-−0.48 (m, 85H, unassigned AlMe)

^{13}C NMR spectroscopy (100 MHz, benzene-d_6): δ 145.8, 143.0, 139.2, 138.9, 130.8, 130.5, 130.2, 128.2, 127.1, 127.0, 124.0, 122.7 (**7a** + **7b** + **11a** + **11b** Ph), 60.5, 54.3 (**11a** CH), 51.8, 51.0, 48.1, 47.8, 47.2, 46.7, 44.8 (**11b** CH_2), 31.6, 30.3, 29.1, 28.2, 27.3 (**11a** + **11b** Me), −7.0 (unassigned AlMe)

^{27}Al NMR spectroscopy (104 MHz, benzene-d_6): δ 170.4, 131.7, 92.6, 79.9

0.1 ml of the **12** + TMA + Me_2AlCl toluene solution was placed in a sealed J Young NMR tube with 0.6 ml of toluene-d_8 and heated to 100 °C for 2 hours.

^{1}H NMR spectroscopy (400 MHz, toluene-d_8): δ 7.15-6.95 (m, **7a** + **7b** + **11a** + **11b** Ph), 6.23 (s, 1H, **7a**), 4.77 (s, 3.3H, **7b** C=CH_2), 4.72 (s, 3.3H, **7b** C=CH_2), 3.40 (d, J = 8.5 Hz 0.3H, **11a** CH), 3.23 (d, J = 10.8 Hz, 0.8H, **11a** CH), 3.13 (s, 7H, **7b** CH_2), 2.72 (s, 2.7H, **11b** CH_2), 1.72 (s, 3.6H, **7a** Me), 1.68 (s, 3.6H, **7a** Me), 1.54 (s, 10.5H, **7b** Me), 1.30 (s, 3.7H, **11b** Me), 1.19 (s, 7.7H, **11b** Me), 0.89-0.77 (m, 15H, **11a** + **11b** Me), 0.17 (s, 8.3H, MeH), −0.10-−0.45 (m, 100H, unassigned AlMe)

^{13}C NMR spectroscopy (100 MHz, toluene-d_8): δ 145.1, 139.9, 139.2, 131.1, 130.7, 130.2, 128.2, 127.1, 127.0, 124.9, 123.0 (**7a** + **7b** + **11a** + **11b** Ph), 112.2 (**7b** =CH_2), 52.1, 51.4, 48.4, 47.6, 47.1, 45.1, 38.7, 38.5 (**11a** + **11b** CH_2), 44.9 (**7b** CH_2), 32.0, 31.8, 30.4, 29.4, 28.6, 27.8, 17.1 (**11a** + **11b** Me), −4.3 (MeH), −6.6 (unassigned AlMe)

^{27}Al NMR spectroscopy (104 MHz, toluene-d_8): δ 183.8, 136.6, 93.0, 80.0

4.2 Reactivity of Tetraesters with Methylaluminium Reagents

4.2.1 Synthesis of Tetraesters

4.2.1.1 Synthesis and characterisation of C{$CH_2OC(O)C_5H_{11}$}$_4$ 14^{Pent}

Hexanoyl chloride **13**^{Pent} (7.0 ml, 50.1 mmol) was added to pentaerythritol (1.36 g, 10.0 mmol) under a N_2 atmosphere and heated to reflux for 2 hours. This resulted in the release of gas and the formation of a pale yellow solution. The solution was removed *in vacuo* at 100 °C for 1 hour to remove any excess hexanoyl chloride. This resulted in a pale yellow liquid.

Yield 4.92 g, 4.95 ml (93% wrt pentaerythritol)

Elemental analysis calculated for $C_{29}H_{52}O_8$ (%): C 65.88, H 9.91; found (%): C 65.71, H 9.80

^{1}H NMR spectroscopy (400 MHz, benzene-d_6): δ 4.26 (s, 8H, CH_2O), 2.07 (t, J = 7.4 Hz, 8H, CH_2), 1.52 (quint, J = 7.4 Hz, 8H, CH_2), 1.22-1.07 (m, 16H, CH_2), 0.82 (t, J = 6.9 Hz, 12H, Me)

^{13}C NMR spectroscopy (100 MHz, benzene-d_6): δ 172.3 (C=O), 61.8 (CH_2O), 42.2 (C_{quat}), 33.7, 31.1, 24.5, 22.3 (CH_2), 13.7 (Me)

4.2.1.2 Synthesis and characterisation of C{$CH_2OC(O)CH_2Ph$}$_4$ 14^{Bn}

Phenylacetyl chloride **13**^{Bn} (5.8 ml, 43.9 mmol) was added to pentaerythritol (1.36 g, 10.0 mmol) under a N_2 atmosphere and heated to 140 °C for 2 hours. This resulted in the release of gas and the formation of a yellow solution. Toluene (8 ml) was added and then the solution cooled to −78 °C. Ethanol (40 ml) was added slowly, resulting in the precipitation of a white solid which was removed by filtration and washed with cold ethanol (20 ml).

Yield 4.73 g (78% wrt pentaerythritol)

^{1}H NMR spectroscopy (400 MHz, benzene-d_6): δ 7.12-7.00 (m, 20H, Ph), 3.89 (s, 8H, CH_2O), 3.20 (s, 8H, CH_2)

^{13}C NMR spectroscopy (100 MHz, benzene-d_6): δ 169.9 (C=O), 133.9 (*i*-Ph), 129.2 (*o*-Ph), 128.5 (*m*-Ph), 127.0 (*p*-Ph), 62.0 (CH_2O), 42.2 (C_{quat}), 40.8 (CH_2)

Elemental analysis calculated for $C_{37}H_{36}O_8$ (%): C 73.01, H 5.96; found (%): C 72.99, H 5.96

Crude **14**^{Bn} (100 mg) was recrystallised from ethanol, with storage at 4 °C producing crystalline colourless needles.

Yield 52 mg

^{1}H NMR spectroscopy (400 MHz, benzene-d_6): δ 7.12-7.00 (m, 20H, Ph), 3.89 (s, 8H, CH_2O), 3.20 (s, 8H, CH_2)

^{13}C NMR spectroscopy (100 MHz, benzene-d_6): δ 169.9 (C=O), 133.9 (*i*-Ph), 129.2 (*o*-Ph), 128.5 (*m*-Ph), 127.0 (*p*-Ph), 62.0 (CH_2O), 42.2 (C_{quat}), 40.8 (CH_2)

Melting Point 72-73 °C

X-ray crystallography $C_{37}H_{36}O_8$, M = 608.66, Monoclinic, $P2_1/c$, a = 17.1214(4), b = 8.0307(2), c = 24.0020(5) Å, α = 90, β = 102.2150(10), γ = 90°, V = 3225.48(13) Å^3, Z = 4, ρ_{calcd} = 1.253 g cm^{-3}, λ = 0.71073 Å, μ = 0.717 mm^{-1}, T = 180(2) K, 33305 reflections collected, 5714 unique, θ_{max} = 66.703°, R_{int} = 0.0823, $R1$ = 0.0388 ($F_{obs} > 4\sigma(F_{obs})$), $wR2$ = 0.0984, S = 1.050, 497 parameters, peak/hole 0.206/−0.178 e Å^{-3}

4.2.2 Reactivity of Tetraesters with TMA

4.2.2.1 Spectroscopic characterisation of 14^{Pent} + TMA reaction mixtures

TMA (0.25, 0.5, 1.0, 2.0 or 3.0 ml, 0.5, 1.0, 2.0, 4.0 or 6.0 mmol, 2.0 M in toluene) was added dropwise to **14**^{Pent} (0.27 ml, 0.5 mmol) under a N_2 atmosphere at −78 °C and allowed to reach room temperature. An aliquot of the solution was analysed by NMR spectroscopy.

1:1 **14**^{Pent}:TMA

^{1}H NMR spectroscopy (400 MHz, benzene-d_6): δ 4.14 (s, 8H, **14**^{Pent}(TMA) CH_2O), 2.12 (t, J = 7.5 Hz, 8H, **14**^{Pent}(TMA) CH_2), 1.50 (quint, J = 7.5 Hz, 8H, **14**^{Pent}(TMA) CH_2), 1.22-1.06 (m, 16H, **14**^{Pent}(TMA) CH_2), 0.82 (t, J = 7.1 Hz, 12H, **14**^{Pent}(TMA) Me), −0.25 (s, 7.4H, **14**^{Pent}(TMA) AlMe)

^{13}C NMR spectroscopy (100 MHz, benzene-d_6): δ 174.1 (**14**^{Pent}(TMA) C=O), 62.4 (**14**^{Pent}(TMA) CH_2O), 42.1 (**14**^{Pent}(TMA) C_{quat}), 33.8, 31.1, 24.4, 22.2 (**14**^{Pent}(TMA) CH_2), 13.6 (**14**^{Pent}(TMA) Me), −7.5 (**14**^{Pent}(TMA) AlMe)

^{27}Al NMR spectroscopy (104 MHz, benzene-d_6): Only background signal

1:2 **14**^{Pent}:TMA

^{1}H NMR spectroscopy (400 MHz, benzene-d_6): δ 4.02 (s, 8H, **14**^{Pent}(TMA) CH_2O), 2.18 (t, J = 7.6 Hz, 8H, **14**^{Pent}(TMA) CH_2), 1.48 (quint, J = 7.5 Hz, 8H, **14**^{Pent}(TMA) CH_2), 1.23-1.05 (m, 16H, **14**^{Pent}(TMA) CH_2), 0.83 (t, J = 7.5 Hz, 12H, **14**^{Pent}(TMA) Me), −0.28 (s, 17.5H, **14**^{Pent}(TMA) AlMe)

^{13}C NMR spectroscopy (100 MHz, benzene-d_6): δ 177.0 (**14**^{Pent}(TMA) C=O), 63.6 (**14**^{Pent}(TMA) CH_2O), 41.9 (**14**^{Pent}(TMA) C_{quat}), 34.0, 31.0, 24.4, 22.1 (**14**^{Pent}(TMA) CH_2), 13.6 (**14**^{Pent}(TMA) Me), −7.5 (**14**^{Pent}(TMA) AlMe)

^{27}Al NMR spectroscopy (104 MHz, benzene-d_6): Only see background signal

1:4 **14**^{Pent}:TMA

^{1}H NMR spectroscopy (400 MHz, benzene-d_6): δ 4.30-2.82 (m 7.8H, **15** CH_2O), 2.31-2.18 (m, 8H, **14**^{Pent}(TMA) CH_2), 1.57-1.39 (m, 8H, **14**^{Pent}(TMA) + **4**^{Pent}(TMA) CH_2), 1.26-1.05 (m, 21H, **14**^{Pent}(TMA) CH_2 + **4**^{Pent}(TMA) CH_2 + Me), 0.88-0.81 (m, 12H, **14**^{Pent}(TMA) + **4**^{Pent}(TMA) Me), 0.10 (s, br, 1.3H, **4**^{Pent}(TMA) $AlMe_b$), −0.30 (s, 18H, **14**^{Pent}(TMA) AlMe), −0.46 (s, 9.6H, **4**^{Pent}(TMA) $AlMe_t$)

^{13}C NMR spectroscopy (100 MHz, benzene-d_6): δ 175.8, 175.3 (**14**^{Pent}(TMA) C=O), 79.2 (**4**^{Pent}(TMA) CO), 62.6, 61.5 (**14**^{Pent}(TMA) CH_2O), 44.2, 32.0, 24.3, 22.6, (**4**^{Pent}(TMA) CH_2), 42.0 (**14**^{Pent}(TMA) C_{quat}), 33.9, 31.1, 31.0, 24.5, 24.4, 22.2 (**14**^{Pent}(TMA) CH_2), 28.4, 13.8 (**4**^{Pent}(TMA) Me), 13.6 (**14**^{Pent}(TMA) Me), −4.5 (**4**^{Pent}(TMA) $AlMe_b$), −7.5 (**4**^{Pent}(TMA) $AlMe_t$), −10.7, −10.8 (**14**^{Pent}(TMA) AlMe)

^{27}Al NMR spectroscopy (104 MHz, benzene-d_6): δ 158.4 (**4**^{Pent}(TMA))

1:8 **14**^{Pent}:TMA

^{1}H NMR spectroscopy (400 MHz, benzene-d_6): δ 4.85-2.90 (m, 8H, **15** CH_2O), 1.44 (m, 8H, **4**^{Pent}(TMA) CH_2), 1.29-1.03 (m, 48H, **4**^{Pent}(TMA) CH_2 + Me), 0.86 (t, J = 7.2 Hz, 12H, **4**^{Pent}(TMA) Me), 0.10 (s, br, 8H, **4**^{Pent}(TMA) $AlMe_b$), −0.27 (s, 12.2H, unassigned AlMe), −0.45 (s, 40H, **4**^{Pent}(TMA) $AlMe_t$)

^{13}C NMR spectroscopy (100 MHz, benzene-d_6): δ 79.2 (**4**^{Pent}(TMA) CO), 44.3, 32.0, 24.3, 22.6 (**4**^{Pent}(TMA) CH_2), 28.4, 13.6 (**4**^{Pent}(TMA) Me), −4.5 (**4**^{Pent}(TMA) $AlMe_b$), −7.5 (**4**^{Pent}(TMA) $AlMe_t$)

^{27}Al NMR spectroscopy (104 MHz, benzene-d_6): δ 157.7 (**4**^{Pent}(TMA))

1:12 **14**^{Pent}:TMA

^{1}H NMR spectroscopy (400 MHz, benzene-d_6): δ 5.05-2.90 (m, 8H, **15** CH_2O), 1.44 (m, 8H, **4**^{Pent}(TMA) CH_2), 1.29-1.03 (m, 48H, **4**^{Pent}(TMA) CH_2 + Me), 0.87 (t, J = 7.2 Hz, 12H, **4**^{Pent}(TMA) Me), 0.10 (s, br, 10H, **4**^{Pent}(TMA) $AlMe_b$), −0.35 (s, 23H, TMA AlMe), −0.45 (s, 44H, **4**^{Pent}(TMA) $AlMe_t$)

^{13}C NMR spectroscopy (100 MHz, benzene-d_6): δ 79.2 (**4**^{Pent}(TMA) CO), 44.3, 32.0, 24.3, 22.6 (**4**^{Pent}(TMA) CH_2), 28.4, 13.8 (**4**^{Pent}(TMA) Me), −4.5 (**4**^{Pent}(TMA) $AlMe_b$), −7.5 (**4**^{Pent}(TMA) $AlMe_t$)

^{27}Al NMR spectroscopy (104 MHz, benzene-d_6): δ 156.0 (**4**^{Pent}(TMA))

4.2.2.2 Synthesis and characterisation of 14^{Pent}(TMA)$_4$

TMA (0.5 ml, 1.0 mmol, 2.0 M in toluene) was added dropwise to **14**^{Pent} (0.27 ml, 0.5 mmol) under a N_2 atmosphere at −78 °C and allowed to reach room temperature. Once the solution reached room temperature it was stored at −27 °C for 1 day to produce colourless crystalline needles. These repeatedly proved impossible to isolate because of their reactivity, preventing the measurement of yield, melting point, NMR spectroscopy and elemental analysis.

X-ray crystallography data $C_{41}H_{88}Al_4O_8$, M = 817.02, Monoclinic, $C2/c$, a = 31.5253(9), b = 8.2240(2) c = 21.0190(6) Å, α = 90, β = 93.346(2), γ = 90°, V = 5440.2(3) Å^3, Z = 4, ρ_{calcd} = 0.998 g cm^{-3}, λ = 0.71073 Å, μ = 1.107 mm^{-1}, T = 180(2) K. 27866 reflections collected, 4809 unique, θ_{max} = 66.607°, R_{int} = 0.0979, $R1$ = 0.0592 ($F_{obs} > 4\sigma(F_{obs})$), $wR2$ = 0.1595, S = 1.021, 248 parameters, peak/hole 0.366/−0.209 e Å^{-3}

4.2.2.3 Spectroscopic characterisation of 14^{Bn} + TMA reaction mixtures

TMA (0.5, 1.0, 2.0 or 3.0 ml, 1.0, 2.0, 4.0 or 6.0 mmol, 2.0 M in toluene) was added dropwise to **14**^{Bn} (304 mg, 0.5 mmol) in toluene (4 ml) under a N_2 atmosphere at −78 °C and allowed to reach room temperature. An aliquot of the solution was analysed by NMR spectroscopy.

1:2 **14**^{Bn}:TMA

^{1}H NMR spectroscopy (400 MHz, benzene-d_6): δ 7.35-6.78 (m, **4**^{Bn}(TMA) + **14**^{Bn}(TMA) Ph), 4.28-3.45 (m, 8H, **14**^{Bn}(TMA) + **15** CH_2O), 3.40-3.18 (m, 7.5H, **14**^{Bn}(TMA) CH_2),

2.86 (s, 0.66H, **4**^{Bn}(TMA) CH_2), 1.11 (s, 2H, **4**^{Bn}(TMA) Me), 0.13 (s, br, 1H, **4**^{Bn}(TMA) $AlMe_b$), −0.17 (s, 4.5H, **14**^{Bn}(TMA)), −0.20-−0.63 (m, 4.7H, unassigned AlMe), −0.42 (s, br, 3.8H, **4**^{Bn}(TMA) $AlMe_t$)

^{13}C NMR spectroscopy (100 MHz, benzene-d_6): δ 170.2 (**14**^{Bn}(TMA)) 133.7, 130.3, 129.2, 128.5 (**4**^{Bn}(TMA) + **14**^{Bn}(TMA) Ph), 77.6 (**4**^{Bn}(TMA) CO), 62.0, 60.9 (CH_2O), 42.2, 40.8 (**14**^{Bn}(TMA) CH_2), 28.3 (**4**^{Bn}(TMA) Me), −8.4 (**14**^{Bn}(TMA))

^{27}Al NMR spectroscopy (104 MHz, benzene-d_6): δ 157.8 (**4**^{Bn}(TMA))

1:4 **14**^{Bn}:TMA

^{1}H NMR spectroscopy (400 MHz, benzene-d_6): δ 7.35-6.78 (m, **4**^{Bn}(TMA) + **14**^{Bn}(TMA) Ph), 4.21-3.38 (m, 8H, **14**^{Bn}(TMA) + **15** CH_2O), 3.37-3.18 (m, 6.3H, **14**^{Bn}(TMA) CH_2), 2.86 (s, 1.4H, **4**^{Bn}(TMA) CH_2), 1.11 (s, 4.2H, **4**^{Bn}(TMA) Me), 0.12 (s, br, 2.1H, **4**^{Bn}(TMA) $AlMe_b$), −0.20 (s, 15H, **14**^{Bn}(TMA)), −0.20-−0.63 (m, 9.7H, unassigned AlMe), −0.42 (s, br, 7.4H, **4**^{Bn}(TMA) $AlMe_t$)

^{13}C NMR spectroscopy (100 MHz, benzene-d_6): δ 136.7, 130.3, 129.1, 128.7, 128.6, 126.7 (**4**^{Bn}(TMA) + **14**^{Bn}(TMA) Ph), 79.5 (**4**^{Bn}(TMA) CO), 50.8 (**4**^{Bn}(TMA) CH_2), 40.9, 40.8 (**14**^{Bn}(TMA) CH_2), 28.0 (**4**^{Bn}(TMA) Me), −7.3 (**4**^{Bn}(TMA) $AlMe_t$)

^{27}Al NMR spectroscopy (104 MHz, benzene-d_6): δ 155.8 (**4**^{Bn}(TMA))

1:8 **14**^{Bn}:TMA

^{1}H NMR spectroscopy (400 MHz, benzene-d_6): δ 7.35-6.78 (m, **4**^{Bn}(TMA) + **14**^{Bn}(TMA) Ph), 4.51-3.21 (m, 8H, **14**^{Bn}(TMA) + **15** CH_2), 2.86 (s, 6.2H, **4**^{Bn}(TMA) CH_2), 1.12 (s, 18H, **4**^{Bn}(TMA) Me), 0.13 (s, br, 8.2H, **4**^{Bn}(TMA) $AlMe_b$), −0.07-−0.69 (m, 35H, unassigned AlMe), −0.42 (s, br, 35H, **4**^{Bn}(TMA) $AlMe_t$)

^{13}C NMR spectroscopy (100 MHz, benzene-d_6): δ 136.7, 130.3, 129.1, 128.7, 128.6, 126.7 (**4**^{Bn}(TMA) + **14**^{Bn}(TMA) Ph), 79.5 (**4**^{Bn}(TMA) CO), 50.7 (**4**^{Bn}(TMA) CH_2), 28.0 (**4**^{Bn}(TMA) Me), −4.5 (**4**^{Bn}(TMA) $AlMe_b$), −7.2 (**4**^{Bn}(TMA) $AlMe_t$)

^{27}Al NMR spectroscopy (104 MHz, benzene-d_6): δ 155.1 (**4**^{Bn}(TMA))

1:12 **14**^{Bn}:TMA

^{1}H NMR spectroscopy (400 MHz, benzene-d_6): δ 7.35-6.78 (m, **4**^{Bn}(TMA) Ph), 4.79-3.56 (m, 8H, **15** CH_2), 2.86 (s, 8H, **4**^{Bn}(TMA) CH_2), 1.11 (s, 24H, **4**^{Bn}(TMA) Me), 0.13 (s, br, 12H, **4**^{Bn}(TMA) $AlMe_b$), −0.15-−0.57 (m, 53H, unassigned AlMe), −0.42 (s, br, 48H, **4**^{Bn}(TMA) $AlMe_t$)

^{13}C NMR spectroscopy (100 MHz, benzene-d_6): δ 136.7, 130.3, 128.1, 126.7 (**4**^{Bn}(TMA) Ph), 79.5 (**4**^{Bn}(TMA) CO), 50.8 (**4**^{Bn}(TMA) CH_2), 28.0 (**4**^{Bn}(TMA) Me), −4.5 (**4**^{Bn}(TMA) $AlMe_b$), −7.0 (**4**^{Bn}(TMA) $AlMe_t$)

^{27}Al NMR spectroscopy (104 MHz, benzene-d_6): δ 160.6 **4**^{Bn}(TMA)

4.2.2.4 Spectroscopic characterisation 14^{Bn} + TMA reaction mixtures heated to reflux

TMA (0.5, 1.0, 1.5 or 2.0 ml, 1.0, 2.0, 3.0 or 4.0 mmol, 2.0 M in toluene) was added dropwise to **14**^{Bn} (304 mg, 0.5 mmol) in toluene (4 ml) under a N_2 atmosphere at −78 °C and allowed to reach room temperature. The solution was then heated to reflux for 2 hours. An aliquot of the solution was analysed by NMR spectroscopy.

1:2 **14**^{Bn}:TMA

^{1}H NMR spectroscopy (400 MHz, benzene-d_6): δ 7.39-6.84 (m, Ph), 4.24 (s, 1.9H, **17**^{Bn}(**4**^{Bn})$_2$ CH_2O), 3.93 (s, 9.1H, **16**^{Bn}(**4**^{Bn}) CH_2O), 3.88 (s, 8.2H, **14**^{Bn} CH_2O), 3.83 (s, 1.7H, **17**^{Bn}(**4**^{Bn})$_2$ CH_2O), 3.62 (s, 3H, **16**^{Bn}(**4**^{Bn}) CH_2O), 3.51 (s, 1.9H, **17**^{Bn}(**4**^{Bn})$_2$ CH_2), 3.32 (s, 9.5H, **16**^{Bn}(**4**^{Bn}) CH_2), 3.20 (s, 8.5H, **14**^{Bn} CH_2), 3.00 (s, 1H, (**4**^{Bn})$_2$ CH_2), 2.88 (m, 4.1H, **16**^{Bn}(**4**^{Bn}) + **17**^{Bn}(**4**^{Bn})$_2$ CH_2), 1.23 (s, 3.0H, (**4**^{Bn})$_2$ Me), 1.13 (s, 13H, **16**^{Bn}(**4**^{Bn}) + **17**^{Bn}(**4**^{Bn})$_2$ Me), −0.27 (s, 3H, (**4**^{Bn})$_2$ AlMe), −0.28 (s, 3H, (**4**^{Bn})$_2$ AlMe), −0.37 (s, 9.5H, **17**^{Bn}(**4**^{Bn})$_2$ AlMe), −0.44 (s, 19H, **16**^{Bn}(**4**^{Bn}) AlMe)

^{13}C NMR spectroscopy (100 MHz, benzene-d_6): δ 169.8 (**14**^{Bn} + **16**^{Bn}(**4**^{Bn}) + **17**^{Bn}(**4**^{Bn})$_2$ C=O), 136.7, 133.9, 133.8, 130.3, 129.2, 128.5, 128.1, 127.0 (**14**^{Bn} + **16**^{Bn}(**4**^{Bn}) + **17**^{Bn}(**4**^{Bn})$_2$ Ph), 61.9 (**14**^{Bn} + **17**^{Bn}(**4**^{Bn})$_2$ CH_2O), 61.0 (**16**^{Bn}(**4**^{Bn}) CH_2O), 51.1 ((**4**^{Bn})$_2$ + **16**^{Bn}(**4**^{Bn}) + **17**^{Bn}(**4**^{Bn})$_2$ CH_2), 43.4 (**17**^{Bn}(**4**^{Bn})$_2$ C_{quat}), 42.2 (**14**^{Bn} C_{quat}), 40.9 (**16**^{Bn}(**4**^{Bn}) + **17**^{Bn}(**4**^{Bn})$_2$ CH_2), 40.8 (**14**^{Bn} CH_2), 28.3 ((**4**^{Bn})$_2$ + **16**^{Bn}(**4**^{Bn}) + **17**^{Bn}(**4**^{Bn})$_2$ Me), −8.5 (**16**^{Bn}(**4**^{Bn}) + **17**^{Bn}(**4**^{Bn})$_2$ AlMe)

^{27}Al NMR spectroscopy (104 MHz, benzene-d_6): Only see background signal

1:4 **14**^{Bn}:TMA

^{1}H NMR spectroscopy (400 MHz, benzene-d_6): δ 7.52-6.78 (m, Ph), 4.60 (s, 0.5H, **18**^{Bn}(**4**^{Bn})$_3$ CH_2O), 4.26 (s, 1.5H, **18**^{Bn}(**4**^{Bn})$_3$ CH_2O), 4.25 (s, 2.5H, **17**^{Bn}(**4**^{Bn})$_2$ CH_2O), 3.93 (s, 1.7H, **16**^{Bn}(**4**^{Bn}) CH_2O), 3.83 (s, 2.7H, **17**^{Bn}(**4**^{Bn})$_2$ CH_2O), 3.74 (s, 0.5H, **18**^{Bn}(**4**^{Bn})$_3$ CH_2), 3.62 (s, 0.6H, **16**^{Bn}(**4**^{Bn}) CH_2O), 3.51 (s, 2.6H, **17**^{Bn}(**4**^{Bn})$_2$ CH_2), 3.32 (s, 1.9H, **16**^{Bn}(**4**^{Bn}) CH_2), 3.00 (s, 1.4H, (**4**^{Bn})$_2$ CH_2), 2.88 (s, 1.7H, **16**^{Bn}(**4**^{Bn}) + **18**^{Bn}(**4**^{Bn})$_3$ CH_2), 2.87 (s, 2.5H, **17**^{Bn}(**4**^{Bn})$_2$ CH_2), 1.22 (s, 4.2H, (**4**^{Bn})$_2$ Me), 1.12 (s, 13H, **16**^{Bn}(**4**^{Bn}) + **17**^{Bn}(**4**^{Bn})$_2$ + **18**^{Bn}(**4**^{Bn})$_3$ Me), −0.22 (s, 9.3H, **18**^{Bn}(**4**^{Bn})$_3$ AlMe), −0.27 (s, 4.4H, (**4**^{Bn})$_2$ AlMe), −0.28 (s, 4.6H, (**4**^{Bn})$_2$ AlMe), −0.37 (s, 17H, **17**^{Bn}(**4**^{Bn})$_2$ AlMe), −0.44 (s, 4.6H, **16**^{Bn}(**4**^{Bn}) AlMe)

^{13}C NMR spectroscopy (100 MHz, benzene-d_6): δ 172.4 (**16**^{Bn}(**4**^{Bn}) + **17**^{Bn}(**4**^{Bn})$_2$ + **18**^{Bn}(**4**^{Bn})$_3$ C=O), 130.3, 129.4, 128.7, 128.6, 128.3 (**16**^{Bn}(**4**^{Bn}) + **17**^{Bn}(**4**^{Bn})$_2$ + **18**^{Bn}(**4**^{Bn})$_3$ Ph), 77.7 ((**4**^{Bn})$_2$ + **16**^{Bn}(**4**^{Bn}) + **17**^{Bn}(**4**^{Bn})$_2$ + **18**^{Bn}(**4**^{Bn})$_3$ CO), 62.0 (**17**^{Bn}(**4**^{Bn})$_2$ CH_2O), 51.2 ((**4**^{Bn})$_2$ CH_2), 51.1 (**16**^{Bn}(**4**^{Bn}) + **17**^{Bn}(**4**^{Bn})$_2$ + **18**^{Bn}(**4**^{Bn})$_3$ CH_2), 41.0 (**18**^{Bn}(**4**^{Bn})$_3$ CH_2), 40.9 (**16**^{Bn}(**4**^{Bn}) + **17**^{Bn}(**4**^{Bn})$_2$ CH_2), 28.5 ((**4**^{Bn})$_2$ Me), 28.3 (**16**^{Bn}(**4**^{Bn}) + **17**^{Bn}(**4**^{Bn})$_2$ + **18**^{Bn}(**4**^{Bn})$_3$ Me), −7.9 (**18**^{Bn}(**4**^{Bn})$_3$ AlMe), −8.5 (**16**^{Bn}(**4**^{Bn}) + **17**^{Bn}(**4**^{Bn})$_2$ AlMe)

^{27}Al NMR spectroscopy (104 MHz, benzene-d_6): δ 8.5

1:6 **14**^{Bn}:TMA

^{1}H NMR spectroscopy (400 MHz, benzene-d_6): δ 7.52-6.78 (m, Ph), 4.60 (s, 0.6H, **18**^{Bn}(**4**^{Bn})$_3$ CH_2O), 4.26 (s, 2.4H, **18**^{Bn}(**4**^{Bn})$_3$ CH_2O), 4.25 (s, 0.5H, **17**^{Bn}(**4**^{Bn})$_2$ CH_2O), 3.94 (s, 1.6H, **19**(**4**^{Bn})$_2$ CH_2O), 3.83 (s, 0.4H, **17**^{Bn}(**4**^{Bn})$_2$ CH_2O), 3.74 (s, 0.9H, **18**^{Bn}(**4**^{Bn})$_3$ CH_2), 3.51 (s, 0.5H, **17**^{Bn}(**4**^{Bn})$_2$ CH_2), 3.00 (s, 1.9H, (**4**^{Bn})$_2$ CH_2), 2.96 (s, 0.8H, **19**(**4**^{Bn})$_2$ CH_2O) 2.88 (s, 3.7H, **17**^{Bn}(**4**^{Bn})$_2$ + **18**^{Bn}(**4**^{Bn})$_3$ CH_2), 2.79 (s, 0.7H, **19**(**4**^{Bn})$_2$ CH_2), 1.22 (s, 6.5H, (**4**^{Bn})$_2$ Me), 1.12 (s, 9.2H, **17**^{Bn}(**4**^{Bn})$_2$ + **18**^{Bn}(**4**^{Bn})$_3$ Me), 1.07 (s, 2.4H, **19**(**4**^{Bn})$_2$ Me), −0.22 (s, 17H, **18**^{Bn}(**4**^{Bn})$_3$ AlMe), −0.27 (s, 4.1H, unassigned AlMe), −0.28 (s, 6.1H, (**4**^{Bn})$_2$ AlMe), −0.35 (s, 2.9H, **19**(**4**^{Bn})$_2$ AlMe), −0.37 (s, 3.4H, **17**^{Bn}(**4**^{Bn})$_2$ AlMe), −0.42 (s, 5.7H, unassigned AlMe), −0.44 (s, 5.7H, unassigned AlMe), −0.46 (s, 5.7H, **19**(**4**^{Bn})$_2$ AlMe)

^{13}C NMR spectroscopy (100 MHz, benzene-d_6): δ 136.7, 130.4, 130.3, 128.7, 128.6, 128.3 (**17**^{Bn}(**4**^{Bn})$_2$ + **18**^{Bn}(**4**^{Bn})$_3$ + **19**(**4**^{Bn})$_2$ Ph), 77.9 (**18**^{Bn}(**4**^{Bn})$_3$ + **19**(**4**^{Bn})$_2$ CO), 77.7 ((**4**^{Bn})$_2$ + **17**^{Bn}(**4**^{Bn})$_2$ CO), 69.8 (**19**(**4**^{Bn})$_2$ CH_2O), 64.0 (**18**^{Bn}(**4**^{Bn})$_3$ CH_2O), 51.2 ((**4**^{Bn})$_2$ CH_2), 51.0 (**17**^{Bn}(**4**^{Bn})$_2$ + **18**^{Bn}(**4**^{Bn})$_3$ + **19**(**4**^{Bn})$_2$ CH_2), 28.5 ((**4**^{Bn})$_2$ Me), 28.4 (**17**^{Bn}(**4**^{Bn})$_2$ + **18**^{Bn}(**4**^{Bn})$_3$ +

19(4^{Bn})$_2$ Me), −7.9 (**18**^{Bn}(4^{Bn})$_3$ AlMe), −8.5 (**17**^{Bn}(4^{Bn})$_2$ + **19**(4^{Bn})$_2$ AlMe), −12.1 (**19**(4^{Bn})$_2$ AlMe)

^{27}Al NMR spectroscopy (104 MHz, benzene-d_6): δ 8.7 (**19**(4^{Bn})$_2$)

1:8 **14**^{Bn}:TMA

^{1}H NMR spectroscopy (400 MHz, benzene-d_6): δ 7.52-6.78 (m, Ph), 4.47 (s, 2H, **15**(4^{Bn})$_4$ CH_2O), 3.94 (s, 3.3H, **19**(4^{Bn})$_2$ CH_2O), 3.00 (s, 2.7H, (4^{Bn})$_2$ CH_2), 2.96 (s, 3.4H, **15**(4^{Bn})$_4$ CH_2 + **19**(4^{Bn})$_2$ CH_2O), 2.86 (s, 1.3H, 4^{Bn}(TMA) CH_2), 2.79 (s, 1H, **19**(4^{Bn})$_2$ CH_2), 1.23 (s, 8.4H, (4^{Bn})$_2$ Me), 1.17 (s, 6.4H, **15**(4^{Bn})$_4$ Me), 1.12 (s, 4.4H, 4^{Bn}(TMA) Me), 1.07 (s, 3.2H, **19**(4^{Bn})$_2$ Me), 0.13 (s, 1.8H, 4^{Bn}(TMA) $AlMe_b$), −0.08 (s, 13H, **15**(4^{Bn})$_4$ AlMe), −0.28 (s, 11H, (4^{Bn})$_2$ AlMe), −0.35 (s, 5.2H, **19**(4^{Bn})$_2$ AlMe), −0.42 (s, 9.8H, 4^{Bn}(TMA) $AlMe_t$), −0.46 (s, 6.1H, **19**(4^{Bn})$_2$ AlMe)

^{13}C NMR spectroscopy (100 MHz, benzene-d_6): δ 137.1, 136.7, 130.3, 128.7, 128.6, 126.6 (4^{Bn}(TMA) + (4^{Bn})$_2$ + **15**(4^{Bn})$_4$ + **19**(4^{Bn})$_2$ Ph), 79.5 (4^{Bn}(TMA) CO), 78.2 (**15**(4^{Bn})$_4$ CO), 77.9 (**19**(4^{Bn})$_2$ CO), 77.6 ((4^{Bn})$_2$ CO), 69.8 (**19**(4^{Bn})$_2$ CH_2O), 62.6 (**15**(4^{Bn})$_4$ CH_2O), 51.2 ((4^{Bn})$_2$ CH_2), 51.1 (**15**(4^{Bn})$_4$ CH_2), 51.0 (**19**(4^{Bn})$_2$ CH_2), 50.8 (4^{Bn}(TMA) CH_2), 46.5 (**15**(4^{Bn})$_4$ C_{quat}), 28.5 ((4^{Bn})$_2$ Me), 28.3 (**15**(4^{Bn})$_4$ + **19**(4^{Bn})$_2$ Me), 28.0 (4^{Bn}(TMA) Me), −5.8 ((4^{Bn})$_2$ AlMe), −6.9 (4^{Bn}(TMA) + **15**(4^{Bn})$_4$ AlMe), −8.5 (**19**(4^{Bn})$_2$ AlMe), −12.1 (**19**(4^{Bn})$_2$ AlMe)

^{27}Al NMR spectroscopy (104 MHz, benzene-d_6): δ 156.8 (**15**(4^{Bn})$_4$ + **19**(4^{Bn})$_2$), 8.7 (**19**(4^{Bn})$_2$)

4.2.2.5 Synthesis and characterisation of {BnC(O)OCH$_2$}$_2$C{(CH$_2$OAlMe$_2$)(Me$_2$AlOCBnMe$_2$)}$_2$ 17^{Bn}(4^{Bn})$_2$

TMA (1.0 ml, 2.0 mmol, 2.0 M in toluene) was added dropwise to **14**^{Bn} (304 mg, 0.5 mmol) in toluene (4 ml) under a N_2 atmosphere at −78 °C and allowed to reach room temperature. The solution was heated to reflux for 2 hours. Addition of hexane (6 ml) and storage at −27 °C resulted in the formation of colourless needle crystals.

Yield 100 mg (22% wrt **14**^{Bn})

Melting point 140-142 °C

Elemental analysis calculated for $C_{49}H_{72}Al_4O_8$ (%): C 65.61, H 8.09; found (%): C 65.46, H 8.01

^{1}H NMR spectroscopy (400 MHz, benzene-d_6): δ 7.28-6.85 (m, 20H, Ph), 4.25 (s, 4H, CH_2O), 3.84 (s, 4H, CH_2O), 3.51 (s, 4H, CH_2), 2.87 (s, 4H, CH_2), 1.12 (s, 12H, Me), −0.37 (s, 24H, AlMe)

^{13}C NMR spectroscopy (100 MHz, benzene-d_6): δ 170.0 (C=O), 136.7, 133.5 (*i*-Ph), 130.3, 129.4 (*o*-Ph), 128.6, 128.0 (*m*-Ph), 127.2, 126.7 (*p*-Ph), 77.7 (CO), 62.1, 62.0(CH_2O), 51.1 (CH_2), 44.2 (C_{quat}), 40.9 (CH_2), 28.4 (Me), −8.4 (AlMe)

^{27}Al NMR spectroscopy (104 MHz, benzene-d_6): Only see background signal

X-ray crystallography $C_{49}H_{72}Al_4O_8$, M = 896.98, Triclinic, $P\bar{1}$, a = 12.3772(4), b = 13.6608(5), c = 17.5106(6) Å, α = 68.249(2), β = 70.040(2), γ = 79.421(2)°, V = 2579.22(16) Å^3, Z = 2, ρ_{calcd} = 1.155 g cm^{-3}, λ = 1.54184 Å, μ = 1.222 mm^{-1}, T = 180(2) K, 74742 reflections, 9120 unique, θ_{max} = 66.810°, R_{int} = 0.1304, $R1$ = 0.0609 ($F_{obs} > 4\sigma(F_{obs})$), $wR2$ = 0.1473, S = 1.017, 562 parameters, peak/hole 0.440/−0.358 e Å^{-3}

4.2.2.6 Synthesis and characterisation of $Al(AlMe_2)_3\{(OCH_2)_3CCH_2OAlMe_2\}_2(Me_2AlOCBnMe_2)_2$ 19(4^{Bn})$_2$

TMA (1.5 ml, 3.0 mmol, 2.0 M in toluene) was added dropwise to **14**^{Bn} (304 mg, 0.5 mmol) in toluene (4 ml) under a N_2 atmosphere at −78 °C and allowed to reach room temperature. The solution was heated to reflux for 2 hours and then the solvent was removed *in vacuo*. The solid was redissolved in hexane (8 ml) and storage at room temperature for 1 day resulted in the formation of colourless crystals.

Yield 40 mg (16% wrt **14**^{Bn})

Melting point 221-224 °C

Elemental analysis calculated for $C_{44}H_{84}Al_8O_{10}$ (%): C 53.44, H 8.56; found (%): C 52.33, H 8.48

^{1}H NMR spectroscopy (400 MHz, benzene-d_6): δ 7.08-6.83 (m, 17H, **19**(**4**^{Bn})$_2$ + (**4**^{Bn})$_2$ Ph), 3.93 (s, 12H, **19**(**4**^{Bn})$_2$ CH_2O), 3.00 (s, 0.72H, (**4**^{Bn})$_2$ CH_2), 2.94 (s, 4H, **19**(**4**^{Bn})$_2$ CH_2O), 2.79 (s, 4H, **19**(**4**^{Bn})$_2$ CH_2), 1.22 (s, 3.1H, (**4**^{Bn})$_2$ Me), 1.06 (s, 12H, **19**(**4**^{Bn})$_2$ Me), −0.27 (s, 2.9H, (**4**^{Bn})$_2$ AlMe), −0.34 (s, 18H, **19**(**4**^{Bn})$_2$ AlMe), −0.46 (s, 24H, **19**(**4**^{Bn})$_2$ AlMe)

^{13}C NMR spectroscopy (100 MHz, benzene-d_6): δ 136.5 (**19**(**4**^{Bn})$_2$ *i*-Ph), 130.3 (**19**(**4**^{Bn})$_2$ *o*-Ph), 128.1 (**19**(**4**^{Bn})$_2$ *m*-Ph), 126.8 (**19**(**4**^{Bn})$_2$ *p*-Ph), 77.9 (**19**(**4**^{Bn})$_2$ CO), 69.8 (**19**(**4**^{Bn})$_2$ CH_2O), 62.2 (**19**(**4**^{Bn})$_2$ CH_2O), 51.2 ((**4**^{Bn})$_2$ CH_2), 51.0 (**19**(**4**^{Bn})$_2$ CH_2), 40.6 (**19**(**4**^{Bn})$_2$ C_{quat}), 28.5 ((**4**^{Bn})$_2$ Me), 28.3 (**19**(**4**^{Bn})$_2$ Me), −8.5 (**19**(**4**^{Bn})$_2$ AlMe), −12.1 (**19**(**4**^{Bn})$_2$ AlMe)

^{27}Al NMR spectroscopy (104 MHz, benzene-d_6): δ 8.7 (**19**(**4**^{Bn})$_2$)

X-ray crystallography $C_{44}H_{84}Al_8O_{10}$, M = 988.95, Monoclinic, $C2/c$, a = 26.8564(8), b = 16.9050(5), c = 13.6338(4) Å, α = 90, β = 108.8420(10), γ = 90°, V = 5858.1(3) Å^3, Z = 4, ρ_{calcd} = 1.121 g cm^{-3}, λ = 1.54184 Å, μ = 1.694 mm^{-1}, T = 180(2) K, 5149 reflections collected, 5149 unique, θ_{max} = 66.623°, R_{int} = 0.0614, $R1$ = 0.0583 ($F_{obs} > 4\sigma(F_{obs})$), $wR2$ = 0.1622, S = 1.154, 291 parameters, peak/hole 0.4371/−0.487 e Å^{-3}

4.2.3 Reactivity of Tetraesters with Me_2AlCl

4.2.3.1 Spectroscopic characterisation of 14^{Bn} + Me_2AlCl reaction mixtures

$AlCl_3$ (267 mg, 2 mmol), toluene (1 ml) and TMA (2 ml, 4 mmol, 2.0 M in toluene) were heated to form Me_2AlCl (6 mmol, 2.0 M in toluene). **14**^{Bn} (304 mg, 0.5 mmol) in toluene (4 ml) was added dropwise at −78 °C and the mixture allowed to warm to room temperature to give a colourless solution. After stirring for 2 hours at the desired temperature an aliquot of the solution was analysed by NMR spectroscopy.

Room temperature reaction

^{1}H NMR spectroscopy (400 MHz, benzene-d_6): δ 7.36-6.76 (m, **4**^{Bn}(Me_2AlCl) + **14**^{Bn}(Me_2AlCl) Ph), 3.97-3.40 (m, br, 16H, **14**^{Bn}(Me_2AlCl) CH_2 + **14**^{Bn}(Me_2AlCl) CH_2O + **20** CH_2O), 2.85 (s, 0.18H, **4**^{Bn}(Me_2AlCl) CH_2), 1.08 (s, 0.6H, **4**^{Bn}(Me_2AlCl) Me), −0.02-−0.48 (m, 100H, **14**^{Bn}(Me_2AlCl) AlMe)

^{13}C NMR spectroscopy (100 MHz, benzene-d_6): δ 172.4 (**14**^{Bn}(Me_2AlCl)), 65.3 (**14**^{Bn}(Me_2AlCl) CH_2O), 41.4 (**14**^{Bn}(Me_2AlCl) CH_2), 27.9 (**4**^{Bn}(Me_2AlCl) Me), −6.8 (**14**^{Bn}(Me_2AlCl) AlMe)

^{27}Al NMR spectroscopy (104 MHz, benzene-d_6): δ 180.0 (**14**^{Bn}(Me_2AlCl))

70 °C reaction

^{1}H NMR spectroscopy (400 MHz, benzene-d_6): δ 7.36-6.76 (m, **4**^{Bn}(Me_2AlCl) + **4**^{Bn}($MeAlCl_2$) + **14**^{Bn}(Me_2AlCl) Ph), 4.50-3.05 (m, br, 12H, **14**^{Bn}(Me_2AlCl) CH_2 + **14**^{Bn}(Me_2AlCl) CH_2O + **20** CH_2O + **21** CH_2O), 2.92 (s, 1.3H, **4**^{Bn}($MeAlCl_2$) CH_2), 2.85 (s, 2.7H, **4**^{Bn}(Me_2AlCl) CH_2), 1.12 (s, 3.9H, **4**^{Bn}($MeAlCl_2$) Me), 1.07 (s, 8.4H, **4**^{Bn}(Me_2AlCl) Me), −0.04 (m, br, 6H, unassigned AlMe), −0.22 (s, 2.3H, **4**^{Bn}($MeAlCl_2$) AlMe), −0.27 (s, 17H, **4**^{Bn}(Me_2AlCl) + **4**^{Bn}($MeAlCl_2$) AlMe), −0.31 (s, 50H, **14**^{Bn}(Me_2AlCl) AlMe), −0.38 (s, 2.2H, **4**^{Bn}($MeAlCl_2$) AlMe), −0.45 (s, 2.6H, unassigned AlMe)

^{13}C NMR spectroscopy (100 MHz, benzene-d_6): δ 81.1 (**4**^{Bn}(Me_2AlCl) CO), 50.4 (**4**^{Bn}(Me_2AlCl) CH_2), 41.2 (**14**^{Bn}(Me_2AlCl) CH_2), 27.9 (**4**^{Bn}(Me_2AlCl) Me), −6.7 (**14**^{Bn}(Me_2AlCl) AlMe)

^{27}Al NMR spectroscopy (104 MHz, benzene-d_6): δ 181.7 (**14**^{Bn}(Me_2AlCl))

80 °C reaction

^{1}H NMR spectroscopy (400 MHz, benzene-d_6): δ 7.36-6.76 (m, **4**^{Bn}(Me_2AlCl) + **4**^{Bn}($MeAlCl_2$) + **14**^{Bn}(Me_2AlCl) Ph), 4.50-3.25 (m, br, 12H, **14**^{Bn}(Me_2AlCl) CH_2 + **14**^{Bn}(Me_2AlCl) CH_2O + **20** CH_2O + **21** CH_2O), 2.92 (s, 2H, **4**^{Bn}($MeAlCl_2$) CH_2), 2.85 (s, 2.4H, **4**^{Bn}(Me_2AlCl) CH_2), 1.13 (s, 5.7H, **4**^{Bn}($MeAlCl_2$) Me), 1.08 (s, 7.2H, **4**^{Bn}(Me_2AlCl) Me), −0.04 (m, br, 7.4H, unassigned AlMe), −0.22 (s, 3.6H, **4**^{Bn}($MeAlCl_2$) AlMe), −0.27 (s, 15.5H, **4**^{Bn}(Me_2AlCl) + **4**^{Bn}($MeAlCl_2$) AlMe), −0.32 (s, 50H, **14**^{Bn}(Me_2AlCl) AlMe), −0.38 (s, 3.2H, **4**^{Bn}($MeAlCl_2$) AlMe), −0.45 (s, 3.2H, unassigned AlMe)

^{13}C NMR spectroscopy (100 MHz, benzene-d_6): δ 83.6 (**4**^{Bn}($MeAlCl_2$) CO), 81.1 (**4**^{Bn}(Me_2AlCl) CO), 50.4 (**4**^{Bn}(Me_2AlCl) CH_2), 50.1 (**4**^{Bn}($MeAlCl_2$) CH_2), 41.6 (**14**^{Bn}(Me_2AlCl) CH_2), 27.9 (**4**^{Bn}(Me_2AlCl) + **4**^{Bn}($MeAlCl_2$) Me), −6.6 (**14**^{Bn}(Me_2AlCl) AlMe)

^{27}Al NMR spectroscopy (104 MHz, benzene-d_6): δ 179.5 (**14**^{Bn}(Me_2AlCl))

90 °C reaction

^{1}H NMR spectroscopy (400 MHz, benzene-d_6): δ 7.36-6.76 (m, **4**^{Bn}(Me_2AlCl) + **4**^{Bn}($MeAlCl_2$) + **7a** + **7b** + **14**^{Bn}(Me_2AlCl) Ph), 4.80 (s, 0.05H, **7b** C=CH_2), 4.75 (s, 0.06H, **7b** C=CH_2), 4.50-3.25 (m, br, 6.2H, **14**^{Bn}(Me_2AlCl) CH_2 + **14**^{Bn}(Me_2AlCl) CH_2O + **20**

CH_2O + **21** CH_2O), 2.92 (s, 4.6H, **4**^{Bn}($MeAlCl_2$) CH_2), 2.85 (s, 5.2H, **4**^{Bn}(Me_2AlCl) CH_2), 1.55 (s, 0.19H, **7b** Me), 1.12 (s, 13.5H, **4**^{Bn}($MeAlCl_2$) Me), 1.07 (s, 15.5H, **4**^{Bn}(Me_2AlCl) Me), −0.02 (m, br, 6.1H, unassigned AlMe), −0.22 (s, 7H, **4**^{Bn}($MeAlCl_2$) AlMe), −0.27 (s, 38H, **4**^{Bn}(Me_2AlCl) + **4**^{Bn}($MeAlCl_2$) AlMe), −0.33 (s, 52H, **14**^{Bn}(Me_2AlCl) AlMe), −0.38 (s, 6.8H, **4**^{Bn}($MeAlCl_2$) AlMe), −0.45 (s, 6.2H, unassigned AlMe)

^{13}C NMR spectroscopy (100 MHz, benzene-d_6): δ 50.4 (**4**^{Bn}(Me_2AlCl) CH_2), 50.1 (**4**^{Bn}($MeAlCl_2$) CH_2), 27.9 (**4**^{Bn}(Me_2AlCl) + **4**^{Bn}($MeAlCl_2$) Me), −6.3 (**14**^{Bn}(Me_2AlCl) AlMe)

^{27}Al NMR spectroscopy (104 MHz, benzene-d_6): δ 178.3 (**14**^{Bn}(Me_2AlCl)), 7.7

100 °C reaction

^{1}H NMR spectroscopy (400 MHz, benzene-d_6): δ 7.36-6.76 (m, **4**^{Bn}($MeAlCl_2$) + **7a** + **7b** + **14**^{Bn}(Me_2AlCl) Ph), 6.28 (s, 0.01H, **7a** CH=C), 4.80 (s, 0.64H, **7b** C=CH_2), 4.76 (s, 0.66H, **7b** C=CH_2), 4.50-3.25 (m, br, 8.4H, **14**^{Bn}(Me_2AlCl) CH_2 + **14**^{Bn}(Me_2AlCl) CH_2O + **20** CH_2O + **21** CH_2O), 3.15 (s, 2H, **7b** CH_2), 2.92 (s, 4H, **4**^{Bn}($MeAlCl_2$) CH_2), 2.85 (s, 2.2H, **4**^{Bn}(Me_2AlCl) CH_2), 1.72 (s, 0.45H, **7a** Me), 1.69 (s, 0.44H, **7a** Me), 1.55 (s, 2.2H, **7b** Me), 1.12 (s, 12H, **4**^{Bn}($MeAlCl_2$) Me), 1.07 (s, 6.6H, **4**^{Bn}(Me_2AlCl) Me), −0.22 (s, 6.5H, **4**^{Bn}($MeAlCl_2$) AlMe), −0.27 (s, 14H, **4**^{Bn}(Me_2AlCl) AlMe), −0.28 (s, 5.3H, **4**^{Bn}($MeAlCl_2$) AlMe), −0.34 (s, 47H, **14**^{Bn}(Me_2AlCl) AlMe), −0.38 (s, 5.5H, **4**^{Bn}($MeAlCl_2$) AlMe)

^{13}C NMR spectroscopy (100 MHz, benzene-d_6): δ 111.8 (**7b** =CH_2), 83.6 (**4**^{Bn}($MeAlCl_2$) CO), 81.1 (**4**^{Bn}(Me_2AlCl) CO), 50.4 (**4**^{Bn}(Me_2AlCl) CH_2), 50.1 (**4**^{Bn}($MeAlCl_2$) CH_2), 44.6 (**7b** CH_2), 27.9 (**4**^{Bn}($MeAlCl_2$) Me), 27.8 (**4**^{Bn}(Me_2AlCl) Me), −6.6 (**14**^{Bn}(Me_2AlCl) AlMe)

^{27}Al NMR spectroscopy (104 MHz, benzene-d_6): δ 181.4 (**14**^{Bn}(Me_2AlCl)), 8.2

Reaction heated to reflux

^{1}H NMR spectroscopy (400 MHz, benzene-d_6): δ 7.36-6.76 (m, **7a** + **7b** + **10** + **11a** + **11b** + **14**^{Bn}(Me_2AlCl) Ph), 6.28 (s, 0.25H, **7a** CH=C), 4.80 (s, 1H, **7b** C=CH_2), 4.76 (s, 1H, **7b** C=CH_2), 4.50-3.25 (m, br, 3H, **14**^{Bn}(Me_2AlCl) CH_2 + **14**^{Bn}(Me_2AlCl) CH_2O + **20** CH_2O + **21** CH_2O), 3.15 (s, 2.1H, **7b** CH_2), 2.76 (s, 0.1H, **11b** CH_2), 2.36 (s, 0.06H, **10** CH_2), 1.72 (s, 1H, **7a** Me), 1.69 (s, 1H, **7a** Me), 1.55 (s, 3.1H, **7b** Me), 1.22 (s, 0.29H, **11b** Me), 0.87 (m, 0.47H, **11a** Me), 0.84 (s, 0.38H, **10** Me), 0.22-−0.50 (m, 28H, unassigned AlMe)

^{13}C NMR spectroscopy (100 MHz, benzene-d_6): δ 144.8, 139.6 (**7b** C), 128.9 (**7b** Ph), 111.8 (**7b** $=CH_2$), 44.6 (**7b** CH_2), 26.4 (**7a** Me), 21.6 (**7b** Me), 18.9 (**7a** Me)

^{27}Al NMR spectroscopy (104 MHz, benzene-d_6): δ 179.3 (**14**^{Bn}(Me_2AlCl)), 8.7

4.2.3.2 Synthesis and characterisation of 14^{Pent}(Me_2AlCl)$_4$

$AlCl_3$ (44 mg, 0.33 mmol), toluene (2 ml) and TMA (0.33 ml, 0.66 mmol, 2.0 M in toluene) were heated to form Me_2AlCl (1 mmol). **14**^{Pent} (0.27 ml, 0.5 mmol) was added dropwise at −78 °C and the mixture allowed to warm to room temperature to give a colourless solution. Once the solution reached room temperature it was stored at –27 °C for 1 day to produce colourless needle crystals.

Yield 75 mg (33% wrt $AlCl_3$)

Melting point 120-123 °C

Elemental analysis calculated for $C_{37}H_{76}Al_4Cl_4O_8$ (%): C 49.45, H 8.52, Cl 15.78; found (%): C 48.64, H 8.24, Cl 15.94

^{1}H NMR spectroscopy (400 MHz, chloroform-*d*): δ 4.54 (s, 8H, CH_2O), 2.75 (t, *J* = 7.6 Hz, 8H, CH_2), 1.74 (quint, *J* = 7.6 Hz, 8H, CH_2), 1.40-1.31 (m, 16H, CH_2), 0.92 (t, *J* = 7.0 Hz, 12H, Me), −0.63 (s, 24H, AlMe)

^{13}C NMR spectroscopy (100 MHz, chloroform-*d*): δ 182.6 (C=O), 65.8 (CH_2O), 42.1 (C_{quat}), 35.2, 31.1, 24.6, 22.1 (CH_2), 13.8 (Me), −7.9 (br, AlMe)

^{27}Al NMR spectroscopy (104 MHz, chloroform-*d*): Only see background signal

X-ray crystallography $C_{37}H_{76}Al_4Cl_4O_8$, *M* = 898.69, Monoclinic, *C*2/*c*, *a* = 31.4647(12), *b* = 8.2194(3), *c* = 20.7543(8) Å, α = 90, β = 92.278(2), γ = 90°, *V* = 5363.3(4) Å^3, *Z* = 4, ρ_{calcd} = 1.113 g cm^{-3}, λ = 1.54184 Å, μ = 2.957 mm^{-1}, *T* = 180(2) K, 53023 reflections, 4735 unique, θ_{max} = 66.699°, R_{int} = 0.0420, *R*1 = 0.0580 ($F_{obs} > 4\sigma(F_{obs})$), *wR*2 = 0.1731, *S* = 1.049, 262 parameters, peak/hole 0.490/−0.748 *e* Å^{-3}

4.2.4 Reactivity of Tetraesters with $MeAlCl_2$

4.2.4.1 Attempted characterisation of 14^{Bn} + $MeAlCl_2$ reaction mixtures

$AlCl_3$ (534 mg, 4 mmol), toluene (2 ml) and TMA (1 ml, 2 mmol, 2.0 M in toluene) were heated to form $MeAlCl_2$ (6 mmol, 2.0 M in toluene). **14**^{Bn} (304 mg, 0.5 mmol) in toluene (4 ml) was added dropwise at −78 °C to give a yellow solution and the mixture allowed to warm to room temperature to give a clear liquid and a white suspension. After stirring for 2 hours the solvent was removed *in vacuo* to give an intractable white solid.

Yield 300 mg

4.2.5 Reactivity of Tetraesters with $Me_{1.5}AlCl_{1.5}$

4.2.5.1 Spectroscopic characterisation of 14^{Bn} + $Me_{1.5}AlCl_{1.5}$ reaction mixtures

$AlCl_3$ (400 mg, 3 mmol), toluene (1.5 ml) and TMA (1.5 ml, 3 mmol, 2.0 M in toluene) were heated to form $Me_{1.5}AlCl_{1.5}$ (6 mmol, 2.0 M in toluene). **14**^{Bn} (304 mg, 0.5 mmol) in toluene (4 ml) was added dropwise at −78 °C to give a yellow solution and the mixture allowed to warm to room temperature to give a clear liquid and a white suspension. After stirring for 2 hours the solvent was removed *in vacuo* to give an intractable white solid.

Yield 480 mg

Heating the toluene solution to reflux for 2 hours produced a yellow solution. An aliquot of the solution was analysed by NMR spectroscopy.

^{1}H NMR spectroscopy (400 MHz, benzene-d_6): δ 7.36-6.76 (m, **7a** + **7b** + **11a** + **11b** + **14**^{Bn}($Me_{1.5}AlCl_{1.5}$) Ph), 6.28 (s, 0.10H, **7a** CH=C), 4.80 (s, 0.11H, **7b** C=CH_2), 4.75 (s, 0.11H, **7b** C=CH_2), 4.65-3.50 (m, br, 8H, **14**^{Bn}($Me_{1.5}AlCl_{1.5}$) CH_2 + **14**^{Bn}($Me_{1.5}AlCl_{1.5}$) CH_2O + **20** CH_2O + **21** CH_2O), 3.15 (s, 0.24H, **7b** CH_2), 2.76 (s, 0.11H, **11b** CH_2), 1.72 (s, 0.4H, **7a** Me), 1.69 (s, 0.4H, **7a** Me), 1.55 (s, 0.3H, **7b** Me), 1.22 (s, 0.22H, **11b** Me), 0.87 (m, 0.4H, **11a** Me), 0.84 (s, 0.16H, **10** Me), 0.10-−0.60 (m, 17H, unassigned AlMe), −0.37 (s, 19H, **14**^{Bn}($Me_{1.5}AlCl_{1.5}$))

^{13}C NMR spectroscopy (100 MHz, benzene-d_6): δ 66.8 (**14**^{Bn}($Me_{1.5}AlCl_{1.5}$ CH_2O), 41.5 (**14**^{Bn}($Me_{1.5}AlCl_{1.5}$ CH_2), −6.9 (**14**^{Bn}($Me_{1.5}AlCl_{1.5}$ AlMe)

^{27}Al NMR spectroscopy (104 MHz, benzene-d_6): δ 179.3 (**14**^{Bn}($Me_{1.5}AlCl_{1.5}$), 131.8

4.2.6 Reactivity of RL 32H with Methylaluminium Reagents

4.2.6.1 Spectroscopic characterisation of RL 32H + TMA reaction mixtures

TMA (3 ml, 6 mmol, 2.0 M in toluene) was added dropwise to RL 32H (0.27 ml, 0.5 mmol) under a N_2 atmosphere at −78 °C and allowed to reach room temperature. An aliquot of the solution was analysed by NMR spectroscopy.

^{1}H NMR spectroscopy (400 MHz, toluene-d_8): δ 4.72-3.40 (m, 6.4H, **15** CH_2O), 1.58-0.99 (m, 59H, **4**^{R}(TMA) CH_2), 1.24, 1.23 (s, 5.7H, **4**^{R}(TMA) Me), 1.14 (s, 9.4H, **4**^{R}(TMA) Me), 1.12 (s, 9.0H, **4**^{R}(TMA) Me), 0.11-0.10 (s, 10.9H, **4**^{R}(TMA) $AlMe_b$), −0.21-−0.62 (m, 36H, **15** AlMe), −0.37 (s, 72H, TMA AlMe), −0.48 (s, 10.9H, **4**^{R}(TMA) $AlMe_t$), −0.50 (s, 17.2H, **4**^{R}(TMA) $AlMe_t$), −0.51 (s, 18.0H, **4**^{R}(TMA) $AlMe_t$)

^{13}C NMR spectroscopy (100 MHz, toluene-d_8): δ 80.4, 79.6, 79.5 (**4**^{R}(TMA) CO), 54.7, 53.6, 44.7, 44.4, 32.2, 31.3, 30.3, 30.0, 29.7, 29.1, 28.8, 28.7, 27.1, 26.8, 25.0, 24.5, 23.3, 23.0, 14.3, 14.1 (**4**^{R}(TMA) CH_2 + Me), −4.2 (**4**^{R}(TMA) $AlMe_b$), −6.6 (br, **4**^{R}(TMA) $AlMe_t$), −6.6 (TMA AlMe)

^{27}Al NMR spectroscopy (104 MHz, toluene-d_8): δ 157.7 (**4**^{R}(TMA))

TMA (2 ml, 4 mmol, 2.0 M in toluene) was added dropwise to RL 32H (0.27 ml, 0.5 mmol) under a N_2 atmosphere at −78 °C and allowed to reach room temperature. The solution was then heated to reflux for 2 hours. An aliquot of the solution was analysed by NMR spectroscopy.

^{1}H NMR spectroscopy (400 MHz, toluene-d_8): δ 4.38-2.89 (m, 8H, CH_2O), 1.89-0.78 (m, 59H, CH_2 + Me), 0.11-0.10 (s, 4.8H, $AlMe_b$), −0.20-−0.60 (m, 58H, AlMe)

^{13}C NMR spectroscopy (100 MHz, toluene-d_8): δ 80.0, 79.2, 78.4, 77.5, 77.0 (CO), 69.8, 65.7, 64.7, 62.4, 54.8, 54.7, 54.3, 53.3, 53.2, 44.9, 44.7, 44.6, 44.4, 44.1, 43.7, 31.8, 30.9, 29.9, 29.7, 29.6, 29.5, 29.3, 28.8, 28.7, 28.6, 28.4, 26.9, 26.8, 26.5, 26.4, 24.7, 24.3, 24.2, 23.0, 22.9, 22.7, 13.9, 13.7 (CH_2 + Me), −4.5, −4.6, −6.9, −7.1, −8.0, −8.2, −8.3, −8.7 (AlMe)

^{27}Al NMR spectroscopy (104 MHz, toluene-d_8): δ 157.3 (**15**(**4**^{R})$_4$ + **19**(**4**^{R})$_2$), 9.1 (**19**(**4**^{R})$_2$)

4.2.6.2 Spectroscopic characterisation of RL 32H + Me_2AlCl reaction mixtures

$AlCl_3$ (267 mg, 2 mmol), toluene (1 ml) and TMA (2 ml, 4 mmol, 2.0 M in toluene) were heated to form Me_2AlCl (6 mmol, 2.0 M in toluene). RL 32H (0.27 ml, 0.5 mmol) was added dropwise at −78 °C and the mixture allowed to warm to room temperature to give a colourless solution. An aliquot of the solution was analysed by NMR spectroscopy.

^{1}H NMR spectroscopy (400 MHz, toluene-d_8): δ 4.95-3.80 (m, 8H, CH_2O), 2.91-0.72 (m, 55H, CH_2 + Me), −0.18-−0.51 (m, 72H, AlMe)

^{13}C NMR spectroscopy (100 MHz, toluene-d_8): δ 185.8, 184.9 (C=O(Me_2AlCl)), 68.3 (CH_2O), 50.7, 45.0, 44.6, 41.7, 36.1, 35.8, 31.5, 31.1, 30.0, 28.9, 28.6, 28.5, 27.0, 25.1, 22.8, 22.4, 14.1, 13.5 (CH_2 + Me), −6.4 (AlMe)

^{27}Al NMR spectroscopy (104 MHz, toluene-d_8): δ 179.8

The NMR sample was then heated in a J Young NMR tube to 70 °C for 24 hours.

^{1}H NMR spectroscopy (400 MHz, toluene-d_8): δ 5.29-3.26 (m, 8H, CH_2O), 4.75 (m, 1.5H, alkene C=CH_2), 2.91-0.72 (m, 67H, CH_2 + Me), 0.17 (s, 1.3H, MeH), 0.08-−0.53 (m, 71H, AlMe)

^{13}C NMR spectroscopy (100 MHz, toluene-d_8): δ 110.1 (alkene C=CH_2), 84.1, 81.3 (CO), 51.1, 44.9, 44.8, 44.6, 44.5, 32.1, 30.2, 29.9, 29.8, 28.6, 27.1, 25.1, 23.1, 23.0, 22.8, 14.3, 14.0 (CH_2 + Me), −6.3 (AlMe)

^{27}Al NMR spectroscopy (104 MHz, toluene-d_8): δ 177.8, 130.5, 8.5

The NMR sample was then heated in a J Young NMR tube to 100 °C for 24 hours.

^{1}H NMR spectroscopy (400 MHz, toluene-d_8): δ 5.29-3.26 (m, 8H, CH_2O), 5.16 (m, 0.4H, alkene C=CH), 4.75 (m, 3.3H, alkene C=CH_2), 1.95-0.68 (m, 56H, CH_2 + Me), 0.17 (s, 3.6H, MeH), 0.06-−0.55 (m, 52H, AlMe)

^{13}C NMR spectroscopy (100 MHz, toluene-d_8): δ 145.9, 145.8, 144.7 (alkene C), 125.3 (alkene C=CH), 112.1, 110.2 (alkene =CH), 51.1, 50.4, 48.7, 38.2, 37.9, 32.2, 32.0, 31.1,

30.4, 30.2, 29.5, 28.5, 28.0, 27.4, 25.8, 23.4, 23.1, 22.8, 22.6, 22.4, 22.2, 17.7, 14.3, 14.2, 14.0 (CH_2 + Me), −4.4 (MeH), −6.4 (AlMe)

^{27}Al NMR spectroscopy (104 MHz, toluene-d_8): δ 178.6, 9.0

4.2.6.3 Spectroscopic characterisation of RL 32H + $MeAlCl_2$ reaction mixtures

$AlCl_3$ (533 mg, 4 mmol), toluene (2 ml) and TMA (1 ml, 2 mmol, 2.0 M in toluene) were heated to form $MeAlCl_2$ (6 mmol, 2.0 M in toluene). RL 32H (0.27 ml, 0.5 mmol) was added dropwise at −78 °C and the mixture allowed to warm to room temperature to give a colourless solution. An aliquot of the solution was analysed by NMR spectroscopy.

^{1}H NMR spectroscopy (400 MHz, toluene-d_8): δ 5.43-4.66 (m, 8H, CH_2O), 3.13-0.78 (m, 54H, CH_2 + Me), 0.05-−0.51 (m, 36H, AlMe)

^{13}C NMR spectroscopy (100 MHz, toluene-d_8): δ 188.5 (C=O(Me_2AlCl)), 75.4, 70.1 (CH_2O), 50.8, 45.4, 43.5, 41.6, 36.7, 36.4, 31.4, 31.2, 29.9, 28.9, 25.5, 22.7, 22.4, 14.1, 13.4 (CH_2 + Me), −6.6 (AlMe)

^{27}Al NMR spectroscopy (104 MHz, toluene-d_8): δ 178.7 (C=O($MeAlCl_2$)), 141.0 ($MeAlCl_2$)

The NMR sample was then heated in a J Young NMR tube to 100 °C for 24 hours.

^{1}H NMR spectroscopy (400 MHz, toluene-d_8): δ 5.12-2.62 (m, 8H, CH_2O), 2.01-0.60 (m, 48H, CH_2 + Me), 0.05-−0.49 (m, 22H, AlMe)

^{13}C NMR spectroscopy (100 MHz, toluene-d_8): δ 239.3 (C=O(Me_2AlCl)), 54.4, 50.2, 50.0, 45.5, 45.2, 31.2, 31.1, 30.5, 29.5, 29.4, 28.0, 27.4, 25.2, 23.4, 22.3, 21.6, 13.8, 13.1 (CH_2 + Me)

^{27}Al NMR spectroscopy (104 MHz, toluene-d_8): δ 137.0, 97.3, 12.1

4.2.6.4 Spectroscopic characterisation of RL 32H + $Me_{1.5}AlCl_{1.5}$ reaction mixtures

$AlCl_3$ (400 mg, 3 mmol), toluene (1.5 ml) and TMA (1.5 ml, 3 mmol, 2.0 M in toluene) were heated to form $Me_{1.5}AlCl_{1.5}$ (6 mmol, 2.0 M in toluene). RL 32H (0.27 ml, 0.5 mmol)

was added dropwise at −78 °C and the mixture allowed to warm to room temperature to give a colourless solution. An aliquot of the solution was analysed by NMR spectroscopy.

^{1}H NMR spectroscopy (400 MHz, toluene-d_8): δ 5.32-4.65 (m, 8H, CH_2O), 3.08-0.72 (m, 56H, CH_2 + Me), 0.12-−0.49 (m, 54H, AlMe)

^{13}C NMR spectroscopy (100 MHz, toluene-d_8): δ 187.3 (C=O($Me_{1.5}AlCl_{1.5}$)), 69.4 (CH_2O), 50.7, 45.2, 41.8, 36.4, 36.1, 31.4, 31.2, 29.9, 28.9, 27.1, 25.3, 22.7, 22.4, 14.1, 13.5 (CH_2 + Me), −6.4 (AlMe)

^{27}Al NMR spectroscopy (104 MHz, toluene-d_8): δ 179.0 (C=O($Me_{1.5}AlCl_{1.5}$))

The NMR sample was then heated in a J Young NMR tube to 100 °C for 24 hours.

^{1}H NMR spectroscopy (400 MHz, toluene-d_8): δ 5.32-4.69 (m, 3H, alkene), 4.46-2.70 (m, 8H, CH_2O), 1.81-0.53 (m, 53H, CH_2 + Me), 0.17 (s, 1.5H, MeH), 0.04-−0.50 (m, 45H, AlMe)

^{13}C NMR spectroscopy (100 MHz, toluene-d_8): δ 110.8 (alkene =CH), 50.4, 45.1, 36.4, 30.3, 30.2, 29.8, 29.5, 22.7, 14.1, 13.4 (CH_2 + Me), −4.4 (MeH), −6.6 (AlMe)

^{27}Al NMR spectroscopy (104 MHz, toluene-d_8): δ 186.2, 136.7, 12.1

4.3 Reactions of Polyols with Methylaluminium Reagents

4.3.1 Synthesis and Characterisation of $MeAl\{Me_2C(CH_2O)_2AlMe_2\}_2$ 22

TMA (1.5 ml, 3 mmol, 2.0 M in toluene) was added dropwise to a solution of neopentyl glycol (208 mg, 2 mmol) in diethyl ether (10 ml) under a N_2 atmosphere at −78 °C. As the solution was allowed to slowly warm to room temperature it started to effervesce. A cloudy white precipitate formed at the same time. The diethyl ether was removed *in vacuo* and was replaced by pentane (10 ml). The solution was filtered and stored at −20 °C, producing colourless crystalline needles.

Yield 70 mg (19% wrt neopentyl glycol)

Melting point 102-105 °C

Elemental analysis calculated for $C_{15}H_{35}Al_3O_4$ (%): C 49.99, H 9.79; found (%): C 50.18, H 10.32

^{1}H NMR spectroscopy (500 MHz, benzene-d_6): δ 3.34 (d, J = 10.4 Hz, 4H, CH_2O), 2.99 (d, J = 10.4 Hz, 4H, CH_2O), 0.92 (s, 6H, Me), 0.14 (s, 6H, Me), −0.42 (s, 6H, AlMe), −0.49 (s, 6H, AlMe), −0.53 (s, 3H, AlMe)

^{13}C NMR spectroscopy (125 MHz, benzene-d_6): δ 72.4 (CH_2O), 34.5 (C_{quat}), 21.6 (Me), 20.6 (Me), −11.0 (br, AlMe)

^{27}Al NMR spectroscopy (130 MHz, benzene-d_6): δ 157.6 (4-coordinate Al)

X-ray crystallography $C_{15}H_{35}Al_3O_4$, M = 360.37, Orthorhombic, $P2_12_12_1$, a = 8.43520(10), b = 15.6400(2), c = 34.2017(4) Å, α = 90, β = 90, γ = 90°, V = 4512.11(9) Å^3, Z = 8, ρ_{calcd} = 1.061 g cm^{-3}, λ = 0.71073 Å, μ = 0.179 mm^{-1}, T = 180(2) K, 25589 reflections collected, 9640 unique, θ_{max} = 27.476°, R_{int} = 0.0453, $R1$ = 0.0499 ($F_{obs} > 4\sigma(F_{obs})$), $wR2$ = 0.1238, S = 1.064, 415 parameters, peak/hole 0.371/−0.358 e Å^{-3}

4.3.2 Synthesis and Characterisation of {Me$_2$C(CH$_2$O)$_2$AlMe(AlMeCl$_2$)}$_2$ 23$_2$

Me_2AlCl (4 ml, 4 mmol, 1.0 M in hexane) was added dropwise to a solution of neopentyl glycol (208 mg, 2 mmol) in toluene (10 ml) under a N_2 atmosphere at −78 °C. As the solution was allowed to slowly warm to room temperature it started to effervesce, with the precipitation of a white solid. Heating dissolved the precipitate and slow cooling produced colourless crystalline needles.

Yield 294 mg (57% wrt neopentyl glycol)

Melting point 188-190 °C

Elemental analysis calculated for $C_{14}H_{32}Al_4Cl_4O_4$ (%): C 32.71, H 6.27, Cl 27.58; found (%): C 33.03, H 6.39, Cl 28.31

^{1}H NMR spectroscopy (400 MHz, benzene-d_6): δ 3.55 (dd, J = 11.6, 1.7 Hz, 2H, CH_2O), 3.40 (dd, J = 11.4, 1.7 Hz, 2H, CH_2O), 3.33 (d, J = 11.4 Hz, 2H, CH_2O), 3.17 (d, J = 11.6 Hz, 2H, CH_2O), 0.57 (s, 6H, Me), 0.15 (s, 6H, Me), −0.24 (s, 6H, AlMe), −0.30 (s, 6H, AlMe)

^{13}C NMR spectroscopy (100 MHz, benzene-d_6): δ 74.9 (CH_2O), 74.7 (CH_2O), 34.9 (C_{quat}), 21.5 (Me), 20.5 (Me)

^{27}Al NMR spectroscopy (104 MHz, benzene-d_6): Only background signal

X-ray crystallography $C_{14}H_{32}Al_4Cl_4O_4$, M = 514.11, Triclinic, $P\bar{1}$, a = 6.6048(3), b = 8.6863(3), c = 11.7813(5) Å, α = 92.4770(10), β = 103.0550(10), γ = 107.9600(10)°, V = 621.69(4) Å^3, Z = 1, ρ_{calcd} = 1.373 g cm^{-3}, λ = 1.54184 Å, μ = 5.845 mm^{-1}, T = 180(2) K, 21769 reflections collected, 2448 unique, θ_{max} = 72.162°, R_{int} = 0.0347, $R1$ = 0.0338 (F_{obs} > 4σ(F_{obs})), $wR2$ = 0.0941, S = 1.067, 122 parameters, peak/hole 0.434/−0.500 e Å^{-3}

4.3.3 Synthesis and Characterisation of (ClAl{$Me_2C(CH_2O)_2AlCl_2$}$_2$)(THF)$_2$ 24(THF)$_2$

Me_2AlCl (4 ml, 4 mmol, 1.0 M in hexane) was added dropwise to a solution of neopentyl glycol (208 mg, 2 mmol) in toluene (10 ml) under a N_2 atmosphere at −78 °C. As the solution was allowed to slowly warm to room temperature it started to effervesce, with the precipitation of a white solid. Addition of THF (1 ml) resulted in solvation to give a colourless solution. The solvent was removed *in vacuo* to give a white solid, which was dissolved in toluene (1 ml) and stored at −27 °C to give colourless crystals.

Yield 70 mg (11% wrt neopentyl glycol)

Melting point turned brown at 220 °C

Elemental analysis calculated for $C_{18}H_{36}Al_3Cl_5O_6$ (%): C 35.64, H 5.98, Cl 29.22; found (%): C 39.85, H 6.63, Cl 21.10 (suggests THF in sample)

^{1}H NMR spectroscopy (400 MHz, benzene-d_6): δ 3.60 (m, br, 8H, CH_2O THF), 3.44 (d, J = 10.7 Hz, 2.6H, CH_2O), 3.22 (d, J = 10.6 Hz, 1.3H CH_2O), 3.01 (d, J = 10.7 Hz, 2.6H, CH_2O), 2.98 (d, J = 10.6 Hz, 1.3H, CH_2O), 1.14 (s, 2H, Me), 1.11 (m, br, 8H, CH_2 THF), 0.94 (s, 2.8H, Me), 0.91 (s, 1.8H, Me), 0.18 (s, 2.1H, Me), 0.03 (s, 2.2H, Me), 0.02 (s, 1.9H, Me)

^{13}C NMR spectroscopy (100 MHz, benzene-d_6): δ 73.4, 73.0, 72.6 (CH_2O), 70.3 (CH_2O THF), 34.4, 34.1, 34.0 (C_{quat}), 24.7 (CH_2 THF), 21.4, 21.0, 20.9, 20.2, 19.8, 19.7 (Me)

^{27}Al NMR spectroscopy (104 MHz, benzene-d_6): δ 53.9 (5-coordinate Al), 45.8 (5-coordinate Al)

X-ray crystallography $C_{18}H_{36}Al_3Cl_5O_6$, M = 606.69, Monoclinic, $P2_1/c$, a = 8.2198(3), b = 38.1620(12), c = 9.2276(3) Å, α = 90, β = 96.3890(10), γ = 90°, V = 2876.57(17) Å^3, Z = 4, ρ_{calcd} = 1.401 g cm^{-3}, λ = 1.54184 Å, μ = 5.747 mm^{-1}, T = 180(2) K, 33970 reflections collected, 4130 unique, θ_{max} = 59.028°, R_{int} = 0.0481, $R1$ = 0.0677 ($F_{obs} > 4\sigma(F_{obs})$), $wR2$ = 0.2014, S = 1.070, 293 parameters, peak/hole 0.872/−1.272 e Å^{-3}

4.3.4 Synthesis and Characterisation of ClAl{Me$_2$C(CH$_2$O)$_2$AlCl$_2$}$_2$ 24

$AlCl_3$ (533 mg, 4 mmol), toluene (2 ml) and TMA (1 ml, 2 mmol, 2.0 M in toluene) were combined and heated to form $MeAlCl_2$ (6 mmol). A solution of neopentyl glycol (312 mg, 3 mmol) in toluene (15 ml) was added dropwise at under a N_2 atmosphere −78 °C. As the solution was allowed to slowly warm to room temperature it started to effervesce, and a white precipitate formed. The precipitate was removed by filtration and storage of the filtrate at −27 °C produced colourless crystalline needles.

Yield 70 mg (15% wrt neopentyl glycol)

Melting point > 250 °C

Elemental analysis calculated for $C_{24}H_{36}Al_3Cl_5O_4$ (%): C 25.97, H 4.36, Cl 38.33; found (%): C 26.73, H 4.54, Cl 33.61

^{1}H NMR spectroscopy (400 MHz, benzene-d_6): δ 3.27 (d, J = 10.7 Hz, 4H, CH_2O), 2.84 (d, J = 10.7 Hz, 4H, CH_2O), 0.82 (s, 6H, Me), −0.19 (s, 6H, Me)

^{13}C NMR spectroscopy (100 MHz, benzene-d_6): δ 73.9 (CH_2O), 33.8 (C_{quat}), 20.4 (Me), 19.0 (Me)

^{27}Al NMR spectroscopy (104 MHz, benzene-d_6): δ 101.6 (4-coordinate Al), 45.8 (5-coordinate Al)

X-ray crystallography $C_{24}H_{36}Al_3Cl_5O_4$, M = 646.72, Triclinic, $P\bar{1}$, a = 8.5045(3), b = 11.5663(5), c = 17.2917(7) Å, α = 97.616(2), β = 99.823(2), γ = 99.338(2)°, V = 1631.16(11) Å^3, Z = 2, ρ_{calcd} = 1.317 g cm^{-3}, λ = 1.54184 Å, μ = 5.059 mm^{-1}, T = 180(2) K, 44477

reflections collected, 5773 unique, θ_{max} = 66.763°, R_{int} = 0.0639, $R1$ = 0.0544 (F_{obs} > 4σ(F_{obs})), $wR2$ = 0.1392, S = 1.055, 361 parameters, peak/hole 0.563/−0.502 e Å^{-3}

4.3.5 Synthesis and Characterisation of Al{MeC(CH$_2$O)$_3$}$_2$(AlMe$_2$)$_3$ 25

TMA (1 ml, 2 mmol, 2.0 M in toluene) was added dropwise to a solution of trimethylolethane (0.120 g, 1 mmol) in THF (10 ml) under a N_2 atmosphere at −78 °C. As the solution was allowed to slowly warm up to room temperature it started to effervesce. It formed a clear solution which, when the solvent was removed *in vacuo*, formed a white solid. The solid was partially dissolved in pentane and filtered. After 3 days at room temperature small colourless crystals formed.

Yield 45 mg (21% wrt trimethylolethane)

Sublimed at 210-212 °C

Elemental analysis calculated for $C_{16}H_{36}Al_4O_6$ (%): C 44.45, H 8.39; found (%): C 42.33, H 8.25

^{1}H NMR spectroscopy (500 MHz, benzene-d_6): δ 3.48 (s, 12H, CH_2O), −0.25 (s, 6H, Me), −0.42 (s, 18H, AlMe)

^{13}C NMR spectroscopy (125 MHz, benzene-d_6): δ 73.1 (CH_2O), 36.3 (C_{quat}), 14.6 (Me), −11.8 (br, AlMe)

^{27}Al NMR spectroscopy (130 MHz, benzene-d_6): δ 163.7 (br, 4-coordinate Al), 7.6 (6-coordinate Al)

X-ray crystallography $C_{16}H_{36}Al_4O_6$, M = 432.37, Monoclinic, $C2$, a = 17.4165(7), b = 9.4901(4), c = 16.6391(8) Å, α = 90, β = 112.240(2), γ = 90°, V = 2545.6(2) Å^3, Z = 4, ρ_{calcd} = 1.128 g cm^{-3}, λ = 0.71073 Å, μ = 0.207 mm^{-1}, T = 180(2) K, 11071 reflections collected, 5067 unique, θ_{max} = 27.574°, R_{int} = 0.0549, $R1$ = 0.0550 (F_{obs} > 4σ(F_{obs})), $wR2$ = 0.1213, S = 1.040, 243 parameters, peak/hole 0.232/−0.289 e Å^{-3}

4.3.6 Reaction of Trimethylolethane with Me$_2$AlCl

Me$_2$AlCl (2 ml, 2 mmol, 1.0 M in hexane) was added dropwise to a solution of trimethylolethane (0.120 g, 1 mmol) in THF (10 ml) under a N_2 atmosphere at −78 °C. As

the solution was allowed to slowly warm up to room temperature it started to effervesce. It formed a clear solution which, when placed under vacuum to remove the solvent, formed a white solid. Attempts to purify the solid proved unsuccessful.

Yield 200 mg

Elemental analysis satisfactory analysis could not be achieved

^{1}H NMR spectroscopy (400 MHz, benzene-d_6): δ 4.20-3.52 (m, br, 12H, CH_2O), 3.48 (m, 12H, THF), 0.94 (m, 12H, THF), −0.28 (s, 6H, AlMe), −0.35 (s, 6H, Me)

^{13}C NMR spectroscopy (100 MHz, benzene-d_6): δ 72.8 (CH_2O), 71.3 (THF), 24.4 (THF), 14.6 (Me), −8.7 (AlMe)

^{27}Al NMR spectroscopy (104 MHz, benzene-d_6): δ 134.2 (br, 4-coordinate Al), 7.6 (6-coordinate Al)

4.3.7 Synthesis and Characterisation of $Al\{MeC(CH_2O)_3\}_2(AlCl_2)_3(THF)_4$ 27$(THF)_4$

$AlCl_3$ (178 mg, 1.33 mmol), toluene (0.67 ml) and TMA (0.33 ml, 0.67 mmol, 2.0 M in toluene) were combined and heated to form $MeAlCl_2$ (2 mmol). A solution of neopentyl glycol (120 mg, 1 mmol) in THF (10 ml) was added dropwise at under a N_2 atmosphere −78 °C. As the solution was allowed to slowly warm up to room temperature it started to effervesce. It formed a clear solution which, when placed under vacuum to remove the solvent, formed a white solid. The solid was redissolved in THF (3 ml) and storage at 4 °C produced small colourless crystals.

Yield 193 mg (42% wrt trimethylolethane)

Melting point 143-146 °C

Elemental analysis calculated for $C_{30}H_{58}Al_4Cl_6O_{11}$ (%): C 39.36, H 6.39, Cl 23.24; found (%): C 39.18, H 6.60, Cl 24.86

^{1}H NMR spectroscopy (400 MHz, chloroform-*d*): δ 4.32-3.70 (m, 32H, CH_2O + THF), 1.95 (m, 20H, THF), 0.80-0.47 (m, 6H, Me)

^{13}C NMR spectroscopy (100 MHz, chloroform-*d*): δ 72.5 (br, CH_2O), 70.1 (THF), 38.0 (br, C_{quat}), 25.5 (THF), 15.8 (br, Me)

^{27}Al NMR spectroscopy (104 MHz, chloroform-*d*): δ 74.2 (5-coordinate Al), 8.2 (6-coordinate Al)

X-ray crystallography $C_{30}H_{58}Al_4Cl_6O_{11}$, M = 915.38, Triclinic, $P\bar{1}$, a = 13.0699(6), b = 13.3031(6), c = 14.0898(6) Å, α = 95.204(2), β = 93.748(2), γ = 117.370(2)°, V = 2150.65(17) Å^3, Z = 2, ρ_{calcd} = 1.414 g cm^{-3}, λ = 0.71073 Å, μ = 4.873 mm^{-1}, T = 180(2) K, 61968 reflections collected, 7590 unique, θ_{max} = 66.799°, R_{int} = 0.0557, $R1$ = 0.0451 (F_{obs} > 4σ(F_{obs})), $wR2$ = 0.1304, S = 1.035, 490 parameters, peak/hole 0.535/−0.475 *e* Å^{-3}

4.3.8 Reaction of Pentaerythritol with TMA

TMA (2 ml, 4 mmol, 2.0 M in toluene) was added dropwise to a solution of pentaerythritol (136 mg, 1 mmol) in pyridine (10 ml) under a N_2 atmosphere at −78 °C. As the solution was allowed to slowly warm to room temperature it started to effervesce. A cloudy white precipitate formed at the same time. The pyridine was removed *in vacuo* to give an intractable white solid.

Yield 500 mg

Elemental analysis found (%): C = 48.88, H = 8.12, N = 4.23

4.4 Reactivity of Ethers with Methylaluminium Reagents

4.4.1 Reactivity of Ethers with TMA

4.4.1.1. Spectroscopic characterisation of MTBE + TMA reaction mixtures

Methyl *tert*-butyl ether (0.36 ml, 3 mmol) was added dropwise to TMA (1.5 ml, 3 mmol, 2.0 M in toluene) under a N_2 atmosphere. The resulting solution was stirred for 2 hours at room temperature. An aliquot of the solution was analysed by NMR spectroscopy.

^{1}H NMR spectroscopy (400 MHz, benzene-d_6): δ 2.93 (s, 3H, MTBE(TMA) OMe), 0.93 (s, 9H, MTBE(TMA) Me), −0.37 (s, 9H, MTBE(TMA) AlMe)

^{13}C NMR spectroscopy (100 MHz, benzene-d_6): δ 84.7 (MTBE(TMA)) CO), 52.2 (MTBE(TMA)) OMe), 26.7 (MTBE(TMA)) Me), −7.7 (MTBE(TMA)) AlMe)

^{27}Al NMR spectroscopy (104 MHz, benzene-d_6): δ 185.4 (MTBE(TMA))

The above toluene solution was heated to reflux for 2 hours and then an aliquot of the solution was analysed by NMR spectroscopy.

^{1}H NMR spectroscopy (400 MHz, benzene-d_6): δ 4.73 (m, 0.1H, **28** C=CH_2), 3.08 (s, 1.3H, **3** OMe), 2.92 (s, 1.7H, MTBE(TMA) OMe), 1.60 (m, 0.4H, **28** Me), 0.92 (m, 5.8H, MTBE(TMA) Me), −0.36 (m, 5.4H, MTBE(TMA) AlMe), −0.59 (s, 2.8H, **3** AlMe)

^{13}C NMR spectroscopy (100 MHz, benzene-d_6): δ 141.6 (**28** C), 110.7 (**28** C=CH_2), 84.7 (MTBE(TMA)) CO), 52.2 (MTBE(TMA)) OMe), 50.4 (**3** OMe), 26.6 (MTBE(TMA)) Me), 23.7 (**28** Me), −5.1 (**3** AlMe)

^{27}Al NMR spectroscopy (104 MHz, benzene-d_6): δ 185.0 (MTBE(TMA)), 153.0 (**3**)

4.4.2 Reactivity of Ethers with Me_2AlCl

4.4.2.1 Spectroscopic characterisation of MTBE + Me_2AlCl reaction mixtures

$AlCl_3$ (133 mg, 1 mmol), toluene (0.5 ml) and TMA (1 ml, 2 mmol, 2.0 M in toluene) were heated to form Me_2AlCl (3 mmol, 2.0 M in toluene). Methyl *tert*-butyl ether (0.36 ml, 3 mmol) was added dropwise under a N_2 atmosphere. The resulting solution was stirred for 2 hours at room temperature. An aliquot of the solution was analysed by NMR spectroscopy.

^{1}H NMR spectroscopy (400 MHz, benzene-d_6): δ 3.02 (s, 3H, MTBE(Me_2AlCl) OMe), 0.96 (s, 9H, MTBE(Me_2AlCl) Me), −0.28 (s, 6H, MTBE(Me_2AlCl) AlMe)

^{13}C NMR spectroscopy (100 MHz, benzene-d_6): δ 87.7 (MTBE(Me_2AlCl)) CO), 52.9 (MTBE(Me_2AlCl)) OMe), 26.7 (MTBE(Me_2AlCl)) Me), −4.2 (MTBE(Me_2AlCl)) AlMe)

^{27}Al NMR spectroscopy (104 MHz, benzene-d_6): δ 162.2 (MTBE(Me_2AlCl))

The above toluene solution was heated to reflux for 2 hours and then an aliquot of the solution was analysed by NMR spectroscopy.

^{1}H NMR spectroscopy (400 MHz, benzene-d_6): δ 4.74 (m, 0.1H, **28** C=CH_2), 3.22, 3.18, 3.14, 3.08 (m, 3H, **5** OMe), 1.59 (m, 0.3H, **28** Me), −0.43, −0.49, −0.60, −0.61 (m, 3H, **5** AlMe)

^{13}C NMR spectroscopy (100 MHz, benzene-d_6): δ 141.6 (**28** C), 110.7 (**28** C=CH_2), 53.0, 52.9, 52.5, 51.7 (**5** OMe), 23.7 (**28** Me)

^{27}Al NMR spectroscopy (104 MHz, benzene-d_6): δ 124.3, 95.0, 48.4, 9.6 (**5**)

0.1 ml of the 1:1 Me_2AlCl:MTBE toluene solution was placed in a sealed J Young NMR tube with 0.6 ml of toluene-d_8 and heated to 100 °C for 2 hours.

^{1}H NMR spectroscopy (400 MHz, toluene-d_8): δ 4.69 (m, 1.3H, **28** C=CH_2), 3.25, 3.22, 3.19, 3.13 (m, 3H, **5** OMe), 1.59 (m, 4.4H, **28** Me), 0.16 (s, 0.7H, MeH), −0.47, −0.50, −0.53, −0.63 (m, 3H, **5** AlMe)

^{13}C NMR spectroscopy (100 MHz, toluene-d_8): δ 141.8 (**28** C), 111.1 (**28** C=CH_2), 53.4, 53.3, 52.8, 52.1 (**5** OMe), 24.1 (**28** Me), −4.4 (MeH), −11.3 (**5** AlMe)

^{27}Al NMR spectroscopy (104 MHz, toluene-d_8): δ 124.2, 95.0 (**5**)

4.4.3 Reactivity of Ethers with $MeAlCl_2$

4.4.3.1 Spectroscopic characterisation of MTBE + $MeAlCl_2$ reaction mixtures

$AlCl_3$ (267 mg, 2 mmol), toluene (1 ml) and TMA (0.5 ml, 1 mmol, 2.0 M in toluene) were heated to form $MeAlCl_2$ (3 mmol, 2.0 M in toluene). Methyl *tert*-butyl ether (0.36 ml, 3 mmol) was added dropwise under a N_2 atmosphere. The resulting yellow solution was stirred for 2 hours at room temperature. An aliquot of the solution was analysed by NMR spectroscopy.

^{1}H NMR spectroscopy (400 MHz, benzene-d_6): δ 3.27 (s, 3H, **6** OMe), 1.21 (s, 9H, **29** Me)

^{13}C NMR spectroscopy (100 MHz, benzene-d_6): δ 150.6 (**29** C), 137.3 (**29** C), 56.5 (**6** OMe), 34.2 (**29** C_{quat}), 31.1 (**29** Me), 21.0 (**29** Me)

^{27}Al NMR spectroscopy (104 MHz, benzene-d_6): δ 102.6, 95.5, 80.6 (**6**)

The above reaction was repeated but toluene was replaced with hexane. After 2 hours stirring at room temperature hexane was removed *in vacuo* to give an orange solid.

Yield 400 mg

^{1}H NMR spectroscopy (400 MHz, benzene-d_6): δ 3.26 (s, 3H, **6** OMe), 1.8-0.4 (m, 6H, polymer)

^{13}C NMR spectroscopy (100 MHz, benzene-d_6): δ 56.5 (**6** OMe), 29.2, 27.2 (polymer)

^{27}Al NMR spectroscopy (104 MHz, benzene-d_6): δ 104.4, 100.1, 95.5, 47.9, 8.1 (**6**)

4.4.3.2 Spectroscopic characterisation of 2-MeTHF + $MeAlCl_2$ reaction mixtures

$AlCl_3$ (533 mg, 4 mmol), toluene (2 ml) and TMA (1 ml, 2 mmol, 2.0 M in toluene) were heated to form $MeAlCl_2$ (6 mmol, 2.0 M in toluene). 2-MeTHF (0.30 ml, 3 mmol) was added dropwise under a N_2 atmosphere. The solution was stirred for 2 hours at room temperature. An aliquot of the solution was analysed by NMR spectroscopy.

^{1}H NMR spectroscopy (400 MHz, toluene-d_8): δ 4.56, 4.47 (m, 1H, 2-MeTHF($MeAlCl_2$) OCH), 3.81 (m, 1H, 2-MeTHF($MeAlCl_2$) CH_2O), 3.60 (m, 1H, 2-MeTHF($MeAlCl_2$) CH_2O), 1.44-1.09 (m, 3H, 2-MeTHF($MeAlCl_2$) CH_2), 0.95-0.82 (m, 4H, 2-MeTHF($MeAlCl_2$) CH_2 +Me), −0.05-−0.50 (m, 6H, 2-MeTHF($MeAlCl_2$) AlMe)

^{13}C NMR spectroscopy (100 MHz, toluene-d_8): δ 86.4, 84.5 (2-MeTHF($MeAlCl_2$) OCH), 73.5, 72.4 (2-MeTHF($MeAlCl_2$) CH_2O), 31.3, 31.1, 23.9, 23.8 (2-MeTHF($MeAlCl_2$) CH_2), 20.0, 19.9 (2-MeTHF($MeAlCl_2$) Me), −6.6 (2-MeTHF($MeAlCl_2$) AlMe)

^{27}Al NMR spectroscopy (104 MHz, toluene-d_8): δ 133.3 ($MeAlCl_2$), 101.7 (2-MeTHF($MeAlCl_2$))

The NMR sample was heated to 100 °C for 2 hours in a sealed J Young NMR tube.

^{1}H NMR spectroscopy (400 MHz, toluene-d_8): δ 2.69 (m, 1H, **34** CH), 2.55 (m, 2H, **34** CH_2), 1.69 (m, 2H, **34** CH_2), 1.51 (m, 2H, **34** CH_2), 1.16 (d, J = 7.0 Hz, 3H, **34** Me), 0.17 (s, 1H, MeH), 0.15 (t, J = 1.9 Hz, 1H, MeD)

^{13}C NMR spectroscopy (100 MHz, toluene-d_8): δ 32.2 (CH), 29.9 (CH_2), 27.3 (CH_2), 23.0 (Me), −4.4 (MeH + MeD)

^{27}Al NMR spectroscopy (104 MHz, toluene-d_8): δ 100.2 (**33**)

4.4.3.3 Spectroscopic characterisation of $^{i}Pr_2O$ + $MeAlCl_2$ reaction mixtures

$AlCl_3$ (533 mg, 4 mmol), toluene (2 ml) and TMA (1 ml, 2 mmol, 2.0 M in toluene) were heated to form $MeAlCl_2$ (6 mmol, 2.0 M in toluene). $^{i}Pr_2O$ (0.42 ml, 3 mmol) was added dropwise under a N_2 atmosphere. The solution was stirred for 2 hours at room temperature. An aliquot of the solution was analysed by NMR spectroscopy.

^{1}H NMR spectroscopy (400 MHz, toluene-d_8): δ 4.37 (sept, J = 6.6 Hz, 1H, $^{i}Pr_2O(MeAlCl_2)$ CH), 4.29 (sept, J = 6.6 Hz, 1H, $^{i}Pr_2O(MeAlCl_2)$ CH), 0.98 (dd, J = 6.6, 1.9 Hz, 6H, $^{i}Pr_2O(MeAlCl_2)$ Me), 0.93 (dd, J = 6.6, 1.9 Hz, 6H, $^{i}Pr_2O(MeAlCl_2)$ Me), −0.05-−0.50 (m, 6H, $^{i}Pr_2O(MeAlCl_2)$ + $MeAlCl_2$ AlMe)

^{13}C NMR spectroscopy (100 MHz, toluene-d_8): δ 79.4, 77.1 ($^{i}Pr_2O(MeAlCl_2)$ CH), 20.7, 20.6 ($^{i}Pr_2O(MeAlCl_2)$ Me), −6.4 ($^{i}Pr_2O(MeAlCl_2)$ + $MeAlCl_2$ AlMe)

^{27}Al NMR spectroscopy (104 MHz, toluene-d_8): δ 131.2 ($MeAlCl_2$), 99.2 ($^{i}Pr_2O(MeAlCl_2)$)

The NMR sample was heated to 100 °C for 2 hours in a sealed J Young NMR tube.

^{1}H NMR spectroscopy (400 MHz, toluene-d_8): δ 5.69 (m, 0.04H, **35** C=CH), 4.97 (m, 0.04H, **35** C=CH_2), 4.91 (m, 0.04H, **35** C=CH_2), 4.36 (sept, J = 6.6 Hz, 1.3H, $^{i}Pr_2O(MeAlCl_2)$ CH), 4.28 (sept, J = 6.6 Hz, 0.7H, $^{i}Pr_2O(MeAlCl_2)$ CH), 3.92 (sept, J = 6.2 Hz, 0.2H, **36** CH), 1.55 (m, 0.14H, **35** Me), 0.97 (m, 10.3H, $^{i}Pr_2O(MeAlCl_2)$ + **36** Me), 0.92 (d, J = 6.6 Hz, 3.8H, $^{i}Pr_2O(MeAlCl_2)$ Me), 0.17(s, 0.2H, MeH), −0.05-−0.50 (m, 5.4H, $^{i}Pr_2O(MeAlCl_2)$ + $MeAlCl_2$ AlMe), −0.22 (s, 0.6H, **36** AlMe)

^{13}C NMR spectroscopy (100 MHz, toluene-d_8): δ 79.4, 77.3 ($^{i}Pr_2O(MeAlCl_2)$ CH), 74.1 (**36** CH), 24.4 (**36** Me), 20.7, 20.6 ($^{i}Pr_2O(MeAlCl_2)$ Me), −6.4 ($^{i}Pr_2O(MeAlCl_2)$ + $MeAlCl_2$ + **36** AlMe)

^{27}Al NMR spectroscopy (104 MHz, toluene-d_8): δ 131.4 ($MeAlCl_2$), 99.0 ($^{i}Pr_2O(MeAlCl_2)$), 87.4

The sample was heated for a further 6 hours in a sealed J Young NMR tube.

^{1}H NMR spectroscopy (400 MHz, toluene-d_8): δ 2.70 (m, 1H, **37a** + **37b** CH), 1.15 (d, J = 7.0 Hz, 6H, **37a** + **37b** Me), 0.17 (s, 0.5H, MeH), 0.15 (t, J = 1.9 Hz, 0.2H, MeD)

^{13}C NMR spectroscopy (100 MHz, toluene-d_8): δ 149.0, 145.8, 126.7, 126.4, 123.7 (**37a** + **37b** Tol), 34.4, 34.0 (**37a** + **37b** CH), 21.3 (**37a** + **37b** Me), −4.4 (MeH + MeD)

^{27}Al NMR spectroscopy (104 MHz, toluene-d_8): δ 102.1 (**33**)

4.4.4 Reactivity of FVC 46D with Methylaluminium Reagents

4.4.4.1 Spectroscopic characterisation of FVC 46D + TMA reaction mixtures

TMA (4.5 ml, 9 mmol, 2.0 M in toluene) was added dropwise to FVC 46D (0.23 ml, 3 mmol) under a N_2 atmosphere at −78 °C and allowed to reach room temperature. An aliquot of the solution was analysed by NMR spectroscopy.

^{1}H NMR spectroscopy (400 MHz, benzene-d_6): δ 4.36-3.23 (m, 3H, CH + CH_2), 1.47-0.59 (m, 4H, CH_2 + Me), −0.37 (s, 27H, AlMe)

^{13}C NMR spectroscopy (100 MHz, benzene-d_6): δ −7.2 (AlMe)

^{27}Al NMR spectroscopy (104 MHz, benzene-d_6): δ 156.9

4.4.4.2 Spectroscopic characterisation of FVC 46D + Me_2AlCl reaction mixtures

$AlCl_3$ (267 mg, 2 mmol), toluene (1 ml) and TMA (2 ml, 4 mmol, 2.0 M in toluene) were heated to form Me_2AlCl (6 mmol, 2.0 M in toluene). FVC 46D (0.23 ml, 3 mmol) was added dropwise at −78 °C and the mixture allowed to warm to room temperature to give a colourless solution. An aliquot of the solution was analysed by NMR spectroscopy.

^{1}H NMR spectroscopy (400 MHz, toluene-d_8): δ 4.95-3.22 (m, 3H, CH + CH_2), 2.83-2.24 (m, 1H, CH_2), 1.66-0.52 (m, 4H, CH_2 + Me), −0.25 (s, 12H, AlMe)

^{13}C NMR spectroscopy (100 MHz, toluene-d_8): δ −6.4 (AlMe)

^{27}Al NMR spectroscopy (104 MHz, toluene-d_8): Only see background signal

The NMR sample was then heated in a J Young NMR tube to 100 °C for 24 hours.

^{1}H NMR spectroscopy (400 MHz, toluene-d_8): δ 5.29-3.27 (m, 3H, CH + CH_2), 3.00 (q, J = 7.3 Hz, 0.5H, **38** CH_2), 2.82-2.26 (m, 1H, CH_2), 1.49-0.42 (m, 4H, CH_2 + Me), 1.02 (t,

J = 7.3 Hz, 0.8H, **38** Me), 0.17 (s, 0.1H, MeH), 0.01 (s, 0.8H, **38** AlMe), −0.11 (s, 0.8H, **38** AlMe), −0.27 (s, 4H, AlMe), −0.40 (s, 0.8H, **38** AlMe)

^{13}C NMR spectroscopy (100 MHz, toluene-d_8): δ 39.7 (**38** CH_2), 18.7 (**38** Me), 1.2 (**38** AlMe), −5.8 (**38** AlMe), −6.4 (AlMe)

^{27}Al NMR spectroscopy (104 MHz, toluene-d_8): δ 167.3 (**38**)

4.4.4.3 Spectroscopic characterisation of FVC 46D + $MeAlCl_2$ reaction mixtures

$AlCl_3$ (533 mg, 4 mmol), toluene (2 ml) and TMA (1 ml, 2 mmol, 2.0 M in toluene) were heated to form $MeAlCl_2$ (6 mmol, 2.0 M in toluene). FVC 46D (0.23 ml, 3 mmol) was added dropwise at −78 °C and the mixture allowed to warm to room temperature to give a colourless solution. An aliquot of the solution was analysed by NMR spectroscopy.

^{1}H NMR spectroscopy (400 MHz, toluene-d_8): δ 4.97-3.38 (m, 3H, CH + CH_2), 2.86-2.28 (m, 1H, CH_2), 1.82-0.70 (m, 4H, CH_2 + Me), −0.37 (s, 6H, AlMe)

^{13}C NMR spectroscopy (100 MHz, toluene-d_8): δ −7.6 (AlMe)

^{27}Al NMR spectroscopy (104 MHz, toluene-d_8): δ 136.0

The NMR sample was then heated in a J Young NMR tube to 100 °C for 24 hours.

^{1}H NMR spectroscopy (400 MHz, toluene-d_8): δ 2.50 (q, *J* = 7.5 Hz, 1.2H, **40** CH_2), 2.45 (q, *J* = 7.5 Hz, 0.8H, **40** CH_2), 1.11 (t, *J* = 7.5 Hz, 1.8H, **40** Me), 1.09 (s, 4H, Me), 1.05 (t, *J* = 7.5 Hz, 1.2H, **40** Me), 0.85 (s, 1.5H, Me), 0.17 (s, 0.7H, MeH), 0.15 (t, *J* = 1.9 Hz, 2H, MeD)

^{13}C NMR spectroscopy (100 MHz, toluene-d_8): δ 29.1, 28.7, 28.6 (CH_2), 26.4, 24.7, 15.9, 14.5 (Me), −4.4 (MeH), −4.8 (MeD)

^{27}Al NMR spectroscopy (104 MHz, toluene-d_8): δ 101.7 (**33**)

4.5 Reactivity of Aluminium-Chloromethane Mixtures with Refrigeration Oils

4.5.1 Reactivity of Aluminium with Chloromethane

Aluminium (4 g), activated 3Å molecular sieves (2 g) and iodine (60 mg) were placed in a Parr reactor. The reactor was connected to a chloromethane cylinder and was purged 3 times to remove any oxygen and water. Chloromethane was added up to a pressure of 5 bar and the vessel was sealed. The vessel was heated to 120 °C for 2 hours with stirring. The reactor was then attached to the vacuum line and a clear liquid was distilled, which was analysed as $Me_{1.5}AlCl_{1.5}$.

Yield 2.27 g (65% wrt MeCl)

Elemental analysis satisfactory analysis could not be achieved

^{1}H NMR spectroscopy (400 MHz, benzene-d_6): δ −0.40 (s, br, $Me_{1.5}AlCl_{1.5}$ AlMe)

^{13}C NMR spectroscopy (100 MHz, benzene-d_6): δ −6.8 (br, $Me_{1.5}AlCl_{1.5}$ AlMe)

^{27}Al NMR spectroscopy (104 MHz, benzene-d_6): δ 176.8 (Me_2AlCl), 134.0 ($MeAlCl_2$)

4.5.2 Reactivity of Aluminium, Chloromethane and RL 32H

The aluminium-chloromethane reaction was repeated, but RL 32H (1.26 g) was added before chloromethane. The reaction was heated to 120 °C for 2 hours with stirring. The reactor was then attached to the vacuum line and a clear liquid was distilled.

Yield 710 mg

Elemental analysis satisfactory analysis could not be achieved

^{1}H NMR spectroscopy (400 MHz, benzene-d_6): δ 1.7-0.5 (m, br, 3H, polymer), −0.46 (s, 3H, $MeAlCl_2$ AlMe)

^{13}C NMR spectroscopy (100 MHz, benzene-d_6): δ 29.2 (polymer Me), 14.0 (polymer Me), −8.3 (br, $MeAlCl_2$ AlMe)

^{27}Al NMR spectroscopy (104 MHz, benzene-d_6): δ 135.1 ($MeAlCl_2$), 100.2 (**9**)

4.5.3 Reactivity of Aluminium, Chloromethane and FVC 46D

The aluminium-chloromethane reaction was repeated, but FVC 46D (1.36 g) was added before the chloromethane. The reaction was heated to 120 °C for 2 hours with stirring. A black solid was produced, which was isolated by dissolving it in THF and then removal of the THF *in vacuo*.

Yield 435 mg

Elemental analysis calculated for $C_8H_{16}AlCl_3O_2$ (%): C 34.62, H 5.81; found (%): C 33.45, H 5.81

^{1}H NMR spectroscopy (400 MHz, benzene-d_6): δ 3.87 (m, 8H, CH_2O THF), 3.74-3.05 (m, br, 2.4H, FVC 46D), 2.30-0.72 (m, br, 8.5H), 1.17 (m, 8H, CH_2 THF)

^{13}C NMR spectroscopy (100 MHz, benzene-d_6): δ 70.9 (CH_2O THF), 24.9 (CH_2 THF)

^{27}Al NMR spectroscopy (104 MHz, benzene-d_6): δ 74.5 ($AlCl_3(THF)_2$)

Chapter 5

Refrigeration Oil Analysis

5.1 Introduction

Refrigeration oils play an important role in the normal functioning of refrigeration units by lubricating moving parts, such as the compressor, and distributing the refrigerant throughout the system. It has been postulated that the counterfeit refrigerant chloromethane can react with aluminium components to produce methylaluminium chlorides. The chemical stability of lubricating oils when exposed to organoaluminiums has not previously been considered. Undertaking reactivity studies on these systems requires detailed knowledge about the chemical composition of refrigeration oils. However, this is not usually disclosed by commercial manufacturers. Therefore, the composition of the lubrication oils must be determined in order to fully understand what *in situ* formed organoaluminiums might do in these systems. In this chapter, characterisation of two commonly used lubricants, RL 32H (a POE) and FVC 46D (a PVE), is reported.

5.2 Analysis of RL 32H

RL 32H is simply described by the manufacturer (CPI Fluid Engineering) as a 'synthetic POE'. A search of POEs revealed that they are based on neopentane structures with multiple alcohol groups, such as neopentyl glycol, trimethylolethane, pentaerythritol or dipentaerythritol.[26,27] At the commencement of this investigation a pristine sample of RL 32H was subjected to IR spectroscopy, NMR spectroscopy, mass spectrometry and elemental analysis.

The IR spectrum of RL 32H (Figure 5.1) revealed that it is primarily ester-based, with a strong absorbance at 1739 cm^{-1} characteristic of the carbonyl stretching frequency in esters.[117] Absorptions at 1236, 1152, 1108 and 1023 cm^{-1} were assigned to C–O stretching. Meanwhile, an absorbance at 2956 cm^{-1} was attributed to saturated C–H stretching.

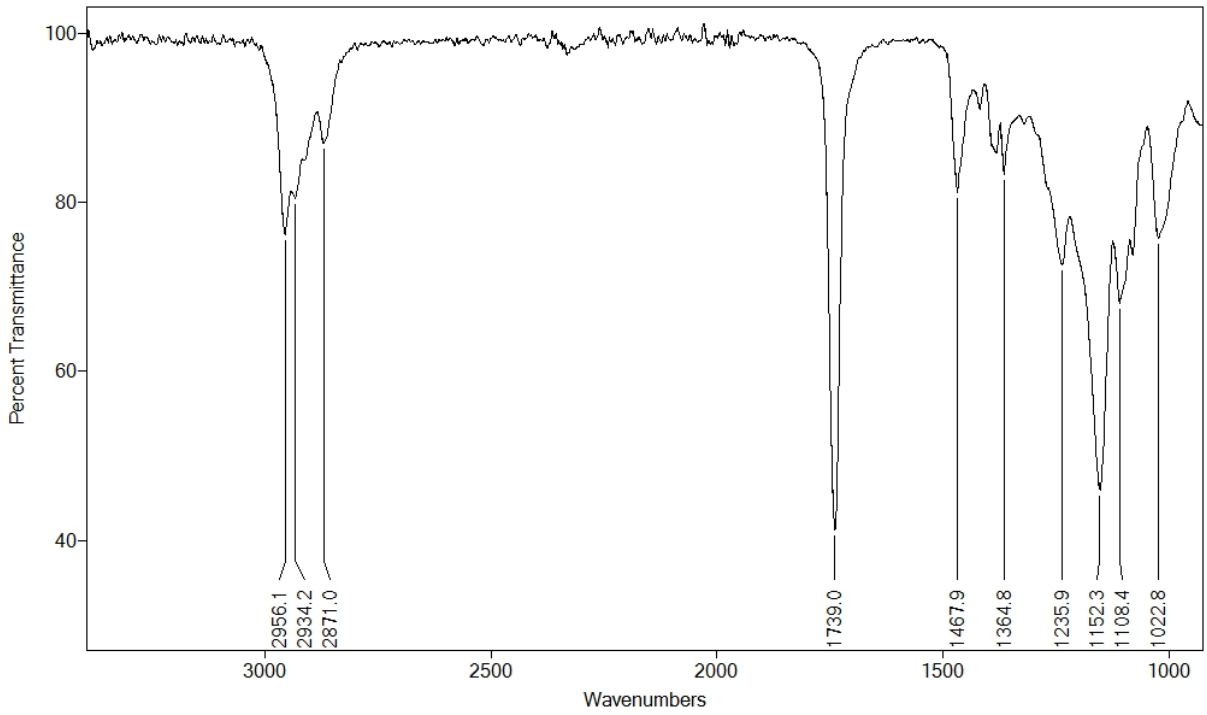

Figure 5.1: IR spectrum of pristine RL 32H oil.

The presence of ester groups was confirmed using ^{13}C NMR spectroscopy (Figure 5.2), with peaks at δ 172.6 and 172.0 ppm corresponding to carbonyl carbons. The observation of two signals showed that there must be different ester environments. The signal at δ 62.3 ppm was assigned to the carbons singly bonded to the oxygen of the esters. It was assumed that only one signal was observed due to the signals overlapping. A DEPT experiment assigned this as a CH_2O carbon. The remaining signals at high field were attributed to aliphatic carbon environments.

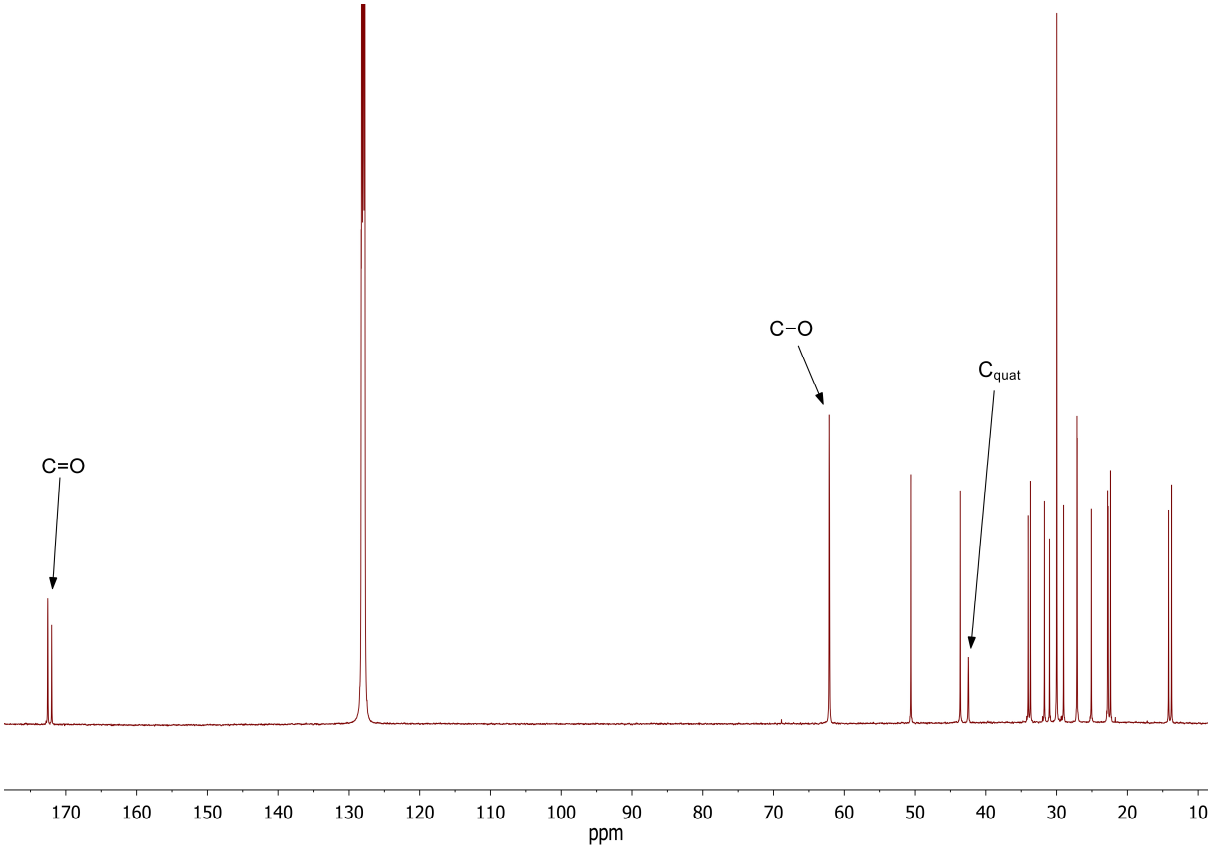

Figure 5.2: ^{13}C NMR spectrum of pristine RL 32H oil. The solvent is benzene-d_6.

^{1}H NMR spectroscopy (Figure 5.3) revealed many peaks in the region δ 2.4-0.7 ppm, suggesting the presence of aliphatic hydrocarbon chains, with the number of signals suggesting a complex mixture of alkyl groups. The set of peaks at *ca.* δ 4.37 ppm was attributed to a $C(=O)OCH_2$ group. The complex pattern seen for this signal pointed to either there being adjacent hydrogens or else multiple ester environments. A COSY experiment showed no correlations to other ^{1}H NMR signals, therefore suggesting the complex pattern is due to multiple ester environments. Integration suggested that for every $C(=O)OCH_2$ group there were about 13 other hydrogen atoms in the aliphatic region.

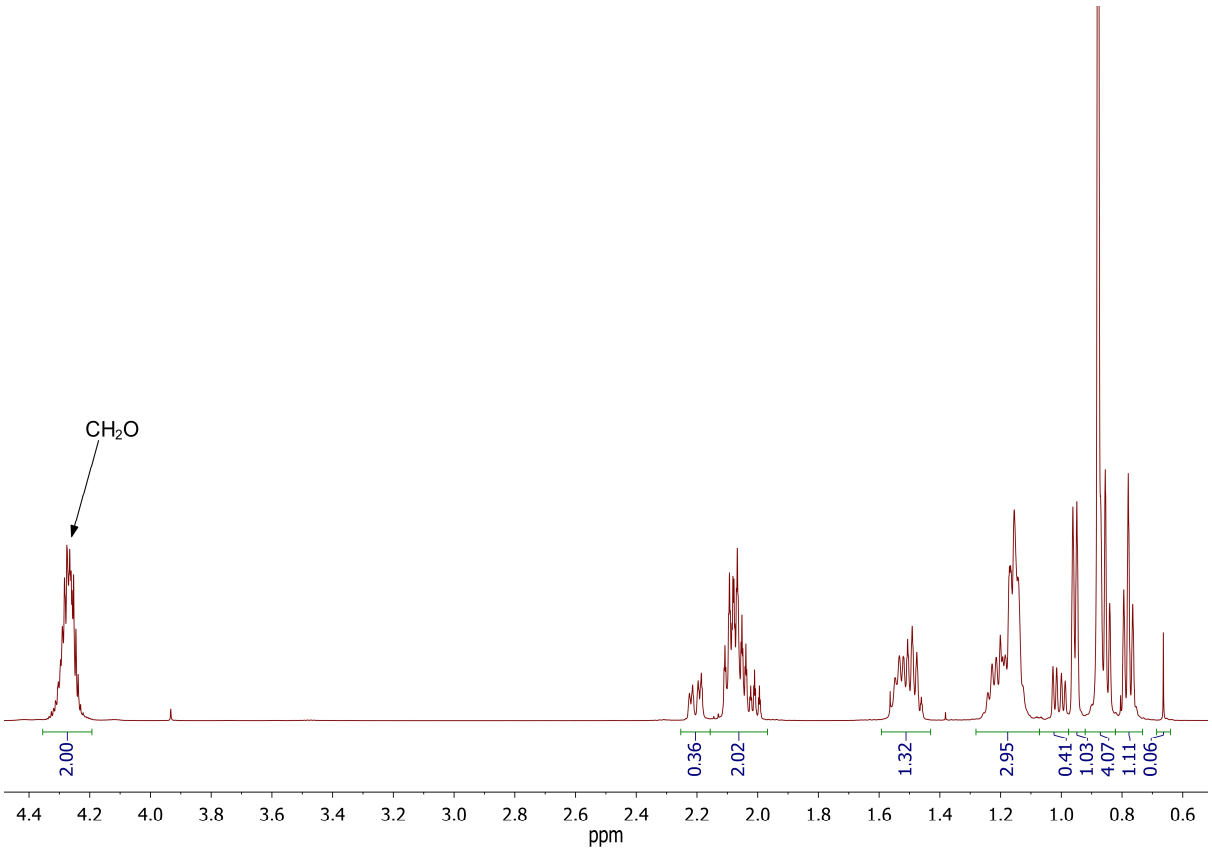

Figure 5.3: ^{1}H NMR spectrum of pristine RL 32H oil. The solvent is benzene-d_6.

To further elucidate the structures of the ester functions a HMBC NMR experiment was performed (Figure 5.4). According to this, the ester signal at δ 172.6 ppm in the ^{13}C NMR spectrum revealed a correlation to the hydrogen atoms at δ 4.32 ppm in the ^{1}H NMR spectrum (C(=O)OCH$_2$). These hydrogen atoms also showed a correlation to the ^{13}C NMR signal at δ 42.5 ppm. This signal suggested a quaternary carbon core to the structure. This view was reinforced by the lack of correlation shown by this resonance in a HSQC NMR experiment (Figure 5.5). This carbon showed correlation *only* to the hydrogens at δ 4.32 ppm (in the HMBC experiment), leading to the conclusion that the core of the molecule is based on pentaerythritol, with a central carbon bonded to four C(=O)OCH$_2$ units (Figure 5.6).

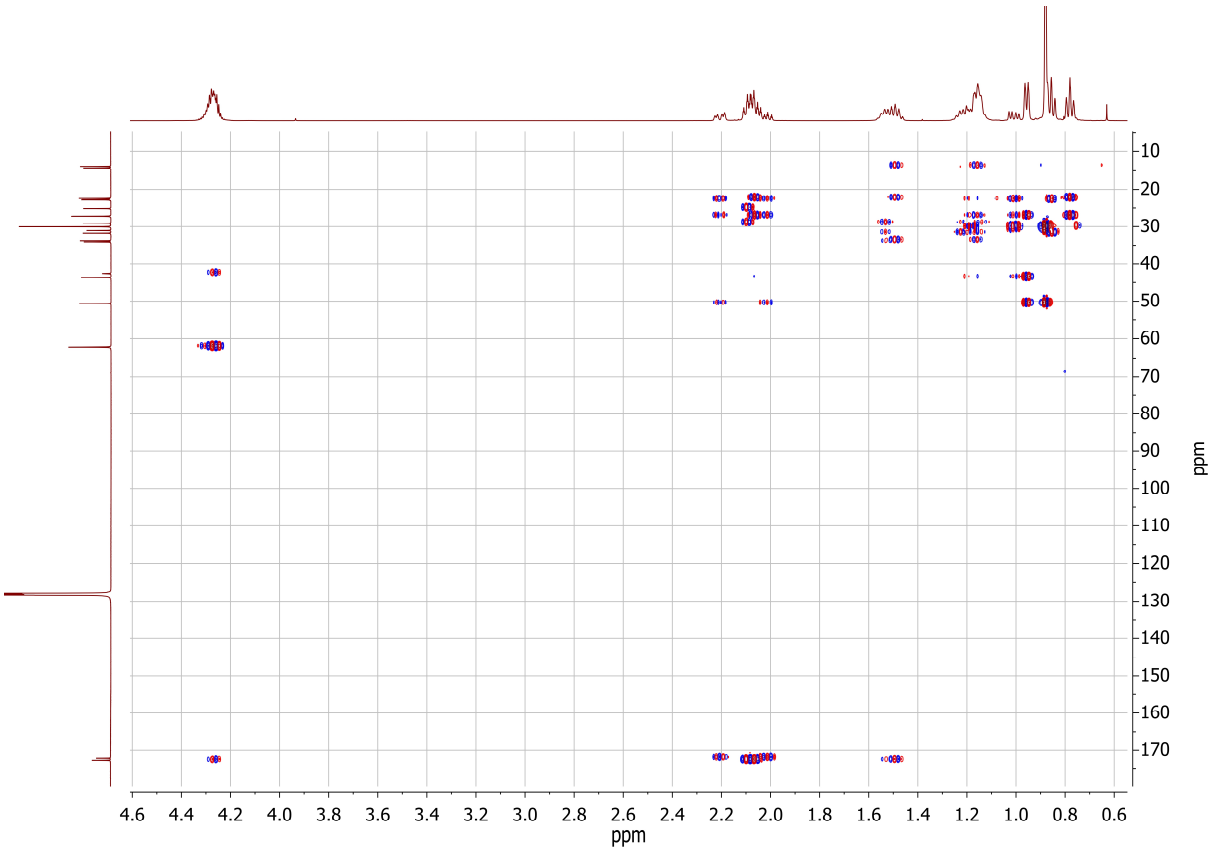

Figure 5.4: HMBC spectrum of pristine RL 32H oil. The solvent is benzene-d_6.

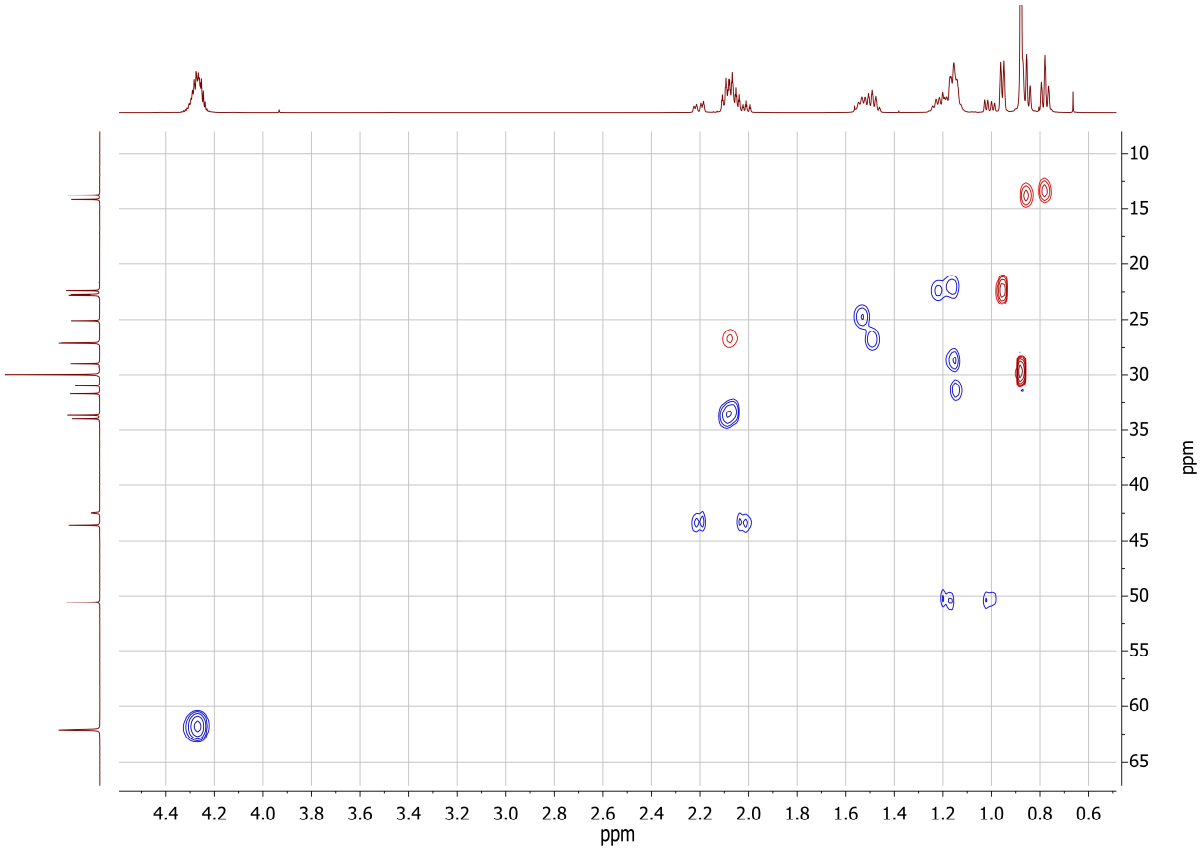

Figure 5.5: HSQC spectrum of pristine RL 32H oil (blue for CH_2 and red for CH or CH_3). The solvent is benzene-d_6.

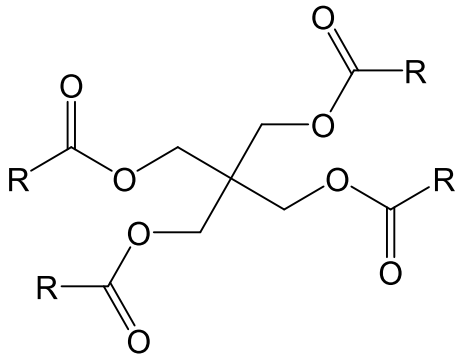

Figure 5.6: Postulated general structure for the types of ester found in RL 32H. The R groups represent alkyl groups.

LC-MS was used to help determine the nature of the alkyl groups present in RL 32H. The main signals are given in Table 5.1.

m/z	**Molecule Detected**
434.4	$C_{21}H_{36}O_8 + NH_4^+$ (PE-core with R = 4 × C_3H_7)
462.4	$C_{23}H_{32}O_8 + NH_4^+$ (PE-core with R = 3 × C_3H_7, 1 × C_5H_{11})
490.3	$C_{25}H_{44}O_8 + NH_4^+$ (PE-core with R = 2 × C_3H_7, 2 × C_5H_{11})
518.4	$C_{27}H_{48}O_8 + NH_4^+$ (PE-core with R = 1 × C_3H_7, 3 × C_5H_{11})
546.4	$C_{29}H_{52}O_8 + NH_4^+$ (PE-core with R = 4 × C_5H_{11})

Table 5.1: m/z values for the main peaks from the LC-MS of pristine RL 32H, PE-core = $C(CH_2OC(O))_4$.

The m/z values observed corresponded to the structure suggested in Figure 5.6; a pentaerythritol-like ($C(CH_2OC(O))_4$) core with the R groups being either C_3H_7 or C_5H_{11}. The extent of branching in the alkyl groups could not be accurately determined by this or other methods, although the appearance of the same m/z values at different retention times in the LC-MS may suggest that different branching is present. From integration of the signals from the LC-MS it seemed that the commercial RL 32H tested incorporated a greater proportion of C_5H_{11} groups relative to C_3H_7 groups. Overall, however, the presence of two alkyl chains of different length by LC-MS was consistent with the observation, by ^{13}C NMR spectroscopy, of two ester environments.

Elemental analysis was conducted on pristine RL 32H oil. The composition was found to be C = 68.06% and H = 10.39%. The expected values for $C_{29}H_{52}O_8$ (containing 4 C_5H_{11}

groups) and $C_{21}H_{36}O_8$ (containing 4 C_3H_7 groups) are C = 65.88%, H = 9.91% and C = 60.56%, H = 8.71%, respectively. The slight differences may be due to unknown additives in the oil, which have higher amounts of carbon and hydrogen than the POEs described above. These could be simple hydrocarbons, which would have NMR signals overlapping with the signals from the POEs.

5.3 Analysis of FVC 46D

FVC 46D is described as a PVE, and when used in refrigeration systems such species often have a $\{CH_2CH(OR)\}_n$ structure, where R is typically a simple alkyl group.[118] As the exact composition of the oil was not disclosed by the manufacturer (Idemitsu Kosan), FVC 46D was analysed by IR spectroscopy, NMR spectroscopy and elemental analysis.

The most prominent features in the IR spectrum of FVC 46D (Figure 5.7) were two strong absorbances, at 1098 and 1078 cm^{-1}, characteristic of C–O stretches. There were also signals at 2972, 2929 and 2869 cm^{-1} attributable to saturated C–H stretches, and at 1443 and 1373 cm^{-1} which were assigned to C–H bending. Overall, these data suggest that ether is the only functionality present.

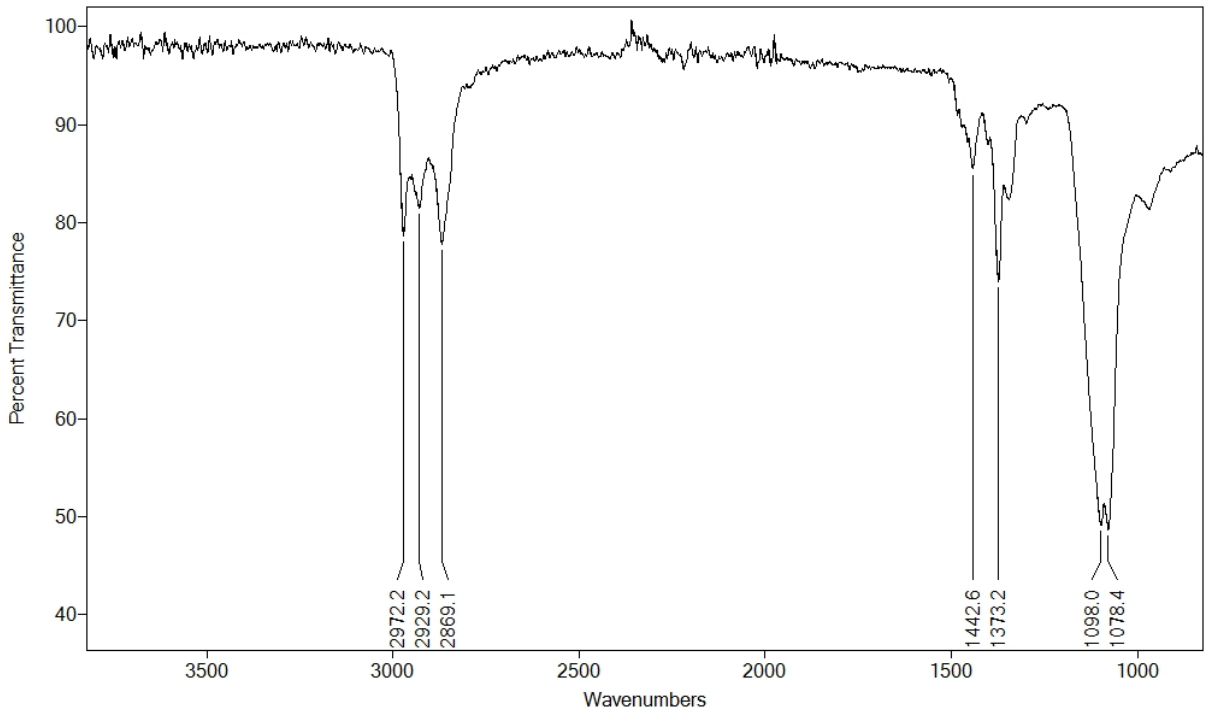

Figure 5.7: IR spectrum of pristine FVC 46D oil.

The ^{1}H NMR spectrum of FVC 46D (Figure 5.8) showed a number of broad signals, which is consistent with a polymeric structure. The signals at δ 4.0-2.9 ppm were assigned to hydrogens adjacent to oxygen atoms, with the signals at δ 2.2-0.7 ppm assigned to aliphatic hydrogens not adjacent to oxygen atoms. Also of note, there were a number of small peaks observed in the aromatic region of the ^{1}H NMR spectrum (Figure 5.8, inset). These were assigned to additives in the refrigeration oil (see Section 1.3.3). Further determination of the source of these signals proved unsuccessful due to limited quantity of it in the oil, with a relative integration of less than 1% compared to the aliphatic signals.

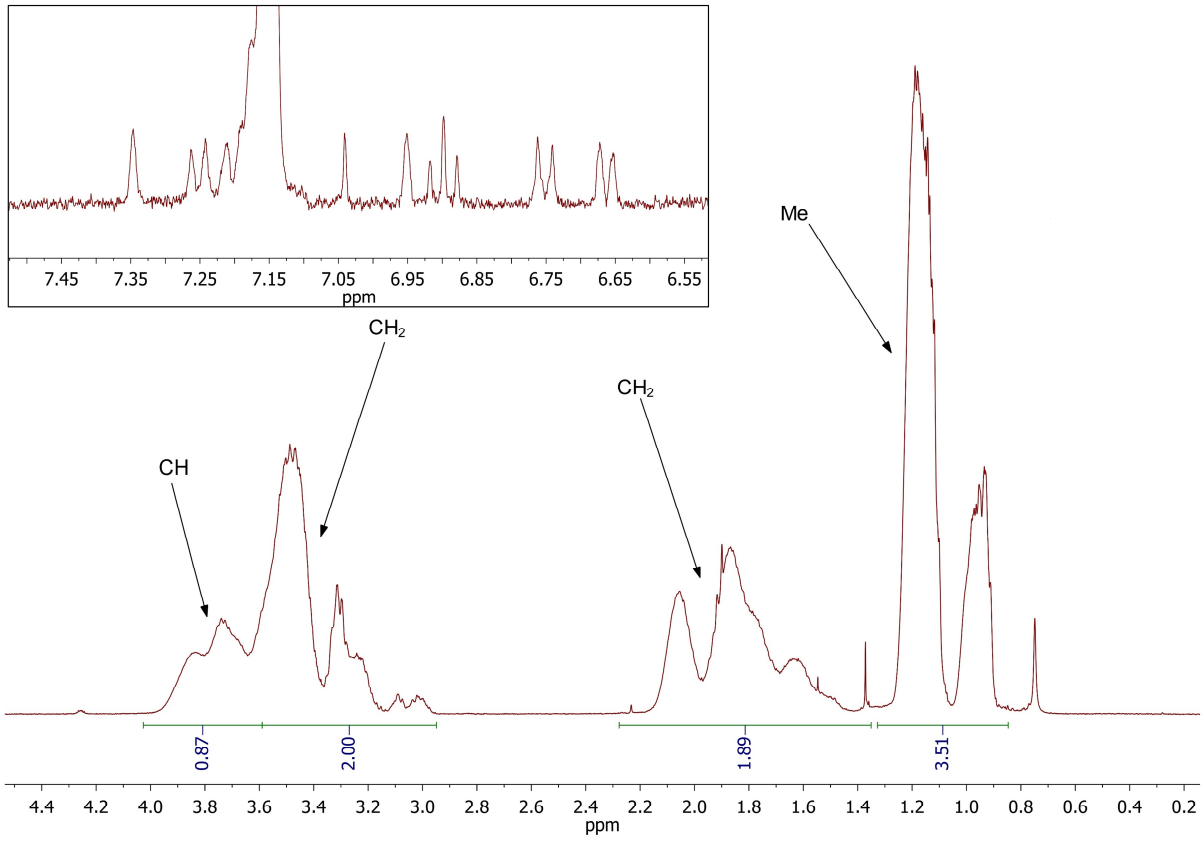

Figure 5.8: ^{1}H NMR spectrum of pristine FVC 46D oil. The inset shows the aromatic region. The solvent is benzene-d_6.

The assignment of the aliphatic signals was corroborated using HSQC spectroscopy (Figure 5.9). From the phase of the signals, the δ 4.0-3.6 ppm region was assigned as CH, the δ 3.6-2.9 and 2.2-1.4 ppm regions as CH_2, and the δ 1.4-0.7 ppm region as Me.

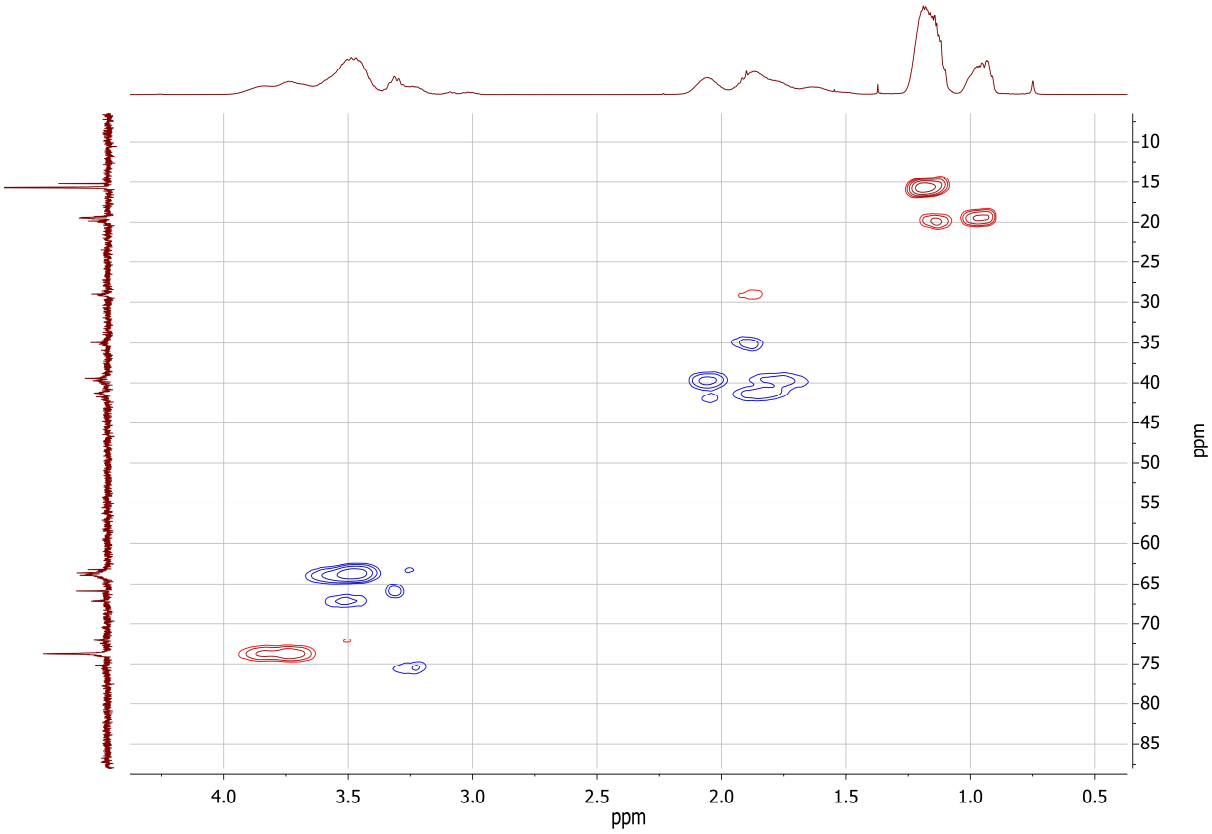

Figure 5.9: HSQC spectrum of pristine FVC 46D oil (blue for CH_2 and red for CH or CH_3). The solvent is benzene-d_6.

A COSY experiment (Figure 5.10) confirmed the presence of ethyl groups in FVC 46D, with a correlation observed between signals at δ 3.5 and 1.2 ppm. There is also a correlation from the signal at δ 1.9 ppm, assigned as CH_2 hydrogens, with signals at δ 3.8 and 1.0 ppm, assigned as CH and Me hydrogens, respectively. This could suggest the presence of branching *sec*-butyl groups instead of ethyl groups. It was difficult to calculate relative proportion of *sec*-butyl groups due to overlapping signals and broad signals. Taken together, these data suggest the major component of FVC 46D oil is poly(ethyl vinyl ether) (Figure 5.11).

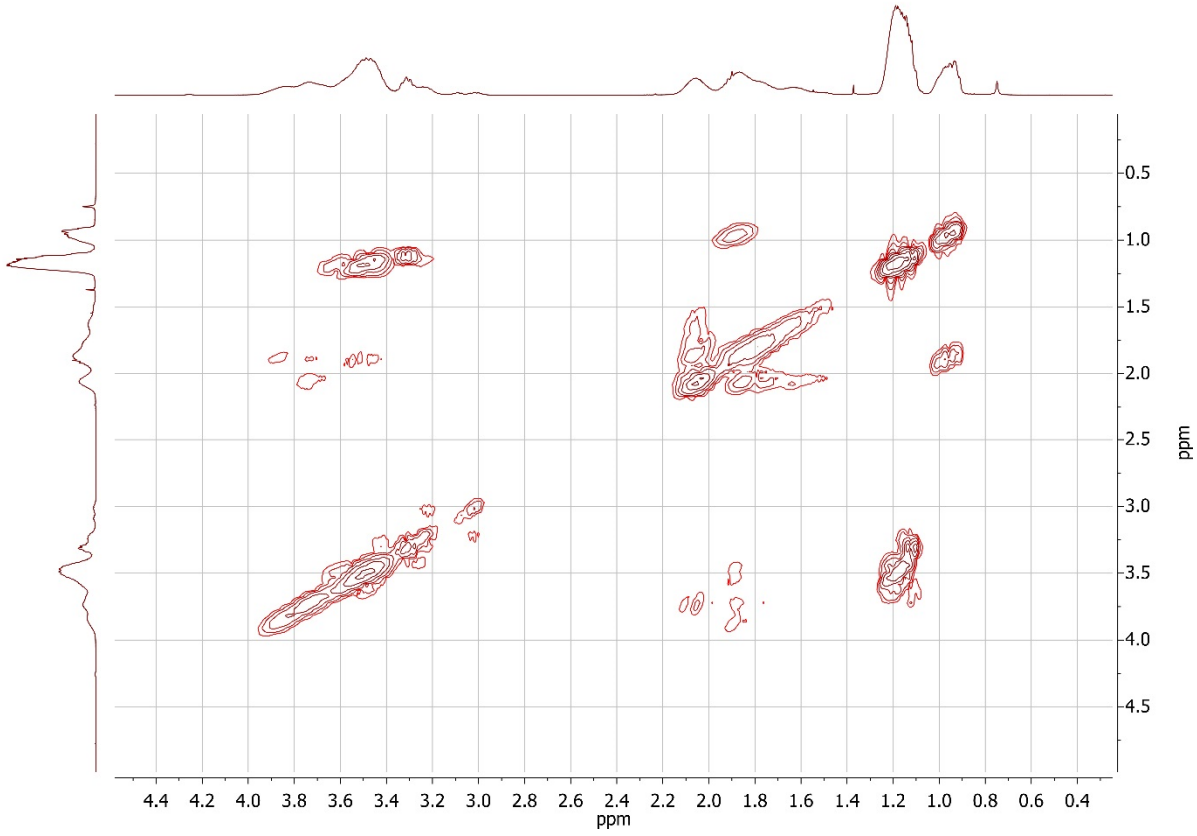

Figure 5.10: COSY spectrum of pristine FVC 46D oil. The solvent is benzene-d_6.

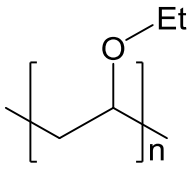

Figure 5.11: The proposed major component of FVC 46D oil.

Elemental analysis was conducted on the pristine FVC 46D oil. The composition was found to be C = 68.01% and H = 11.93%, which compares fairly well the values expected for a polyvinyl ether with ethyl side groups as shown above (C = 66.63%, H = 11.18%). The expected values for poly(*sec*-butyl vinyl ether) are C = 71.95%, H = 12.08%, suggesting the oil is a mixture of PVEs based on these two structures. However, the differences between experiment and calculation may alternatively be due to unidentified additives, such as those which gave aromatic signals in the ^{1}H NMR spectrum (Figure 5.8, inset).

5.4 Summary

The analysis of the two refrigerant oils that will form the basis of reactivity studies in this thesis, RL 32H and FVC 46D, suggests the former to be composed mainly of pentaerythritol-derived esters, whilst the latter reveals spectroscopic data most consistent with a poly(ethyl vinyl ether). However, the presence of other minor components cannot be ruled out, with the presence of small amounts of an aromatic species detected in FVC 46D. Additionally, there may be also be spectroscopically silent species, which would not have been observed in the above analysis. In the following chapters, the reactions between model esters and ethers with methylaluminium chlorides will therefore be investigated. This will aim to mimic the reactions with lubrication oils that are expected to occur in contaminated industrial refrigeration units containing methylaluminium chlorides, that could be reasonably expected to have been generated from aluminium reacting with chloromethane.

Chapter 6
Reactivity of Monoesters with Methylaluminium Reagents

6.1 Introduction

As shown in Chapter 5, the refrigeration oil RL 32H is polyolester based. Experiments carried out by CRT have shown the significant alteration of RL 32H when combined with aluminium and chloromethane in a sealed reaction vessel (see Section 1.3.4). This modification was expected to be from the *in situ* formation of organoaluminium compounds. It is therefore crucial to understand how polyolesters interact with organoaluminiums. Of particular interest, is the interaction of polyolesters with methylaluminium chlorides, as these species are expected to result from the reaction of aluminium with chloromethane. The reaction of organoaluminium compounds with esters has previously been the subject of some study, but the specifics of the mechanism remain surprisingly obscure and, in particular, reaction intermediates have not been fully characterised. Nevertheless, it is known that an adduct is initially formed between the Lewis acidic organoaluminium and the Lewis basic ester. This has been evidenced by infrared spectroscopy, where a decrease in the ester stretching frequency has been interpreted as being due to electron density donation to the aluminium.[119,120] An adduct having formed, the ester has been shown to then undergo addition of an organyl group from the organoaluminium. Hence, the reaction of $AlEt_3$ with esters in an equimolar ratio has been reported to give ketones after hydrolysis.[121] Similarly, the ketonisation of heteroaromatic esters using 1 equivalent of TMA has been documented.[122,123] Meanwhile, the use of an excess of TMA has been reported in the alkylation of acetates.[124] The reduction of cyclic ketones by TMA in the presence of ancillary ester groups showed good chemoselectivity towards ketones at low temperatures, suggesting low reactivity between TMA and esters.[105,125,126] The addition of TMA to methyl benzoate in a 1:1 ratio at 98 °C for 10 hours, followed by hydrolysis, resulted in 40% conversion to 2-phenylpropan-2-ol. This was the result of nucleophilic addition of two methyl groups. On the other hand, replacing the TMA with Me_2AlCl resulted in limited reactivity, with analysis suggesting

no 2-phenylpropan-2-ol, 5% conversion to an alkene and 5% conversion to a trimethylated species (Scheme 6.1). However, the proposed intermediate organoaluminium species were not isolated, with analysis having only been on hydrolysis products.[127] The mechanism of these reactions and the structures of intermediate species therefore currently remain unexplored.

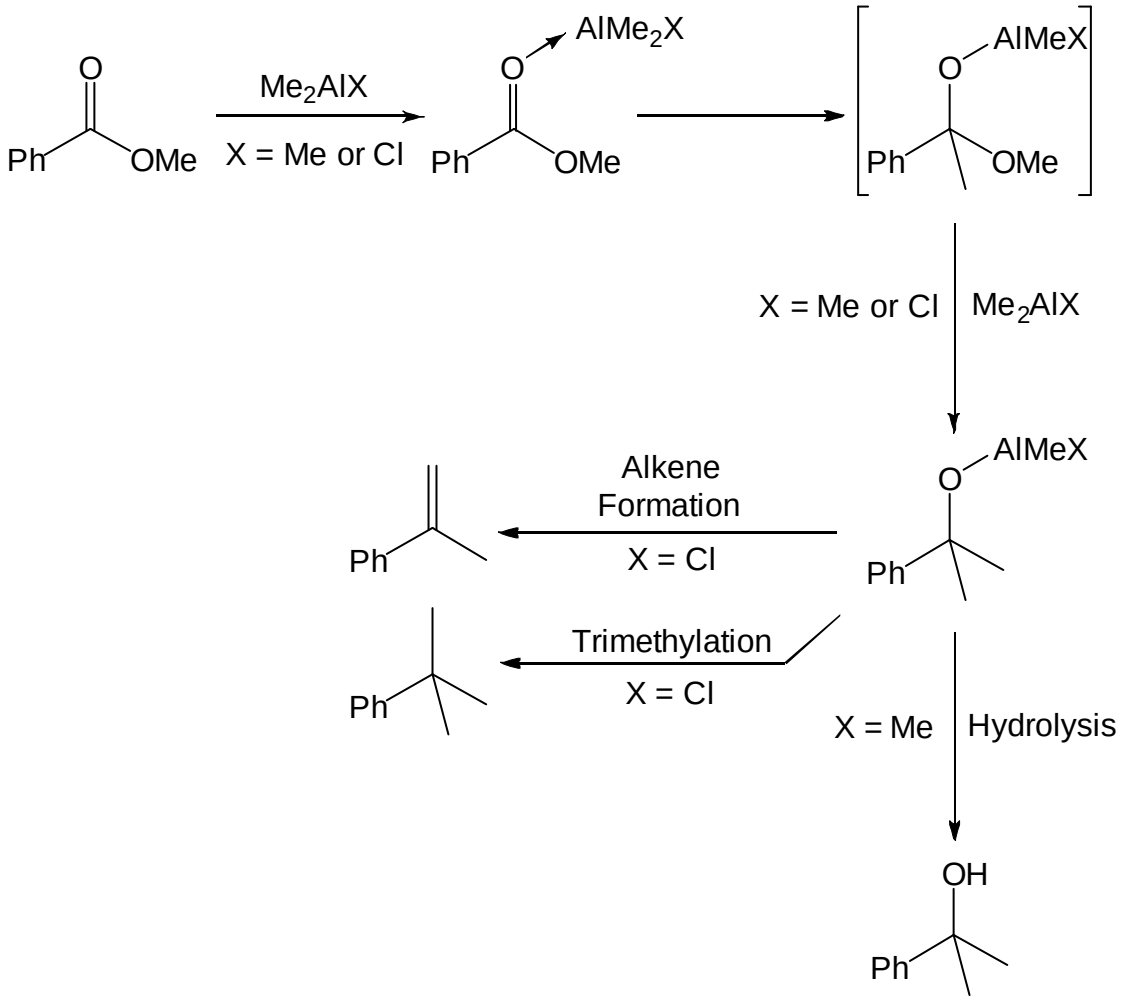

Scheme 6.1: The proposed reaction of methyl benzoate with Me_2AlX (X = Me or Cl), resulting in dimethylation of the ester. With Me_2AlCl, alkene formation and trimethylation was observed.[127]

As the formation of an alkene and a trimethylated species were not fully understood in the above work,[127] the reactions of simple monoesters (as models for the POE RL 32H) with methylaluminium reagents will be investigated. Work will include the isolation and full characterisation of reaction intermediates where possible. Reactions will be undertaken with TMA, Me_2AlCl, $MeAlCl_2$ and $Me_{1.5}AlCl_{1.5}$ using different stoichiometries and temperatures.

6.2 Reactivity of Monoesters with TMA

Initially, attempts to model the reactivity of organoaluminium reagents with monoesters were initiated using TMA and the simple monoester methyl propionate **1**^{Et}. Hence, a solution of TMA in toluene was added dropwise to **1**^{Et} (1:1) at −78 °C. Though this system failed to readily produce isolable products, the observation of a pale green solution upon heating, which became colourless upon cooling to room temperature, suggested the interaction of **1**^{Et} and TMA. This prompted further investigations; therefore, an excess of TMA was added to **1**^{Et} (3:1) at −78 °C. After reaching room temperature, the solution was stirred for 2 hours, whereupon the NMR spectra of an aliquot was collected. ^{1}H NMR spectroscopy (Figure 6.1, top) and COSY suggested the formation of two species, with ^{13}C NMR spectroscopy confirming the complete absence not only of ester but of C=O groups from each species. These data suggested that the 2:1 reaction of TMA with ester had occurred, 1 equivalent of TMA expelling methoxide to induce the formation of the reactive intermediate EtMeC=O **2**^{Et}, alongside Me_2AlOMe **3** (^{1}H δ 3.06 and −0.59 ppm).[59] Then a second equivalent of TMA reacted with the ketone to give the dimethylaluminium alkoxide $Me_2AlOCEtMe_2$ **4**^{Et}. Integration of the ^{1}H NMR signals at δ 3.06 (**3**) and 0.61 ppm (**4**^{Et}) suggested the two products to be present in the anticipated 1:1 ratio. Finally, the observation of signals at δ −0.47 and −0.59 ppm in a 2:1 integral ratio suggested that **4**^{Et} trapped the final, unreacted equivalent of TMA present to give $Me_2AlOCEtMe_2$(TMA) **4**^{Et}(TMA) (Scheme 6.2). These spectroscopic data were assigned to an unusual 4-membered Al_2OC metallacycle. This metallacycle has five aluminium-bonded methyl groups, with four equivalent terminal methyl groups ($AlMe_t$) which resonated at δ −0.47 ppm and the remaining unique bridging group ($AlMe_b$) with a signal at δ 0.09 ppm. ^{13}C NMR spectroscopy reinforced this assignment, with a sharp signal at δ −4.1 ppm due to the bridging methyl in **4**^{Et}(TMA) and broad signals at δ −6.7 and −10.7 ppm from terminal AlMe groups in **4**^{Et}(TMA) and **3**, respectively.

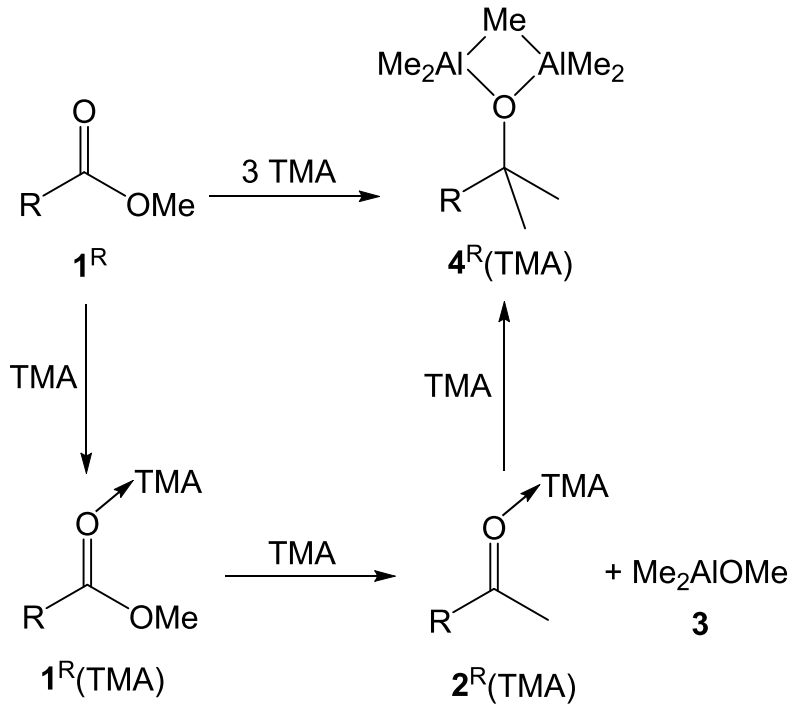

Scheme 6.2: The reaction of **1**^{R} and TMA at room temperature (R = Et, Bn).

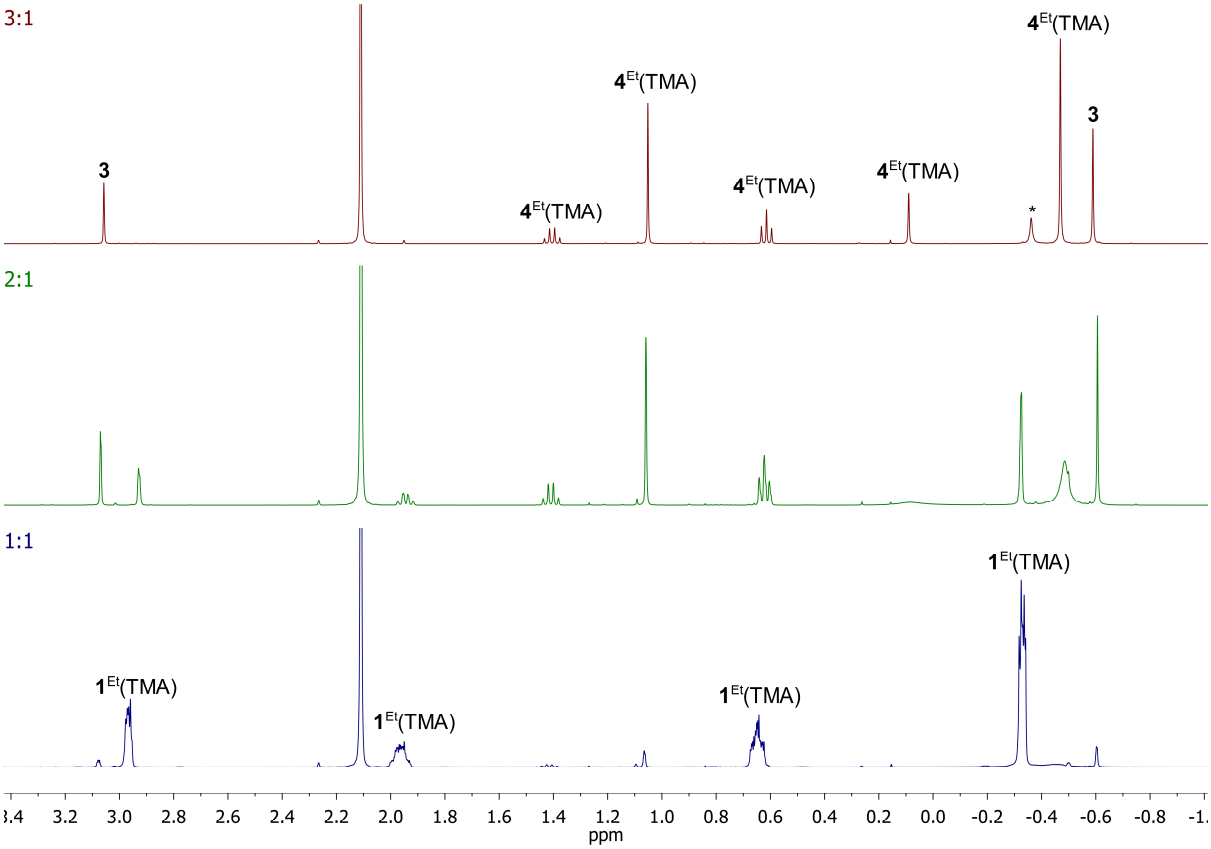

Figure 6.1: ^{1}H NMR spectra of aliquots from the reaction between TMA and methyl propionate **1**^{Et} in toluene (δ 2.11 ppm) employing 3:1 (top), 2:1 (middle) and 1:1 (bottom) stoichiometries. The solvent is benzene-d_6. * = Free TMA.

To further clarify the co-formation of **4**^{Et}(TMA) and **3**, the same synthetic process was repeated using 2:1 and 1:1 TMA:**1**^{Et} ratios. The ^{1}H NMR spectrum of the 1:1 ratio was dominated by the formation of an adduct between **1**^{Et} and TMA (Figure 6.1, bottom), with signals from free **1**^{Et}, at δ 3.32, 1.99 and 0.93 ppm, moved to δ 2.98, 1.97 and 0.65 ppm, whilst coordinated TMA was found downfield (δ −0.33 ppm) of free TMA (δ −0.35 ppm). ^{13}C NMR spectroscopy revealed retention of ester functionality in **1**^{Et}(TMA) (δ 181.4 ppm, cf. δ 173.9 ppm in **1**^{Et}) and the presence of coordinated TMA (δ −7.7 ppm). This system also revealed 6% conversion of the complex **1**^{Et}(TMA) into addition product **4**^{Et}(TMA) and **3**. Similarly, the 2:1 TMA:**1**^{Et} system also revealed the existence of **1**^{Et}(TMA), **4**^{Et}(TMA) and **3** in solution (Figure 6.1, middle). Integration of the ^{1}H NMR signals revealed that 56% of **1**^{Et} had converted to **4**^{Et}(TMA) and 44% to **1**^{Et}(TMA). Meanwhile, ^{27}Al NMR spectroscopy supported the trend from **1**^{Et}(TMA) towards the formation of **4**^{Et}(TMA) and **3** by the gradual replacement of a dominant signal at δ 185.0 ppm in the 1:1 system (**1**^{Et}(TMA)) with a signal at δ 156.2 ppm in the 3:1 system (**4**^{Et}(TMA) and **3**).

Spectroscopy pointed to an $Me_4Al_2(\mu_2\text{-}Me)(\mu_2\text{-}OCEtMe_2)$ formulation based on a symmetrical Al_2OC metallacycle for **4**^{Et}(TMA). However, while this would be similar to motifs previously proposed,[100] the thermal stability of such a motif in the presence of another organoaluminium species had not previously been reported. With this in mind, the reaction mixture resulting from the introduction of TMA in toluene to **1**^{Et} in a 3:1 ratio (spectroscopically characterised as ostensibly a 1:1 mixture of **4**^{Et}(TMA) and **3**, Figure 6.1, top) was heated to reflux for 4 hours. NMR spectroscopic analysis of aliquots obtained after 0, 1, 2, 3 and 4 hours revealed a gradual thermal rearrangement (Figure 6.2), with the spectra demonstrating the *in situ* reformation of free TMA (^{1}H NMR δ −0.36 ppm) together with the appearance of a new complex, **4**^{Et}(**3**) $Me_4Al_2(\mu_2\text{-}OMe)(\mu_2\text{-}OCEtMe_2)$ (Scheme 6.3). Evidence for the symmetry of an Al_2O_2 ring in **4**^{Et}(**3**) came from the development of a single ^{1}H NMR signal at δ −0.48 ppm from the terminal AlMe groups. Meanwhile, residual **4**^{Et}(TMA) (δ −0.47 ppm) and **3** (δ −0.59 ppm) remained clearly identifiable. Integration revealed that thermal rearrangement of **4**^{Et}(TMA) and **3** to give **4**^{Et}(**3**) and TMA proceeded to *ca*. 54% completion after heating to reflux for 4 hours.

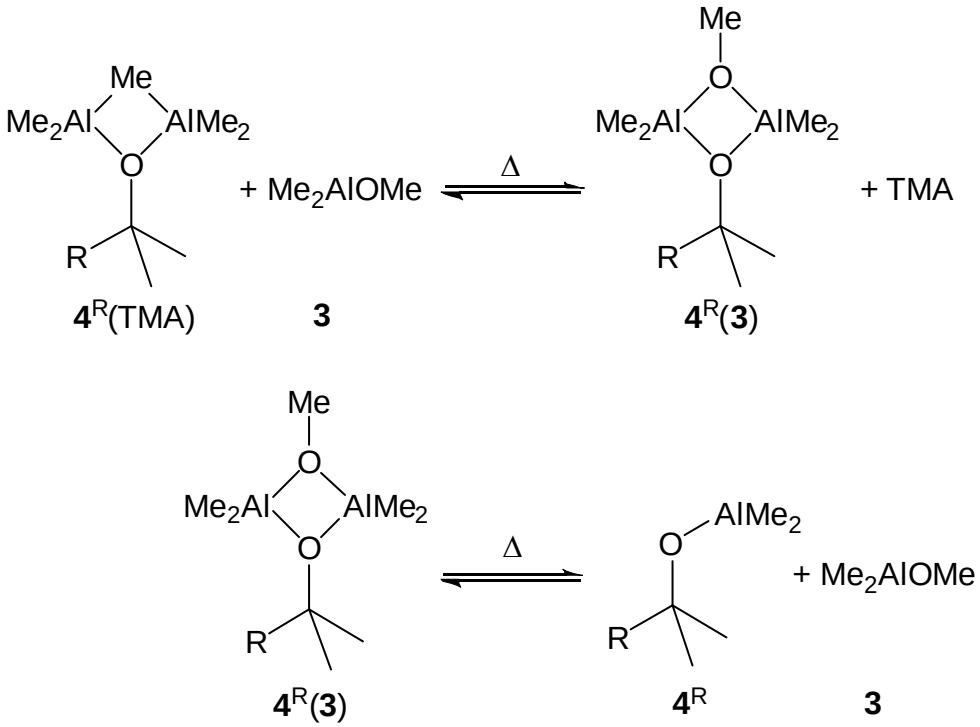

Scheme 6.3: The thermally induced rearrangement of **4**^{R}(TMA) and **3** (R = Et, Bn).

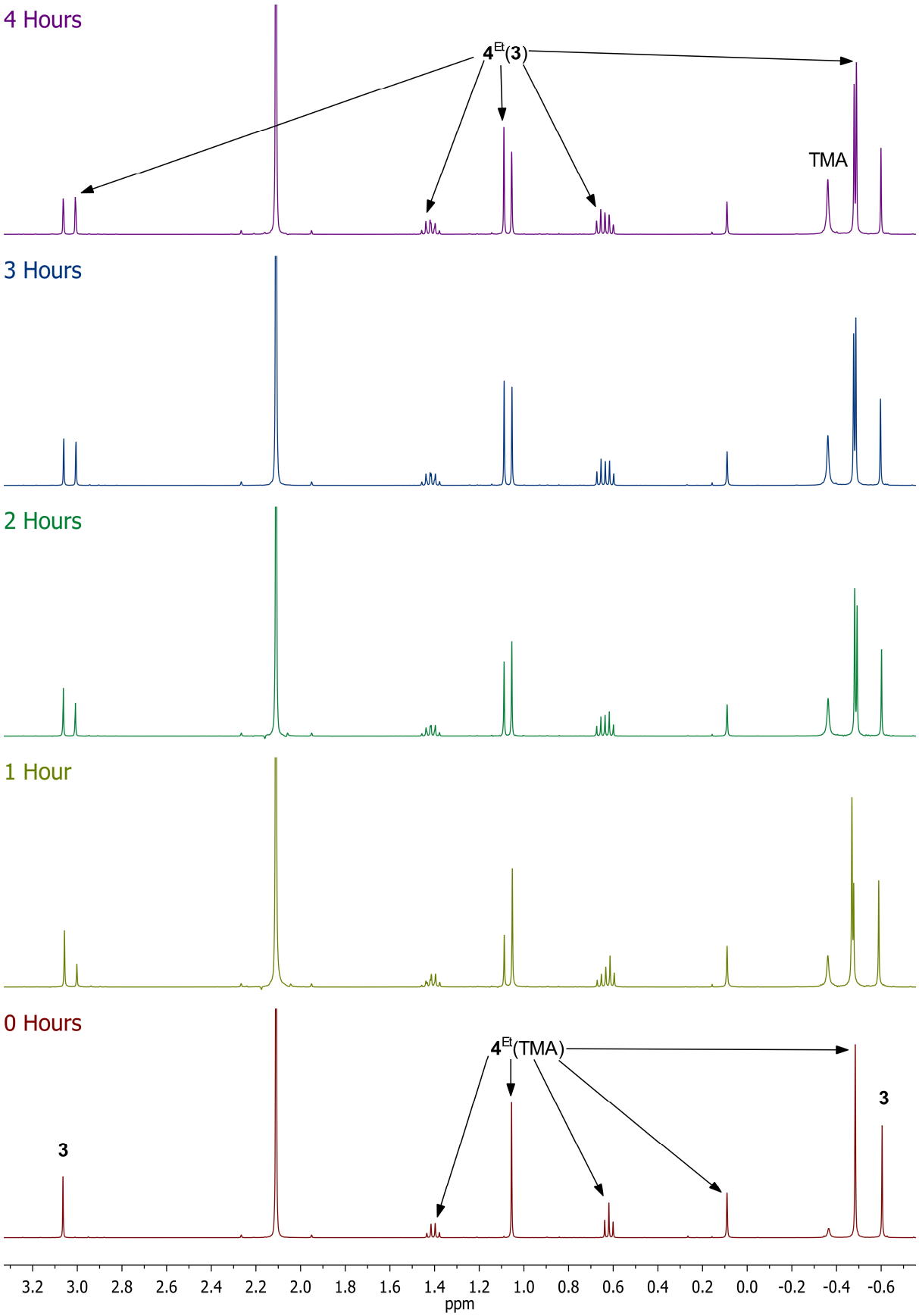

Figure 6.2: ^{1}H NMR spectra of aliquots from the 1:1 reaction between **4**^{Et}(TMA) and **3**, heated to reflux in toluene (δ 2.11 ppm), after time = 0-4 hours. The solvent is benzene-d_6.

Further study of the thermal rearrangement of **4**^{Et}(TMA) focused on heating the reaction mixtures resulting from the 1:1 and 2:1 reaction of TMA with **1**^{Et}. The 1:1 combination of TMA and **1**^{Et} without heating resulted in very limited reaction, with only traces of **4**^{Et}(TMA) and **3** found to exist alongside adduct **1**^{Et}(TMA). Even heating of this reaction mixture to reflux failed to completely react all of **1**^{Et} and instead *ca*. 50% unreacted **1**^{Et} was observed after 2 hours (δ 3.32 ppm, Figure 6.3, bottom). This could be explained by viewing **1**^{Et} as having reacted with 3 equivalents of TMA to yield **4**^{Et}(TMA) and **3**, which then underwent thermal exchange to give **4**^{Et}(**3**) and TMA. This regenerated TMA could then react with the remaining **1**^{Et}, eventually converting half of the available **1**^{Et} into **4**^{Et}(**3**). In the 2:1 TMA:**1**^{Et} system, the greater amount of TMA present aided the formation of **4**^{Et}(TMA) and **3** (Figure 6.3, top). These then acted as a source of further **4**^{Et}(**3**) and TMA when heated to reflux. The eventual outcome of this cycle was the complete removal of both **1**^{Et}(TMA) and TMA from the system, and this explained the prevalence of **4**^{Et}(**3**) in this system. In addition to **4**^{Et}(**3**), **3** was also observed. This could be understood by the appearance of a further species **4**^{Et}, characterised by ^{1}H NMR resonances at δ 1.50, 1.15, 0.68, −0.40 ppm. Literature precedent has suggested that this species would likely exist as a dimer in solution.[59] It appears therefore that **4**^{Et}(**3**) was in equilibrium with its constituent parts (Scheme 6.3), clearly suggested by noting the 1:1 integral of the signals at δ −0.40 and −0.59 ppm (**4**^{Et} and **3**, respectively). Based on ^{1}H NMR spectroscopy, this equilibrium lay heavily on the side of **4**^{Et}(**3**) (*ca*. 88:12 **4**^{Et}(**3**):(**4**^{Et} + **3**)). This equilibrium of heterodimers to form homodimers (or homotrimers) has been shown to occur very slowly, due to the strength of the Al−O−Al bridge bonding.[100] This suggests the 88:12 ratio may not represent the final thermodynamic mixture.

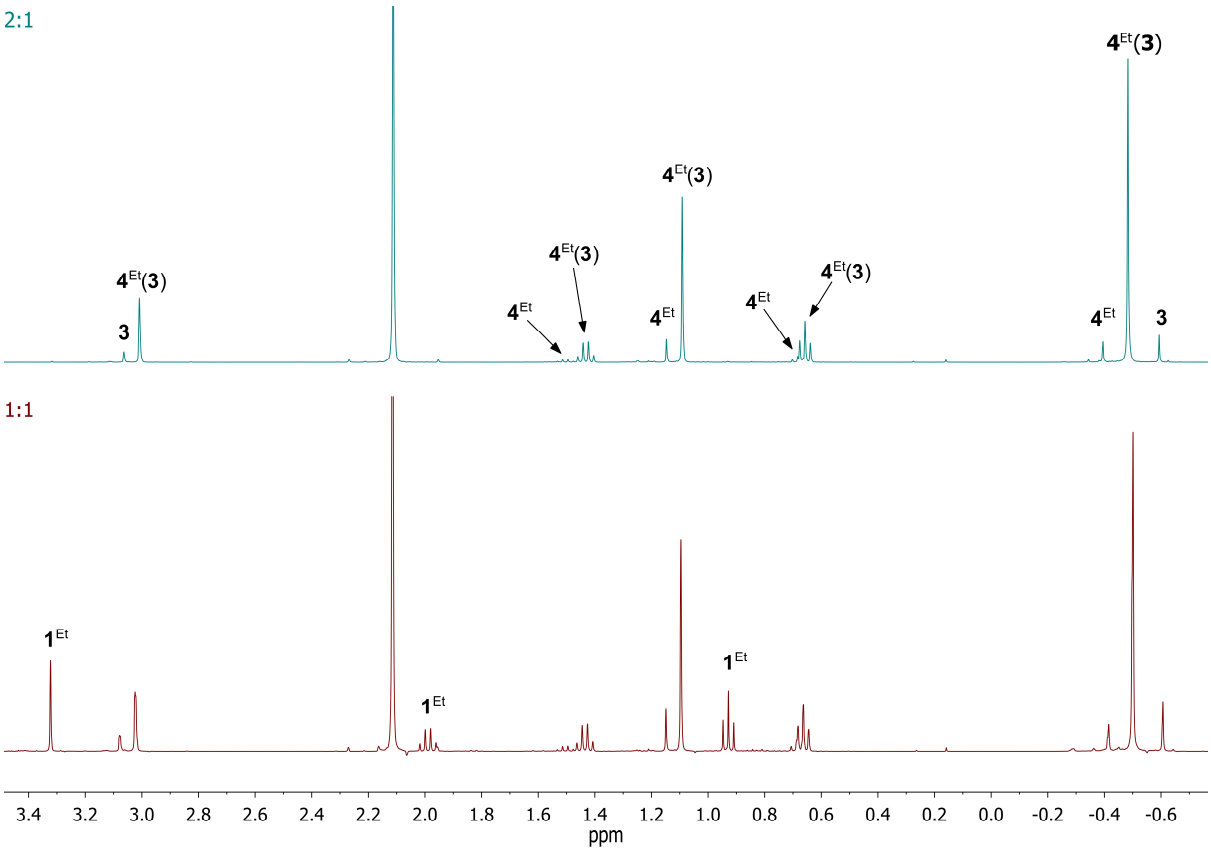

Figure 6.3: ^{1}H NMR spectra of aliquots from the 2:1 (top) and 1:1 (bottom) reactions between TMA and **1**^{Et}, heated to reflux in toluene (δ 2.11 ppm) for 2 hours. The solvent is benzene-d_6.

Repeated attempts to isolate crystalline products of reaction between methyl propionate **1**^{Et} and TMA proved unsuccessful, due to the low melting point of **4**^{Et}(TMA). This led to the replacement of **1**^{Et} with methyl phenylacetate **1**^{Bn} as the benzyl group was expected to increase the melting point. Hence, TMA in toluene was added dropwise to **1**^{Bn} (1:1, 2:1 or 3:1 TMA:**1**^{Bn}). NMR spectroscopic analysis of the resulting mixtures revealed similar behaviour to that observed for the methyl propionate **1**^{Et} system, with the formation of initial adduct **1**^{Bn}(TMA) in the presence of 1 equivalent of TMA, followed by reaction to give **4**^{Bn}(TMA) and **3** in the presence of more than 1 equivalent of TMA (Scheme 6.2). As with **4**^{Et}(TMA), the capture of excess TMA by **4**^{Bn} could be inferred from the ^{1}H NMR spectroscopic observation of **4**^{Bn}(TMA), with signals at δ 0.13 and −0.42 ppm in a 1:4 ratio corresponding to bridging and terminal AlMe groups, alongside retention of the singlet at δ −0.59 ppm due to **3**. ^{13}C NMR spectroscopy corroborated the co-presence of **3** alongside **4**^{Bn}(TMA) through the observation of a broad resonance at δ −11.1 ppm (**3**) alongside signals at δ −4.5 (**4**^{Bn}(TMA), $AlMe_b$) and −7.0 ppm (**4**^{Bn}(TMA), $AlMe_t$). For the 3:1 TMA:**1**^{Bn} combination, the liquid remaining after reaction was concentrated *in vacuo* and stored at 4 °C for 1 day to produce colourless crystals that analysed as a mixture of

4^{Bn}(TMA) and **3**. It was now possible to confirm the identity of **4**^{Bn}(TMA) as $Me_4Al_2(\mu_2$-Me)(μ_2-OCBnMe_2), with X-ray diffraction establishing the symmetry of the Al_2OC metallacycle formed by the capture of TMA and the presence of the expected μ_2-bridging ($AlMe_b$) and terminal ($AlMe_t$) methyl groups (Figure 6.4). The Al−Me bonding shows a significant difference between the bridging and terminal bond lengths; Al−Me_b 2.133(3) Å, Al−Me_t 1.951 Å (mean). The Al_2OC ring has a kite shape, due to the shorter Al−O bond (1.8240(15) Å).

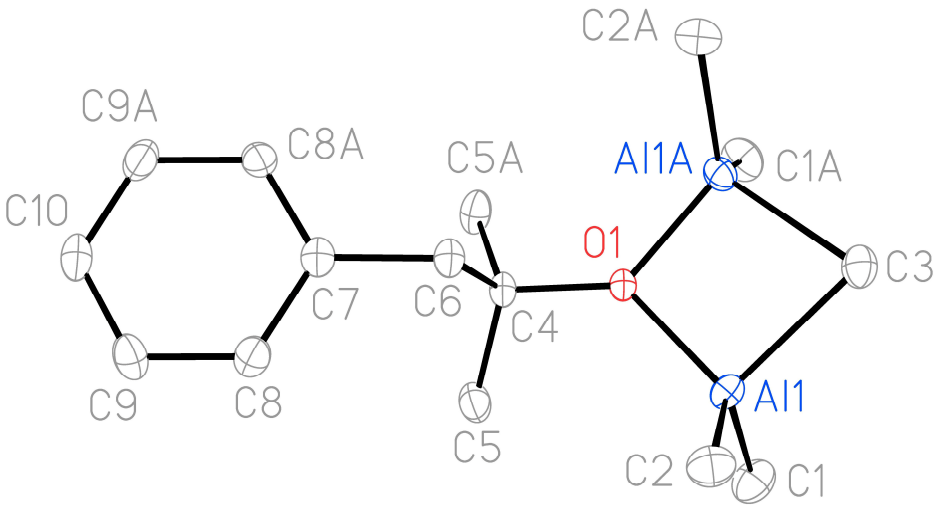

Figure 6.4: Thermal ellipsoid plot of **4**^{Bn}(TMA) (30% probability). H-atoms omitted for clarity. Selected bond lengths (Å) and angles (°): Al1–O1 1.8240(15), Al1–C1 1.952(3), Al1–C2 1.949(3), Al1–C3 2.133(3), Al1–O1–Al1A 96.79(10), Al1–C3–Al1A 79.50(12), O1–Al1–C3 90.97(8).

Diffraction data for the symmetrical $Me_4Al_2(\mu_2$-Me)(μ_2-OR) metallacyclic motif has only previously been reported in the electron diffraction analysis of the hemialkoxide $Me_4Al_2(\mu_2$-Me)(μ_2-O^{t}Bu) in the gas phase (Al−Me_b 2.103(10) Å, Al−Me_t 1.948(7) Å (mean)).[128] Even in the solid-state, there are few examples of an Al_2OC metallacyclic motif, with a search of the Cambridge Crystallographic Database returning only six results. Of these, only four show adducted TMA, demonstrating the highly uncommon nature of this phenomenon. The nearest analogues of **4**^{Bn}(TMA) are based on asymmetric bis(oxyphenyl) structures (Figure 6.5) demonstrated by tetraaluminium bis(bis(oxyphenyl)methyl)anthracene and -dibenzofuran complexes and the dialuminium derivative of a 1,1´-bis-2,2´-oxynaphthyl ligand.[129–131]

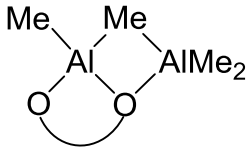

Figure 6.5: The structural motif shown for asymmetric bis(oxyphenyl) compounds.

Attempts were made to isolate one component of the **4**^{Bn}(TMA)-**3** mixture using an alternative solvent. Excess Et_2O was added to an equimolar mixture of **4**^{Bn}(TMA) and **3** (from the 3:1 reaction of TMA with **1**^{Bn} at room temperature). This resulted in the precipitation of a white solid, which was recrystallised to produce colourless blocks. ^{1}H NMR spectroscopic analysis of the blocks indicated the presence of phenyl groups, but not of Et_2O and only one AlMe signal, observed at δ −0.28 ppm, with an integration of 6H per phenyl group. These data suggested the removal of TMA as an ether solvate, resulting in the formation of (**4**^{Bn})$_2$ (Scheme 6.4). The structure was confirmed crystallographically by the observation of a simple dimer based on an Al_2O_2 core, a motif common in aluminium alkoxide chemistry (Figure 6.6).[95,132,133] The Al_2O_2 core is planar and has a rhombus shape. The mean O−Al−O and Al−O−Al angles are 81.3 and 98.7°, respectively.

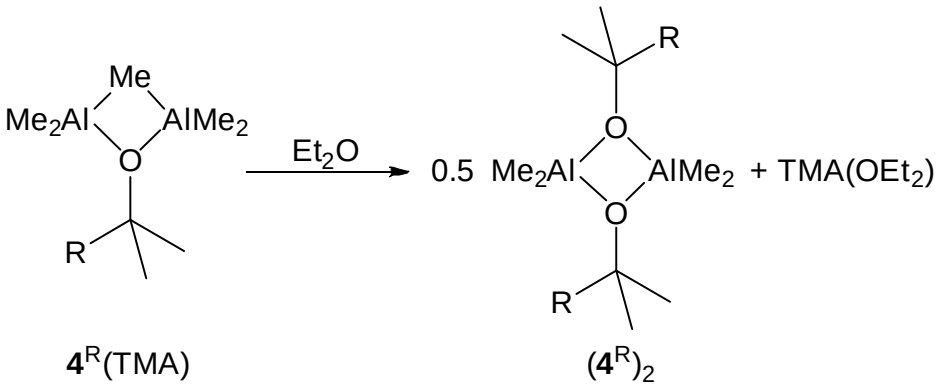

Scheme 6.4: The rearrangement of **4**^{R}(TMA) with Et_2O to form (**4**^{R})$_2$ and TMA(OEt$_2$) (R = Et, Bn).

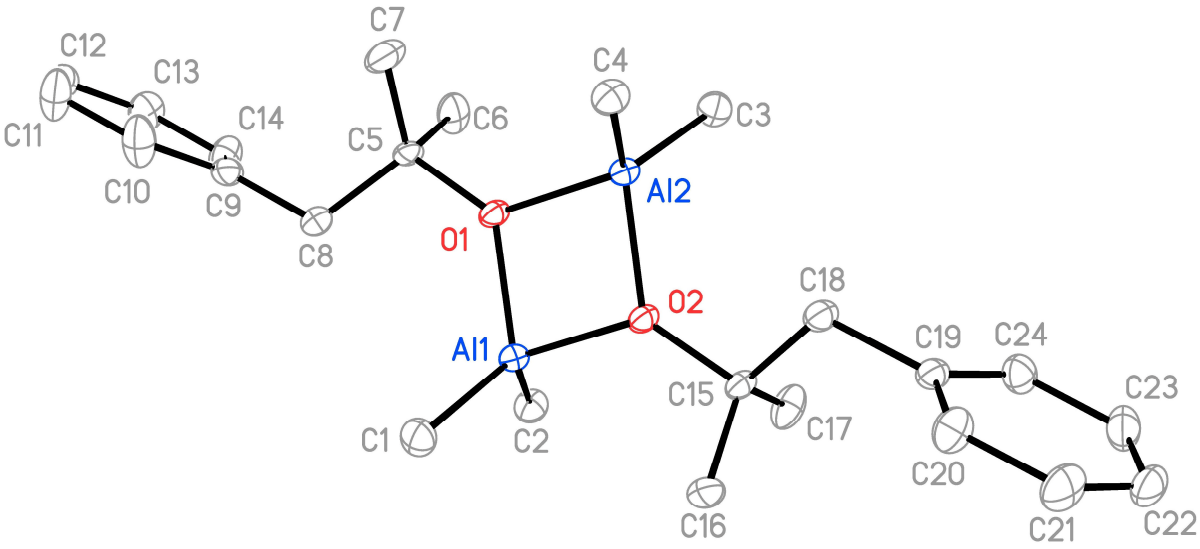

Figure 6.6: Thermal ellipsoid plot of **4**$^{Bn}_2$ (30% probability). H-atoms and minor disorder omitted for clarity. Selected bond lengths (Å) and angles (°): Al1–O1 1.8457(10), Al1–O2 1.8526(10), Al1–C1 1.9522(16), Al1–C2 1.9559(16), Al2–O1 1.8493(10), Al2–O2 1.8447(10), Al2–C3 1.9565(15), Al2–C4 1.9492(15), Al1–O1–Al2 98.76(5), Al1–O2–Al2 98.68(5), O1–Al1–O2 81.20(4), O1–Al2–O2 81.32(4).

6.3 Reactivity of Monoesters with Me_2AlCl

In the previous section, it was shown that methyl propionate and methyl phenylacetate exhibited the same reactivity towards TMA. The use of methyl phenylacetate in particular proved advantageous, as it permitted the isolation of crystalline material. Hence, in the following sections, focus will be placed on studying the reactivity of this monoester. The work will now investigate the reactivity with Me_2AlCl, as this species more closely resembles the products from the reaction of chloromethane with aluminium. Previous literature is scant, but has suggested the formation of alkenes and trimethylated species (Scheme 6.1).[127]

A hexane solution of Me_2AlCl was added to methyl phenylacetate **1**^{Bn} in a 3:1 ratio at −78 °C, after which the mixture was left to reach room temperature. A 3-fold excess of Me_2AlCl was used based on the observed preference for reaction of TMA with esters when the former was in excess (see above). However, in contrast to the 3:1 TMA:**1**^{Bn} reaction which quantitatively give **4**^{Bn}(TMA), work with Me_2AlCl was dominated by adduct formation, with ^{13}C NMR spectroscopy revealing a C=O signal at δ 182.3 ppm for **1**^{Bn}(Me_2AlCl) (cf. δ 170.9 ppm for **1**^{Bn}). The same spectrum suggested limited formation of another species, with signals at δ 50.4 and 28.0 ppm attributable to CH_2 and Me from a dimethylated species. The ^{1}H NMR spectrum (Figure 6.7) reinforced this message,

pointing to 96% adduct formation through the observation of characteristic signals at δ 3.54 and 2.78 ppm (CH_2 and OMe, respectively). The presence of the dimethylated species (4%) was evidenced by minor signals for CH_2 and Me in a 1:3 ratio at δ 2.85 and 1.08 ppm. These shifts were comparable to those seen for **4**^{Bn}(TMA) (δ 2.86 and 1.11 ppm), and suggested 3:1 reaction of Me_2AlCl with ester, initially yielding intermediate BnMeC=O **2**^{Bn} and MeAl(OMe)Cl **5**, before forming a dimethylated species. A signal at δ −0.27 ppm revealed an integral twice that of the signal at δ 1.08 ppm. This suggested that, although it might be expected that the dimethylation of **1**^{Bn}(Me_2AlCl) should yield **4**^{Bn}($MeAlCl_2$), as it was thought each aluminium would retain a chloride ligand, instead **4**^{Bn} traps Me_2AlCl to form **4**^{Bn}(Me_2AlCl). In this species, the chloride ligand bridges the two aluminium centres, leaving four identical AlMe groups (Scheme 6.5).

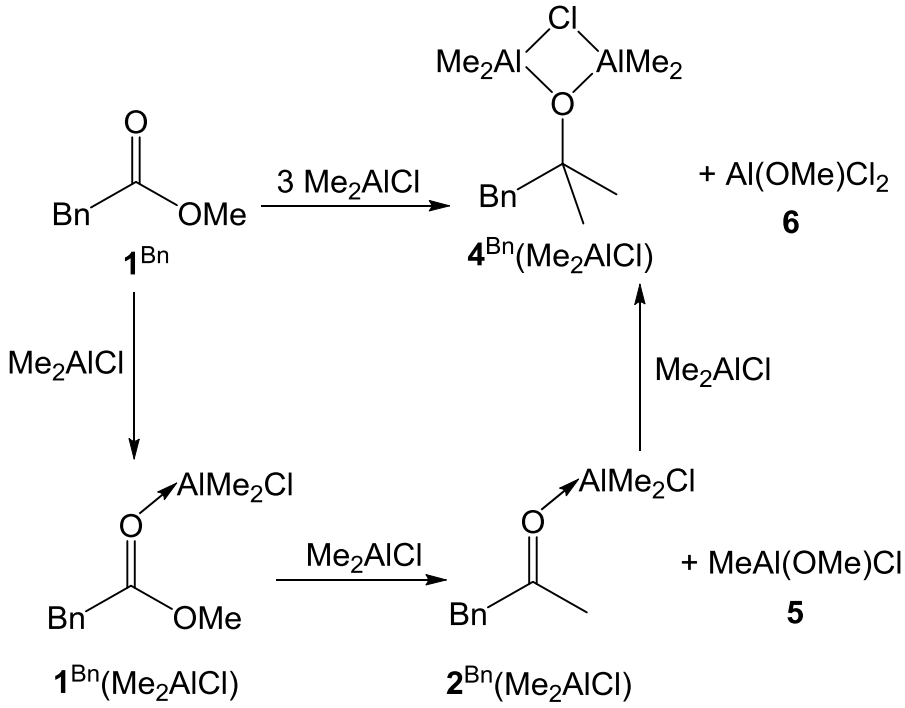

Scheme 6.5: The reaction of methyl phenylacetate **1**^{Bn} with Me_2AlCl at room temperature.

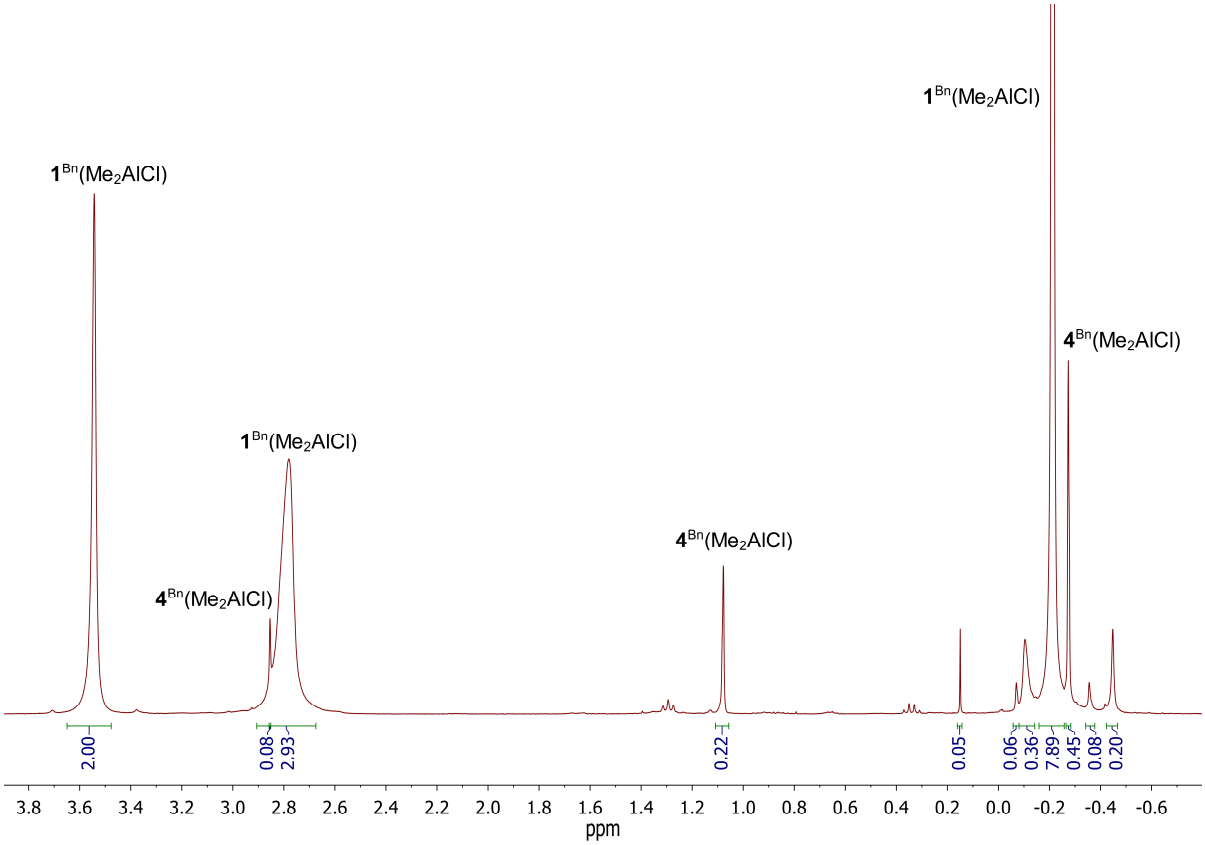

Figure 6.7: ^{1}H NMR spectrum of the reaction mixture from the room temperature reaction between Me_2AlCl and methyl phenylacetate **1**^{Bn} (3:1) in hexane. The solvent is benzene-d_6.

The temperature dependence of the Me_2AlCl-**1**^{Bn} reaction was investigated by heating the reaction mixture to reflux for 24 hours. Spectroscopic analysis of an aliquot revealed substantial growth of the δ 50.4 and 28.0 ppm ^{13}C NMR peaks, pointing to increased formation of the dimethylated species **4**^{Bn}(Me_2AlCl). ^{1}H NMR spectroscopy corroborated this assignment and suggested a mixture containing multiple components. A new set of peaks attributable to a different dimethylated species were observed (δ 2.92 and 1.12 ppm), suggesting another adduct of **4**^{Bn}. This species was identified, using a ^{1}H,^{1}H-NOESY experiment, as the expected product of the dimethylation of **1**^{Bn}, **4**^{Bn}($MeAlCl_2$), through the observation of NOE signals between the Me signal at δ 1.12 ppm and three different AlMe signals at δ −0.22, −0.32 and −0.37 ppm. This species was proposed to be produced from the reaction of **4**^{Bn}(Me_2AlCl) with $Al(OMe)Cl_2$ **6** (Scheme 6.6). The main species in the final reaction mixture were the adducts **1**^{Bn}(Me_2AlCl) (44%), **4**^{Bn}(Me_2AlCl) (26%) and **4**^{Bn}($MeAlCl_2$) (28%). However, two minor species present were alkenes **7** in a 2% combined yield of **7a** (PhCH=CMe_2, δ 6.28, 1.71 and 1.68 ppm) and **7b** (BnC(=CH_2)Me, δ 4.80, 4.75 and 1.55 ppm). These were thought to be produced from the elimination of $Me_3Al_2(OH)Cl_2$ **8** from **4**^{Bn}($MeAlCl_2$) (Scheme 6.6). This elimination was thought to have

proceeded via a thermal syn elimination, resulting in the formation of an alkene and the organoaluminium hydroxide **8**. This elimination reaction did not occur when esters were reacted with TMA, which is thought to be due to the lower Lewis acidity of TMA. The chloride groups of **4**^{Bn}($MeAlCl_2$) have an increased electron withdrawing ability and result in a more basic organoaluminium, enabling thermal elimination. The increased Lewis acidity of Me_2AlCl relative to TMA was previously demonstrated by the thermal decomposition of organoaluminiums, with a greater number of chloride groups resulting in reactions at lower temperatures.[102]

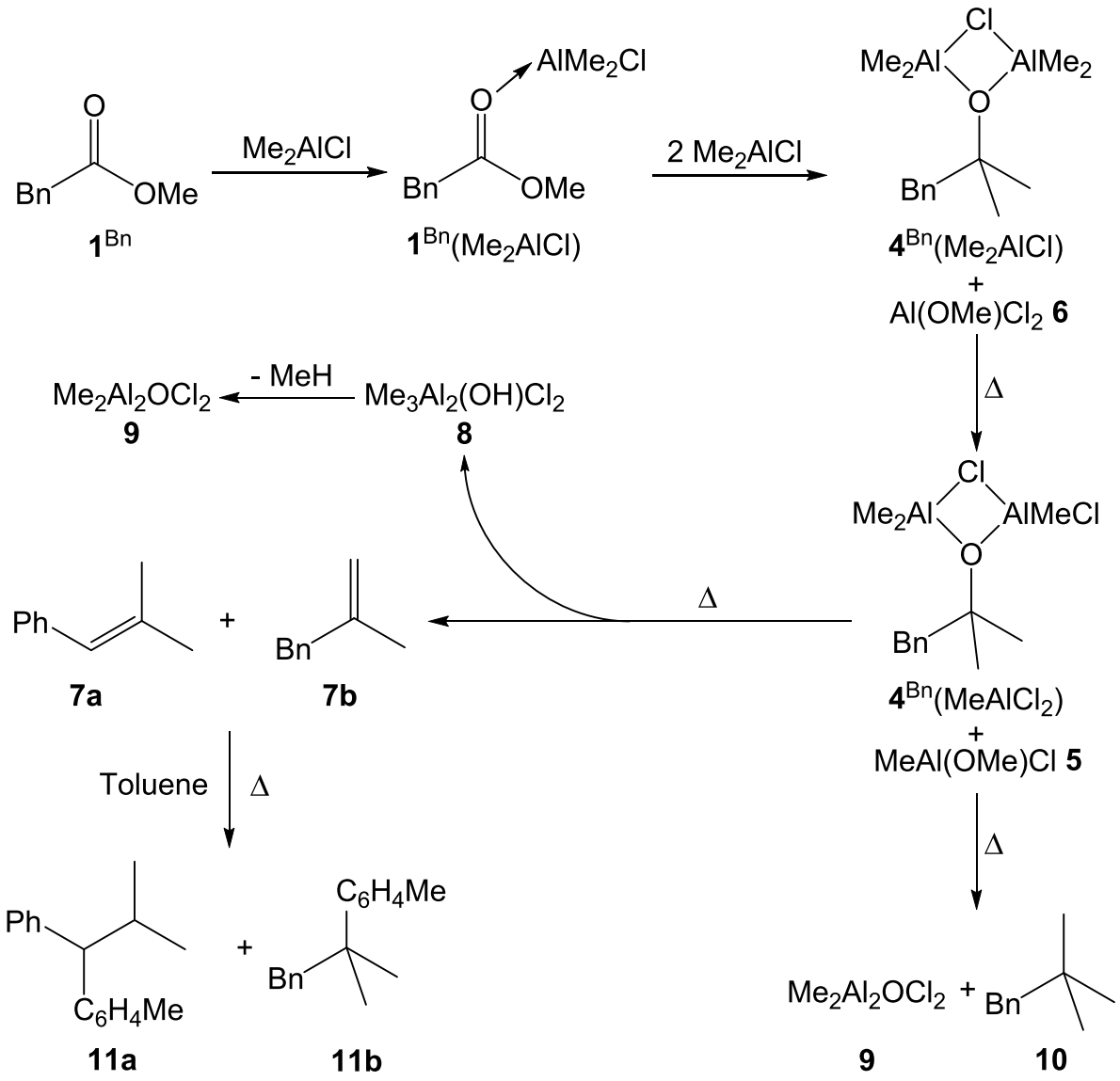

Scheme 6.6: The proposed reaction of methyl phenylacetate **1**^{Bn} with Me_2AlCl in toluene at raised temperatures.

The same 3:1 reaction was heated to 100 °C for 24 hours in toluene-d_8 in a sealed J Young NMR tube. The resulting mixture revealed signals consistent with methane (^{1}H NMR δ

0.17 ppm, ^{13}C NMR δ −4.3 ppm, Figure 6.8),[134] suggesting that **8** had converted to the aluminoxane $Me_2Al_2OCl_2$ **9**.

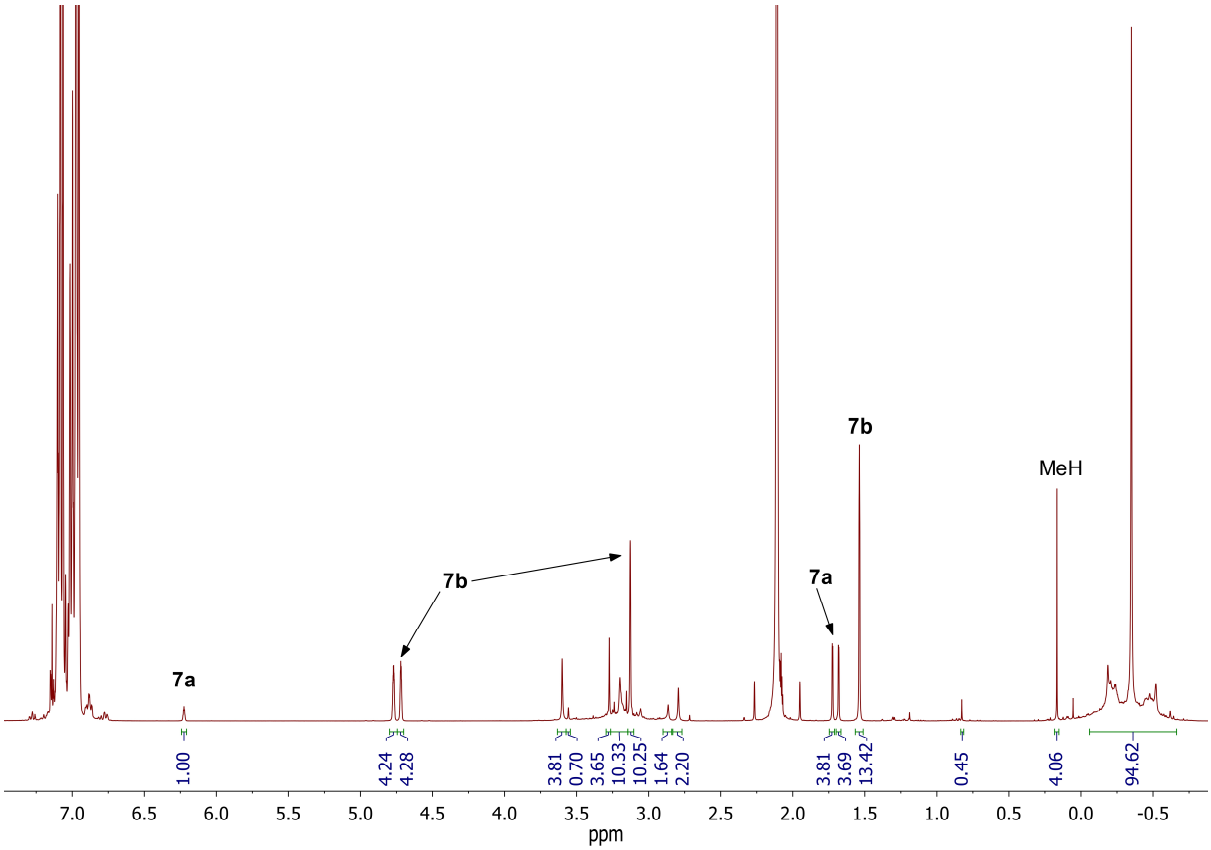

Figure 6.8: ^{1}H NMR spectrum of an aliquot from the reaction of Me_2AlCl with methyl phenylacetate **1**^{Bn} in a 3:1 ratio, after heating to 100 °C for 24 hours in toluene-d_8 in a sealed J Young NMR tube.

The 3:1 Me_2AlCl:**1**^{Bn} was repeated in toluene to further study the effect of temperature on the reaction. While heating to reflux for 2 hours yielded **1**^{Bn}(Me_2AlCl) (40%) and alkenes **7** (60%, 1:4 **7a**:**7b**), heating for 24 hours resulted in Friedel-Crafts reaction of the solvent.[135] Nevertheless, variable temperature studies in toluene successfully revealed alkene formation from 60 °C and exhaustive methylation to give Bn^{t}Bu **10** from 80 °C with adducts of **4**^{Bn} not observed at temperatures in excess of 70 °C (Scheme 6.6 and Figure 6.9). The proportions of each product as a function of temperature are plotted in Figure 6.10. Lastly, investigation of reaction stoichiometry revealed data consistent with the mechanism in Scheme 6.6; **1**^{Bn}(Me_2AlCl) (42%) and alkenes **7** (58%) formed when using 2:1 Me_2AlCl:**1**^{Bn} in toluene, while a 1:1 ratio led to the dominance of **1**^{Bn}(Me_2AlCl).

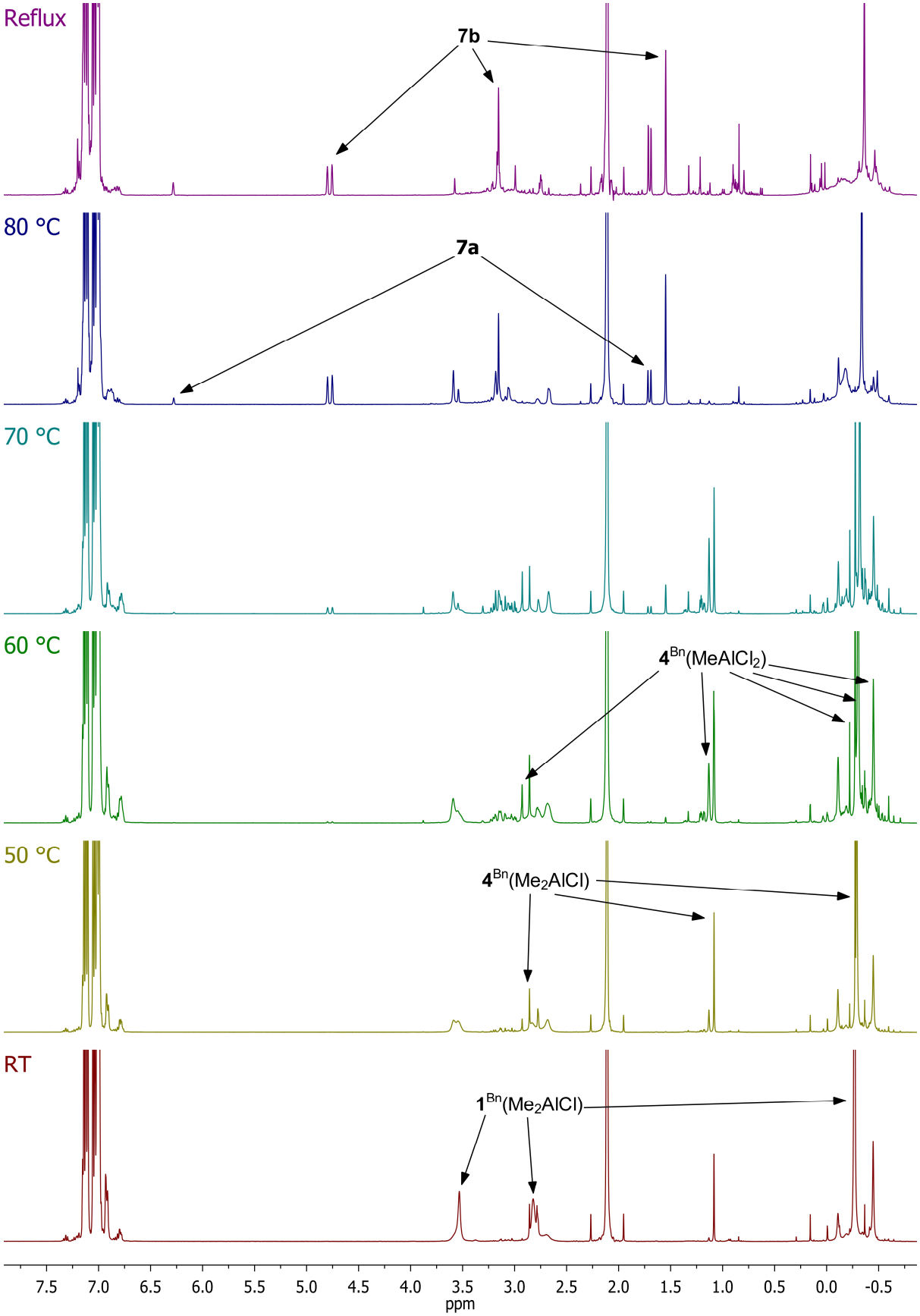

Figure 6.9: ^{1}H NMR spectra of aliquots from the reaction of Me_2AlCl and methyl phenylacetate $\mathbf{1}^{Bn}$ in a 3:1 ratio in toluene, heated at the stated temperature for 24 hours. The solvent is benzene-d_6.

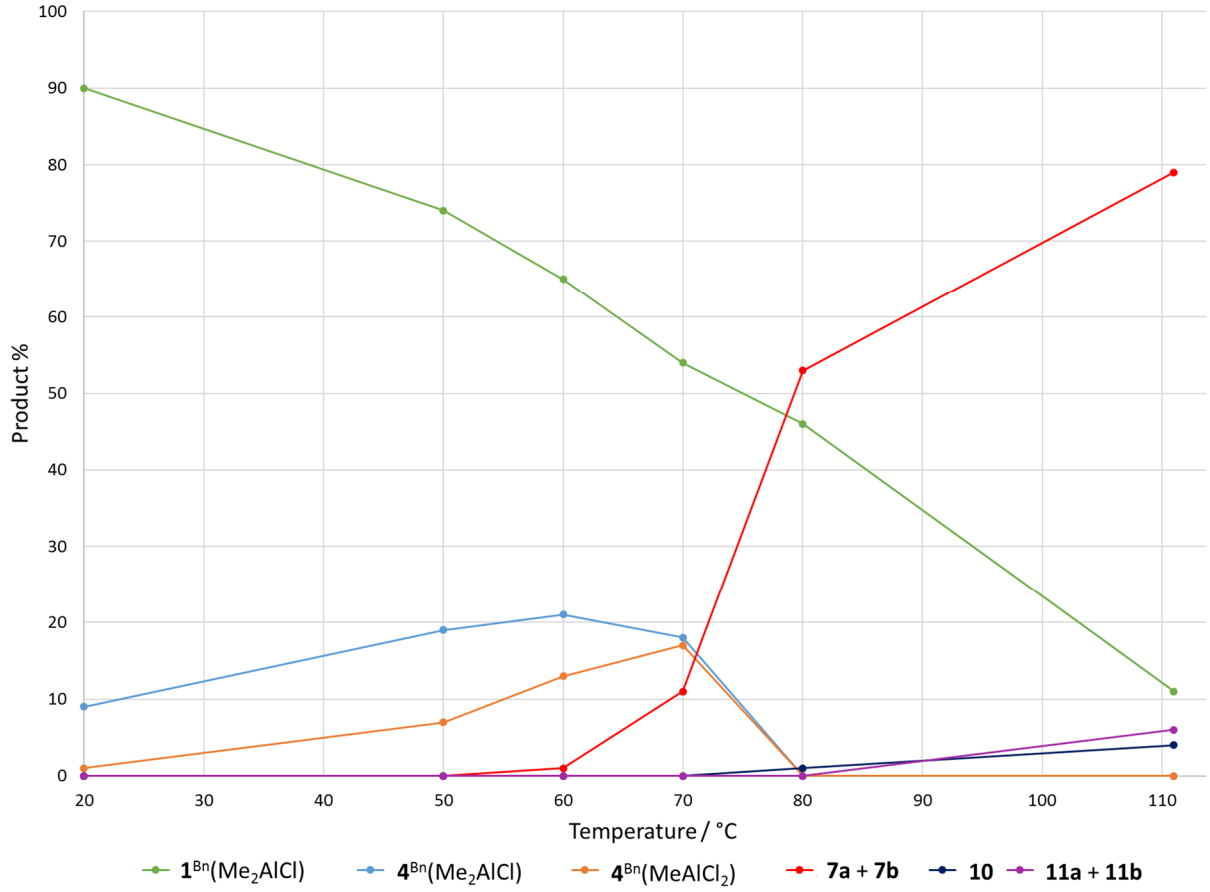

Figure 6.10: The proportions of products obtained from the reaction of Me_2AlCl and methyl phenylacetate **1**^{Bn} in a 3:1 ratio in toluene, heated at the stated temperature for 24 hours. The proportions are calculated by integration of the ^1H NMR spectra.

Attempts to isolate **4**^{Bn}(Me_2AlCl) and **4**^{Bn}($MeAlCl_2$) were undertaken. The Me_2AlCl-**1**^{Bn} reaction mixture that was heated to 60 °C for 24 hours was shown spectroscopically to yield the greatest proportion of dimethylation products. The solvent and volatiles were therefore removed *in vacuo* to give a liquid which solidified upon standing at room temperature. Recrystallisation from the melt yielded material suitable for X-ray analysis (Figure 6.11). Diffraction revealed metallacyclic $Me_4Al_2(\mu_2\text{-}Cl)(\mu_2\text{-}OCBnMe_2)$, **4**^{Bn}($Me_2AlCl$). This general structure is similar to that seen for **4**^{Bn}(TMA) and is consistent with the structure predicted from NMR spectroscopy. Compared to **4**^{Bn}(TMA), the bridging Al–Cl bond (2.308(2) Å) is longer than the bridging Al–Me bond (2.133(3) Å) due to the larger chloride ligand. Slight differences are also observed in the bond lengths within the 4-membered ring. Hence, the Al–O–Al bond angle in **4**^{Bn}(TMA) (96.79(10)°) is significantly reduced relative to that found in **4**^{Bn}(Me_2AlCl) (107.8(2)°). This increase can similarly be attributed to steric factors. The structural motif demonstrated by **4**^{Bn}(Me_2AlCl) is highly unusual, with fully characterised $Al_2(\mu_2\text{-}O)(\mu_2\text{-}Cl)$ metallacycles being rare.

Currently, only two other examples have been crystallographically characterised – both the result of $AlCl_3$ adduct formation and containing no Al–C bonds.[136,137] Unfortunately, the coexistence of **4**^{Bn}(Me_2AlCl) and **4**^{Bn}($MeAlCl_2$) as a mixture of crystalline products made it impossible to obtain accurate elemental analysis and high quality spectroscopic data.

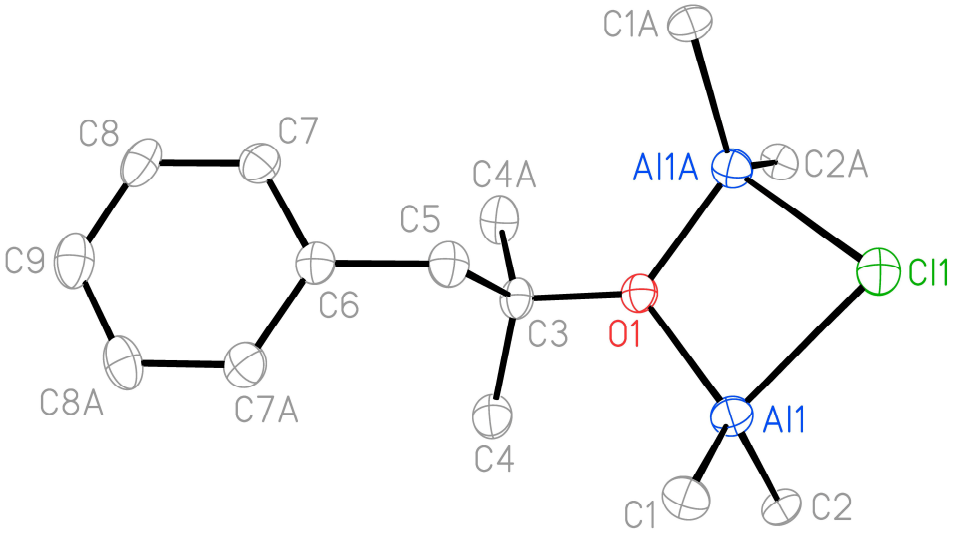

Figure 6.11: Thermal ellipsoid plot of **4**^{Bn}(Me_2AlCl) (30% probability). H-atoms omitted for clarity. Selected bond lengths (Å) and angles (°): Al1–O1 1.837(3), Al1–C1 1.954(5), Al1–C2 1.982(5), Al1–Cl1 2.308(2), Al1–O1–Al1A 107.8(2), Al1–Cl1–Al1A 80.06(9), Cl1–Al1–O1 85.08(13).

6.4 Reactivity of Monoesters with $MeAlCl_2$

The following section will aim to repeat the above reactions, but with Me_2AlCl replaced with $MeAlCl_2$. This is because a more accurate view (than expressed at the start of Section 6.3) of the product of the reaction between chloromethane and aluminium is that it is, in fact, methylaluminium sesquichloride, which is an equimolar mixture of Me_2AlCl and $MeAlCl_2$. The increased Lewis acidity of $MeAlCl_2$ led to the predominance of adduct formation. Analysis of the room temperature reaction of **1**^{Bn} with 3 equivalents of $MeAlCl_2$ revealed a C=O signal at δ 184.2 ppm in the ^{13}C NMR spectrum due to **1**^{Bn}($MeAlCl_2$) (cf. δ 170.9 ppm for **1**^{Bn}). Heating the reaction mixture to reflux for 24 hours resulted in a dark brown solution. ^{13}C NMR spectroscopy now revealed a C=O signal at δ 214.8 ppm, which suggested the formation of a ketone-organoaluminium adduct.[99] Hydrolysis of the reaction mixture and extraction of the organic layer with toluene gave a brown oil. ^{13}C NMR spectroscopy of this oil revealed that the C=O peak had moved to δ 195.8 ppm, attributed to an adduct-free ketone. ^{1}H NMR spectroscopy revealed several signals in the aromatic

region, multiple CH_2 signals, centred at *ca.* δ 3.9 ppm, and multiple methyl signals. HMBC suggested that these were attributable to multiple organic species. Further attempts to elucidate the identity of these species proved futile. However, taken together, the spectroscopic data suggested that a Friedel-Crafts acylation with toluene had occurred, due to the Lewis acidity of $MeAlCl_2$, forming **12** (Figure 6.12).[138] Friedel-Crafts acylation has previously been observed with esters, using indium tribromide as a Lewis acid catalyst.[139] Consistent with this hypothesis, repeating the reaction in heptane resulted in only adduct formation, even after heating to reflux for 24 hours.

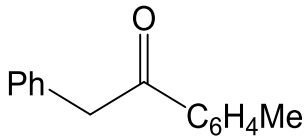

12

Figure 6.12: The proposed structure of the product from the 3:1 reaction of $MeAlCl_2$ with methyl phenylacetate $\mathbf{1}^{Bn}$ in toluene, which was heated to reflux for 24 hours.

6.5 Reactivity of Monoesters with $Me_{1.5}AlCl_{1.5}$

The reactivity of esters with an equimolar mixture of Me_2AlCl and $MeAlCl_2$ ($Me_{1.5}AlCl_{1.5}$, methylaluminium sesquichloride) is of particular interest as this should be the composition of the material produced from the aluminium-chloromethane reactions believed to occur in contaminated refrigeration units. The 3:1 reactions of $Me_{1.5}AlCl_{1.5}$ with methyl phenylacetate $\mathbf{1}^{Bn}$ yielded activity intermediate of that seen for Me_2AlCl and $MeAlCl_2$. Room temperature reactions produced the adduct $\mathbf{1}^{Bn}(Me_{1.5}AlCl_{1.5})$ (presumed to be a rapid equilibrium between $\mathbf{1}^{Bn}(Me_2AlCl)$ and $\mathbf{1}^{Bn}(MeAlCl_2)$) with a ^{13}C NMR signal δ 183.6 ppm pointing to Lewis acidity intermediate with respect to that of Me_2AlCl and $MeAlCl_2$ (cf. δ 182.3 ppm for $\mathbf{1}^{Bn}(Me_2AlCl)$, δ 184.2 ppm for $\mathbf{1}^{Bn}(MeAlCl_2)$). Below 60 °C, adduct formation dominated and dimethylation was not detected. At 70 °C and above, reaction occurred; alkenes **7**, trimethylated **10** and Friedel-Crafts products **11** were identified in the reaction mixture (Figure 6.13). The expected mixture of dimethylated species $\mathbf{4}^{Bn}(Me_2AlCl)$ and $\mathbf{4}^{Bn}(MeAlCl_2)$ was not observed at any temperature. However, the existence of alkenes **7** suggested that these species had formed, albeit as rapidly consumed intermediates. The difference in reactivity compared to Me_2AlCl can be understood in terms of $Me_{1.5}AlCl_{1.5}$ being less nucleophilic and more Lewis acidic than Me_2AlCl,

resulting in slower addition and faster elimination.[140,141] The reactions of **1**^{Bn} with $Me_{1.5}AlCl_{1.5}$ therefore followed the same overall pathway as seen for Me_2AlCl (Scheme 6.6), albeit at a slower rate due to the sesquichloride being a weaker nucleophile.

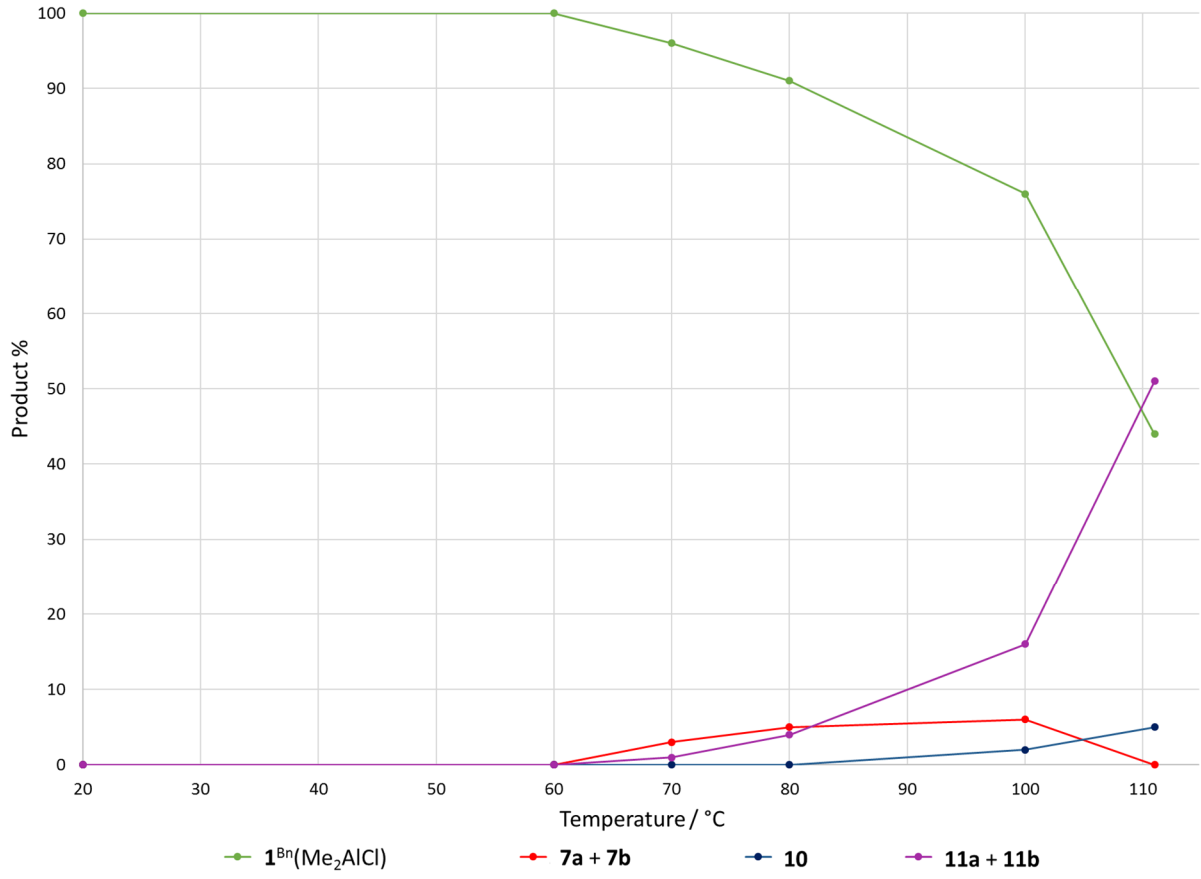

Figure 6.13: The proportions of products obtained from the reaction of $Me_{1.5}AlCl_{1.5}$ and methyl phenylacetate **1**^{Bn} in a 3:1 ratio in toluene, heated at the stated temperature for 24 hours. The proportions are calculated by integration of the ^{1}H NMR spectra.

6.6 Reactions of Phenylacetyl Chloride with TMA and Me_2AlCl

To further investigate methane production from the products of Me_2AlCl-**1**^{Bn} reactions, attempts were made to separately isolate **4**^{Bn}(Me_2AlCl) and **4**^{Bn}($MeAlCl_2$) via an alternative method. The reaction of phenylacetyl chloride **13**^{Bn} with 2 equivalents of TMA resulted in complete conversion to **4**^{Bn}(Me_2AlCl), as determined by ^{1}H NMR spectroscopy. This was believed to proceed by TMA first undergoing methyl-chloride exchange with **13**^{Bn} to produce phenylacetone **2**^{Bn} (and Me_2AlCl), which then reacted with TMA to produce **4**^{Bn}(Me_2AlCl) (Scheme 6.7). Heating a toluene solution of **4**^{Bn}(Me_2AlCl) to reflux for 2 hours resulted in 10% conversion to (**4**^{Bn})$_2$ but failed to yield either alkenes or methane.

Concentration of the room temperature reaction mixture and storage at −27 °C resulted in the formation of crystalline material. Crystallographic unit cell check and further analysis confirmed these crystals to be **4**^{Bn}(Me_2AlCl); the same product as that obtained from the Me_2AlCl-**1**^{Bn} reaction (Figure 6.11).

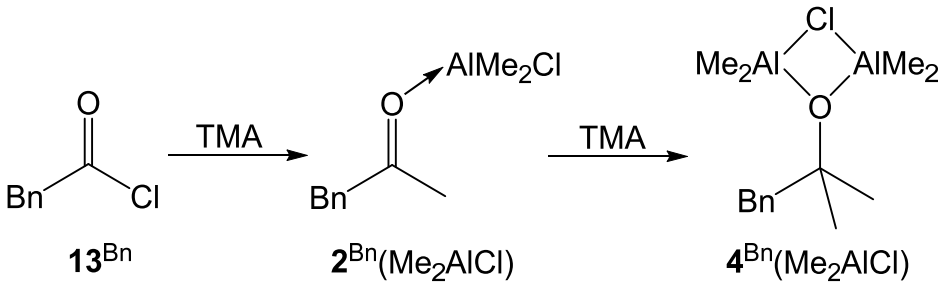

Scheme 6.7: The reaction of phenylacetyl chloride **13**^{Bn} with 2 equivalents of TMA, producing **4**^{Bn}(Me_2AlCl).

Attempts to produce **4**^{Bn}($MeAlCl_2$) involved reacting **13**^{Bn} with TMA and Me_2AlCl (1 equivalent of each). This was expected to initially form **2**^{Bn} and 2 equivalents of Me_2AlCl, with reaction between these species then occurring slowly (due to the reduced nucleophilicity of Me_2AlCl compared to that of TMA). Stirring at room temperature for 2 hours resulted in 49% **2**^{Bn}, 33% **4**^{Bn}(Me_2AlCl) and 18% **4**^{Bn}($MeAlCl_2$) (Figure 6.14). Meanwhile, raising the reaction temperature to 60 °C led to an increase in the amount of **4**^{Bn}($MeAlCl_2$) (8% **2**^{Bn}, 31% **4**^{Bn}(Me_2AlCl) and 61% **4**^{Bn}($MeAlCl_2$)). However, above 70 °C, the formation of alkenes **7a** and **7b** was observed, and Friedel-Crafts reaction with toluene to form products **11a** and **11b** was also now seen (Scheme 6.8). Furthermore, heating the reaction mixture to 100 °C in toluene-d_8 in a sealed J Young NMR tube for 2 hours revealed the presence of methane (^{1}H NMR δ 0.17 ppm, ^{13}C NMR δ −4.3 ppm), indicating that it is **4**^{Bn}($MeAlCl_2$) and not **4**^{Bn}(Me_2AlCl) that represents a source of methane. This difference in reactivity is attributed to the higher Lewis acidity of $MeAlCl_2$, which promoted more facile elimination of the alkene.

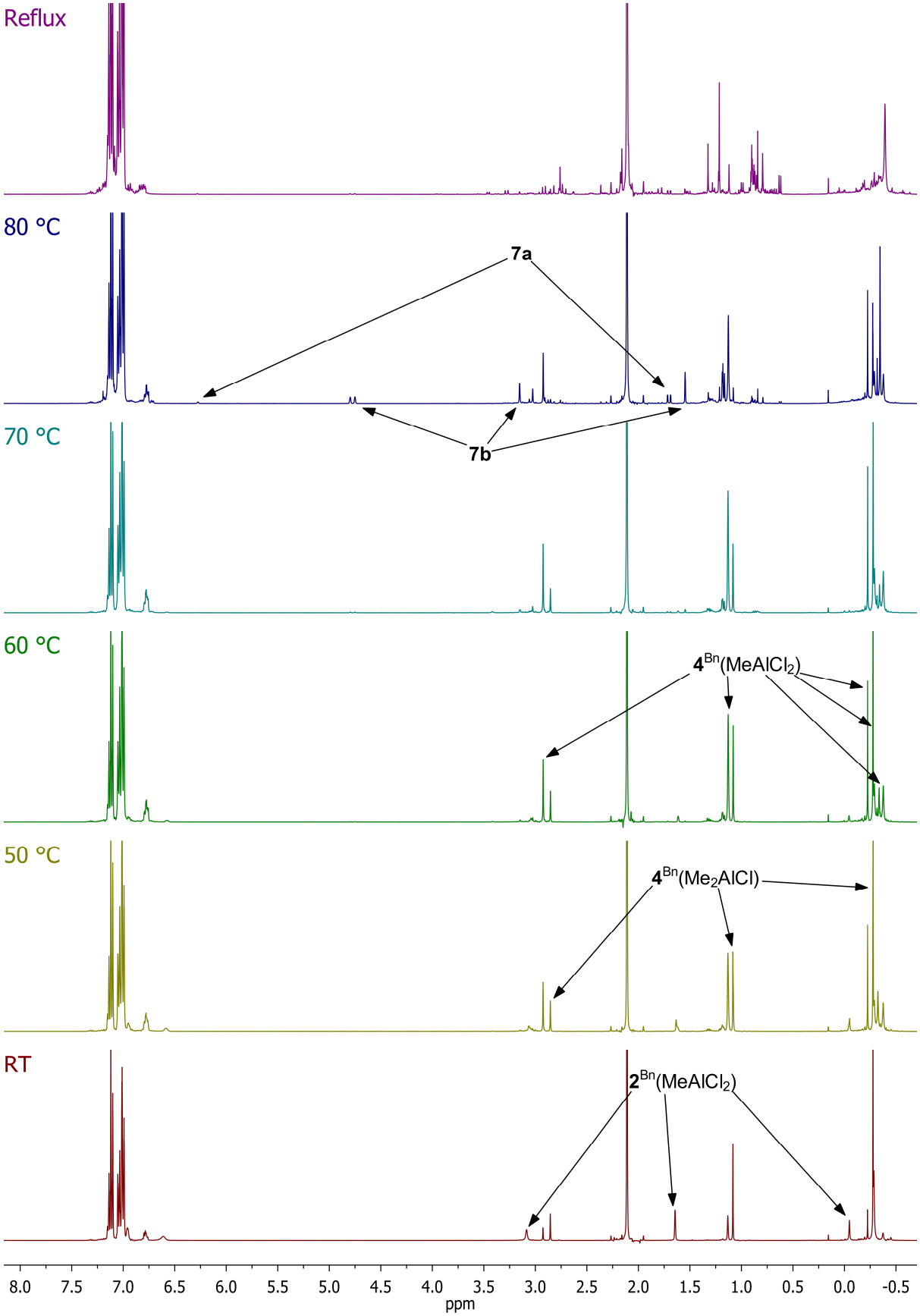

Figure 6.14: ^{1}H NMR spectra of aliquots from the reaction of TMA, Me_2AlCl and phenylacetyl chloride **13**^{Bn} in a 1:1:1 ratio in toluene heated at the stated temperatures for 2 hours. The solvent is benzene-d_6.

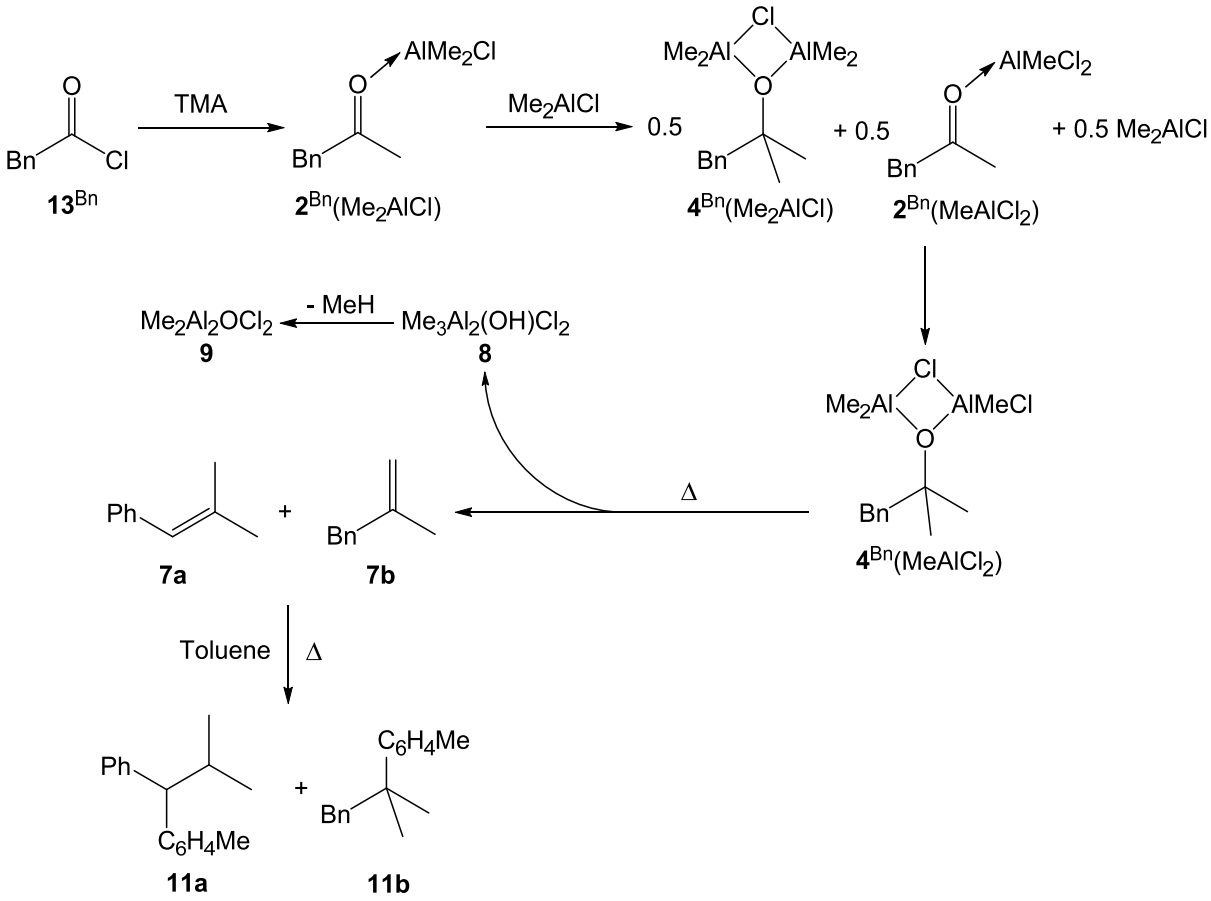

Scheme 6.8: The reaction of phenylacetyl chloride **13**^{Bn} with TMA and Me_2AlCl (1 equivalent of each).

6.7 Summary

The reaction of methylaluminium reagents with POE refrigeration oils was modelled using monoesters. The addition of 1 equivalent of TMA to monoester **1**^{R} (R = Et, Bn) has resulted in the formation of an adduct **1**^{R}(TMA). Addition of further equivalents of TMA resulted in the formation of the aluminium alkoxides **4**^{R}(TMA) and **3** from nucleophilic addition, with complete reaction occurring with 3 equivalents of TMA. The heating of **4**^{R}(TMA) and **3** resulted in an exchange reaction to form **4**^{R}(**3**) and release TMA. This thermal rearrangement allowed for the formation of a stable Al_2O_2 metallacycle and the entropically favourable release of TMA. The released TMA proved capable of reacting with remaining **1**^{R}, resulting in 2 equivalents of TMA being required overall for full ester cleavage. This ester cleavage would clearly be problematic in refrigeration systems, as **4**^{R}(TMA), **3** or **4**^{R}(**3**) would not be able to act as lubricants. The use of methyl phenylacetate **1**^{Bn} resulted in the isolation of crystalline **4**^{Bn}(TMA), which was based on a rare example

of a symmetrical Al_2OC metallacycle. The addition of the Lewis base Et_2O to **4**^{Bn}(TMA) then resulted in the extraction of TMA and the formation of **4**^{Bn} which crystallises as the dimer (**4**^{Bn})$_2$.

Using Me_2AlCl instead of TMA resulted in a more sluggish reaction, with reactions at room temperature predominately leading to the formation of the adduct **1**^{Bn}(Me_2AlCl) and small amounts of **4**^{Bn}(Me_2AlCl). This decreased reactivity was attributed to the reduced nucleophilicity of Me_2AlCl compared to TMA. Increasing the temperature of the reaction resulted in an increase in the amount of **4**^{Bn}(Me_2AlCl) and the appearance of a second dimethylated species, **4**^{Bn}($MeAlCl_2$). Above 60 °C, evidence for the generation of alkenes **7a** and **7b** could be observed by ^{1}H NMR spectroscopy. Furthermore, increasing the temperature resulted in increased amounts of these alkenes and a decrease in the proportion of **4**^{Bn}(Me_2AlCl) and **4**^{Bn}($MeAlCl_2$). The alkenes were proposed to form from a thermal elimination reaction of **4**^{Bn}($MeAlCl_2$). The fact that elimination was observed for reactions with Me_2AlCl, but not with TMA, was associated with the inclusion of chloride ligands, increasing the Lewis acidity of the aluminium centre. This elimination reaction also produced (by deduction) $Me_3Al_2(OH)Cl_2$ **8**, which could then release methane and (logically) form $Me_2Al_2OCl_2$ **9**. The formation of methane gas was confirmed through its observation by *in situ* NMR spectroscopy. At higher temperatures a trimethylated species **10** and the Friedel-Crafts products **11a** and **11b** (from reaction with toluene) were also observed. From the reaction at 60 °C, crystals of **4**^{Bn}(Me_2AlCl) were obtained and X-ray crystallography revealed a symmetrical metallacycle similar to that found in **4**^{Bn}(TMA), but with the bridging methyl group replaced by a chloride.

Replacement of Me_2AlCl with $MeAlCl_2$ initially resulted in ketone formation due to Friedel-Craft acylation with the solvent (toluene). Meanwhile, replacing toluene with heptane led to only the adduct **1**^{Bn}($MeAlCl_2$) as $MeAlCl_2$ is a weak nucleophile. Using a mixture of Me_2AlCl and $MeAlCl_2$ (methylaluminium sesquichloride) resulted in activity similar to that of Me_2AlCl. However, the dimethylated species **4**^{Bn}(Me_2AlCl) and **4**^{Bn}($MeAlCl_2$) were not observed at any temperature. In spite of this, the production of alkenes **7a** and **7b** suggested that the **4**^{Bn} adducts might play a role as short-lived intermediates in the reactions occurring. This could be attributed to the reduced nucleophilicity of $Me_{1.5}AlCl_{1.5}$ relative to Me_2AlCl, resulting in slower formation of

4^{Bn}(Me_2AlCl) and **4**^{Bn}($MeAlCl_2$), and its increased Lewis acidity, resulting in faster elimination.

The production of methane in the reactions reported here is significant for the industrial refrigeration sector, due to the potential for explosions. To further investigate its production, the individual syntheses of **4**^{Bn}(Me_2AlCl) and **4**^{Bn}($MeAlCl_2$) were attempted via alternative methods. Hence, the reaction of 2 equivalents of TMA with phenylacetyl chloride **13**^{Bn} resulted in complete conversion to **4**^{Bn}(Me_2AlCl). However, heating a toluene solution of analytically pure **4**^{Bn}(Me_2AlCl) to reflux resulted in neither methane nor alkene production. Replacing 1 equivalent of TMA with Me_2AlCl resulted in a slower reaction which produced a mixture of phenylacetone **2**^{Bn}, **4**^{Bn}(Me_2AlCl) and **4**^{Bn}($MeAlCl_2$). Heating this mixture resulted in methane production above 70 °C according to NMR spectroscopy. This suggested that it is **4**^{Bn}($MeAlCl_2$) that undergoes thermal elimination. This was attributed to the greater number of chloride ligands, which increases the Lewis acidity of the aluminium and promotes elimination.

As the refrigeration oil RL 32H contains ester functionalities, the reactions discussed above present a model for industrial systems. The breakdown of the ester is a concern as the aluminium alkoxides (**4**^{R} and **3**) and alkenes (**7a** and **7b**) formed will not be able to provide the same lubricity as the refrigeration oil. The increased friction may lead to higher internal temperatures within the refrigeration system, which may in turn accelerate decomposition of the lubricating oil. Subsequent elimination reactions of aluminium alkoxides (observed for higher chlorine-content organoaluminiums) is a particularly concerning result, as the production of large amounts of methane and alkenes could lead to potentially explosive conditions. This work will be extended in the following chapter wherein the reactions of methylaluminium reagents with tetraesters (which more closely model commercial refrigeration POEs) will be reported.

Chapter 7

Reactivity of Tetraesters with Methylaluminium Reagents

7.1 Introduction

In the previous chapter, it was shown that the interaction of monoesters with methylaluminium reagents resulted in cleavage of the ester. Furthermore, reactions with Me_2AlCl and $Me_{1.5}AlCl_{1.5}$ led to the release of methane above 70 °C. The scope of this reactivity will now be extended, using tetraesters that closely mimic the refrigeration oil RL 32H (see Section 5.2 for details on the composition of RL 32H). This will involve the synthesis of model POEs containing only one type of ester group to simplify analysis. There is currently little literature concerning the interaction between organoaluminiums and polyolesters. The addition of $AlCl_3$ to diesters and triesters has been reported to result in 1:1 $AlCl_3$ to ester adduct formation, with X-ray crystal structures reported for both of these species.[142,143] The reaction of a dimethylaluminium alkoxide with lactide (a cyclic diester) resulted in opening of the lactide and intramolecular adduct formation with the ester groups (Scheme 7.1).[144]

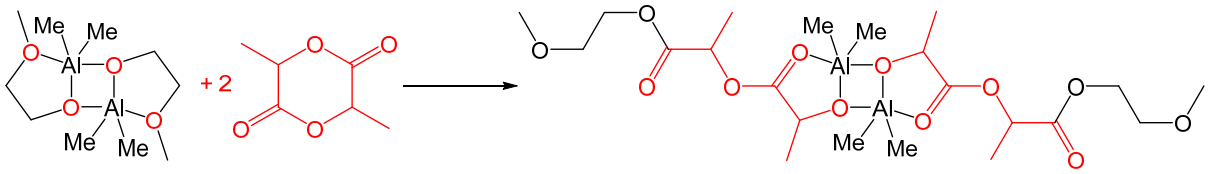

Scheme 7.1: The insertion of a dimethylaluminium alkoxide into lactide, resulting in intramolecular ester adduct formation.[144]

Meanwhile, the 1:1 reaction of Me_2AlF with triethyl citrate (a hydroxylated triester) leads to deprotonation of the triester and the formation of a dimeric aluminium alkoxide species. In this case, the retained ester groups show adduct formation to the aluminium atoms (Scheme 7.2).[145]

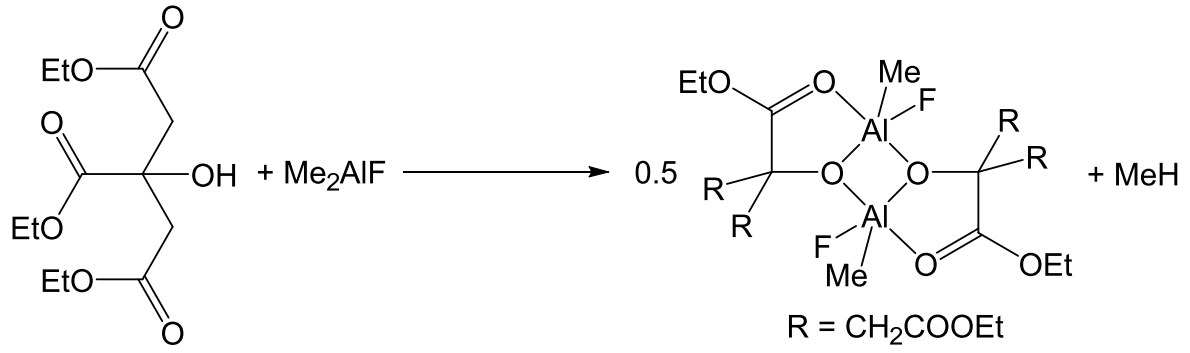

Scheme 7.2: The reaction of triethyl citrate with Me_2AlF.[145]

7.2 Synthesis of Tetraesters

Initially, a tetraester mimicking RL 32H and containing external pentyl groups was synthesised. The reaction of pentaerythritol with an excess of hexanoyl chloride **13**^{Pent} heated to reflux for 2 hours, followed by removal of the excess hexanoyl chloride *in vacuo* left the tetraester **14**^{Pent} as a pale yellow oil (Scheme 7.3). The product **14**^{Pent} was shown to be pure by NMR spectroscopy, with a single ^{13}C NMR signal observed at δ 172.3 ppm. In Chapter 6 it was shown that monoesters with benzyl groups aided the isolation of crystalline products for analysis. Therefore, a benzyl tetraester was produced by reacting pentaerythritol with phenylacetyl chloride **13**^{Bn}, with heating to 140 °C for 2 hours. Addition of cold toluene and ethanol resulted in precipitation of tetraester **14**^{Bn} as a white solid, which was then isolated by filtration. Recrystallisation of **14**^{Bn} from ethanol produced crystals suitable for X-ray diffraction, confirming the structure of **14**^{Bn} (Figure 7.1).

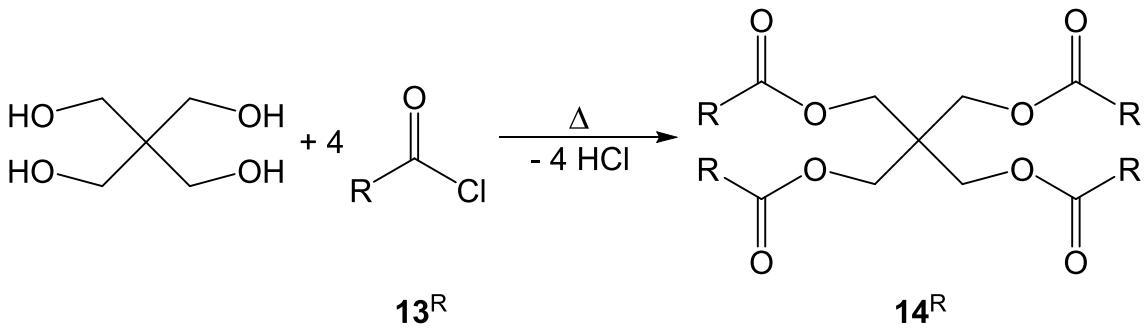

Scheme 7.3: The synthesis of tetraester **14**^{R} (R = C_5H_{11}, Bn).

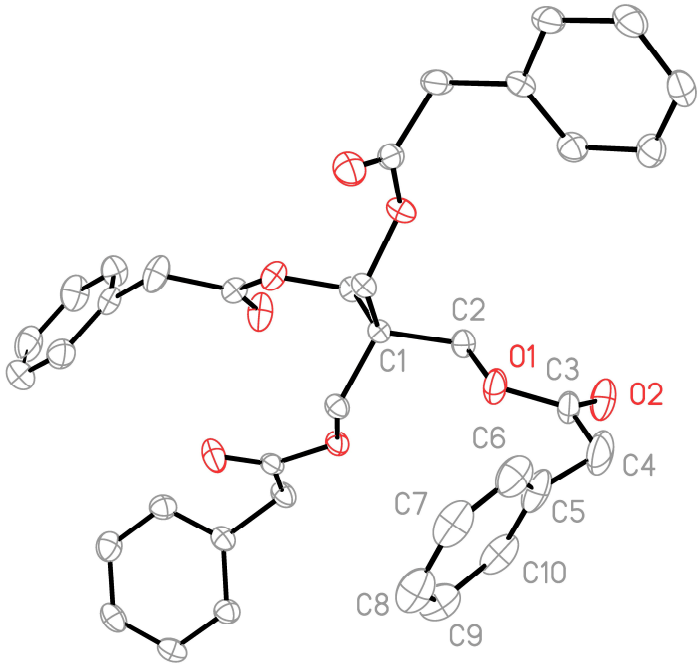

Figure 7.1: Thermal ellipsoid plot of **14**^{Bn} (30% probability). H-atoms and minor disorder omitted for clarity.

7.3 Reactivity of Tetraesters with TMA

Initially, reactions were attempted using **14**^{Pent}, as this tetraester most closely resembled polyolester RL 32H according to the analysis presented in Chapter 5. TMA was introduced to **14**^{Pent} in 1:1, 2:1, 4:1, 8:1 and 12:1 stoichiometries at −78 °C and the resulting mixture slowly warmed to room temperature. The first of these systems yielded only evidence for 1:1 adduct formation, with a ^{13}C NMR signal at δ 174.1 ppm from an average of one adducted and three non-adducted carbonyls (cf. δ 172.3 ppm for **14**^{Pent}, δ 181.4 ppm for **1**^{Et}(TMA)). However, the 2:1 system proved more variable. Immediately after combination, NMR spectroscopy revealed empirically 2:1 adduct formation (i.e. formally half of the ester functions in all the **14**^{Pent} were complexed), with exchange averaging the resulting ester signal to δ 177.0 ppm in the ^{13}C NMR spectrum. However, after 12 hours at room temperature, ^{1}H NMR spectroscopy revealed the evolution of a singlet at δ 1.11 ppm from dimethylated adduct $C_5H_{11}CMe_2OAlMe_2$(TMA) **4**^{Pent}(TMA) (Figure 7.2).

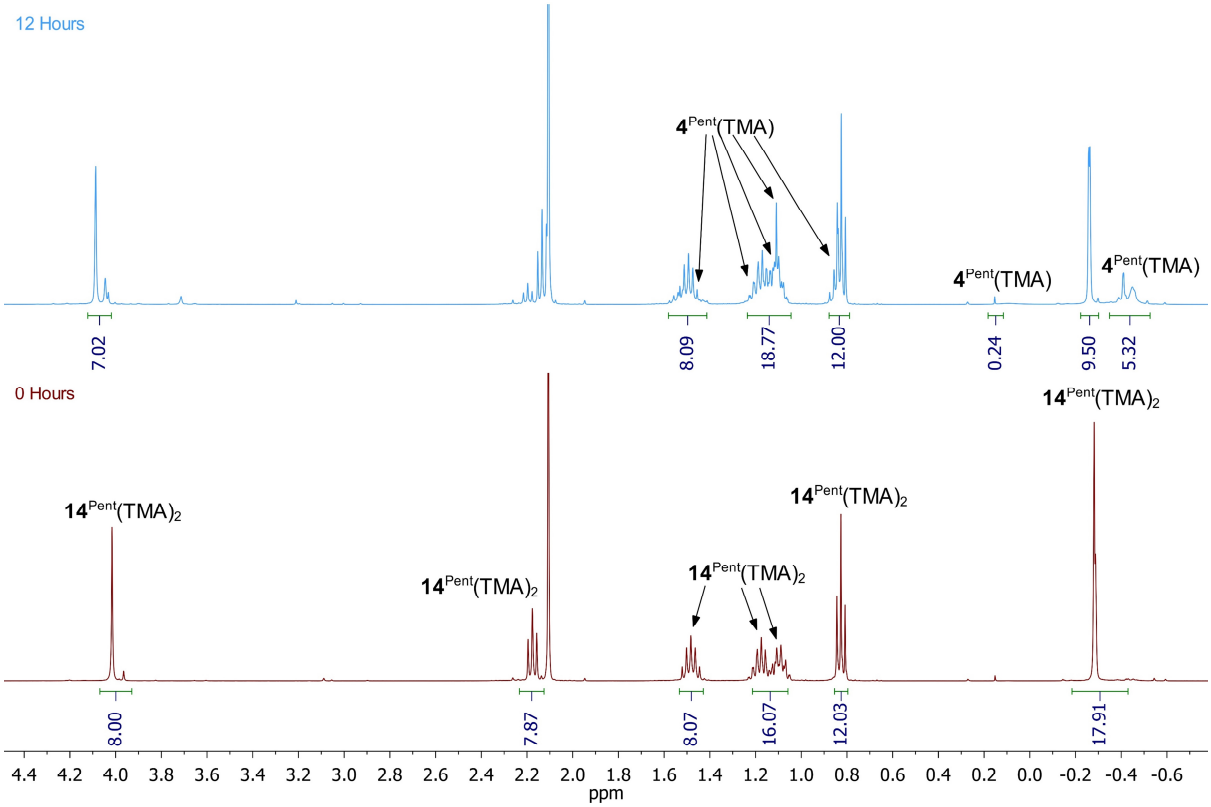

Figure 7.2: ^{1}H NMR spectra of aliquots from the introduction of TMA to **14**^{Pent} in a 2:1 ratio at −78 °C in toluene (visible at δ 2.11 ppm) after reagent combination (bottom) and 12 hours at room temperature (top). The solvent is benzene-d_6.

Based on the observations made for the 2:1 system, attempts were made to isolate the initial species that resulted when TMA and **14**^{Pent} were combined. While spectroscopy suggested that the 2:1 combination of TMA with **14**^{Pent} gave a 2:1 adduct, chilling of the mixture to −27 °C immediately after combination of the reagents led to crystallisation of a material which proved highly reactive at room temperature and largely resisted thorough characterisation. However, X-ray crystallography revealed tetraadduct **14**^{Pent}(TMA)$_4$ (Figure 7.3). This suggested that half of the **14**^{Pent} had formed **14**^{Pent}(TMA)$_4$, with the other half remaining as **14**^{Pent} (Scheme 7.4).

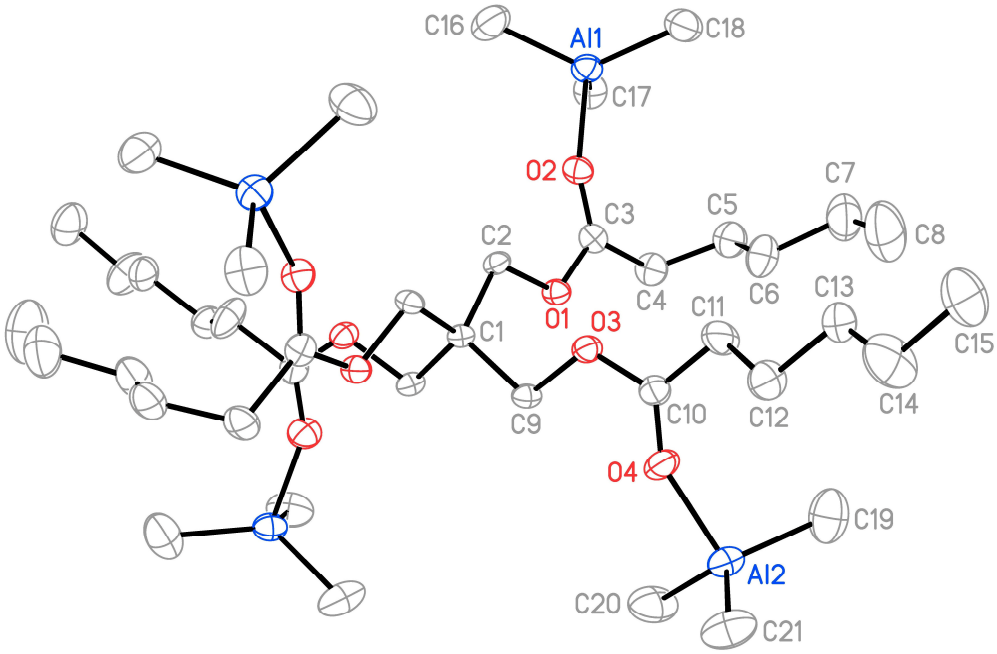

Figure 7.3: Thermal ellipsoid plot of **14**^{Pent}(TMA)$_4$ (30% probability). H-atoms omitted for clarity. Selected bond lengths (Å) and angles (°): Al1–O2 1.931(2), O2–C3 1.223(4), Al1–C16 1.960(4), Al1–C17 1.993(3), Al1–C18 1.967(4), Al2–O4 1.909(2), O4–C10 1.222(4), Al2–C19 1.954(4), Al2–C20 1.973(4), Al2–C21 1.954(4), C3–O2–Al1 147.3(2), C10–O4–Al2 152.7(2).

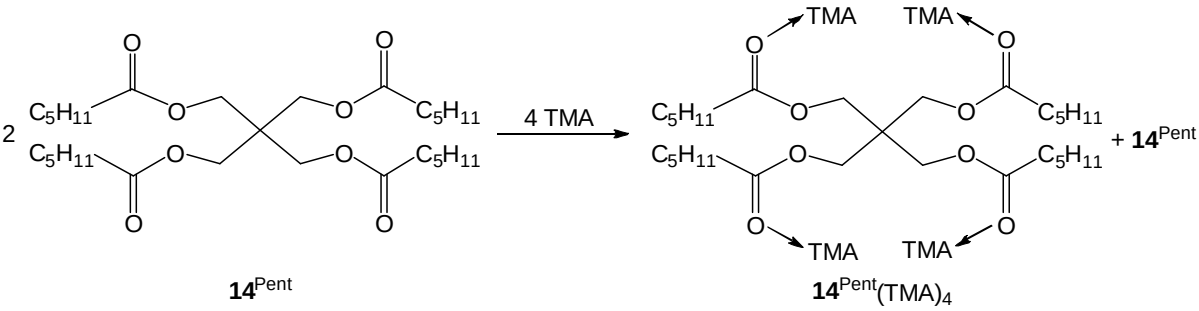

Scheme 7.4: The reaction of **14**^{Pent} with 4 equivalents of TMA at low temperature.

The 4:1 reaction of TMA and **14**^{Pent} revealed a ^{1}H NMR spectrum similar to that produced by the 2:1 reaction, with ester functionality still present (^{13}C NMR δ 175.8 and 175.3 ppm), along with the dimethylated peak at δ 1.11 ppm, which had increased in size. These were accompanied by the appearance of signals at δ 0.10 and −0.46 ppm that were attributed to the bridging and terminal AlMe groups of **4**^{Pent}(TMA). Aliquots from the 8:1 and 12:1 combinations of reagents revealed an absence of ester groups, and all of the peaks for the dimethylated adduct **4**^{Pent}(TMA) could be clearly observed. The ^{1}H NMR spectrum (Figure 7.4) revealed aliphatic signals at δ 1.44, 1.22, 1.12, 1.11, 1.10 and 0.87 ppm, along with signals at δ 0.10 and −0.45 ppm from bridging and terminal AlMe groups, respectively. In the analogous monoester work, the reaction of **1** with 3 equivalents of TMA produced **4**(TMA) and **3** (see Section 6.2). However, in the current case, spectroscopy of the 12:1

reaction revealed less clear evidence for the presence of the expected tetrolate-based elimination by-product. A very broad signal centred at *ca.* δ 3.8 ppm in the ^{1}H NMR spectra (Figure 7.4) could be tentatively attributed to the CH_2O region of the tetrolate-based elimination by-product $C(CH_2OAlMe_2)_4$ **15** (Scheme 7.5). This broad feature showed the correct integration (2H per dimethylated **4**^{Pent}(TMA)).

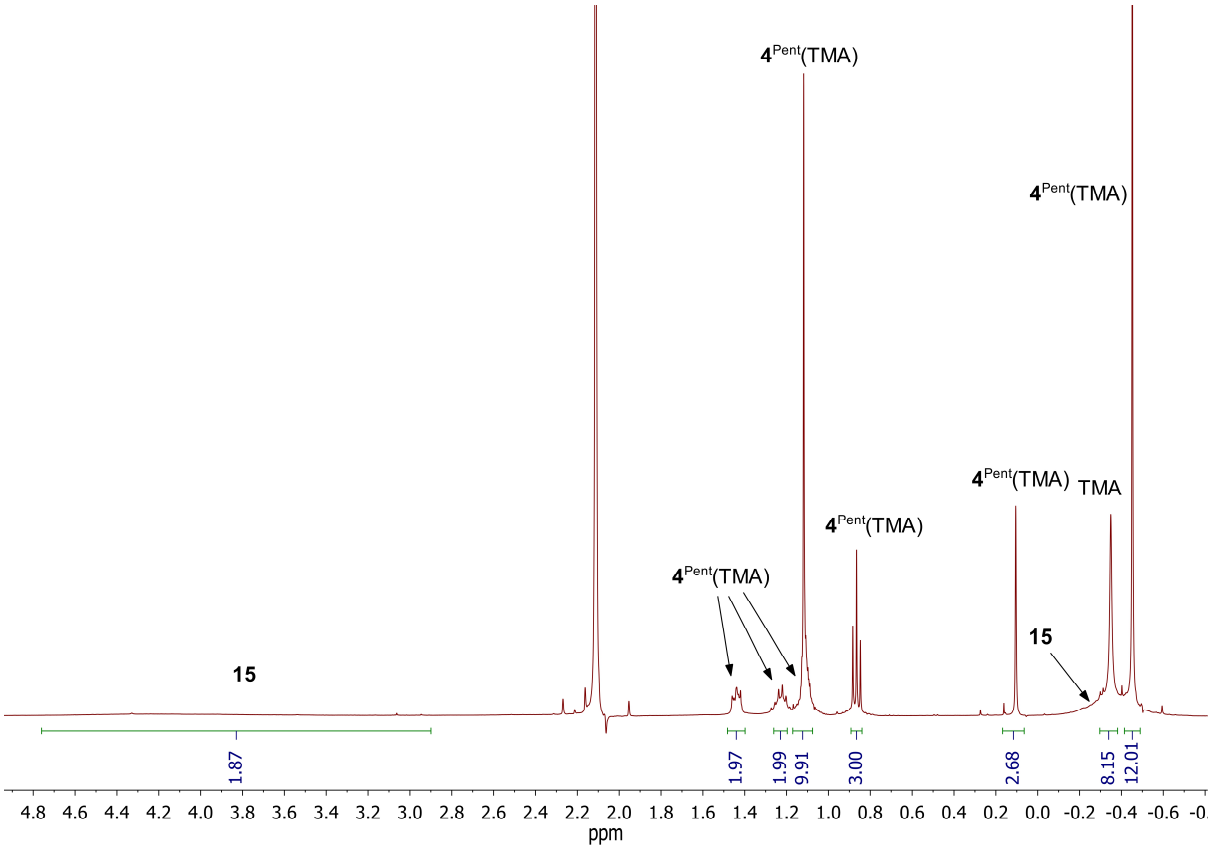

Figure 7.4: ^{1}H NMR spectrum of an aliquot from the 12:1 reaction of TMA with **14**^{Pent} at room temperature in toluene (δ 2.11 ppm). The solvent is benzene-d_6.

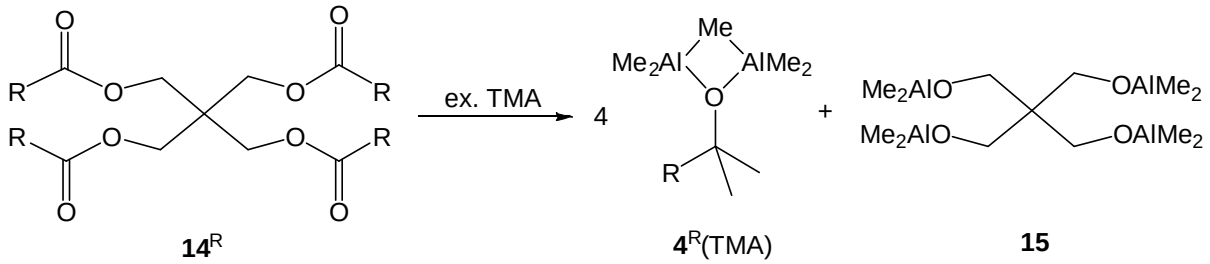

Scheme 7.5: The reaction of **14**^{R} with an excess of TMA at room temperature (R = C_5H_{11}, Bn).

Repeated attempts to isolate products of reaction between TMA and **14**^{Pent} failed. This led to the use of the benzyl tetraester **14**^{Bn}, in the hope that inclusion of the benzyl group would aid recrystallisation. TMA was introduced to **14**^{Bn} in 2:1, 4:1, 8:1 and 12:1 stoichiometries. NMR spectroscopic analysis of aliquots of the resulting mixtures suggested analogous

behaviour to that seen for **14**^{Pent}. This was evidenced by the observation of **4**^{Bn}(TMA) (^{1}H NMR δ 2.86, 1.11, 0.13 and −0.42 ppm, ^{13}C NMR δ 136.7, 130.3, 128.1, 126.7, 79.5, 50.8, 28.0, −4.5 and −7.0 ppm) and retention of a broad signal at *ca*. 4.0 ppm due to **15** (Scheme 7.5).

To further investigate the breadth demonstrated in the central tetrolate core region of the ^{1}H NMR spectra of the various TMA-**14**^{R} mixtures, the TMA-**14**^{Bn} reactions were repeated but were heated to reflux for 2 hours, as it had previously been shown that heating a TMA-monoester mixture resulted in the formation of an OMe-bridged species, **4**^{R}(**3**) (R = Et, Bn; see Section 6.2). Reactions were undertaken at 2:1, 4:1, 6:1 and 8:1 TMA to **14**^{Bn} ratios. Spectroscopically, two types of dimethylaluminium alkoxide products of reaction were identified. The first was dimethylated **4**^{Bn} and the second was the tetrolate-based product of ester cleavage retaining 3, 2, 1 or 0 unreacted ester groups (**16**^{Bn}, **17**^{Bn}, **18**^{Bn} or **15**). A ^{1}H,^{1}H-NOESY experiment revealed that these two types of alkoxide formed adducts based on 4-membered Al_2O_2 rings (Scheme 7.6).

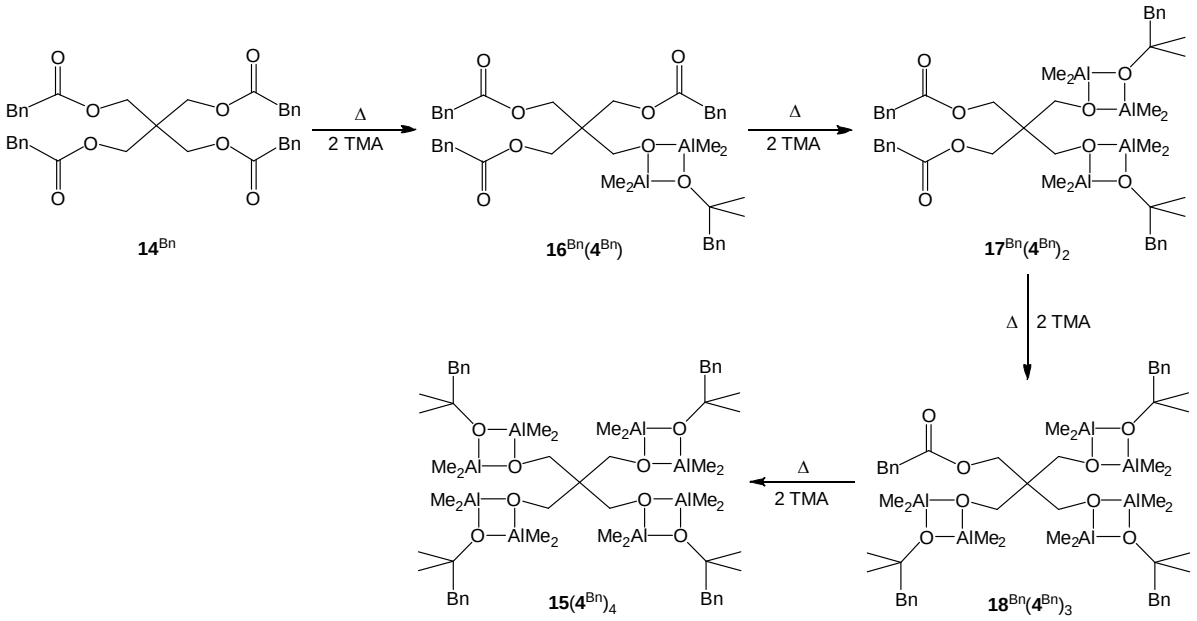

Scheme 7.6: The reaction of **14**^{Bn} with TMA (shown here for 8 equivalents), heated to reflux in toluene.

The ^{1}H NMR spectra from the TMA-**14**^{Bn} reactions heated to reflux revealed a number of sharp peaks in the δ 4.6-3.2 ppm region that could be assigned to CH_2O and CH_2 protons in **14**^{Bn}, **15**(**4**^{Bn})$_4$, **16**^{Bn}(**4**^{Bn}), **17**^{Bn}(**4**^{Bn})$_2$ and **18**^{Bn}(**4**^{Bn})$_3$ (Figure 7.5).

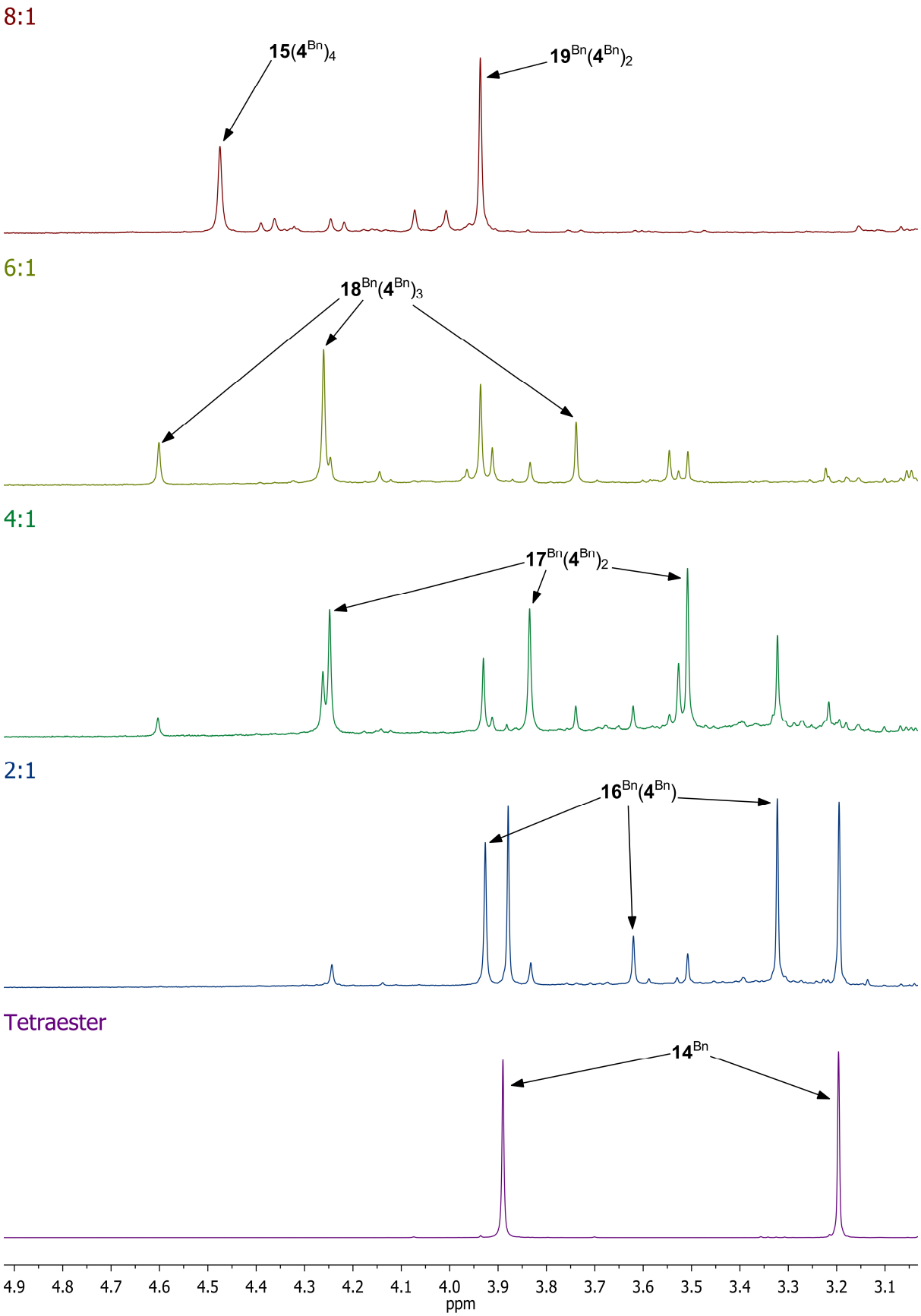

Figure 7.5: Selected ^{1}H NMR data of aliquots from the reaction of TMA with **14**^{Bn} in 2:1, 4:1, 6:1 and 8:1 stoichiometries after heating for 2 hours in toluene, showing the formation of ester cleavage products **15**(**4**^{Bn})$_4$ - **19**(**4**^{Bn})$_2$. The solvent is benzene-d_6.

The ^{1}H NMR spectrum (Figure 7.6) of an aliquot of the 8:1 reaction of TMA with **14**^{Bn} that had been heated to reflux revealed the presence of two tetrolate-containing species, with all ester groups having reacted. Data suggested the co-existence of **15**(**4**^{Bn})$_4$ alongside a species with ^{1}H NMR signals at δ 3.94, 2.96, 2.79, 1.07, −0.35 and −0.46 ppm (suggested to be one species by NOESY). The δ 3.94 and 2.96 ppm signals, which exist in a 3:1 ratio, were assigned (with the aid of a HSQC experiment) as CH_2O hydrogen atoms from a tetrolate. The AlMe signals at δ −0.35 and −0.46 ppm revealed a 3:4 integration ratio. Taken together, these data suggested that 2 equivalents of **15**(**4**^{Bn})$_4$ had undergone the elimination of 6 equivalents of dimethylated **4**^{Bn} and 2 equivalents of TMA to form tetrolate product **19**(**4**^{Bn})$_2$, 4 equivalents of **4**^{Bn} (presumed to exist as two dimers; ^{1}H NMR δ 3.00, 1.23 and −0.28 ppm) and 2 equivalents of **4**^{Bn}(TMA) (^{1}H NMR δ 2.86, 1.12, 0.13 and −0.42 ppm) (Scheme 7.7).

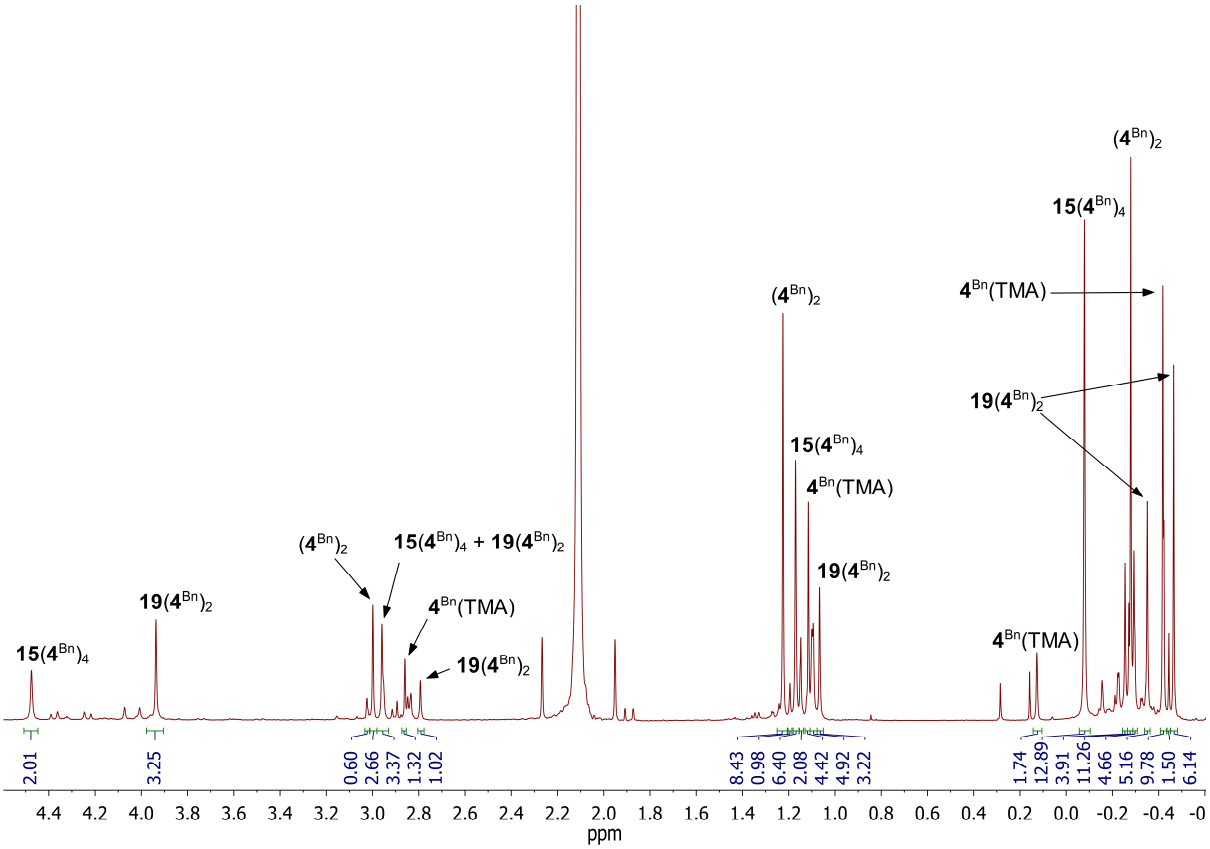

Figure 7.6: ^{1}H NMR spectrum of an aliquot from the reaction of TMA with **14**^{Bn} in an 8:1 ratio after heating to reflux for 2 hours in toluene (δ 2.11 ppm), showing the formation and subsequent reaction of **15**(**4**^{Bn})$_4$ to give **19**(**4**^{Bn})$_2$. The solvent is benzene-d_6.

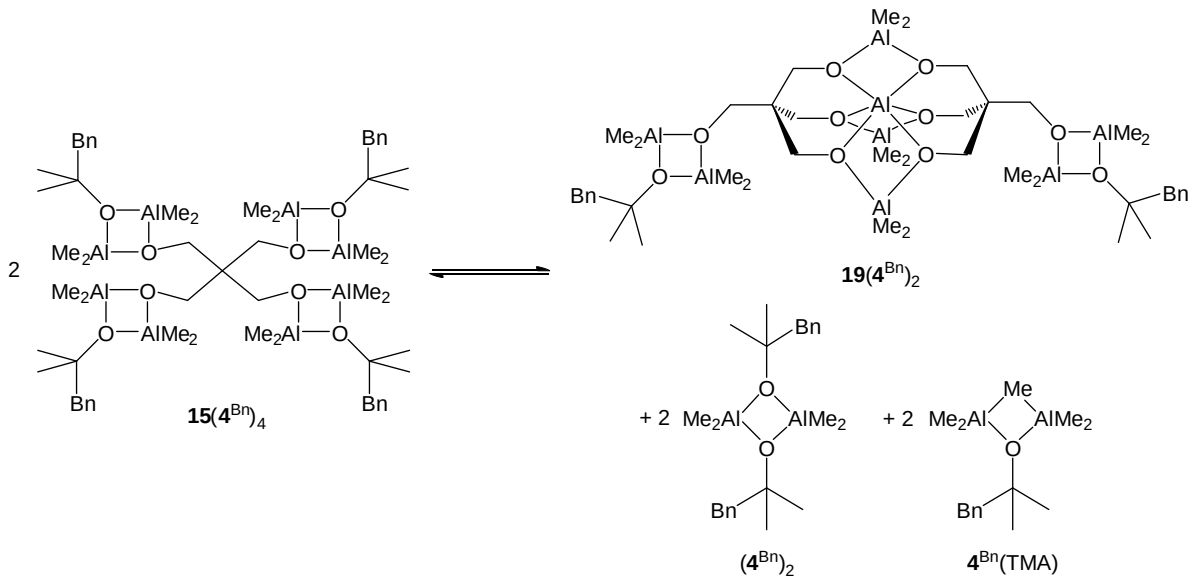

Scheme 7.7: The presumed thermal rearrangement of **15**(**4**^{Bn})$_4$ to give **19**(**4**^{Bn})$_2$, (**4**^{Bn})$_2$ and **4**^{Bn}(TMA) based on ^{1}H NMR spectroscopic analysis.

Beyond the spectroscopic data described above, further observations are significant in extracting a structure for **19**(**4**^{Bn})$_2$. First, the nature of the tetrolate ligand, whereby the retention of 1 equivalent of **4**^{Bn} per tetrolate suggests the availability of three alkoxide O-centres for further bonding. In addition, a sharp signal at δ 8.7 ppm in the ^{27}Al NMR spectrum is characteristic of 6-coordinate aluminium. Taken together, these data are consistent with the creation of a Mitsubishi molecule,[146] which is based on an Al_4O_6 core in which a central Al^{3+} is coordinated by six O-centres – in this case provided by two tridentate alkoxide ligands that also capture three $AlMe_2$ moieties (Scheme 7.7).

The proportions of **14**^{Bn} and **15**(**4**^{Bn})$_4$ - **19**(**4**^{Bn})$_2$ formed from the TMA-**14**^{Bn} reactions heated to reflux are given in Table 7.1. Data revealed that for every 2 equivalents of TMA added, approximately one ester group had reacted. This observation replicates the reactivity of monoesters (see Section 6.2). The binomial distribution of products seen indicated a lack of cooperativity between esters groups within the same molecule. This was contrary to expectation, since it was thought that the reaction of an ester group would have affected the reactivity of other esters groups within the same molecule, i.e. that $OAlMe_2$ groups would have been able to coordinate to unreacted esters and enhance its reactivity.

TMA (eq.) wrt **14**^{Bn}	% ester groups reacted					Total % ester groups reacted
	0 (**14**^{Bn})	1 (**16**^{Bn}(**4**^{Bn}))	2 (**17**^{Bn}(**4**^{Bn})$_2$)	3 (**18**^{Bn}(**4**^{Bn})$_3$)	4 (**15**(**4**^{Bn})$_4$ + **19**(**4**^{Bn})$_2$)	
0	100	0	0	0	0	0
2	35	50	15	0	0	20
4	0	25	54	21	0	49
6	0	0	16	50	34	80
8	0	0	0	0	100	100

Table 7.1: Proportions of substrate **14**^{Bn} and ester cleavage products **15**(**4**^{Bn})$_4$ - **19**(**4**^{Bn})$_2$ as a function of equivalents of TMA relative to **14**^{Bn} from integration of the ^{1}H NMR spectra. Analysis based on aliquots withdrawn after heating to reflux in toluene for 2 hours. The solvent is benzene-d_6.

Attempts to crystallise the products of reaction between TMA and **14**^{Bn} gave mixed results. The addition of hexane to the 4:1 TMA:**14**^{Bn} reaction mixture that had been heated to reflux in toluene allowed the isolation of crystalline material. X-ray diffraction confirmed this to be **17**^{Bn}(**4**^{Bn})$_2$ (Figure 7.7). In this species, two of the four ester groups had reacted, resulting in a structure consistent with the NMR spectroscopy data. The isolation of this material established further important points. First, in line with the reaction stoichiometry, only two out of a possible four ester groups in **14**^{Bn} had undergone dimethylation. Second, like for **4**^{R}(**3**) (R = Et, Bn), the 4-membered Al_2O_2 metallacycles incurred by ester cleavage/alkoxide capture were symmetrical and based on $(AlMe_2)_2(\mu_2\text{-}OR)_2$ metallacycles. These metallacycles are flat and have a rhombus shape, with all Al–O bond lengths within error of each other (*ca*. 1.85 Å). The mean O–Al–O and Al–O–Al angles are 81.0 and 98.9°, respectively. The crystal structure of **17**^{Bn}(**4**^{Bn})$_2$ reveals that the molecule has a relatively flat conformation. Of note, the two reacted ester groups are projected directly away from each other in the molecule, which is attributed to the larger steric bulk of the adducts they form with **4**^{Bn} relative to that of the unreacted esters. In addition, the unreacted esters groups do not coordinate to the aluminium centres, in contrast to the

examples shown in Schemes 7.1 and 7.2. This failure to coordinate is attributed to the formation of a less thermodynamically favoured 8-membered ring that would from between the carbonyl oxygen and the aluminium centre (O6 and Al1 in Figure 7.7). Instead the aluminium centres in the reacted ester groups are stabilised by coordination to **4**^{Bn}.

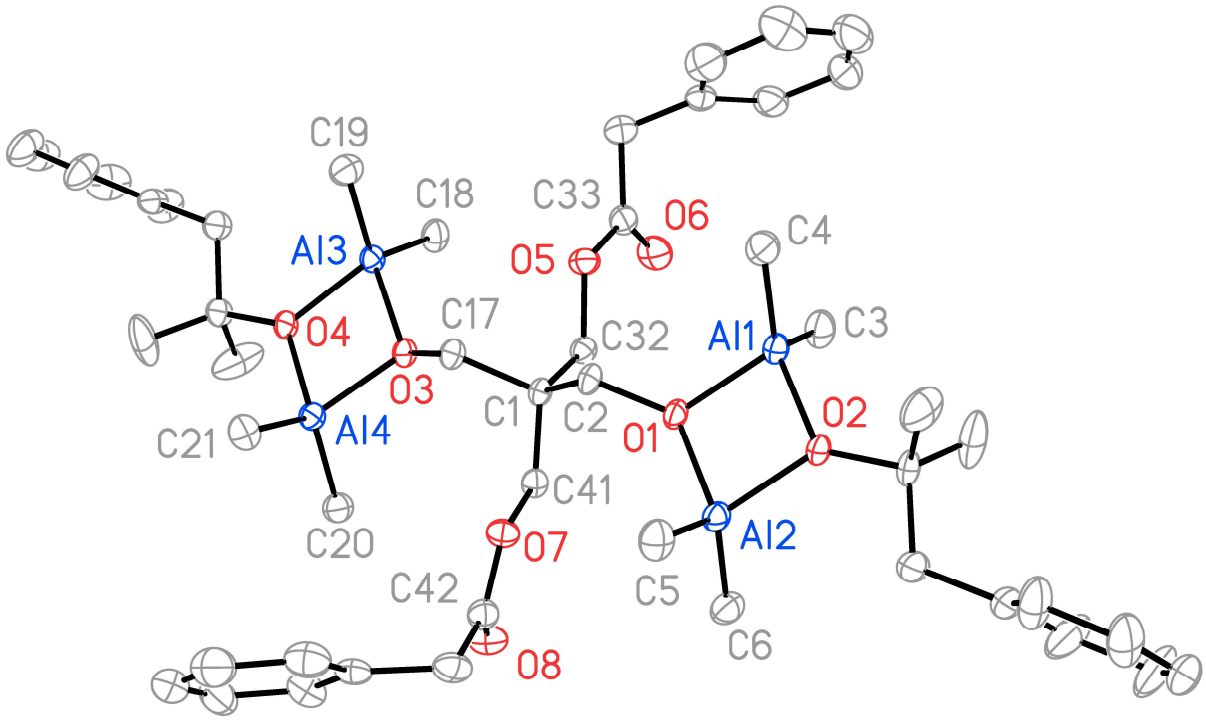

Figure 7.7: Thermal ellipsoid plot of **17**^{Bn}(**4**^{Bn})$_2$ (30% probability). H-atoms omitted for clarity. Selected bond lengths (Å) and angles (°): Al1–O1 1.851(2), Al1–O2 1.848(2), Al1–C3 1.938(4), Al1–C4 1.948(4), Al2–O1 1.853(2), Al2–O2 1.854(2), Al2–C5 1.948(4), Al2–C6 1.944(4), Al1–O1–Al2 99.00(10), Al1–O2–Al2 99.07(10), O1–Al1–O2 81.07(10), O1–Al2–O2 80.86(10).

In a similar vein to the 4:1 TMA:**14**^{Bn} reaction, removal of solvent from the 6:1 TMA:**14**^{Bn} reaction mixture produced a white solid, which could be redissolved in hexane. This solution yielded crystals that X-ray diffraction confirmed to be the octaaluminium species **19**(**4**^{Bn})$_2$ (Figure 7.8), establishing reaction of all four ester groups of **14**^{Bn}. The structure of **19**(**4**^{Bn})$_2$ reveals a central Al_4O_6 unit - a Mitsubishi-type structure. The formation of Mitsubishi molecules is common for methylaluminium sesquialkoxides.[146] Their structures allow for all of the alkoxide groups to act as bridging ligands, which is thermodynamically favourable. In the current reaction the formation of a Mitsubishi-type species is attributed to the elimination of **4**^{Bn} and **4**^{Bn}(TMA), which is favoured entropically. Also, it is expected that **15**(**4**^{Bn})$_4$ would be sterically crowded, due to having four Al_2O_2 metallacycles surrounding the core of the molecule, whereas **19**(**4**^{Bn})$_2$ has much less crowding. Two peripheral **4**^{Bn} units, which form Al_2O_2 metallacycles from

coordination to the $OAlMe_2$ groups, point away from the centre of the molecule. Similar to **17**^{Bn}(**4**^{Bn})$_2$, the peripheral Al_2O_2 metallacycles form rhombuses, with a mean Al–O bond length of 1.85 Å. The central unit is composed of two tetrolates (each contributing three alkoxide groups), a central aluminium and three $AlMe_2$ units. The central aluminium coordinates to the six available alkoxides and the $AlMe_2$ groups bridge between the tetrolates. The central 6-coordinate aluminium has a distorted octahedral geometry with O–Al–O angles from adjacent oxygen centres occurring within the range 77.96(10)-104.13(11)°. The distortion from octahedral geometry is attributed to the acute angle at aluminium in the Al_2O_2 metallacycles. These bond angles are similar to those reported for the Mitsubishi molecule $Al\{(\mu\text{-}OEt)_2AlMe_2\}_3$.[147] The Al_4O_6 core shows mean Al–O bond lengths of 1.82 and 1.88 Å for 4- and 6-coordinate aluminium, respectively.

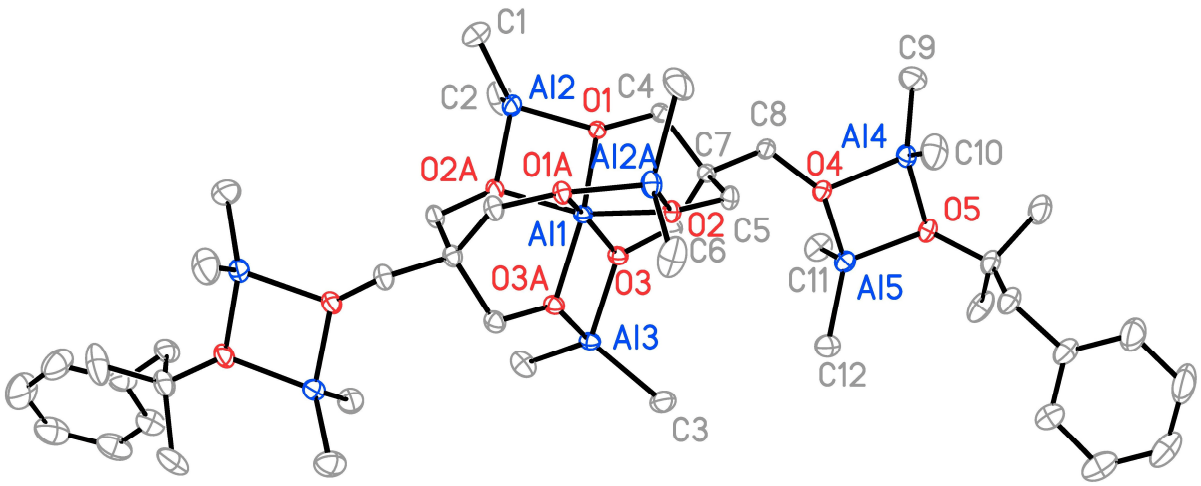

Figure 7.8: Thermal ellipsoid plot of **19**(**4**^{Bn})$_2$ (30% probability). H-atoms omitted for clarity. Selected bond lengths (Å) and angles (°): Al1–O1 1.874(2), Al1–O2 1.888(2), Al1–O3 1.880(3), Al2–O1 1.822(2), Al2–O2A 1.824(3), Al2–C1 1.948(5), Al2–C2 1.954(5), Al3–O3 1.828(2), Al3–C3 1.943(4), Al4–O4 1.858(3), Al4–O5 1.838(3), Al4–C9 1.953(5), Al4–C10 1.945(5),Al5–O4 1.851(3), Al5–O5 1.848(3), Al5–C11 1.948(4), Al5–C12 1.950(4), Al1–O1–Al2 100.72(11), Al1–O2A–Al2 100.11(11), O1–Al1–O2A 77.96(10), O1–Al2–O2A 80.96(11), Al1–O3–Al3 100.21(12), O3–Al1–O3A 78.43(15), O3–Al3–O3A 81.15(15), Al4–O4–Al5 98.42(11), Al4–O5–Al5 99.21(12), O4–Al4–O5 81.07(11), O4–Al5–O5 81.00(11).

7.4 Reactivity of Tetraesters with Me_2AlCl

The study of tetraesters was next extended to using Me_2AlCl as the organoaluminium component, as this more closely resembles the organoaluminiums produced in industrial refrigeration systems. The use of **14**^{Bn} with 12 equivalents of Me_2AlCl (3 equivalents per ester group, which was the amount shown in Section 6.3 to be required for full reaction between **1**^{Bn} and Me_2AlCl) in toluene resulted in limited reactivity that was, nonetheless, similar to that of the monoester (see Section 6.3). ^{1}H NMR spectroscopy revealed that only

2% of the ester groups had reacted to form **4**^{Bn}(Me_2AlCl) (presumably alongside $C(CH_2OAlCl_2)_4$ **20**) after 2 hours at room temperature, with most of the tetraester instead just forming an adduct with Me_2AlCl; **14**^{Bn}(Me_2AlCl)$_4$ (Scheme 7.8 and Figure 7.9). Heating to reflux in toluene for 2 hours resulted in complete reaction of the tetraester to give alkenes **7a** and **7b**, while a small amount of exhaustive methylation gave Bn^{t}Bu **10** and Friedel-Crafts products **11a** and **11b** were also noted (Scheme 7.8 and Figure 7.9). ^{1}H NMR spectroscopy revealed a broad signal, centred at *ca.* δ 3.9 ppm, which is tentatively attributed to the CH_2O region of the tetrolate-based by-product of complete reaction, $C(CH_2OAlMeCl)_4$ **21**. Similar to the monoester-Me_2AlCl reactions (Section 6.3), the reaction of Me_2AlCl with **14**^{Bn} was investigated by heating an identical 12:1 reaction mixture to a range of temperatures for 2 hours (Figure 7.9). For the 70 °C reaction, ^{1}H NMR spectroscopy of an aliquot of the reaction revealed the conversion of 35% of the ester groups to give **4**^{Bn}(Me_2AlCl) and 16% to give **4**^{Bn}($MeAlCl_2$). A very broad signal centred at *ca.* δ 3.8 ppm resulted from the remaining esters and various CH_2OAl groups present. In contrast to the monoester system, carefully raising the reaction temperature now resulted in an increase in the amount of **4**^{Bn}(Me_2AlCl) and **4**^{Bn}($MeAlCl_2$) produced, with **4**^{Bn}($MeAlCl_2$) becoming most abundant at 100 °C. Formation of alkenes **7a** and **7b** (along with methane) was now seen from 90 °C, which again contrasts with Me_2AlCl-monoester reactions, where alkene formation was seen from 60 °C.

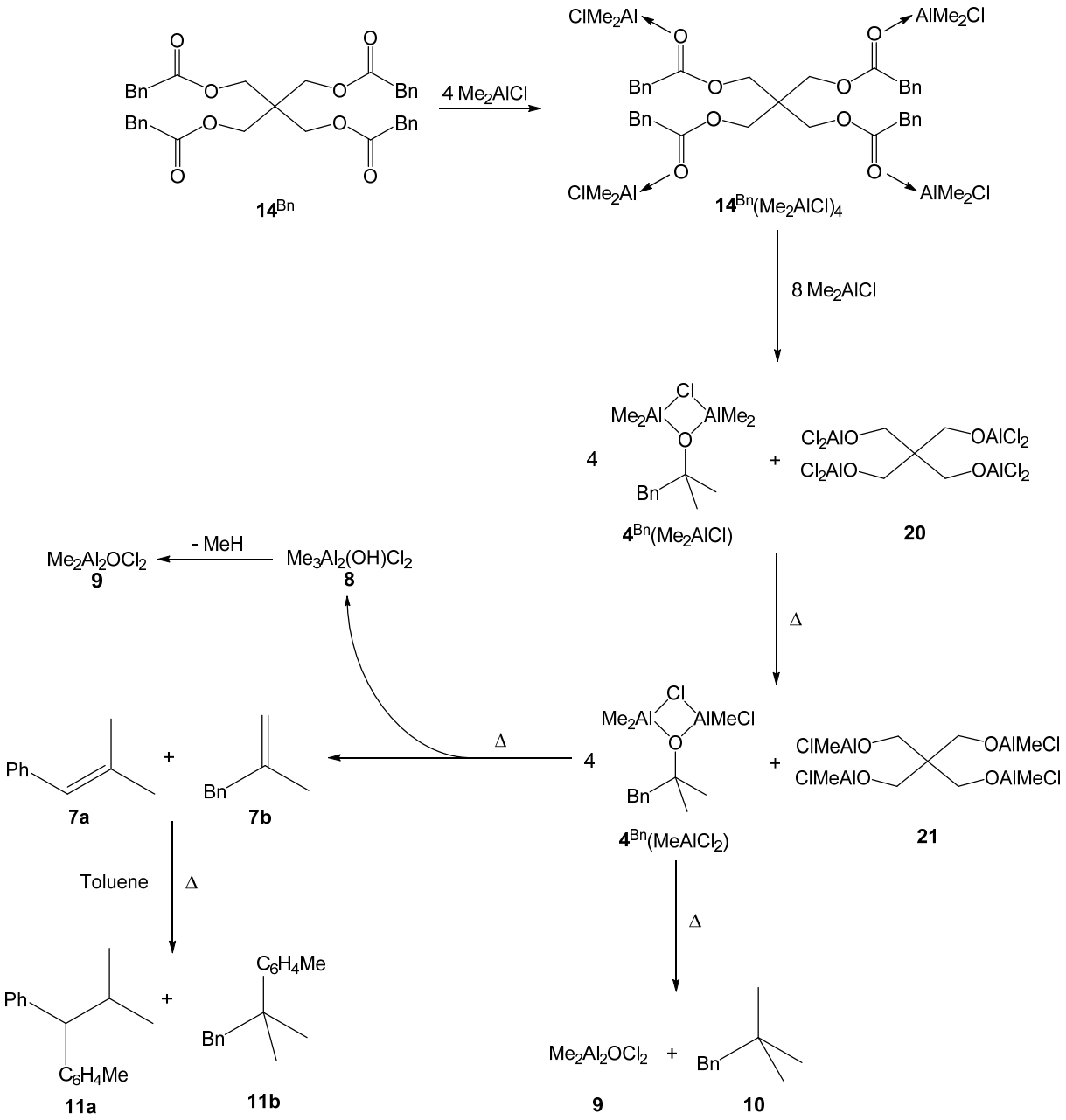

Scheme 7.8: The proposed reaction of tetraester **14**^{Bn} with Me_2AlCl at raised temperature.

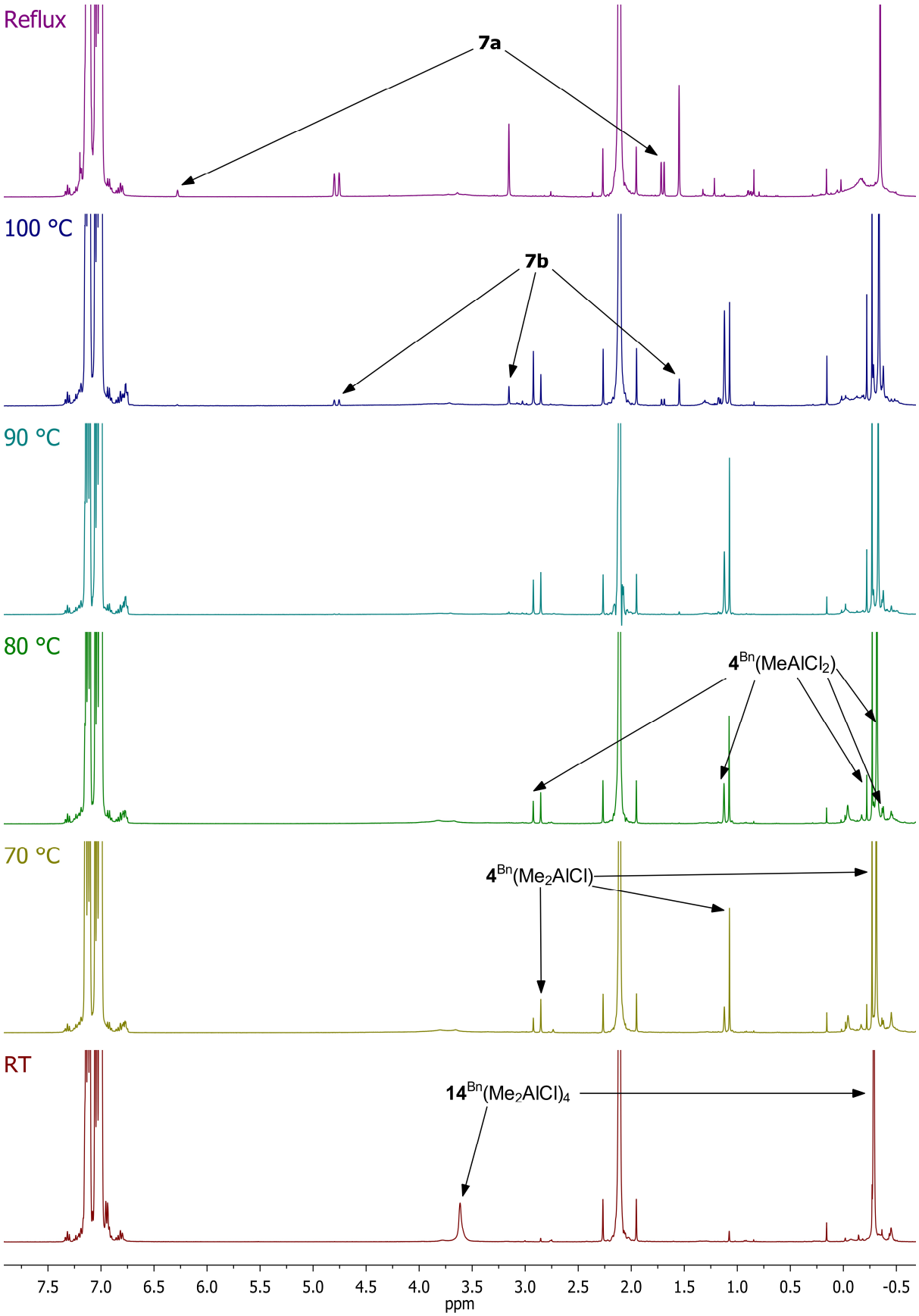

Figure 7.9: ^{1}H NMR spectra of aliquots from the reaction of Me_2AlCl and tetraester **14**^{Bn} in a 12:1 ratio in toluene, heated at the stated temperature for 2 hours. The solvent is benzene-d_6.

The observation that **14**^{Pent}(TMA)$_4$ crystallised (Figure 7.3), but that it did so as a highly sensitive material that proved difficult to analyse, led to attempts to produce the analogous Me_2AlCl structure. The addition of 2 equivalents of Me_2AlCl to **14**^{Pent} allowed the isolation of crystalline **14**^{Pent}(Me_2AlCl)$_4$ (Figure 7.10). Relative to like-structured **14**^{Pent}(TMA)$_4$, the Al–O distances are shorter (mean 1.845 Å vs. mean 1.920 Å in the TMA adduct). This is consistent with Me_2AlCl being a stronger Lewis acid, and appeared to impart additional stability that enabled more thorough characterisation of the adduct. ^{13}C NMR spectroscopy confirmed the structure, with a signal at δ 182.6 ppm attributed to the carbonyl (cf. δ 172.3 ppm for **14**^{Pent}) and a broad signal at δ −7.9 ppm attributed to the AlMe groups.

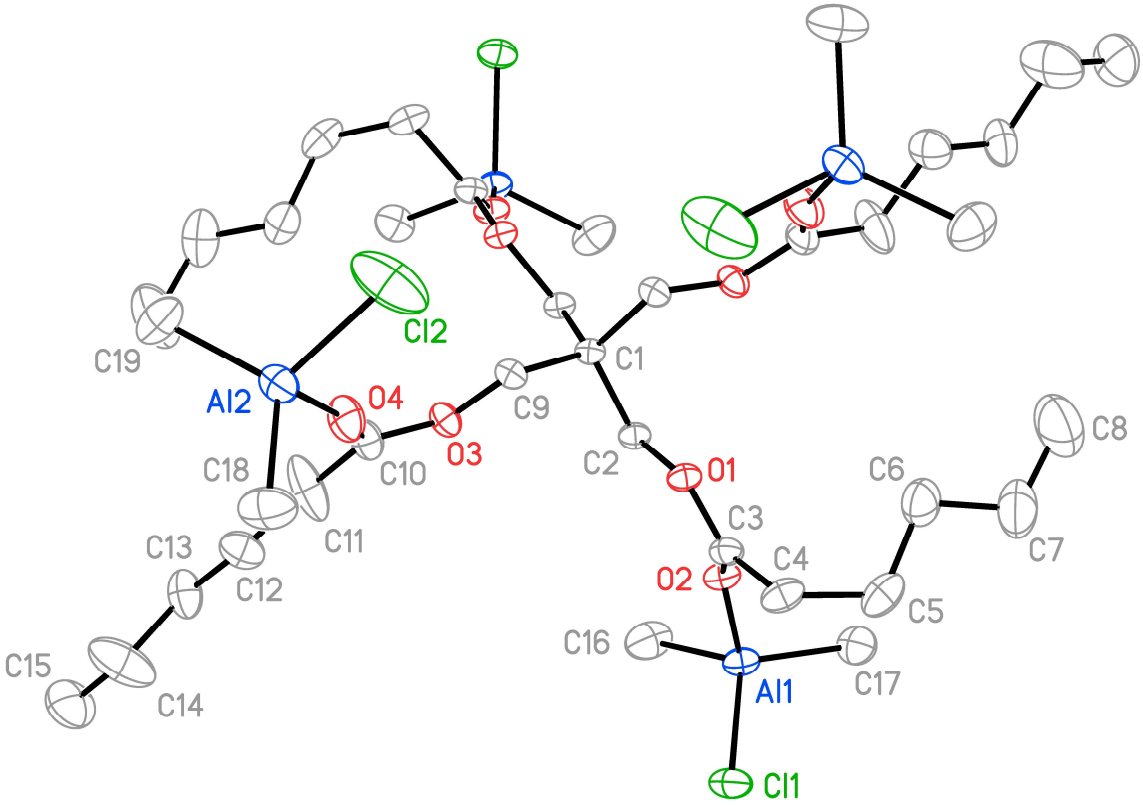

Figure 7.10: Thermal ellipsoid plot of **14**^{Pent}(Me_2AlCl)$_4$ (30% probability). H-atoms and minor disorder omitted for clarity. Selected bond lengths (Å) and angles (°): Al1–O2 1.8729(18), O2–C3 1.227(3), Al1–C16 1.944(3), Al1–C17 1.960(3), Al1–Cl1 2.1839(10), Al2–O4 1.817(9), O4–C10 1.221(3), Al2–C18 1.958(14), Al2–C19 1.974(12), Al2–Cl2 2.172(8), C3–O2–Al1 149.15(16), C10–O4–Al2 163.6(3).

7.5 Reactivity of Tetraesters with $MeAlCl_2$

The use of $MeAlCl_2$ in place of Me_2AlCl resulted in the formation of a white precipitate when it was introduced to **14**^{Bn} in a 12:1 ratio (to give a 3:1 Me_2AlCl to ester ratio). This

material proved intractable, with heating to reflux resulting in no change in the material. The intractable species is presumed to be the tetraadduct **14**^{Bn}($MeAlCl_2$)$_4$. Attempts to analyse this species by IR spectroscopy proved unsuccessful as it was too air sensitive.

7.6 Reactivity of Tetraesters with $Me_{1.5}AlCl_{1.5}$

The reaction of an equimolar mixture of Me_2AlCl and $MeAlCl_2$ ($Me_{1.5}AlCl_{1.5}$) with **14**^{Bn} (6 equivalents of each of Me_2AlCl and $MeAlCl_2$ per **14**^{Bn}, so 12 equivalents of organoaluminium per ester as before) resulted in similar reactivity to that seen using $MeAlCl_2$, with a white precipitate formed at lower temperatures. However, in contrast to the $MeAlCl_2$ reaction above, heating the reaction to reflux in toluene produced a yellow solution. NMR spectroscopy of an aliquot revealed the presence of alkenes **7a** and **7b**, trimethylated **10**, Friedel-Crafts products **11a** and **11b**, and a broad set of peaks, at δ 4.5-3.5 ppm, which suggested a mixture of unreacted ester groups and CH_2OAl units. This pointed to similar reactivity to that seen between monoester **1**^{Bn} and $Me_{1.5}AlCl_{1.5}$ (see Section 6.5), where at low temperatures, adduct formation dominated and heating led to the creation of alkenes and methane, presumably via the formation of **4**^{Bn}(Me_2AlCl) and **4**^{Bn}($MeAlCl_2$), which underwent immediate elimination.

7.7 Reactivity of RL 32H with Methylaluminium Reagents

Initially, the monoesters **1**^{Et} and **1**^{Bn} were reacted with methylaluminium reagents, to model the reactivity expected to be seen for RL 32H. These reactions revealed that using TMA, Me_2AlCl or $Me_{1.5}AlCl_{1.5}$ resulted in ester cleavage (with $Me_{1.5}AlCl_{1.5}$ requiring elevated temperatures). Spectroscopy also revealed that reactions with Me_2AlCl and $Me_{1.5}AlCl_{1.5}$ produced alkenes (**7a** and **7b**) and methane above 70 °C. Subsequently, the reactions with methylaluminium reagents were repeated with the tetraesters **14**^{Pent} and **14**^{Bn}. This revealed similar reactivity to that seen with the monoesters. It was expected that RL 32H would show the same essential reactivity as that described above, but that analysis of the spectra would likely be more complex due to the oil containing multiple different alkyl fragments (see Section 5.2). Also, the presence of additives in the oil could affect both reaction rate and complexity, as well as enabling fundamentally new reactions not seen in the pure, model systems.

To begin with, TMA was reacted with RL 32H (12:1) at room temperature. ^{27}Al NMR spectroscopy revealed a peak at δ 157.7 ppm, similar to the chemical shifts observed in the reaction mixtures of **14**^{Pent} and **14**^{Bn} with 12 equivalents of TMA (δ 156.0 and 160.6 ppm, respectively). ^{1}H NMR spectroscopy of the TMA-RL 32H mixture aliquot revealed a spectrum (Figure 7.11) that resembled that obtained from the TMA-**14**^{Pent} reaction aliquots, with a broad signal at *ca.* δ 4.0 ppm, which corresponded with that previously seen for $C(CH_2OAlMe_2)_4$ **15** (Figure 7.4). Two large peaks were observed, at δ 1.14 and 1.12 ppm, alongside two minor peaks, at δ 1.24 and 1.23 ppm, which were attributed to the methyl groups of **4**^{R}(TMA) (cf. ^{1}H NMR of methyl groups of **4**^{Et}(TMA) and **4**^{Bn}(TMA) δ 1.05 and 1.12 ppm, respectively). The observation of multiple peaks with similar chemical shifts that are attributable to **4**^{R}(TMA) species can be explained by the presence of different alkyl groups originating from RL 32H. In Section 5.2, it was suggested that these were propyl (C_3H_7) and pentyl (C_5H_{11}) groups, based on mass spectrometry, although the extent of branching was not known. The AlMe region of the ^{1}H NMR spectrum (Figure 7.11) suggests the existence of three different **4**^{R}(TMA) species, with $AlMe_t$ signals seen at δ −0.48, −0.50 and −0.51 ppm, along with three overlapping broad signals, at δ 0.11, 0.11 and 0.10 ppm, from the three different $AlMe_b$ groups (Figure 7.11, inset).

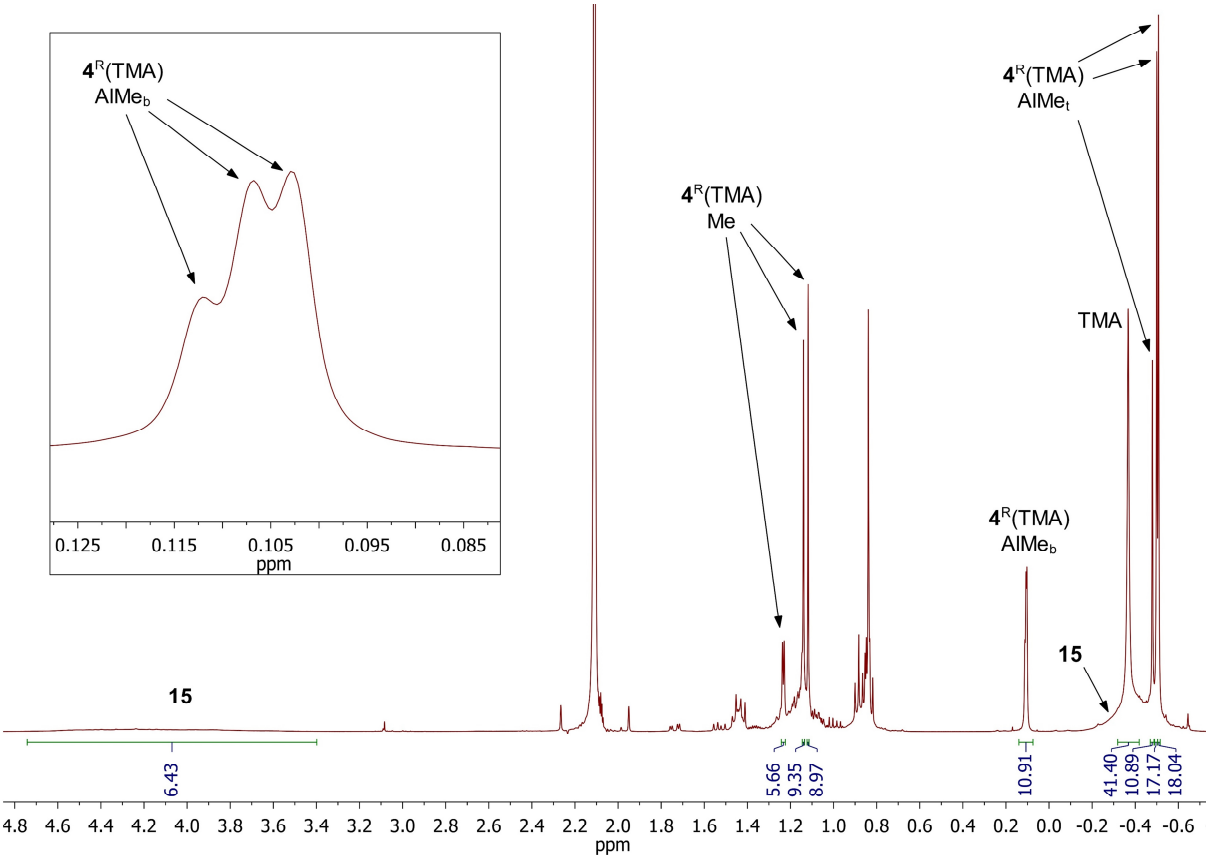

Figure 7.11: ^{1}H NMR spectrum of an aliquot from the reaction of TMA with RL 32H in a 12:1 ratio at room temperature in toluene (visible at δ 2.11 ppm). The inset shows three separate AlMe$_b$ signals. The solvent is toluene-d_8.

The use of ^{1}H,^{1}H-NOESY (Figure 7.12) showed NOE signals between peaks at δ 1.23, 1.14 and 1.12 ppm and the peaks at δ −0.48, −0.50 and −0.51 ppm, respectively. The exact nature of these different **4**^{R}(TMA) species is difficult to determine due to the large number of overlapping signals in the ^{1}H NMR spectrum, but it is clear that three different **4**^{R}(TMA) species are present in the reaction mixtures, originating from three different alkyl groups from RL 32H. Mass spectrometry study of RL 32H (see Section 5.2) suggested only C_3H_7 or C_5H_{11} groups, therefore suggesting that one of these two groups is present in two isomeric forms.

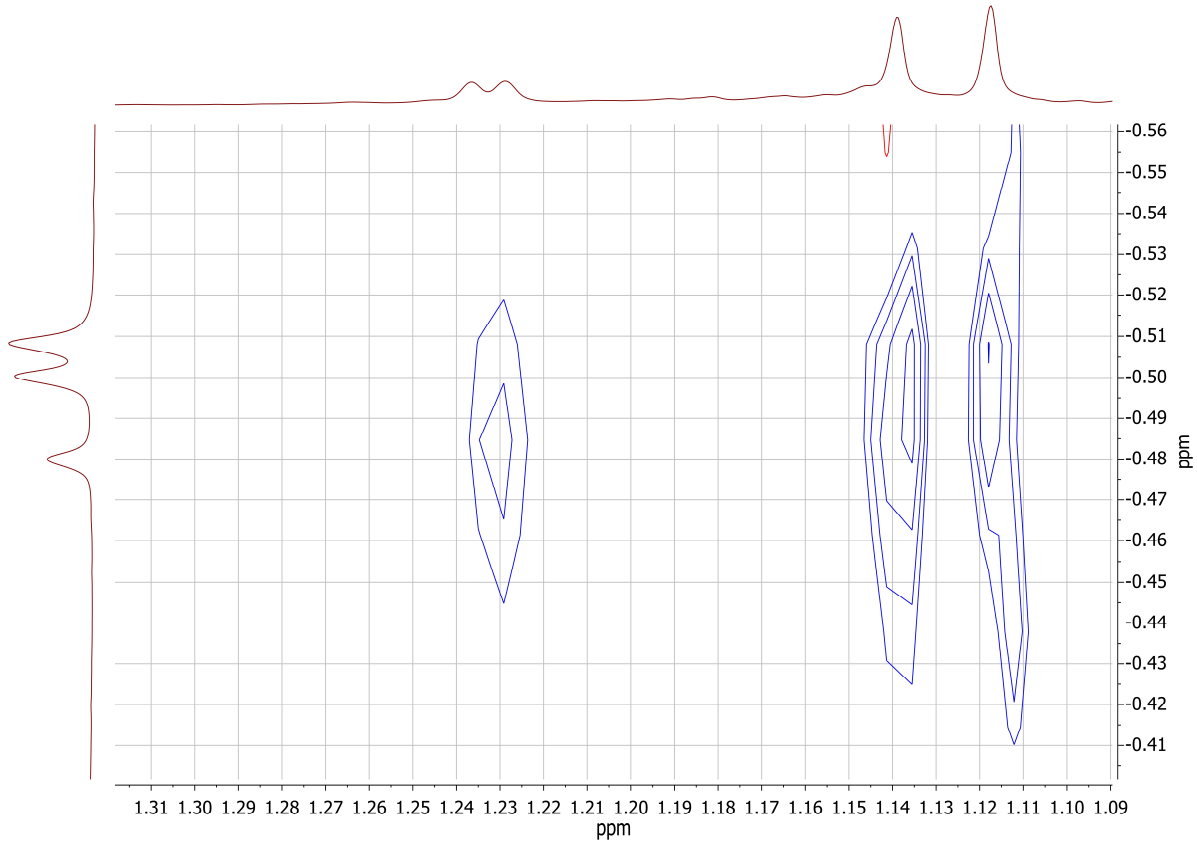

Figure 7.12: ^{1}H,^{1}H-NOESY spectrum (τ = 0.6 s) of an aliquot from the reaction of TMA with RL 32H in a 12:1 ratio at room temperature in toluene. The solvent is toluene-d_8.

^{13}C NMR spectroscopy corroborated the suggestion from ^{1}H NMR spectroscopy that three **4**^{R}(TMA) species had formed, with the observation of three signals from CO carbons, at δ 80.4, 79.6 and 79.5 ppm. HMBC showed correlations between the methyl hydrogens in the ^{1}H NMR spectrum and these CO carbons. Meanwhile, the AlMe region of the ^{13}C NMR spectrum revealed a sharp peak at δ −4.2 ppm due to the bridging methyl groups and a broad signal at δ −6.6 ppm from the multiple terminal methyl groups. This assignment was confirmed by a HSQC experiment.

Next, the reaction between TMA and RL 32H was investigated at elevated temperatures, using an 8:1 stoichiometry. This ratio was selected as it was previously shown that heating of **14**^{Bn} with 8 equivalents of TMA resulted in the formation of the octaaluminium species **19**(**4**^{Bn})$_2$, which exhibited a characteristic signal at δ 8.7 ppm in the ^{27}Al NMR spectrum due to the symmetrical octahedral aluminium environment at the core of the cluster (see Section 7.3). After heating the 8:1 TMA:RL 32H mixture to reflux in toluene for 2 hours, ^{27}Al NMR spectroscopy revealed signals at δ 157.3 and 9.1 ppm, which are characteristic of 4- and 6-coordinate aluminium, therefore suggesting formation of the Mitsubishi

molecule **19**(**4**^{R})$_2$ (Figure 7.13). ^{1}H NMR spectroscopy corroborated this, with the appearance of a number of sharp signals in the δ 4.4-3.8 ppm region that were interpreted in terms of the CH_2O hydrogens of **19**(**4**^{R})$_2$ and other molecular species, such as **15**(**4**^{R})$_4$ (see Figure 7.5). Further evidence for the formation of **19**(**4**^{R})$_2$ came from the observation of a correlation between ^{1}H NMR signals at δ 3.89 and 2.95 ppm by ^{1}H,^{1}H-NOESY, which paralleled the spectroscopic observations on **19**(**4**^{Bn})$_2$ (δ 3.93 and 2.94 ppm). The ^{1}H NMR integrals of these signals also showed the expected 3:1 ratio.

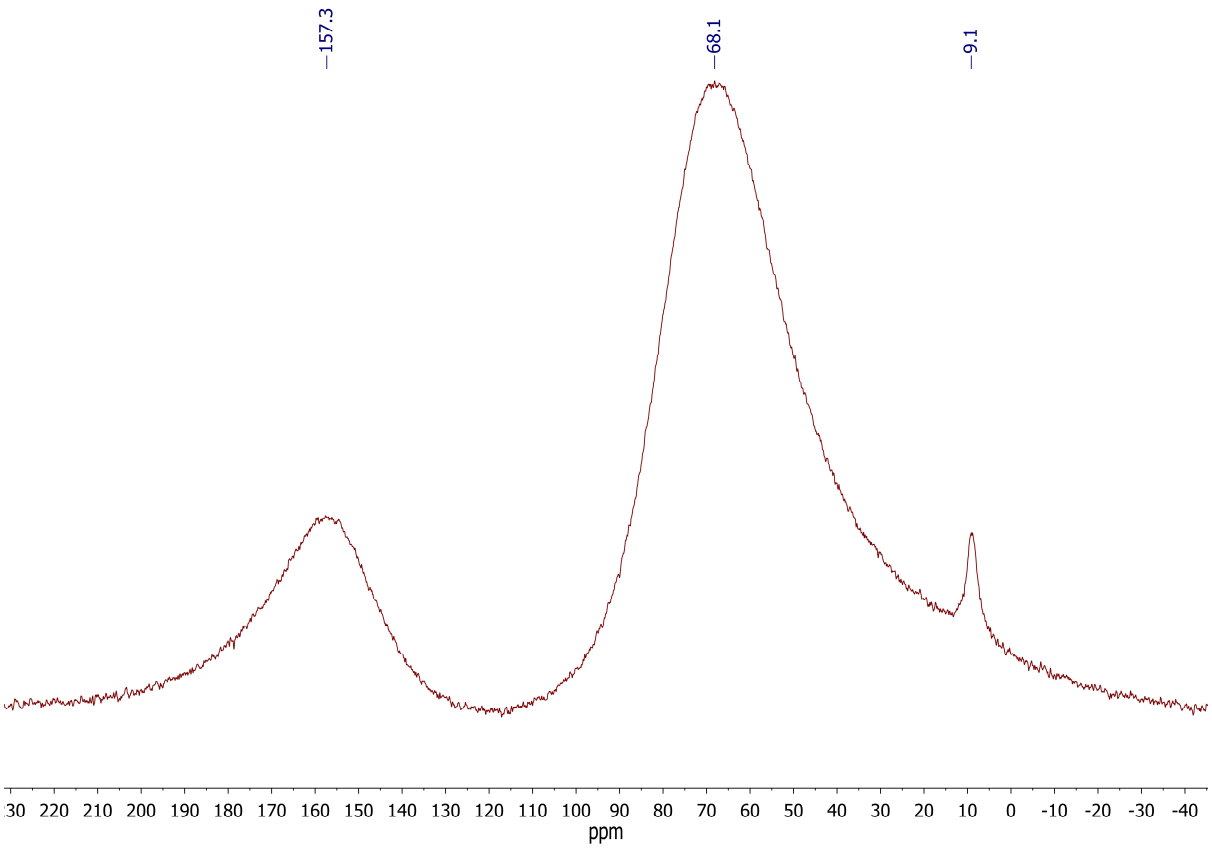

Figure 7.13: ^{27}Al NMR spectrum of an aliquot from the reaction of TMA with RL 32H in an 8:1 ratio after heating to reflux for 2 hours in toluene. The peak at δ 68.1 ppm is a background signal due to the NMR instrument. The solvent is toluene-d_8.

The reaction of 12 equivalents of Me_2AlCl with RL 32H was analysed by an NMR experiment in toluene-d_8. At room temperature adduct formation dominated, with ^{13}C NMR spectroscopy revealing carbonyl signals at δ 185.8 and 184.9 ppm (cf. δ 172.6 and 172.0 ppm for RL 32H). ^{1}H NMR spectroscopy (Figure 7.14, bottom) also indicated adduct formation, with a number of broad signals moved relative to those seen in pristine RL 32H and an AlMe signal seen at δ −0.29 ppm (cf. δ −0.35 ppm for Me_2AlCl). Heating the NMR sample to 70 °C for 24 hours resulted in the appearance of two sharp peaks in the ^{1}H NMR spectrum (Figure 7.14, middle), at δ 1.12 and 1.10 ppm. These could be

attributed to the methyl hydrogens of **4**^{R}(Me_2AlCl) or **4**^{R}($MeAlCl_2$) (based on the monoester reactions with **1**^{Bn}, see Section 6.3). Also of interest, the appearance of a small, sharp signal at δ 0.17 ppm indicated the production of methane. Meanwhile, a signal down field at δ 4.75 ppm suggested the formation of alkenes. These assignments were corroborated by HSQC data, which revealed a correlation between the presumed alkene signal at δ 4.75 ppm and a signal at δ 110.2 ppm in the ^{13}C NMR spectrum. These signals are very similar to those seen for the alkene **7b** (^{1}H NMR δ 4.77 and 4.72 ppm, ^{13}C NMR δ 112.2 ppm, see Section 6.3). Heating the NMR sample to 100 °C for 24 hours (Figure 7.14, top) resulted in complete disappearance of the signals at δ 1.12 and 1.10 ppm, along with the growth of signals at δ 5.16, 4.75 and 0.17 ppm. These signals were attributed to elimination from the dimethylated species to form multiple alkenes and methane. Such reactivity was similar to that seen for the tetraesters with Me_2AlCl (see Section 7.4). From the previous tetraester work it was expected that the alkenes would constitute two possible isomers (Figure 7.15). Unfortunately, due to overlapping signals it proved difficult to determine the exact structures of the alkenes formed, but a HSQC experiment allowed for the assignment of the δ 5.16 and 4.75 ppm ^{1}H NMR signals to CH=C and C=CH_2 environments (by correlations to ^{13}C NMR signals at δ 125.3 and 110.2 ppm).

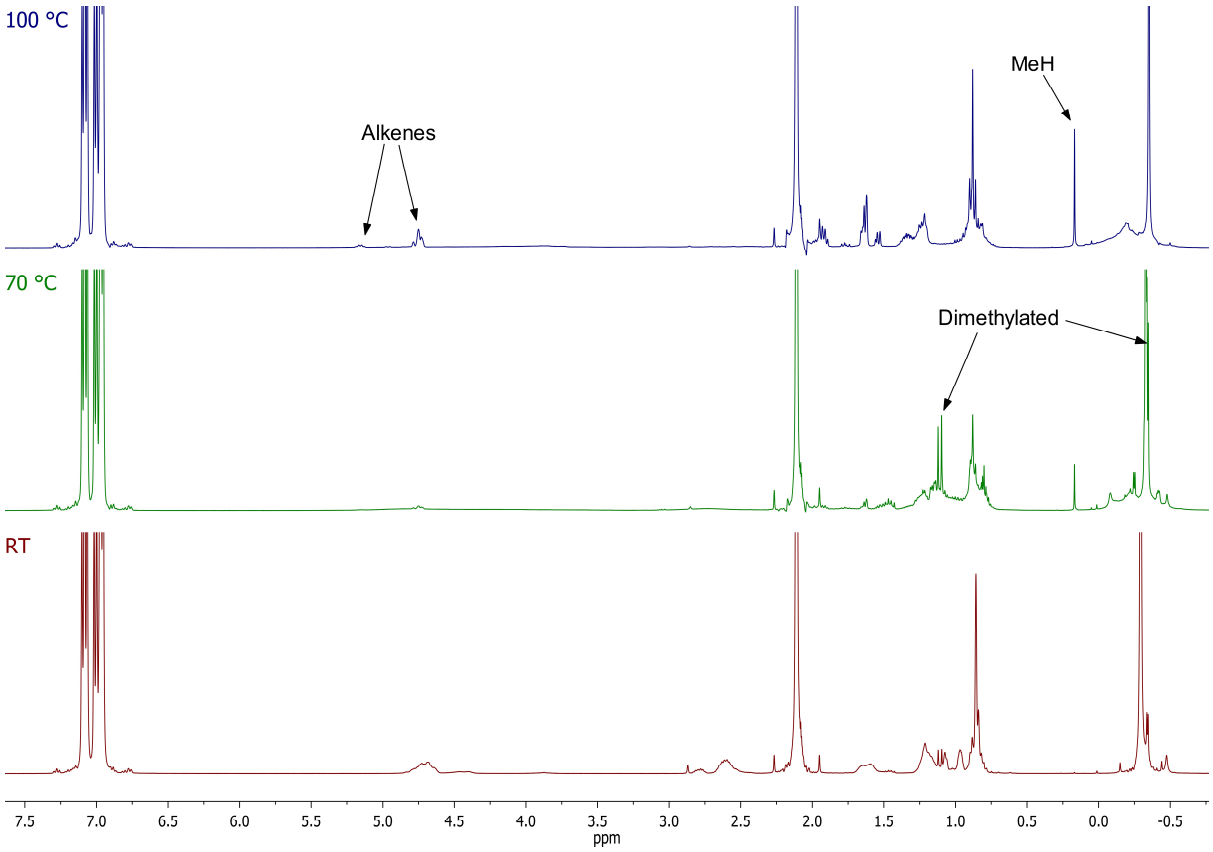

Figure 7.14: ^{1}H NMR spectra of aliquots from the reaction of Me_2AlCl and RL 32H in a 3:1 ratio in toluene, heated at the stated temperature for 24 hours in toluene-d_8 in a sealed J Young NMR tube.

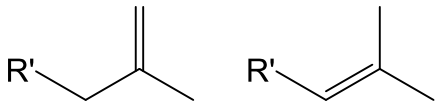

Figure 7.15: The proposed structures of the alkenes formed from the 12:1 reaction of Me_2AlCl and RL 32H in toluene (heated to 100 °C for 24 hours, R′ = C_2H_5 or C_4H_9).

Moving to more Lewis acidic $MeAlCl_2$, addition to RL 32H resulted in only adduct formation, similar to the behaviour seen for the addition of $MeAlCl_2$ to tetraesters (see Section 6.4). Adduct formation was identified by ^{27}Al NMR spectroscopy, which revealed a signal at δ 178.7 ppm (cf. δ 135 ppm for $MeAlCl_2$) and a peak at δ 188.5 ppm in the ^{13}C NMR spectrum (cf. δ 172.6 and 172.0 ppm for RL 32H). Heating the NMR sample to 100 °C for 24 hours resulted in a significant change, with ^{13}C NMR spectroscopy suggesting ketone formation, through the observation of a resonance at δ 239.3 ppm. This replicated the reactivity shown between **1**^{Bn} and $MeAlCl_2$, with Friedel-Crafts acylation of toluene generating a ketone which formed an adduct with $MeAlCl_2$ (see Section 6.4).

The reaction of RL 32H with $Me_{1.5}AlCl_{1.5}$ showed reactivity intermediate between that of reactions with Me_2AlCl and $MeAlCl_2$. At room temperature adduct formation was

observed, with a ^{13}C NMR signal at δ 187.3 ppm and a ^{27}Al NMR signal at δ 179.0 ppm. Heating the NMR sample to 100 °C for 24 hours again showed the formation of alkenes and methane, with the corresponding ^{1}H NMR signals seen at δ 5.18, 4.72 and 0.17 ppm.

7.8 Summary

The reaction of methylaluminium reagents and polyolester oil RL 32H was modelled using tetraesters **14**^{Pent} and **14**^{Bn}. Initially, TMA was used to model the reactivity. The reactions of TMA with **14**^{Pent} and **14**^{Bn} showed similar results to those obtained using monoesters **1**^{Et} and **1**^{Bn} (see Section 6.2). At low TMA:tetraester stoichiometry, adduct formation dominated. The tetraadduct **14**^{Pent}(TMA)$_4$ was observed crystallographically, but was only stable at low temperatures and defied characterisation beyond X-ray diffraction despite repeated attempts at isolation and handling. With more than one equivalent of TMA per ester, addition resulted in the formation of **4**^{R}(TMA) (R = Pent, Bn). Along with **4**^{R}(TMA), the ^{1}H NMR spectrum revealed a very broad signal at *ca.* δ 3.8 ppm which was attributed to the tetrolate-based elimination product C(CH$_2$OAlMe$_2$)$_4$ **15**. The broadness of this signal was attributed to **15** existing as a polymeric species. Heating of the different stoichiometry TMA:**14**^{Bn} reaction mixtures resulted in adduct formation between **4**^{Bn} and the tetrolate-based product of ester cleavage, demonstrating the retention of 3, 2, 1 or 0 unreacted ester groups (**16**^{Bn}, **17**^{Bn}, **18**^{Bn} or **15**). For full ester cleavage, 8 equivalents of TMA were required. NMR spectroscopy revealed these adducts to contain Al$_2$O$_2$ metallacycles similar to those seen for **4**^{R}(**3**). In the 8:1 reaction of TMA with **14**^{Bn}, it was revealed that **15**(**4**^{Bn})$_4$ could undergo elimination of (**4**^{Bn})$_2$ and **4**^{Bn}(TMA) to form the octaaluminium species **19**(**4**^{Bn})$_2$. This species was shown crystallographically to contain an Al$_4$O$_6$ Mitsubishi-type core. This thermal rearrangement was explained by the formation of the thermodynamically stable Al$_4$O$_6$ core and a reduction in the number of **4**^{Bn} adducts, from four in **15**(**4**^{Bn})$_4$ to two in **19**(**4**^{Bn})$_2$, resulting in less steric crowding.

Replacing TMA with Me$_2$AlCl resulted in much less reactive systems due to the reduced nucleophilicity of Me$_2$AlCl. The 12:1 reaction of Me$_2$AlCl with **14**^{Bn} resulted in only 2% of the ester groups cleaving to form **4**^{Bn}(Me$_2$AlCl) after 2 hours at room temperature. Increasing the temperature resulted in an increase in the amount of **4**^{Bn}(Me$_2$AlCl) formed and also the observation of **4**^{Bn}(MeAlCl$_2$). The formation of alkenes **7a** and **7b** was detected

after the system was heated to 90 °C due to thermal elimination, with trimethylated **10** and Friedel-Crafts products **11a** and **11b** also observed upon heating to reflux. In these reactions, a broad signal in the ^{1}H NMR spectrum was also observed to develop. This was attributed to the tetrolate-based by-product of complete de-esterification, $C(CH_2OAlMeCl)_4$ **21**. In contrast to the products of the TMA reactions, this central tetrolate core did not complex dimethylated **4**^{Bn}. This is consistent with the removal of **4**^{Bn} from the reaction mixture when **4**^{Bn}(Me_2AlCl) and **4**^{Bn}($MeAlCl_2$) undergo elimination reactions at raised temperatures to form alkenes **7a** and **7b**. Concomitant with alkene formation was the observation of methane, in a manner similar to that observed in the monoester reactions.

The use of $MeAlCl_2$ produced in an intractable solid (presumed to be the tetraadduct **14**^{Bn}($MeAlCl_2)_4$). The reaction of tetraesters with $Me_{1.5}AlCl_{1.5}$ at room temperature, resulted in adduct formation dominating. However, heating to reflux in toluene resulted in the formation of alkenes **7a** and **7b**, trimethylated **10**, Friedel-Crafts products **11a** and **11b** and methane. Similar to the monoester reactions with $Me_{1.5}AlCl_{1.5}$, **4**^{Bn}(Me_2AlCl) and **4**^{Bn}($MeAlCl_2$) were not directly observed due to fast thermal elimination undergone by these species.

The above reactions were repeated, but with industrial lubricant RL 32H as the tetraester resulted in similar patterns of reactivity to those observed in the model systems described above. The addition of 12 equivalents of TMA to RL 32H produced **4**^{R}(TMA) and **15** at room temperature. Three different species of the type **4**^{R}(TMA) were observed by NMR spectroscopy, suggesting that three different alkyl groups may be present in RL 32H. Heating RL 32H with 8 equivalents of TMA resulted in the formation of the Mitsubishi-type species **19**(**4**^{R})$_2$, as suggested by the observation of a characteristic and sharp ^{27}Al NMR signal at δ 9.1 ppm. Meanwhile, the reaction of RL 32H with Me_2AlCl resulted in behaviour analogous to that seen between **14**^{Bn} and Me_2AlCl. Adduct formation was observed at room temperature, followed by the production of dimethylated **4**^{R}(Me_2AlCl) and **4**^{R}($MeAlCl_2$) at 70 °C, and finally the detection of alkenes and methane after heating to 100 °C. The use of $Me_{1.5}AlCl_{1.5}$ and $MeAlCl_2$ as organoaluminium reagents resulted in the same reactivity as seen for **14**^{Bn}, with only adduct formation seen at room temperature. However, heating the $Me_{1.5}AlCl_{1.5}$-containing mixture to reflux produced alkenes and

methane. These reactions therefore revealed essentially the same patterns of reactivity to those observed in the model systems described above.

To summarise, the model for industrial refrigeration oils used here, with their well-defined tetraester structures and compositions, revealed similar reactivity towards organoaluminiums as did the monoesters, whose chemistry was reported in Chapter 6. Ester cleavage was observed in reactions with TMA and Me_2AlCl at room temperature, while reactions with $Me_{1.5}AlCl_{1.5}$ required elevated temperatures for cleavage. These results essentially lead to the same problems raised in Section 6.7, which were a loss of lubrication and the formation of flammable species, such as methane and alkenes.

Chapter 8

Reactions of Polyols with Methylaluminium Reagents

8.1 Introduction

In Chapter 7 it was shown that reactions between tetraesters and organoaluminiums at room temperature resulted in the formation of polymeric species. These polymers were produced from tetrolate cores (which were formed by cleavage of all four ester functions in the tetraester reagent), bridged by aluminium centres. This was evidenced by broad signals in the ^{1}H NMR spectrum. Heating the TMA-tetraester reaction mixtures resulted in incorporation of the tetrolate into the products, as seen crystallographically for **17**^{Bn}(**4**^{Bn})$_2$ and **19**(**4**^{Bn})$_2$. A tetrolate can adopt several different coordination modes, depending on its denticity and the number of metal centres that it coordinates. However, pentaerythritolate is geometrically restricted to act, at most, as a tridentate ligand to a single metal centre. The coordination modes expected for a tetrolate can be mimicked by reacting diols and triols with organoaluminium reagents, revealing possible aggregation and structure-types.

As discussed in the introduction (see Section 1.4.3.1), the 1:1 reaction of alcohols with trialkylaluminiums results in the formation of dialkylaluminium alkoxides (which generally form dimers or trimers) and alkanes.[59,148] The use of polyols instead of alcohols can lead to more complex structures due to the chelating nature of the ligands. Reactions between diols and organoaluminiums are dominated by the formation of trialuminium species, the structures of which contain one central 5-coordinate aluminium and two 4-coordinate aluminiums (Scheme 8.1).[149–151] These species are observed with 1.5 equivalents or more of organoaluminium to diol.

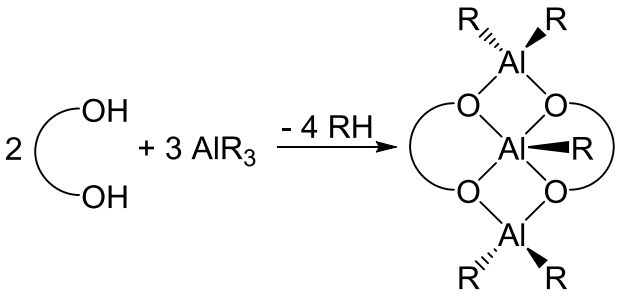

Scheme 8.1: The general reaction of diols with trialkylaluminiums (AlR_3) to produce trialuminium species.

On the other hand, the use of sterically bulky organoaluminium Al^tBu_3 has been reported to stabilise monodeprotonated diols. These dialuminium species possess two unreacted hydroxyl groups (Scheme 8.2). The observation of unusually downfield hydroxyl hydrogens (δ 17-15 ppm) by ^1H NMR spectroscopy supported the crystallographic interpretation of hydrogens bridging the diolate moiety.[67,152,153]

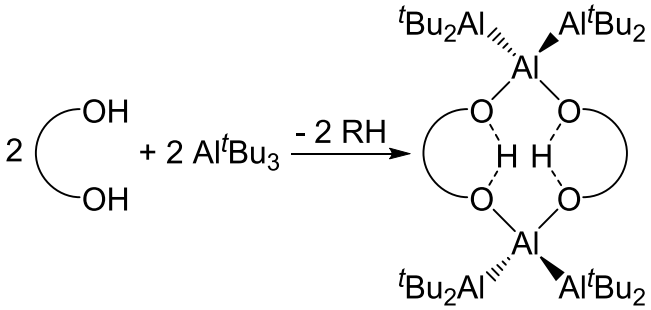

Scheme 8.2: The reaction of diols with Al^tBu_3 resulted in the formation of a dialuminium species which retained hydroxyl hydrogens.[67,152,153]

As noted already, the reaction between organoaluminiums and diols is highly dependent on the stoichiometry of these components. An excess of organoaluminium reagent results in the formation of molecular species. However, using equimolar amounts of organoaluminiums and diol can result in the formation of oligomeric and polymeric species (so-called alucones). These species are insoluble in organic solvents. The structure of these alucones has been suggested to be based on linear chains with aluminium atoms bridging the diolate groups (Figure 8.1).[154,155]

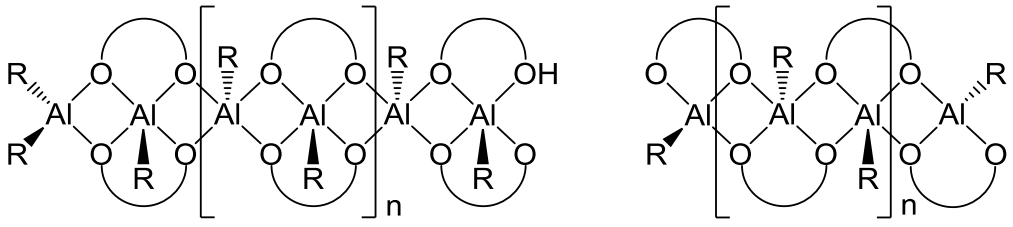

Figure 8.1: The proposed structure of linear alucones, formed from the equimolar reaction of a trialkylaluminium (AlR_3) with a diol.[154,155]

Further reduction in the AlR_3:diol stoichiometry was reported to form polymeric sheets. In these polymers all alkyl groups had reacted, resulting in cross-linking between aluminium chains to form 3D structures (Figure 8.2). The structure of these species was determined through the use of solid-state ^{27}Al NMR spectroscopy, thermogravimetric analysis and mass spectrometry.[156]

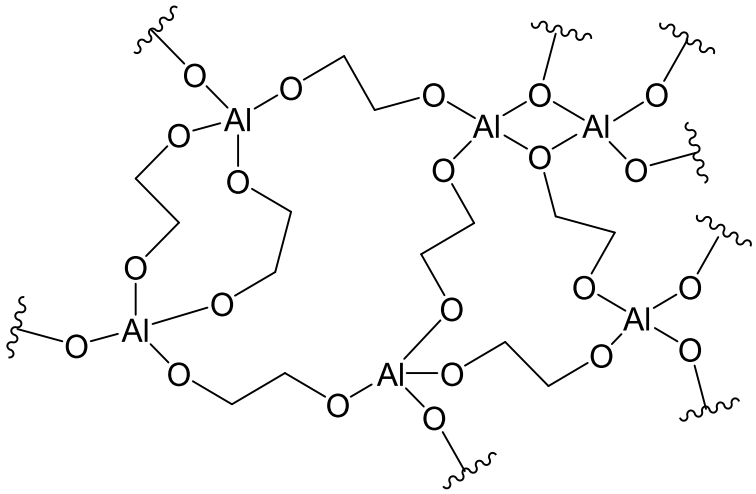

Figure 8.2: The proposed structure of a cross-linked alucone polymer, formed by reacting an excess of diol with a trialkylaluminium reagent.[156]

There is little literature on the reaction of triols with organoaluminium compounds. The most prevalent use is in the formation of Anderson-type clusters. In these clusters, a central octahedrally-coordinated metal (e.g. aluminium) is bridged to six equatorial metal atoms by oxygen-based ligands. A triol unit can coordinate to one or two faces of the cluster and act as a tridentate ligand to the central aluminium (Figure 8.3, left).[157,158] Examples of these clusters also include the use of tetrol ligands. This results in one of the alcohol groups remaining protonated and pointing away from the cluster, due to geometric constraints (Figure 8.3, right).[157,159]

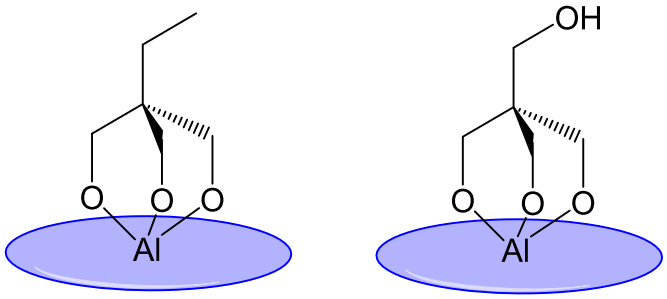

Figure 8.3: The structure of Anderson-type clusters with triol and tetrol ligands. The blue oval represents an $AlMo_6O_{18}(OH)_3$ fragment, with the triolate moiety in each case chelating the central aluminium.[157]

8.2 Reactions of Diols with Methylaluminium Reagents

Initially, the diol neopentyl glycol was reacted with TMA in a number of different stoichiometries to further understand how the tetrolate core from tetraesters may behave. The 3:2 combination of TMA with the diol in Et_2O at −78 °C produced a white precipitate. Recrystallisation from pentane at −20 °C produced crystals of the trialuminium species $MeAl\{Me_2C(CH_2O)_2AlMe_2\}_2$ **22** (Scheme 8.3).

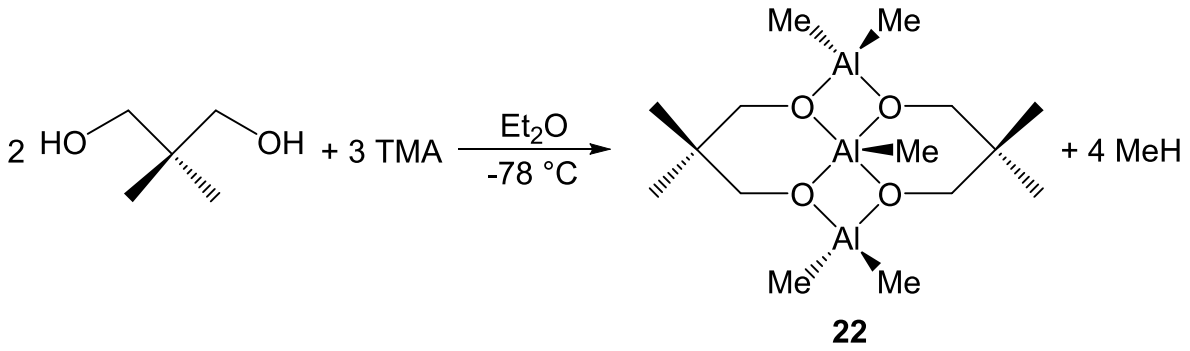

22

Scheme 8.3: The 3:2 reaction between TMA and neopentyl glycol to produce **22**.

The crystal structure of **22** (Figure 8.4) indicated that each alcohol had undergone deprotonation, resulting in the elimination of 4 equivalents of methane for each molecule of **22** formed. The geometry of the central 5-coordinate aluminium atom is distorted square based pyramidal, with four oxygen atoms in the basal positions and a methyl group in the apical position. The 4-coordinate aluminiums each have distorted tetrahedral geometry. In **22**, the central aluminium has a mean Al−O bond length of 1.868 Å, whereas the outer 4-coordinate aluminiums have a mean Al−O bond length of 1.826 Å, slightly shorter due to the decreased coordination number. The Al_2O_2 rings show smaller mean O−Al−O angles at the 5-coordinate aluminium (77.1°) compared to the 4-coordinate aluminiums (79.2°). The Al_2O_2 rings are close to planar, with internal angles summing to 359.1 and 359.4°. The geometry around the oxygen atoms is close to trigonal planar, with the mean sum of the angles (359.5°) suggesting the oxygens are sp^2 hybridised. The 6-membered AlOCCCO rings have a distorted chair conformation.

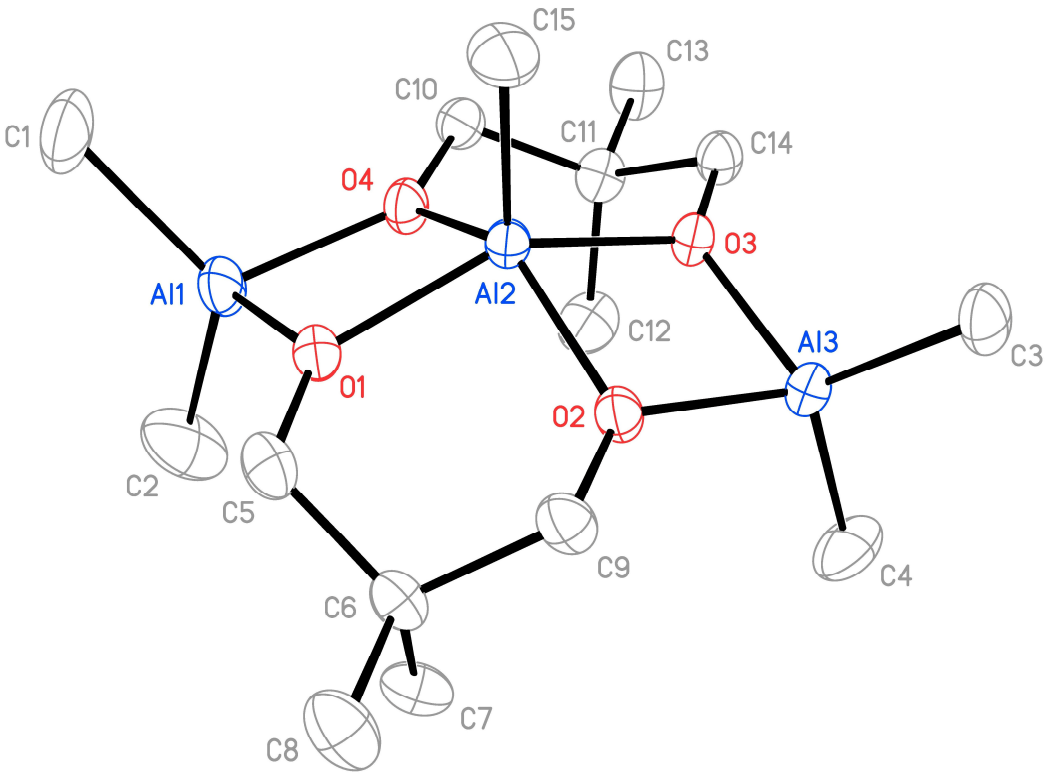

Figure 8.4: Thermal ellipsoid plot of **22** (30% probability). H-atoms omitted for clarity and only one representative molecule from the asymmetric unit cell shown. Selected bond lengths (Å) and angles (°): Al1–O1 1.814(3), Al1–O4 1.833(3), Al1–C1 1.945(6), Al1–C2 1.950(6), Al2–O1 1.881(3), Al2–O2 1.851(3), Al2–O3 1.881(3), Al2–O4 1.857(3), Al2–C15 1.942(4), Al3–O2 1.827(3), Al3–O3 1.830(3), Al3–C3 1.951(4), Al3–C4 1.949(5), Al1–O1–Al2 101.22(14), Al1–O4–Al2 101.41(14), O1–Al1–O4 79.38(13), O1–Al2–O4 77.07(13), O1–Al2–O2 89.73(12), O3–Al2–O4 90.88(12), Al2–O2–Al3 102.15(13), Al2–O3–Al3 100.94(12), O2–Al2–O3 77.19(11), O2–Al3–O3 79.09(12).

The ^{1}H NMR spectrum of **22** (Figure 8.5) suggested that the solid-state structure is retained in solution, as indicated by the observation of three distinct aluminium-bound methyl environments in a 2:2:1 ratio (δ −0.42, −0.49 and −0.53 ppm, respectively). The spectrum also showed geminal coupling between the CH_2O hydrogens (δ 3.34 and 2.99 ppm, ^{2}J = 10.4 Hz), revealing that they are non-equivalent in solution. A single broad AlMe resonance is observed in the ^{13}C NMR spectrum from the overlap of signals.

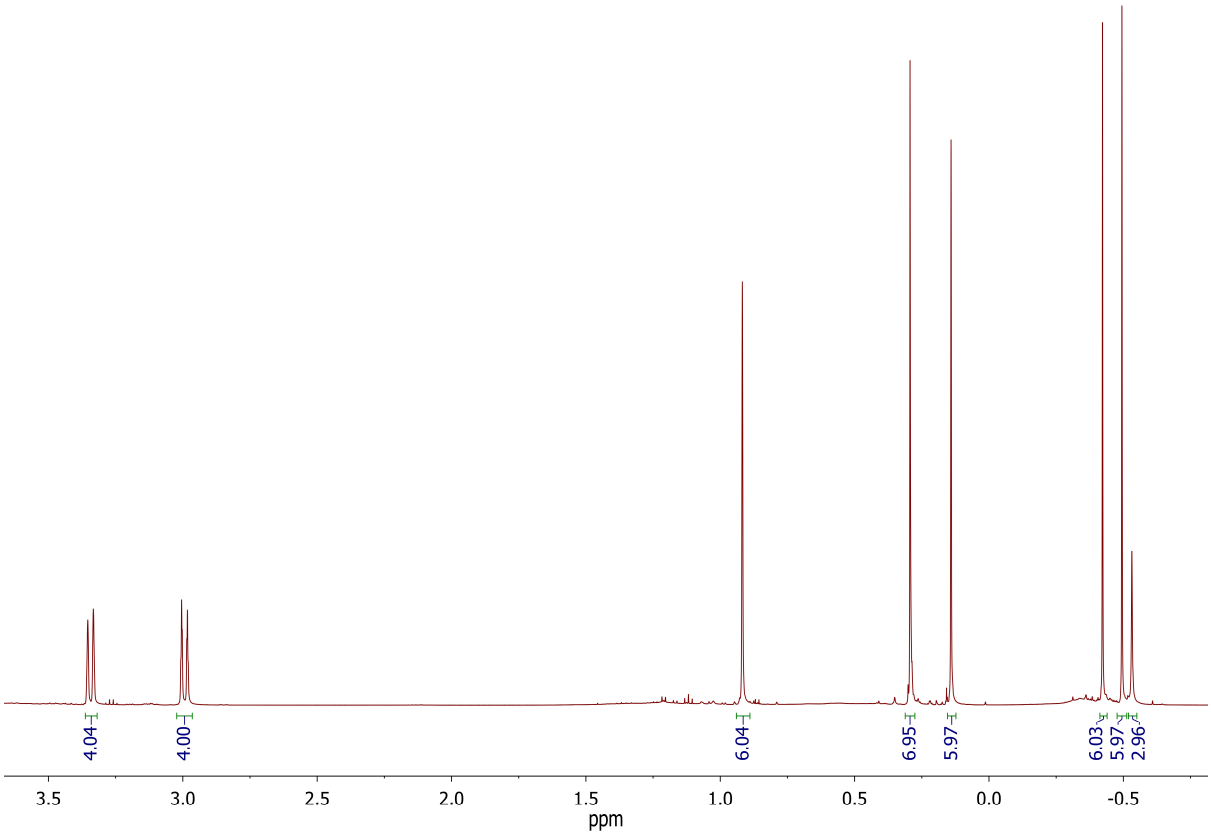

Figure 8.5: ^{1}H NMR spectrum of **22**. The signal at δ 0.29 ppm is an impurity from Si grease. The solvent is benzene-d_6.

Reactions between neopentyl glycol and Me_2AlCl showed a marked difference to those with TMA. The 2:1 combination of Me_2AlCl with the diol in toluene at −78 °C produced a white precipitate. This precipitate was dissolved in toluene, with storage at room temperature producing crystalline needles. X-ray diffraction revealed these to be $\{Me_2C(CH_2O)_2AlMe(AlMeCl_2)\}_2$ **23**$_2$ (Scheme 8.4). The crystal structure of **23**$_2$ (Figure 8.6) revealed that the methyl groups had performed deprotonation, rather than the chloride. This selectivity has previously been observed in reactions between methylaluminium chlorides and alcohols.[160–162] This is attributed to the weakness of the Al−C bond compared to the Al−Cl bond.[72]

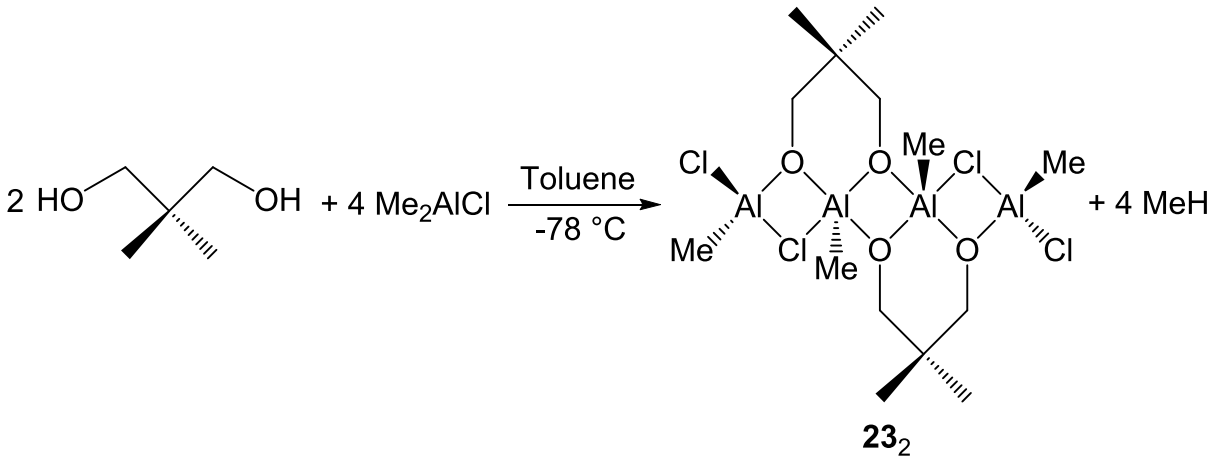

23$_2$

Scheme 8.4: The 2:1 reaction between Me_2AlCl and neopentyl glycol to produce **23**$_2$.

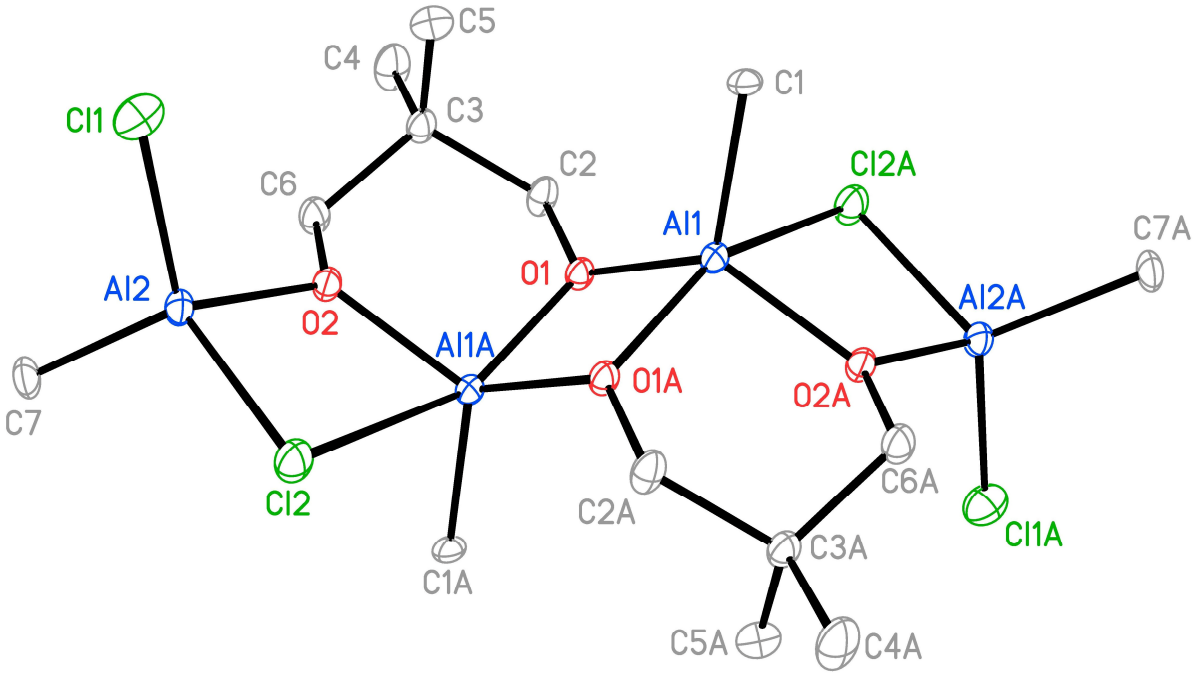

Figure 8.6: Thermal ellipsoid plot of **23**$_2$ (30% probability). H-atoms omitted for clarity. Selected bond lengths (Å) and angles (°): Al1–O1 1.8131(14), Al1–O1A 1.8601(14), Al1–O2A 1.8225(14), Al1–C1 1.9574(19), Al1–Cl2A 2.7416(7), Al2–O2 1.8108(14), Al2–C7 1.943(2), Al2–Cl1 2.1303(8), Al2–Cl2 2.1910(8), O1–Al1–O1A 78.97(6), O1A–Al1–O2A 93.96(6), O2A–Al1–Cl2A 73.97(5), O1–Al1–Cl2A 86.05(5), Al1–O1–Al1A 101.03(6), Al2–O2–Al1A 118.13(7), Al2–Cl2–Al1A 77.48(3), O2–Al2–Cl2 89.99(5), O2–Al1A–Cl2 73.97(5).

The tetraaluminium species **23**$_2$ has a dimeric structure, composed of dialuminium diolates. The geometry around Al1 is square based pyramidal, with the methyl group occupying the apical position. The geometry around Al2 is distorted tetrahedral, with the distortion occurring due to the 4-membered Al_2OCl ring. The Al_2O_2 ring in the centre of the structure (containing two 5-coordinate aluminiums) is planar, with the internal angles summing to 360°. The Al_2OCl rings show a non-symmetrical bonding mode for the bridging chlorine, Cl2 (Figure 8.7). The Al2–Cl2 bond length (2.1910(8) Å) is significantly

shorter than the Al1–Cl2 bond length (2.7416(7) Å). Furthermore, the difference in Al–Cl bond lengths (0.5506(14) Å) is significantly greater than could potentially be explained by differences in aluminium coordination number or steric effects. The suggested stronger interaction of Cl2 with Al2 is in accordance with the increased Lewis acidity expected for the lower coordinate Al centre. This type of asymmetrical Al–Cl–Al bridge bonding is uncommon. A previous example is in arene borylation with $AlCl_3$, and was also explained by the stronger Lewis acidity of the lower coordinate aluminium centre.[137] The overall structure of **23**$_2$ can be viewed as a central $\{(Me_2C(CH_2O)_2)(AlMe)\}_2$ unit, adducted with two units of $MeAlCl_2$.

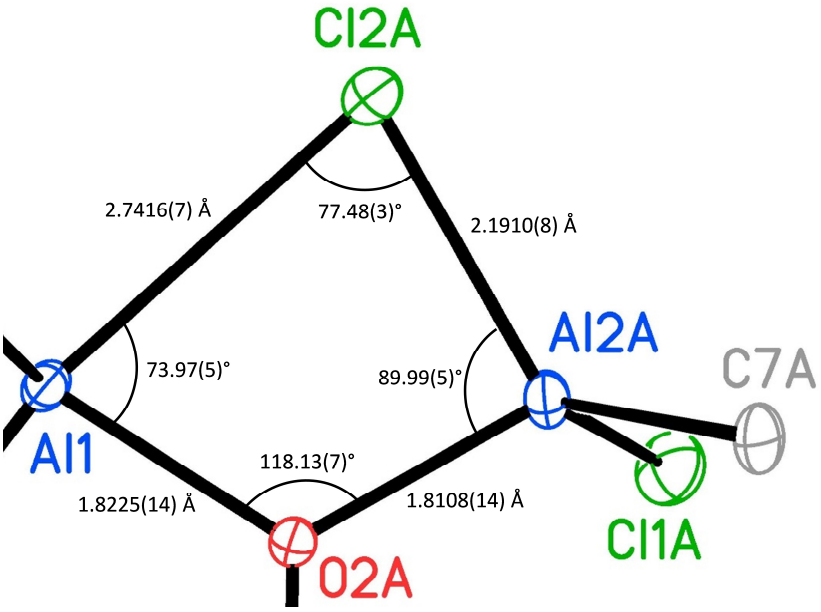

Figure 8.7: The thermal ellipsoid plot of a part of **23**$_2$ (30% probability). H-atoms omitted for clarity.

The ^{1}H NMR spectrum for **23**$_2$ (Figure 8.8) suggested that the solid-state structure is retained in solution. Four different CH_2O hydrogen signals were observed (δ 3.55, 3.40, 3.33 and 3.17 ppm) with geminal coupling between hydrogens (δ 3.55 and 3.17 ppm, ^2J = 11.6 Hz; δ 3.40 and 3.33 ppm, ^2J = 11.4 Hz). There was also a ^4J coupling observed between the signals at δ 3.55 and 3.40 ppm (^4J = 1.7 Hz), which was due to W-coupling.[163] This W-coupling led to the assignment of the signals at δ 3.55 and 3.40 ppm as pseudo-equatorial hydrogens and points to conformational rigidity. The presence of two AlMe environments (δ −0.24 and −0.30 ppm) in a 1:1 ratio corroborated the retention of the structure in solution. The use of a ^{1}H,^{1}H-NOESY experiment allowed for the assignment of the signal at δ −0.30 ppm as the AlMe featuring the 5-coordinate aluminium through a

NOE correlation with the signal at δ 0.57 ppm, which is attributable to a methyl group in the diolate (*viz*. C1···C5 3.686(3) Å in Figure 8.6).

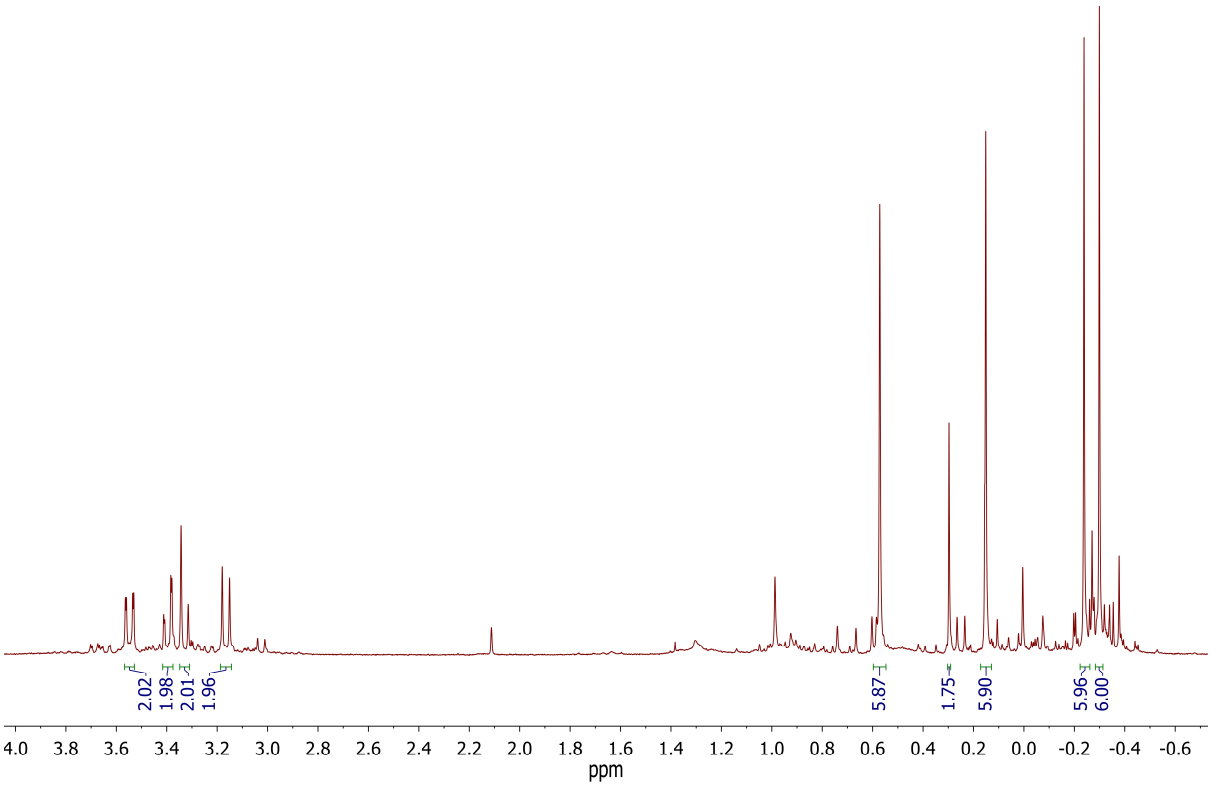

Figure 8.8: ^{1}H NMR spectrum of **23**$_2$. The signal at δ 0.30 ppm is an impurity from Si grease. The solvent is benzene-d_6.

Attempts to dissolve the precipitate from the Me_2AlCl-diol reaction mixture with an excess of THF resulted in solvation. Removal of the solvent *in vacuo* and recrystallisation in toluene led to the isolation of the trialuminium species $(ClAl\{Me_2C(CH_2O)_2AlCl_2\}_2)(THF)_2$ **24**$(THF)_2$ (Figure 8.9). This shows the same structure-type as seen for **22**, but the aluminium-bound methyl groups are replaced by chlorides and THF is coordinated to the peripheral aluminium centres. This results in a distorted trigonal bipyramidal geometry for the peripheral aluminium centres, with an alkoxide and a THF in the axial positions. The addition of THF resulted in a preference for retention of chloride ligands over methyl ligands in the Al-diolate complex. This is because THF can act as a Lewis base and having chloride ligands increases the Lewis acidity of the aluminium, increasing the strength of the adduct interaction. The observation of $AlCl_2$ groups indicates that a rearrangement of ligands has occurred. This suggests that a by-product with AlMe groups was also formed, such as $TMA(THF)_2$, but further analysis of the remaining material proved unsuccessful.

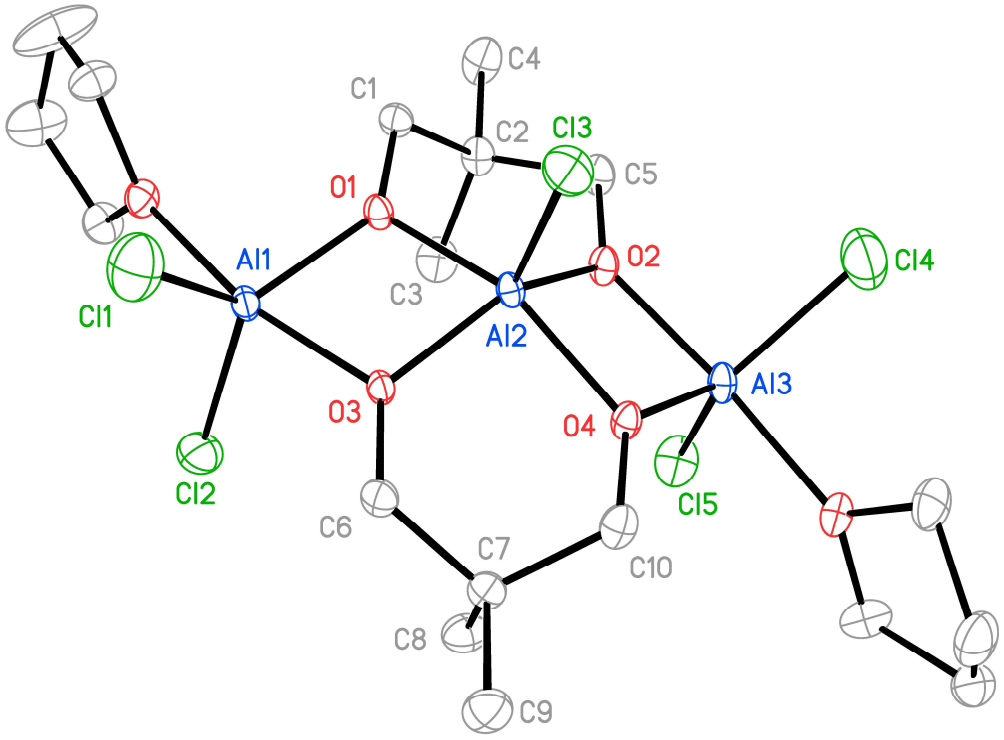

Figure 8.9: Thermal ellipsoid plot of **24**$(THF)_2$ (30% probability). H-atoms omitted for clarity. Selected bond lengths (Å) and angles (°): Al1–O1 1.835(3), Al1–O3 1.897(3), Al1–Cl1 2.105(2), Al1–Cl2 2.157(2), Al2–O1 1.878(3), Al2–O2 1.802(3), Al2–O3 1.793(3), Al2–O4 1.884(3), Al2–Cl3 2.1452(19), Al3–O2 1.891(4), Al3–O4 1.829(3), Al3–Cl4 2.123(2), Al3–Cl5 2.147(2), Al1–O1–Al2 102.99(16), Al1–O3–Al2 103.85(16), O1–Al1–O3 75.79(14), O1–Al2–O3 77.29(15), O1–Al2–O2 93.06(15), O3–Al2–O4 93.54(15), Al2–O2–Al3 103.65(17), Al2–O4–Al3 102.91(16), O2–Al2–O4 77.00(15), O2–Al3–O4 76.18(15).

NMR spectroscopy on **24**$(THF)_2$ in benzene-d_6 revealed multiple signals in the ^{1}H and ^{13}C NMR spectra, suggesting that **24**$(THF)_2$ undergoes dissociation in solution to give multiple, currently unidentified species. On the other hand, ^{27}Al NMR spectroscopy revealed peaks at δ 53.9 and 45.8 ppm, which could be attributed to the two 5-coordinate aluminium environments observed in the crystal structure of **24**$(THF)_2$, suggesting that **24**$(THF)_2$ could be partially retained in solution.

Attempts to further understand the structure-type of **24**$(THF)_2$ led to use of $MeAlCl_2$. The addition of 2 equivalents of $MeAlCl_2$ to neopentyl glycol in toluene resulted in the precipitation of a white solid. The solution was stored at −27 °C, producing colourless crystalline needles of $ClAl\{Me_2C(CH_2O)_2AlCl_2\}_2$ **24** (Scheme 8.5). The crystal structure of **24** (Figure 8.10) showed that $MeAlCl_2$ acted preferentially as an alkyl base, with the central aluminium having also lost one chloride ligand to generate HCl. However, instead of producing HCl it is also possible that the $MeAlCl_2$ may have undergone disproportionation to form Me_2AlCl and $AlCl_3$, with only the Me_2AlCl reacting with the

diol. Evidence for this is the low yield of the product (15% wrt the diol), as $AlCl_3$ may not react with diol.

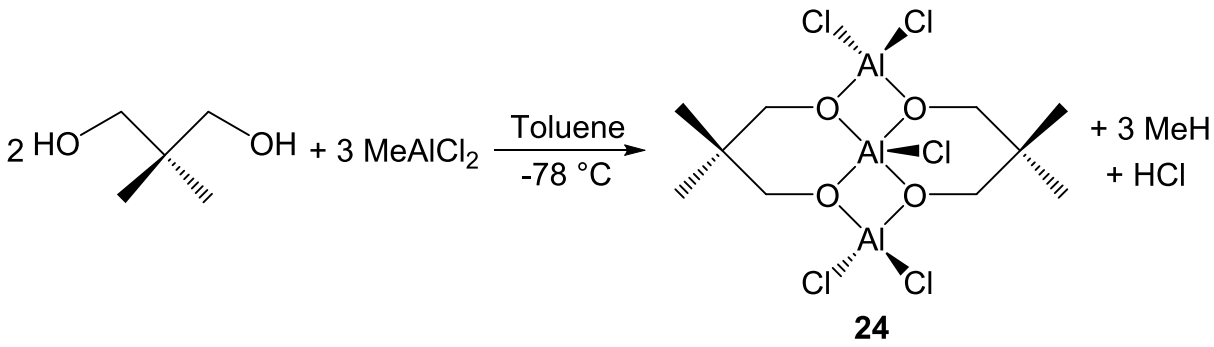

24

Scheme 8.5: The 3:2 reaction between $MeAlCl_2$ and neopentyl glycol to produce **24**.

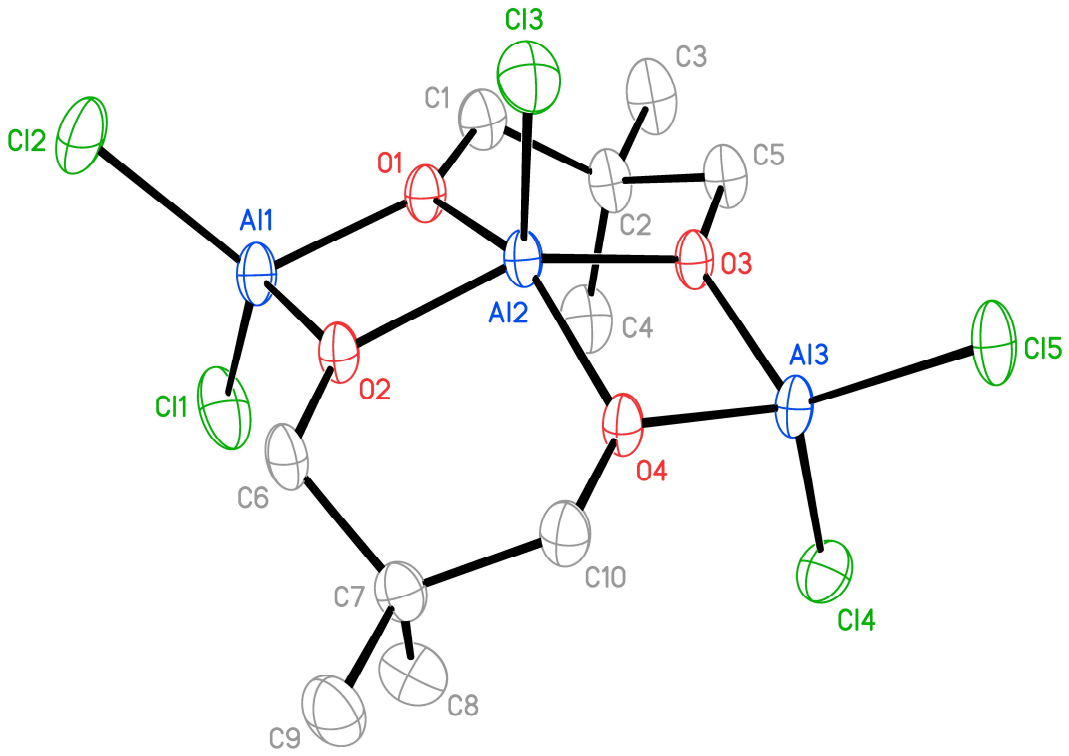

Figure 8.10 Thermal ellipsoid plot of **24** (30% probability). H-atoms and toluene of crystallisation omitted for clarity. Selected bond lengths (Å) and angles (°): Al1–O1 1.779(3), Al1–O2 1.778(3), Al1–Cl1 2.0985(17), Al1–Cl2 2.0821(17), Al2–O1 1.853(2), Al2–O2 1.855(3), Al2–O3 1.843(2), Al2–O4 1.850(3), Al2–Cl3 2.1236(15), Al3–O3 1.787(3), Al3–O4 1.783(2), Al3–Cl4 2.0924(16), Al3–Cl5 2.0853(14), Al1–O1–Al2 100.48(13), Al1–O2–Al2 100.49(13), O1–Al1–O2 81.43(11), O1–Al2–O2 77.46(11), O1–Al2–O3 92.07(11), O2–Al2–O4 91.32(12), Al2–O3–Al3 100.17(12), Al2–O4–Al3 100.05(12), O3–Al2–O4 78.09(11), O3–Al3–O4 81.35(11).

The X-ray structure of **24** shows a structure very similar to that of **22**, but with the methyl groups replaced by chlorides, and **24**$(THF)_2$, but without coordination by THF. Comparing the bond lengths in **24** with those in **22** reveals a shorter mean Al–O bond length (1.816 Å for **24**, 1.847 Å for **22**). This shortening of the mean Al–O bond length

can be attributed to the chloride ligands, as they lead to more positively charged aluminium centres and therefore stronger interactions with the electronegative oxygens.

NMR spectroscopy on **24** revealed spectra very similar to those seen for **22**. There are two distinct ^{1}H NMR signals from the CH_2O groups, at δ 3.27 and 2.84 ppm, and two methyl signals at δ 0.82 and −0.19 ppm. This suggested that **24**, like **22**, appears to retain its structure in solution. This is in contrast to **24**$(THF)_2$, which seemed to undergo dissociation in to multiple species. The ^{27}Al NMR spectrum revealed two signals at δ 101.6 and 45.8 ppm, which were assigned to the 4- and 5-coordinate aluminium environments of **24**, respectively. The signal for 4-coordinate aluminium in **24** (δ 101.6 ppm) revealed a higher field signal compared to that in **22** (δ 157.6 ppm). This difference was attributed to the replacement of methyl groups with the more electronegative chlorides. Meanwhile, the signal for 5-coordinate aluminium in **24** (δ 45.8 ppm) was the same as that in **24**$(THF)_2$, due to the almost identical coordination environment.

The species **22**, **23**$_2$, **24**$(THF)_2$ and **24** were all acquired using at least a 3:2 organoaluminium reagent to diol ratio. However, using fewer equivalents of organoaluminium yielded a gel that proved intractable. It is thought that this resulted from aluminium centres forming links between the diols to create oligomeric or polymeric structures (Figure 8.11, see also Figure 8.1).[154]

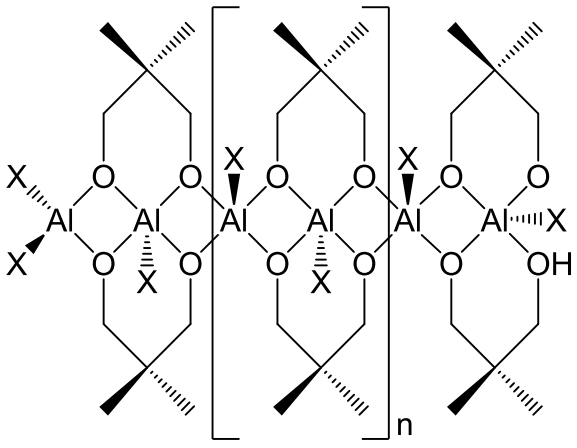

Figure 8.11: The proposed production of an oligomeric or polymeric species from the 1:1 reaction of neopentyl glycol with an organoaluminium reagent (X = Me or Cl).

To summarise, the reactions between the diol neopentyl glycol and methylaluminium reagents produced two different type of structures, with the trialuminium structural motif, shown by **22**, **24**$(THF)_2$ and **24**, dominating. This can be contrasted with the structure of **17**^{Bn}(**4**^{Bn})$_2$ (see Section 7.3) in which two ester groups, originally from a tetraester, had

reacted to produce a diolate species. The structure of **17**^{Bn}(**4**^{Bn})$_2$ revealed that the alkoxides of **17**^{Bn} did not act cooperatively as a chelating diolate, instead forming separate Al_2O_2 metallacycles with **4**^{Bn}. Considering the structural data on organoaluminium diolates reported in this chapter and elsewhere in the literature, it might be expected that **17**^{Bn}(**4**^{Bn})$_2$ would undergo rearrangement to form a trialuminium species (Scheme 8.6). The fact that this species is not observed could be explained by the bulky peripheral ester groups preventing aggregation of two **17**^{Bn} species. It may also not have occurred due to the large structural rearrangement required, suggesting **17**^{Bn}(**4**^{Bn})$_2$ to be the kinetic product.

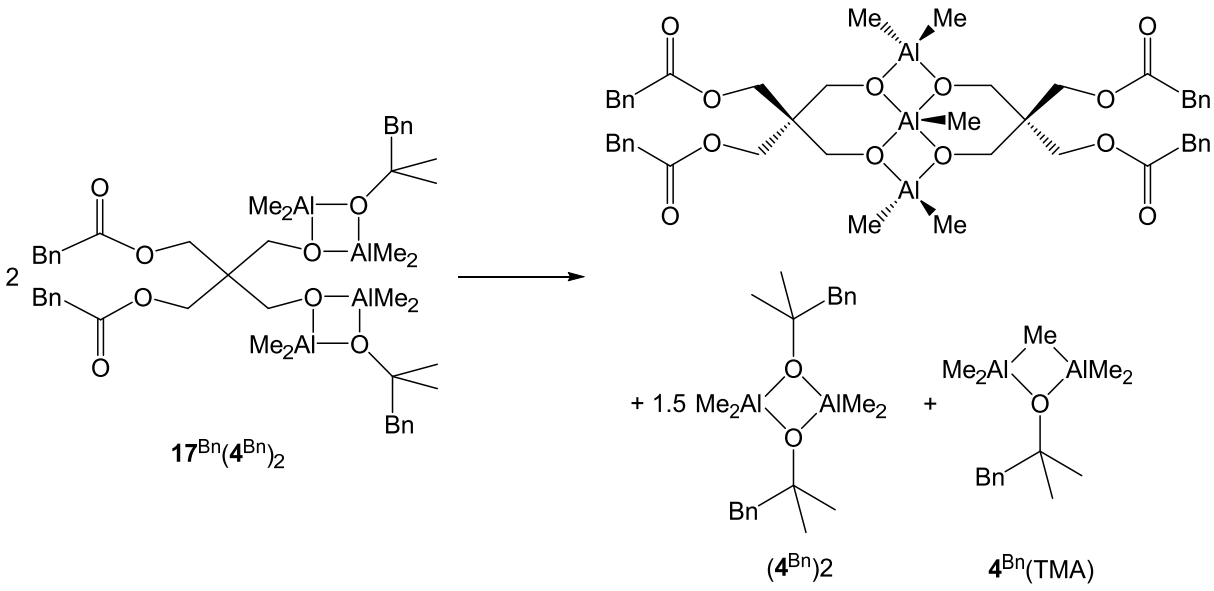

Scheme 8.6: The possible rearrangement of **17**^{Bn}(**4**^{Bn})$_2$ to give a trialuminium species, with a core similar to that seen in **22**.

8.3 Reactions of Triols with Methylaluminium Reagents

To further extend the study of the reactivity of methylaluminium reagents with polyols, TMA was combined with the triol trimethylolethane in a 2:1 ratio in THF at −78 °C. This resulted in the formation of a white solid, which was recrystallised in pentane to give $Al\{MeC(CH_2O)_3\}_2(AlMe_2)_3$ **25** (Scheme 8.7) and the elimination of 6 equivalents of methane.

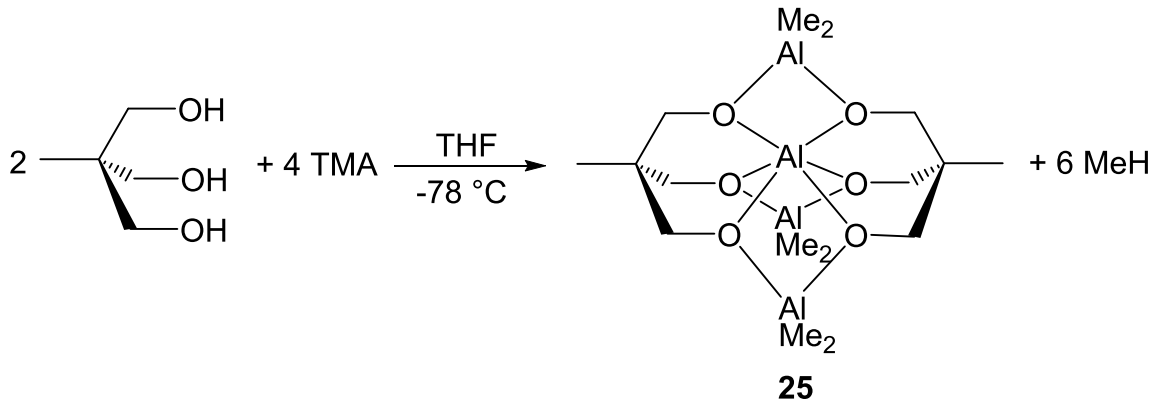

25

Scheme 8.7: The 2:1 reaction between TMA and trimethylolethane to produce **25**.

Crystallography of **25** revealed the formation of a Mitsubishi molecule (Figure 8.12).[146,147] This structure is based on an Al_4O_6 core which forms three rhombic Al_2O_2 metallacycles, related by threefold symmetry (resembling the Mitsubishi logo). The two triolate ligands act not only as tridentate ligands to the central 6-coordinate aluminium, but also act as bridging ligands to the three peripheral $AlMe_2$ units. Overall this structure has D_3 symmetry, with a C_3 axis perpendicular to the Al_4 plane. The three Al_2O_2 metallacycle planes are all flat and form a propeller like structure.

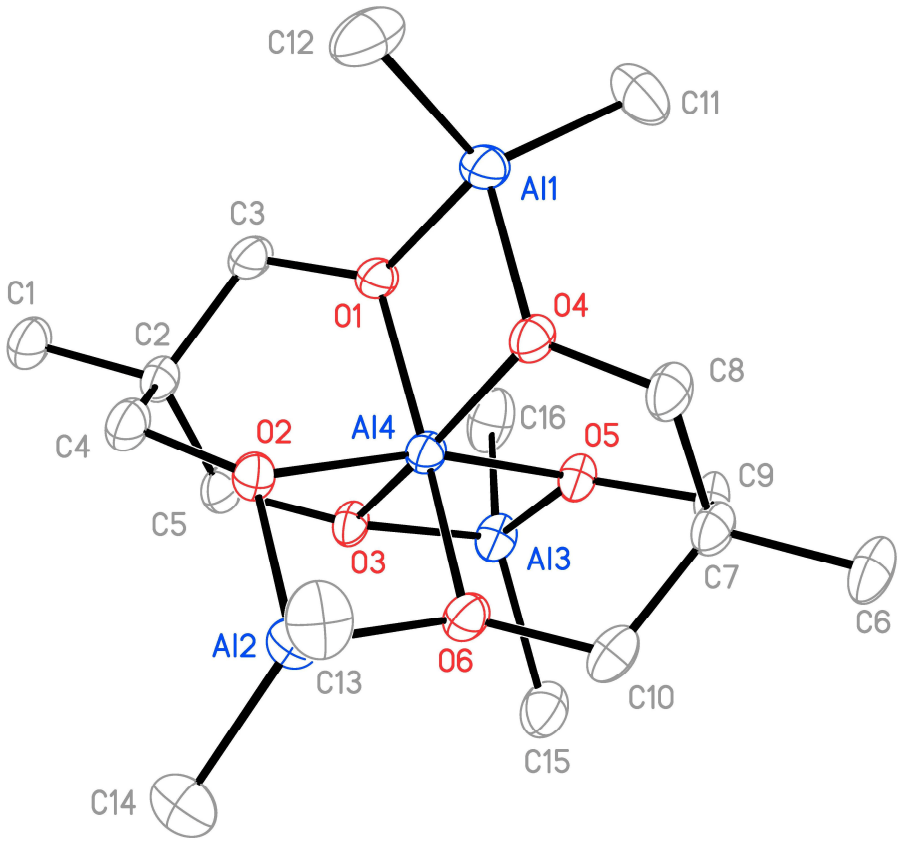

Figure 8.12: Thermal ellipsoid plot of **25** (30% probability). H-atoms omitted for clarity. Selected bond lengths (Å) and angles (°): Al1–O1 1.820(3), Al1–O4 1.828(3), Al1–C11 1.965(8), Al1–C12 1.943(7), Al2–O2 1.830(3), Al2–O6 1.828(4), Al2–C13 1.953(6), Al2–C14 1.943(5), Al3–O3 1.828(4), Al3–O5 1.823(3), Al3–C15 1.946(6), Al3–C16 1.946(6), Al4–O1 1.871(3), Al4–O2 1.880(4), Al4–O3 1.884(3), Al4–O4 1.884(3), Al4–O5 1.873(4), Al4–O6 1.873(3), Al1–O1–Al4 100.46(15), Al1–O4–Al4 99.68(16), O1–Al1–O4 81.23(15), O1–Al4–O4 78.45(14), Al2–O2–Al4 99.61(16), Al2–O6–Al4 99.94(17), O2–Al2–O6 81.45(16), O2–Al4–O6 78.99(16), Al3–O3–Al4 99.41(16), Al3–O5–Al4 100.02(16), O3–Al3–O5 81.65(16), O3–Al4–O5 78.86(15).

In **25** the mean Al–O bond lengths for the 4- and 6-coordinate aluminium centres are 1.826 and 1.878 Å, respectively. This is similar to Al{(μ-OEt)$_2$AlMe$_2$}$_3$ where the mean distances are 1.813 and 1.897 Å.[147] This difference in bond length for 4- and 6- coordinate aluminium is expected as ligand-ligand repulsion increases with coordination number. The central 6-coordinate aluminium shows approximately octahedral symmetry with all O–Al–O angles involving adjacent oxygens being between 78.45(14) and 101.39(16)°. However, the 4-coordinate aluminium has a mean O–Al–O angle of 81.5° and a mean C–Al–C angle of 120.2°, so has a distorted tetrahedral geometry. The distortion from octahedral and tetrahedral geometry is due to the geometrically constraining 4-membered Al_2O_2 rings. Also of interest, there is no THF coordination to any of the aluminium centres, unlike that seen for **24**(THF)$_2$. This is attributed to lower Lewis acidity of the aluminium centres in **25**, as there are no chloride ligands.

Spectroscopic results were essentially consistent with crystallography. The AlMe region (δ −0.42 ppm) of the ^{1}H NMR spectrum was consistent with the high symmetry of the complex, with all aluminium-bonded methyl groups equivalent. The carbon bonded methyl groups (see C1 and C6 in Figure 8.12) showed an unusually upfield ^{1}H NMR shift (δ −0.25 ppm), similar to the CH_2O groups seen in **19**(**4**^{Bn})$_2$. The source of this low shift is not currently known, but can tentatively be attributed to magnetic anisotropy as these methyl groups lie on the C_3 axis. ^{27}Al NMR spectroscopy revealed a very sharp signal at δ 7.6 ppm from the 6-coordinate aluminium, the narrowness being due to the highly symmetric nature of the octahedrally coordinated aluminium, and also a broad signal centred at δ 163.7 ppm consistent with 4-coordinated aluminium (Figure 8.13).

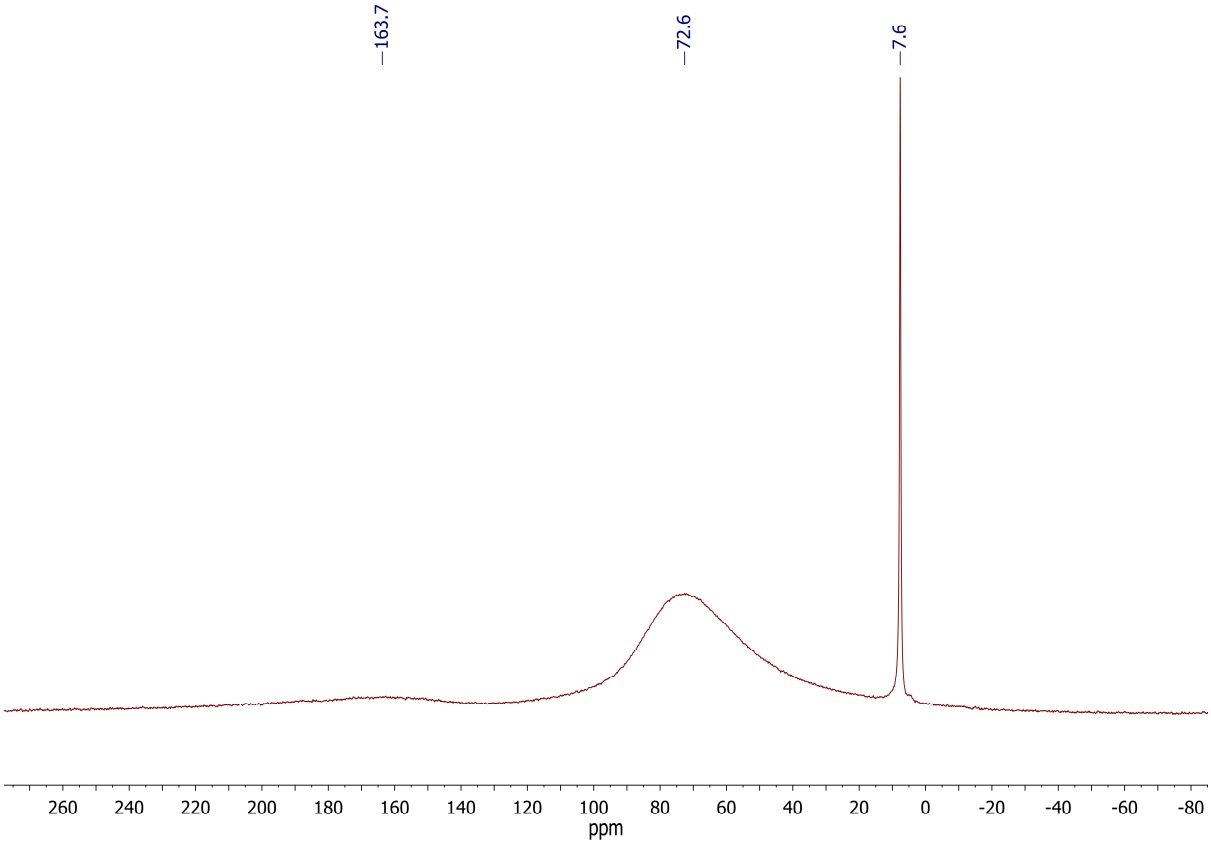

Figure 8.13: ^{27}Al NMR spectrum of **25**. The peak at δ 72.6 ppm is a background signal due to the NMR instrument. The solvent is benzene-d_6.

Attempts to react trimethylolethane with Me_2AlCl were less successful. The addition of Me_2AlCl to the triol in THF resulted in the production of a white solid, but purification of this material proved unsuccessful. ^{27}Al NMR spectroscopy on the crude material revealed peaks at δ 134.2 and 7.6 ppm, indicative of 5- and 6-coordinate aluminium respectively. This suggested a Mitsubishi structure similar to that seen for **25**, with a central 6-coordinate aluminium, but with a different periphery due to the presence of chloride

groups and THF coordination. The ^{1}H NMR spectrum (Figure 8.14) revealed aluminium-coordinated THF (δ 3.48 and 0.94 ppm). In the high field region, two peaks were observed in a 1:1 integral ratio (δ −0.29 and −0.35 ppm), thought to be from Me and AlMe groups, respectively. This assignment was confirmed by a HSQC experiment that showed correlations between the ^{1}H NMR signals at δ −0.29 and −0.35 ppm and the ^{13}C NMR signals at δ 14.6 and −8.7 ppm, respectively. The location of the CH_2O hydrogens was not clear, but a broad region, centred at *ca.* δ 3.8 ppm with an integration of 12 hydrogens, was most consistent with this group. These data suggested the formation of **26**$(THF)_3$ (Scheme 8.8). The broad spectroscopic feature could be accounted for by fluxionality in solution.

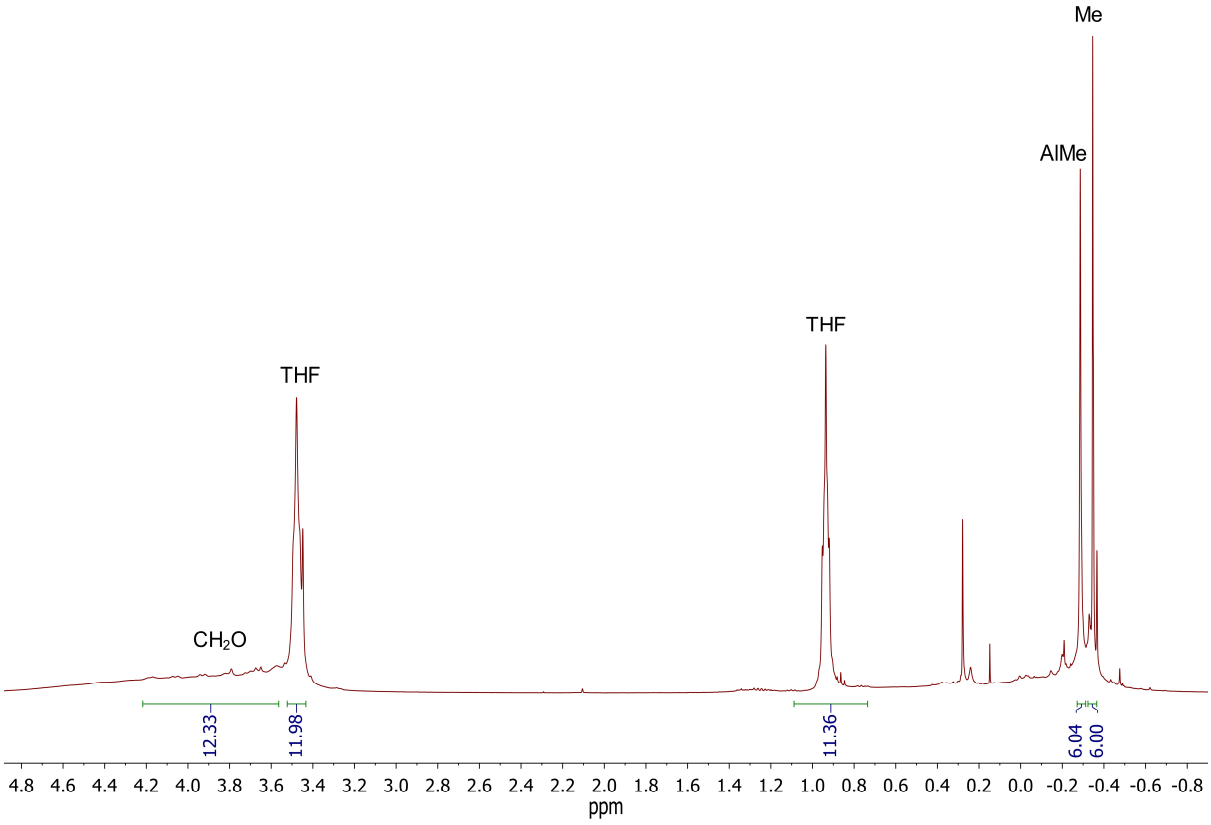

Figure 8.14: ^{1}H NMR spectrum of the product from the reaction of trimethylolethane with 2 equivalents of Me_2AlCl. The signal at δ 0.28 ppm is an impurity from Si grease. The solvent is benzene-d_6.

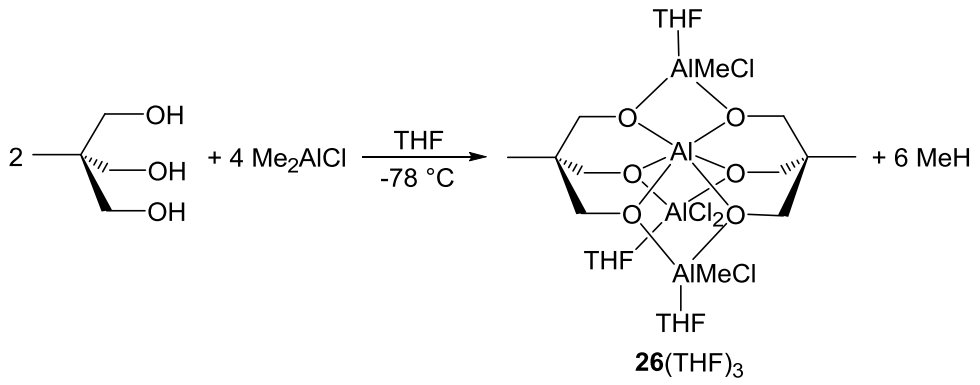

Scheme 8.8: The proposed 2:1 reaction between Me_2AlCl and trimethylolethane to produce **26**$(THF)_3$.

The addition of 2 equivalents of $MeAlCl_2$ to the triol in THF resulted a clear solution. Concentration of the solution *in vacuo* and storage at 4 °C produced small colourless crystals of $Al\{MeC(CH_2O)_3\}_2(AlCl_2)_3(THF)_4$ **27**$(THF)_4$ (Scheme 8.9), as evidenced by X-ray crystallography. As discussed previously, the production of HCl may not occur due to disproportionation of $MeAlCl_2$ to Me_2AlCl and $AlCl_3$. The crystal structure of **27**$(THF)_4$ (Figure 8.15) reveals a Mitsubishi structure, similar to that seen for **25**, but with the methyl-bound aluminium replaced by chloride-bound aluminium. In contrast to **25**, solvation of the peripheral aluminium centres by THF is observed. However, this occurs in an unsymmetrical manner as two of the aluminiums are coordinated by one THF, with another coordinated by two THF molecules. The final aluminium centre is located in the centre of the Mitsubishi molecule. This results in two 6-coordinate and two 5-coordinate aluminium centres in the structure of **27**$(THF)_4$.

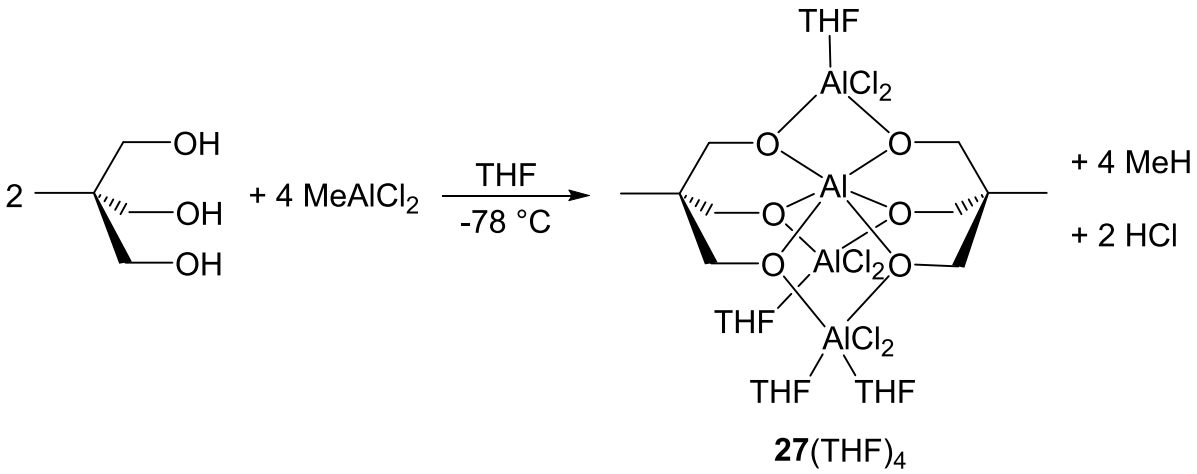

Scheme 8.9: The 2:1 reaction between $MeAlCl_2$ and trimethylolethane to produce **27**$(THF)_4$.

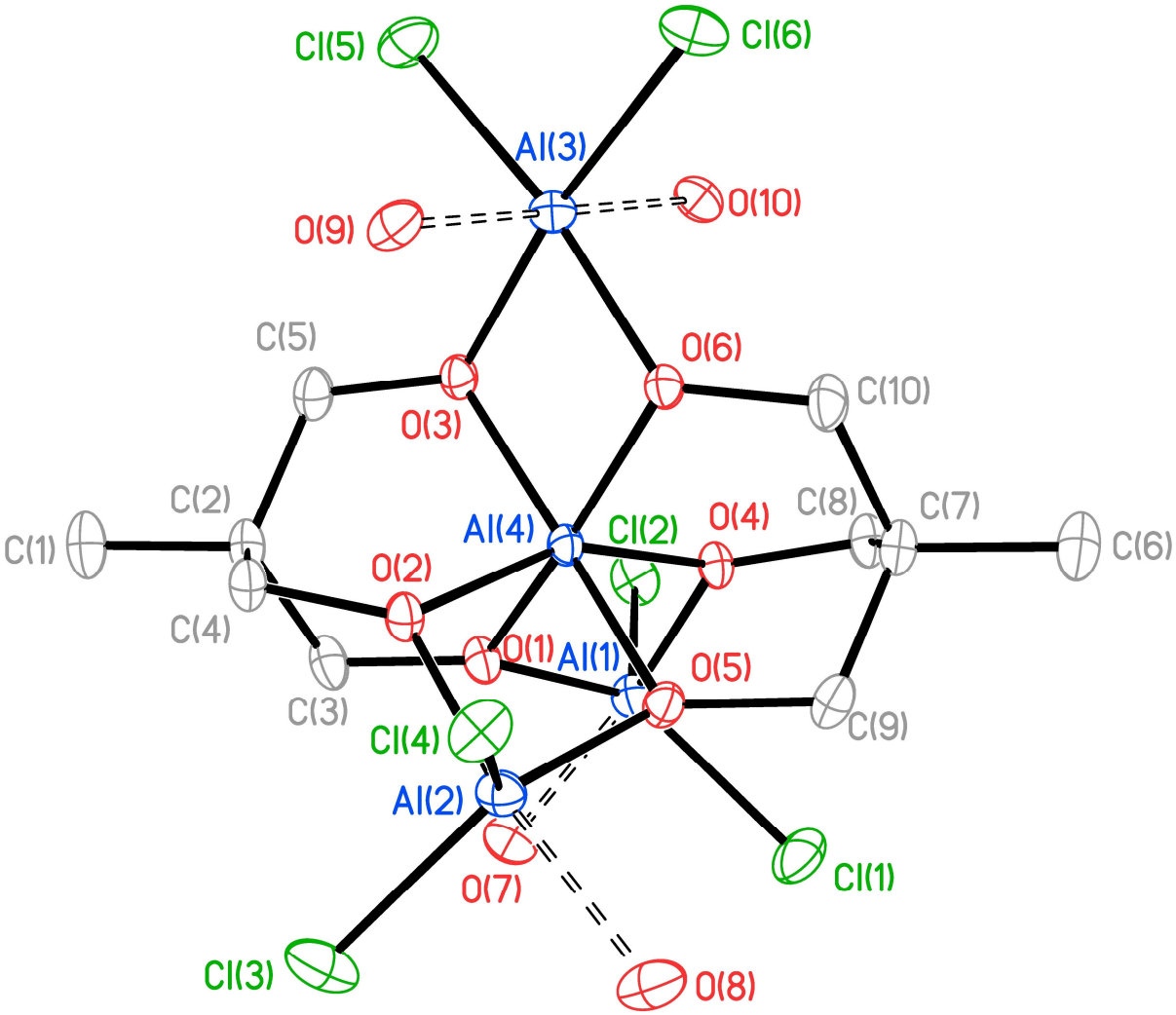

Figure 8.15: Thermal ellipsoid plot of **27**(THF)$_4$ (30% probability). H-atoms, C-atoms of THF and THF of crystallisation omitted for clarity. Selected bond lengths (Å) and angles (°): Al1–O1 1.802(2), Al1–O4 1.868(2), Al1–Cl1 2.1780(12), Al1–Cl2 2.1529(12), Al2–O2 1.864(2), Al2–O5 1.802(2), Al2–Cl3 2.1940(12), Al2–Cl4 2.1488(11), Al3–O3 1.880(2), Al3–O6 1.879(2), Al3–Cl5 2.2461(12), Al3–Cl6 2.2631(11), Al4–O1 1.887(2), Al4–O2 1.8770(19), Al4–O3 1.854(2), Al4–O4 1.8788(19), Al4–O5 1.894(2), Al4–O6 1.847(2), Al1–O1–Al4 103.71(10), Al1–O4–Al4 101.49(9), O1–Al1–O4 77.99(9), O1–Al4–O4 75.67(8), Al2–O2–Al4 101.62(9), Al2–O5–Al4 103.30(10), O2–Al2–O5 78.55(9), O2–Al4–O5 75.98(9), Al3–O3–Al4 103.36(9), Al3–O6–Al4 103.66(9), O3–Al3–O6 75.79(8), O3–Al4–O6 77.19(9).

The ^{1}H NMR spectrum of **27**(THF)$_4$ showed a number of broad peaks for the CH_2O and Me hydrogens of the triolate ligands. This suggested that **27**(THF)$_4$ was undergoing dynamic exchange in solution, with the THF molecules able to exchange. ^{13}C NMR spectroscopy supported this view, with broad signals from the CH_2O, C_{quat} and Me carbons at δ 72.5, 38.0 and 15.8 ppm, respectively, along with broad signals from THF at δ 70.1 and 25.5 ppm. ^{27}Al NMR spectroscopy revealed peaks at δ 74.2 and 8.2 ppm, attributed to 5- and 6-coordinate aluminium environments, respectively.

Similar to the reactions with diols, the use of less than 2 equivalents of organoaluminium reagent resulted in the formation of intractable gels. Again, this could potentially be

explained by the formation of polymeric species with the triolate groups bridged by aluminium.

The structures obtained from reactions of organoaluminiums with trimethylolethane, **25** and **27**$(THF)_4$, each exhibited a Mitsubishi structure. This motif has been commonly observed for alkylaluminium sesquialkoxides, $R_{1.5}Al(OR')_{1.5}$. These species have been produced previously through the reaction of trialkylaluminiums with alcohols or aluminium alkoxides.[147,164,165] There are only three previously reported examples of Mitsubishi molecules formed from tridentate alkoxide ligands.[166] The tetraaluminium species **25** and **27**$(THF)_4$ exhibit very similar structures to that seen for the central region of **19**$(\mathbf{4}^{Bn})_2$ produced from the 6:1 and 8:1 reaction between TMA and $\mathbf{14}^{Bn}$, heated to reflux. However, this general structure-type was not observed for $\mathbf{18}^{Bn}(\mathbf{4}^{Bn})_3$. Instead, NMR spectroscopy revealed that $\mathbf{18}^{Bn}$ underwent adduct formation with three equivalents of $\mathbf{4}^{Bn}$, forming three Al_2O_2 rings. The difference in structure between **19**$(\mathbf{4}^{Bn})_2$ and $\mathbf{18}^{Bn}(\mathbf{4}^{Bn})_3$ was attributed to the steric bulk of the Al_2O_2 rings. The crystal structure of $\mathbf{17}^{Bn}(\mathbf{4}^{Bn})_2$ revealed that the two Al_2O_2 rings are pointing away from each other due to steric effects, but for **15**$(\mathbf{4}^{Bn})_4$ there are now four Al_2O_2 rings resulting in steric crowding. This therefore favours the thermal rearrangement to **19**$(\mathbf{4}^{Bn})_2$, whereas for $\mathbf{17}^{Bn}(\mathbf{4}^{Bn})_2$ and $\mathbf{18}^{Bn}(\mathbf{4}^{Bn})_3$ the steric influence of two and three Al_2O_2 rings respectively, is not as large.

8.4 Reactions of Tetrols with Methylaluminium Reagents

Attempts to isolate the products of reaction from the combination of organoaluminium reagents with the tetrol pentaerythritol proved unsuccessful. The addition of TMA, Me_2AlCl or $MeAlCl_2$ to the tetrol in pyridine (chosen due to the limited solubility of pentaerythritol) resulted in effervescence (presumed to be methane or HCl) and the precipitation of intractable solids, which proved difficult to analyse. Elemental analysis of the solid produced from the reaction of the tetrol with an excess of TMA in pyridine gave C = 48.88%, H = 8.12% and N = 4.23% (the presence of nitrogen was due to the solvent, pyridine). These insoluble solids were presumed to be polymeric species, similar to those proposed in Chapter 7 from the reaction of organoaluminiums with tetraesters. The formation of intractable solids was attributed to the increased denticity of the tetrol ligand, and the fact that geometry allows for only three of the alkoxide functions to coordinate to a single aluminium centre. The remaining alkoxide would therefore be available to form

a Me_2AlO unit which could go on to form an adduct with another Me_2AlO unit. This has the potential to produce a polymeric structure (Figure 8.16).

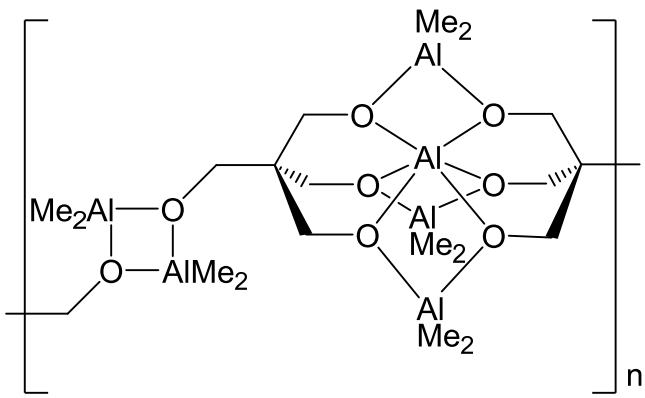

Figure 8.16: The proposed polymeric structure resulting from the reaction of pentaerythritol with an excess of TMA.

8.5 Summary

The reactions of organoaluminiums with a diol or triol resulted in the formation of molecular species. Reactions with diols tended to produce a trialuminium species, demonstrating the structure-types seen for **22**, **24**$(THF)_2$ and **24**. In these structures, two diolate units coordinate three aluminium centres, resulting in the formation of two Al_2O_2 rings. Reacting organoaluminiums with triols resulted in the formation of tetraaluminium Mitsubishi molecules, shown by **25** and **27**$(THF)_4$. The structure for these molecules revealed two triolate units coordinating four aluminium centres, which all lay in one plane. The central aluminium attained a distorted octahedral geometry. The attempted reactions of methylaluminium reagents with tetrols produced intractable solids.

In Chapter 6 it was shown that reactions between monoesters and organoaluminiums resulted in the formation of organoaluminium alkoxides (e.g. Me_2AlOMe **3**), which have a 1:1 aluminium to alkoxide ratio. However, the work in this chapter has revealed that fewer equivalents of aluminium reagent are required to stabilise diols and triols. For example, the species **22**, **24**$(THF)_2$ and **24** revealed a 3:4 aluminium to alkoxide group ratio. This is important in understanding how the tetrolate unit of a polyolester behaves when reacted with an organoaluminium (resulting in cleavage, which produces a polyalkoxide). This reduced number of aluminium centres was observed for the rearrangement of $\mathbf{15}^{Bn}(\mathbf{4}^{Bn})_4$ to form $\mathbf{19}(\mathbf{4}^{Bn})_2$, where $\mathbf{4}^{Bn}$(TMA) was eliminated (see Section 7.3). This results in fewer equivalents of organoaluminium reagents being required for

ester cleavage of polyolesters compared to multiple monoesters. This means that in refrigeration systems breakdown of the polyolesters requires the presence of less organoaluminium reagent than might have hitherto been expected.

Chapter 9

Reactivity of Ethers with Methylaluminium Reagents

9.1 Introduction

Chapters 6, 7 and 8 concerned, directly or indirectly, the reactivity of polyolester refrigeration oils with organoaluminium reagents. Results showed that the polyolesters degraded in the presence of organoaluminiums, with the formation of alkenes and methane observed at elevated temperatures. This degradation is potentially dangerous as the loss of lubricity and formation of methane could lead to explosive consequences. Therefore, investigations into the reactivity of other refrigeration oils will be undertaken. This will involve understanding what other reactions might arise if different functional groups are present. Another common type of refrigeration oil is based upon polyvinyl ethers; in Section 5.3, it was shown that FVC 46D refrigeration oil is primarily composed of poly(ethyl vinyl ether). Hence, in this chapter the reactions between ethers and organoaluminiums will be investigated. Initially, this will be studied through the reaction of organoaluminiums with an ether that will represent a simplified model for FVC 46D, before reactions with FVC 46D itself are undertaken.

Ethers are used extensively in synthetic chemistry as polar, aprotic solvents. They are also commonly used as reagents, where they can act as either a Lewis base or a Brønsted base. Most ethers are relatively inert, with C–O bonds showing good stability. However, despite their apparent low chemical reactivity, they can undergo chemical transformations with certain chemical species.

The cleavage of ether C–O bonds has been reported under strongly acidic or basic conditions. In the presence of mineral acids, such as hydrobromic acid or hydroiodic acid, an acid catalysed nucleophilic substitution reaction can occur. This reaction occurs via either a S_N1- or S_N2-type mechanism, depending on the sterics of the ether. The S_N1-type mechanism is promoted by a bulky ether and stabilisation of the carbocation intermediate. These reactions result in the formation of an alcohol and a haloalkane (Scheme 9.1).[167]

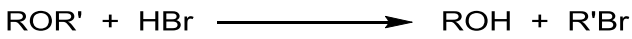

Scheme 9.1: Ether cleavage by hydrobromic acid.[167]

Ethers can also undergo cleavage in the presence of an organometallic base. Ethers are common solvents for organolithium reagents, where they enhance solubility and reactivity by promoting the formation of adducts. Whilst these adducts are generally stable at low temperature, α-metalation occurs with increasing temperature. This can result in a 1,2-Wittig rearrangement, where after deprotonation the unreacted alkyl group can migrate to the deprotonated alkyl, producing a lithium alkoxide.[168] For cyclic ethers, such as THF, this can result in the formation of an alkene and a lithium alkoxide (Scheme 9.2).[169–171]

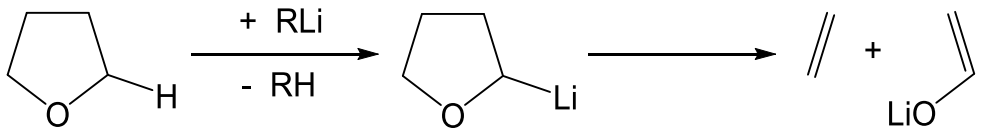

Scheme 9.2: The ring-opening ether cleavage of THF by an organolithium reagent.[171]

Lewis acids, such as $TiCl_4$, PCl_5 or $MgBr_2$, have also been used to achieve ether cleavage.[167] By way of a further example, the addition of aluminium chloride to anisole has been reported to form an adduct at room temperature. However, heating above 40 °C resulted in decomposition to phenoxyaluminium dichloride and chloromethane (Scheme 9.3).[172] Aluminium-based Lewis acids have been used in numerous ether cleavage reactions, including the use of aluminium chloride in the selective ether cleavage of methyl ethers adjacent to carbonyls in arenes.[173]

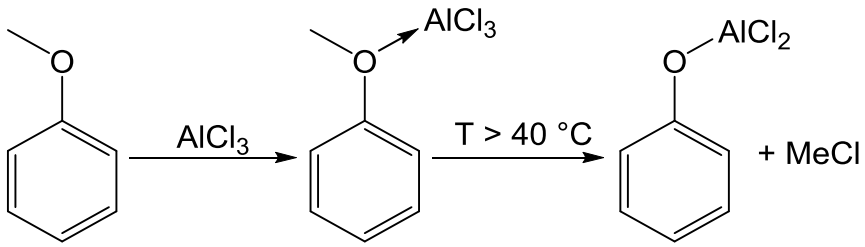

Scheme 9.3: The reaction between anisole and aluminium chloride.[172]

Methylaluminium chlorides Me_2AlCl and $MeAlCl_2$ are the expected products from the reaction between aluminium and chloromethane in industrial refrigeration systems. Both of these species are Lewis acids and organometallic bases, so may be able to perform ether cleavage on polyvinyl ether refrigeration oils. Therefore, the reactivity of these organoaluminiums with ethers will be investigated. Current literature reports extensively on adduct formation, but subsequent reactivity is largely unexplored.[174–177]

9.2 Reactivity of Ethers with TMA

Initially, reactions were attempted with TMA to simplify analysis and a range of ethers (Et_2O, $^iPr_2O$, THF, 2-MeTHF and methyl *tert*-butyl ether (MTBE)) were used to understand how ether structure affected reactivity. The addition of TMA to Et_2O, $^iPr_2O$, THF or 2-MeTHF resulted in only adduct formation, even after heating to reflux in toluene for 2 hours, as evidenced by NMR spectroscopy. However, the 1:1 combination of MTBE with TMA in toluene showed unexpected reactivity. At room temperature only adduct formation was indicated; through the observation of a ^{27}Al NMR signal at δ 185.4 ppm (cf. δ 182 ppm for THF(TMA))[178] and ^{1}H NMR signals at δ 2.93, 0.93 and −0.37 ppm. However, heating the toluene solution to reflux for 2 hours resulted in the appearance of a new ^{27}Al NMR signal at δ 153.0 ppm. ^{1}H NMR spectroscopy now revealed the presence of Me_2AlOMe **3** (δ 3.08 and −0.59 ppm) and the alkene isobutene **28** (δ 4.73 and 1.60 ppm), alongside unreacted MTBE(TMA) (Figure 9.1). These products suggested that MTBE had undergone elimination to form **28**, **3** and methane (Scheme 9.4). Integration of the ^{1}H NMR signals suggested that 45% of the MTBE had undergone reaction.

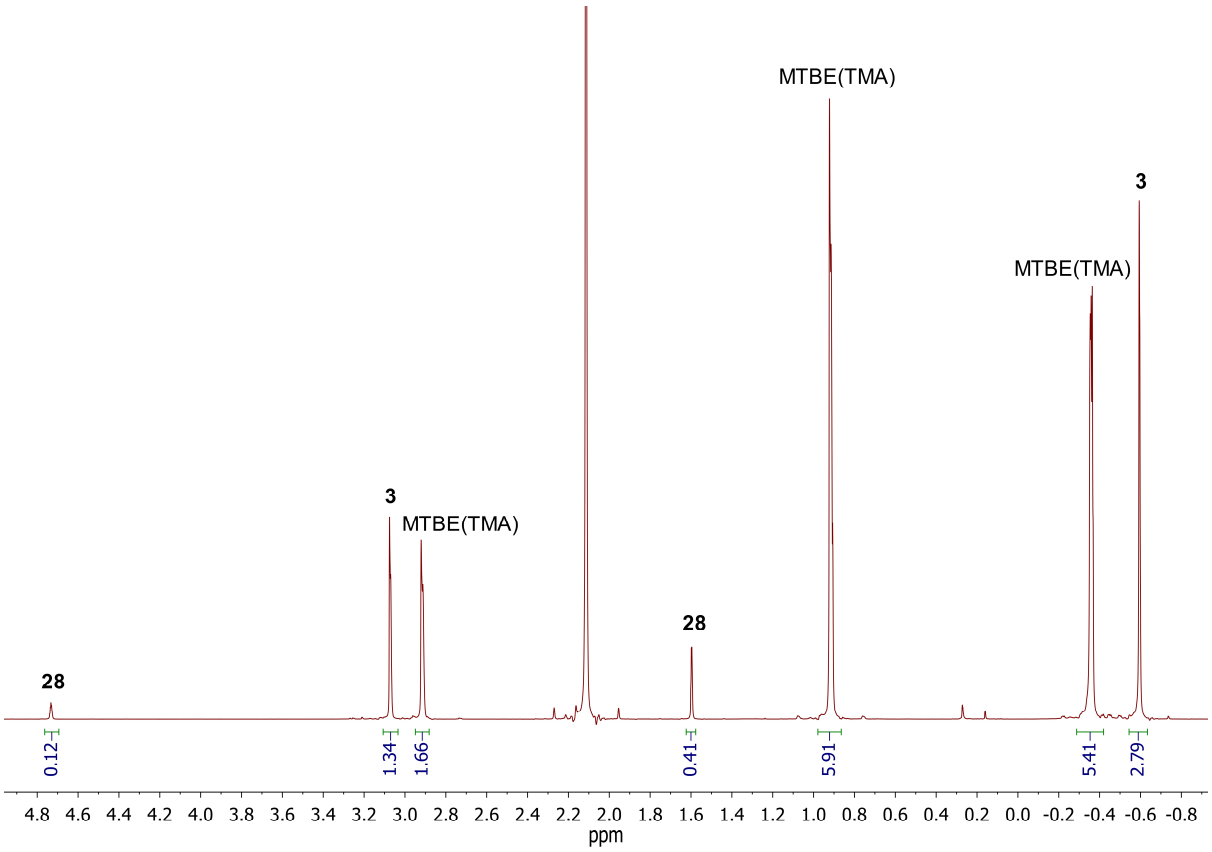

Figure 9.1: ^{1}H NMR spectrum of an aliquot from the reaction of TMA with MTBE in toluene (δ 2.11 ppm) in a 1:1 ratio, after heating to reflux for 2 hours in toluene. The solvent is benzene-d_6.

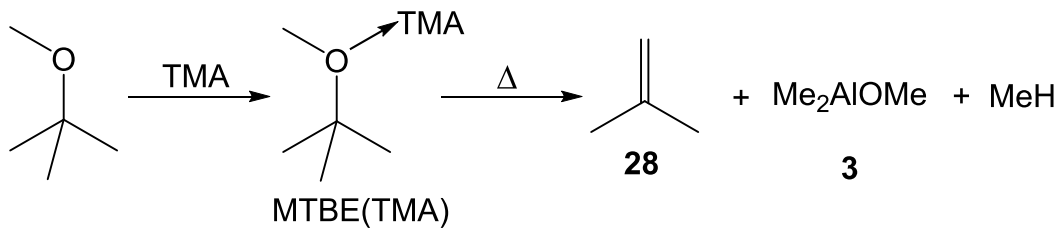

Scheme 9.4: The reaction of MTBE with TMA.

Reaction with TMA was only observed for MTBE. This was attributed to the presence of a tertiary carbon centre adjacent to the oxygen. The tertiary alkyl group results in a disubstituted alkene, and these are thermodynamically more stable than unsubstituted or monosubstituted alkenes. Another contributing factor is the geometry of MTBE, which means that at least one of the methyl groups from the *tert*-butyl must be directed towards the organoaluminium at the adduct stage. The ethers with primary or secondary alkyl groups can rotate the C–O bond to reduce steric clash between the methyl groups and the organoaluminium. The elimination reaction is proposed to occur via a concerted mechanism (Figure 9.2). This reaction is very similar to the elimination seen for the

organoaluminium-ester reactions (cf. elimination reaction of **4**^{Bn}($MeAlCl_2$), see Section 6.3).

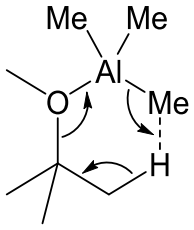

Figure 9.2: Rearrangement of the proposed transition state for the reaction of MTBE with TMA.

9.3 Reactivity of Ethers with Me_2AlCl

Replacing TMA with Me_2AlCl was expected to aid the elimination reaction from the ether, due to the increased Lewis acidity of Me_2AlCl relative to that of TMA. The combination of Et_2O, $^iPr_2O$, THF or 2-MeTHF with Me_2AlCl still resulted in only adduct formation, with NMR spectroscopy revealing the retention of ether functionality. The 1:1 mixture of MTBE with Me_2AlCl showed similar reactivity to that seen with TMA, with the observation of adduct formation at room temperature (^{27}Al NMR δ 162.2 ppm) and ether cleavage when heated to reflux in toluene for 2 hours. The products of this reaction were identified as **28**, MeAl(OMe)Cl **5** and methane (Scheme 9.5).

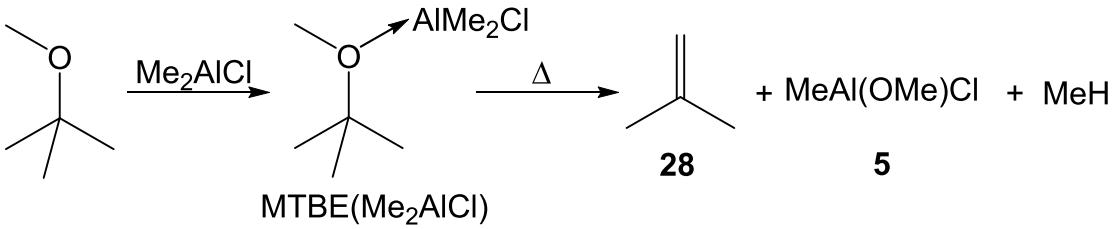

Scheme 9.5: The reaction of MTBE with Me_2AlCl.

Meanwhile, repeating the reaction at 100 °C in a sealed J Young NMR tube with toluene-d_8 as a solvent resulted in the clear spectroscopic observation of **28** (^{1}H NMR δ 4.69 and 1.59 ppm) and methane (^{1}H NMR δ 0.16 ppm) (Figure 9.3). The presence of **5** was confirmed by the observation of ^{1}H NMR signals at δ 3.22, 3.18, 3.14 and 3.08 ppm from the OMe hydrogens, and signals at δ −0.43, −0.49, −0.60 and −0.61 ppm from the AlMe hydrogens. In contrast to **3**, a greater number of NMR signals were observed for **5** than were expected based upon its formula. It was proposed that **5** could exist as several different structures that are in equilibrium. This has previously been observed for

aluminium chloride alkoxides, which have previously been shown to exist as dimers and trimers.[162,179] Another possibility is that **5** can undergo a disproportion of ligands to form trialuminium or tetraaluminium species (and eliminate Me_2AlCl).[180] Possible species that might form in such a way from MeAl(OMe)Cl are shown in Figure 9.4. ^{27}Al NMR spectroscopy strengthens this interpretation by revealing peaks at δ 124.3, 95.0, 48.4 and 9.6 ppm, suggesting 4-, 5- and 6-coordinate aluminium, respectively.[70]

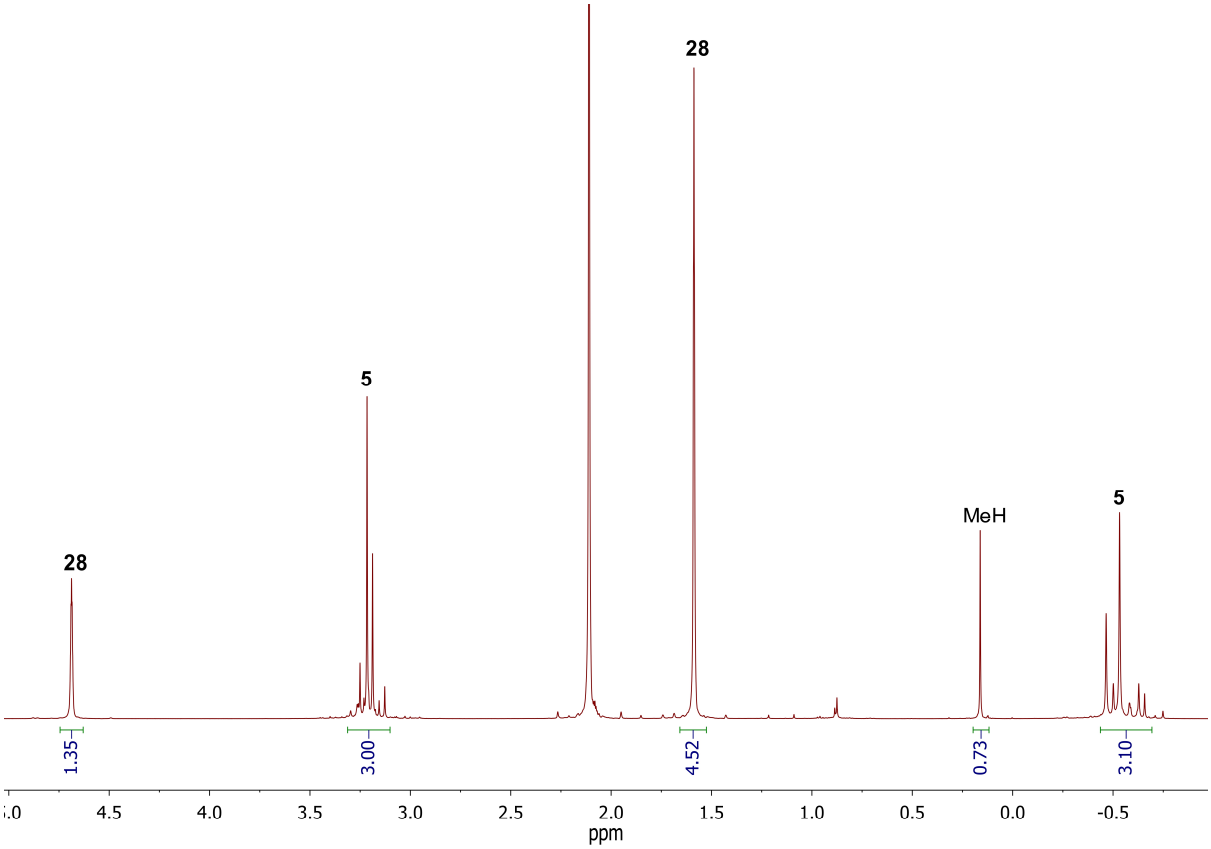

Figure 9.3: ^1H NMR spectrum of an aliquot from the reaction of Me_2AlCl with MTBE in toluene (δ 2.11 ppm) in a 1:1 ratio, after heating to 100 °C for 2 hours in toluene-d_8 in a sealed J Young NMR tube.

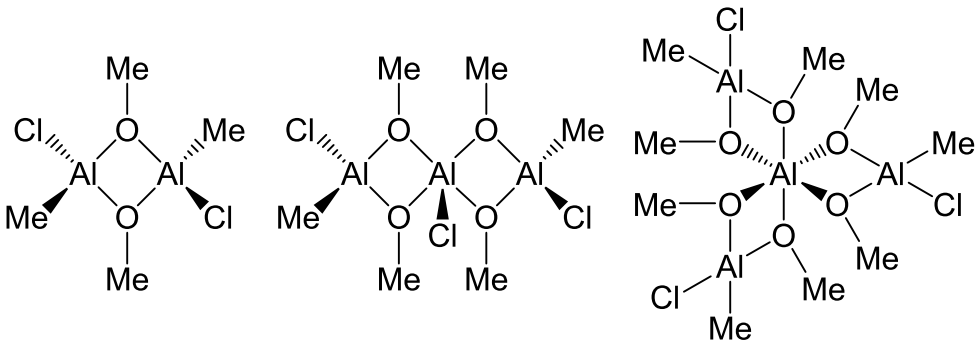

Figure 9.4: Possible structures resulting from the aggregation and redistribution of **5**.

9.4 Reactivity of Ethers with $MeAlCl_2$

In a similar way to the behaviour observed for TMA and Me_2AlCl, combination of $MeAlCl_2$ with Et_2O and THF showed only adduct formation, even after refluxing in toluene. On the other hand, reactions with MTBE were much more vigorous, with effervescence observed without any heating. The elimination reaction was evidenced by ^{1}H NMR spectroscopy, with a signal at δ 3.27 ppm corresponding to $Al(OMe)Cl_2$ **6**. However, in contrast to the TMA / Me_2AlCl-based systems, described above, isobutene **28** could not be detected by ^{1}H NMR spectroscopy. This can be explained by *in situ* Friedel-Crafts reaction of **28** with the toluene solvent, giving **29a** and **29b** (Scheme 9.6). The failure to observe this reactivity in the systems described above can be attributed to the presence of more Lewis acidic (and therefore more effective) catalysts, such as $MeAlCl_2$ or **6**, in the present system. Using hexane instead of toluene as the solvent still resulted in the formation of **6** (^{1}H NMR δ 3.26 ppm). However, even in the absence of aromatic reagents, **28** could not be observed, ostensibly due to its polymerisation (suggested by the observation of very broad peaks, at δ 1.8–0.4 ppm, by ^{1}H NMR spectroscopy) and this is once again consistent with higher Lewis acidity of this system (Scheme 9.6).

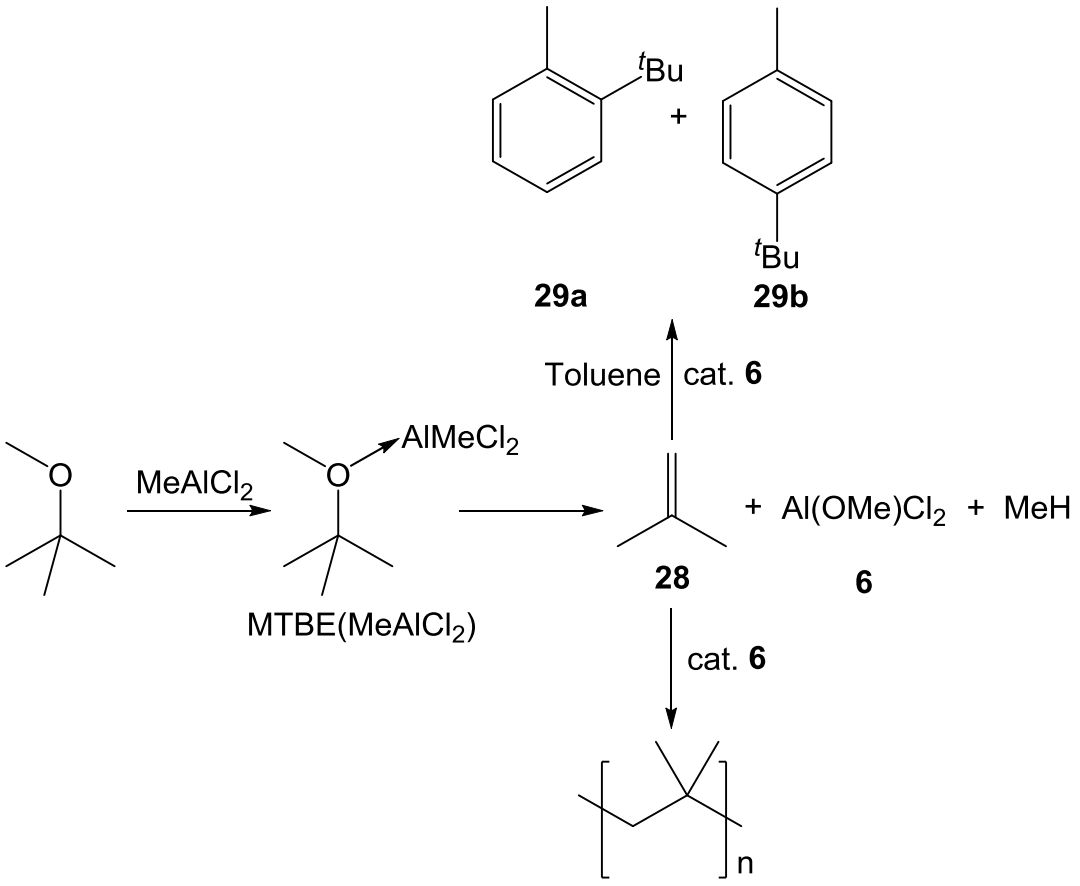

Scheme 9.6: The reaction of MTBE with $MeAlCl_2$, in the presence or absence of toluene.

Also of interest was the fact that, in contrast to the case of TMA and Me_2AlCl, 2-MeTHF and $^{i}Pr_2O$ did undergo reaction with $MeAlCl_2$. The 1:1 combination with both ethers resulted only in adduct formation at all temperatures. However, heating a 2:1 mixture of $MeAlCl_2$ and 2-MeTHF to 100 °C in a sealed J Young NMR tube with toluene-d_8 as a solvent for 2 hours resulted in a brown solid and solution, in contrast to the colourless solutions obtained previously. One of the expected products, based on an elimination reaction, would be the aluminium alkoxide **30** (Scheme 9.7). However, instead of revealing alkene hydrogens, ^{1}H NMR spectroscopy suggested the presence of CH_2 groups (δ 1.69, 1.51 and 1.16 ppm). A HMBC experiment revealed that these signals were due to the alkyl groups of a substituted toluene derivative. This could be explained by **30** undergoing further elimination to form diene **31** (also producing **32**, which then produces aluminoxane **33** and methane), with **31** undergoing Friedel-Crafts addition to toluene to form **34**. The aluminoxane **33** was detected by ^{27}Al NMR spectroscopy, with a single peak observed at δ 100.2 ppm. The observation of methane (^{1}H NMR δ 0.17 ppm) and methane-*d* (^{1}H NMR 1:1:1 triplet at δ 0.15 ppm) was attributed to reaction with toluene-d_8.

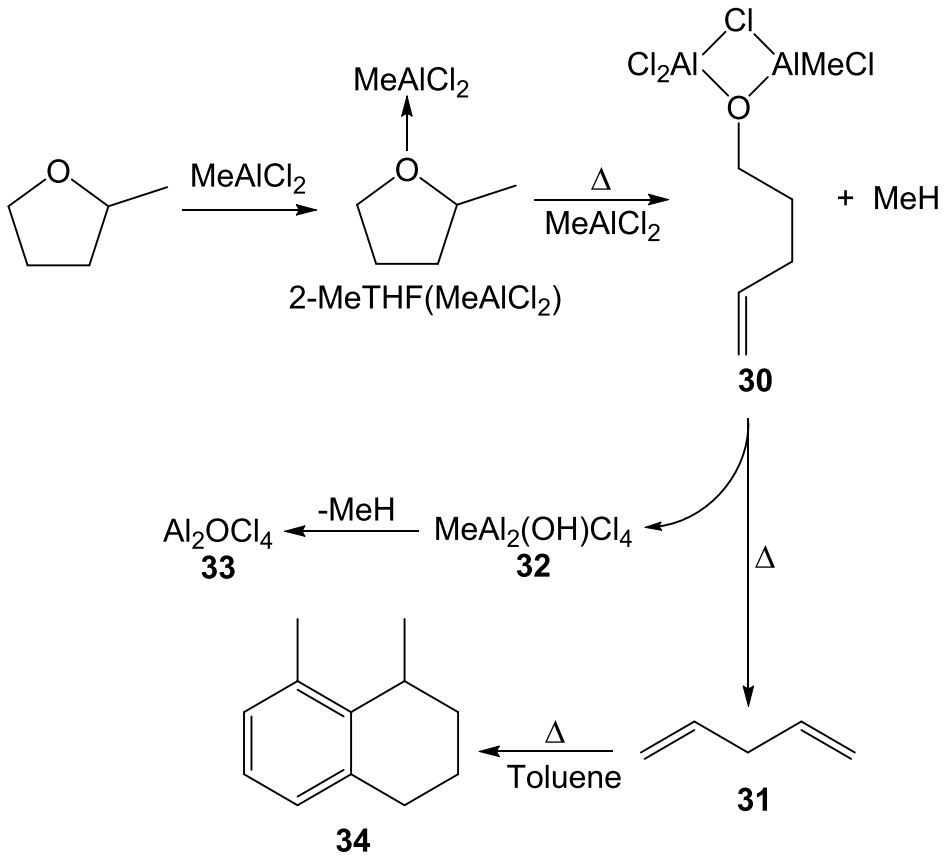

Scheme 9.7: The reaction of 2-MeTHF with 2 equivalents of $MeAlCl_2$.

The use of $^{i}Pr_2O$ showed similar reactivity to that seen for 2-MeTHF. The requirement of 2 equivalents of $MeAlCl_2$ was still observed, but the reaction proceeded at a much slower rate compared to 2-MeTHF. After 2 hours of heating to 100 °C in a sealed J Young NMR tube with toluene-d_8 as a solvent, ^{1}H NMR spectroscopy revealed 10% conversion of $^{i}Pr_2O(MeAlCl_2)$ to the alkene propene **35** (δ 5.69, 4.97, 4.91 and 1.55 ppm), the organoaluminium alkoxide **36** (δ 3.92, 0.97 and −0.22 ppm) and methane (δ 0.17 ppm). Heating the mixture for 8 hours at 100 °C resulted in full reaction of the ether and the formation of the Friedel-Crafts products **37a** and **37b**, from reaction with toluene (Scheme 9.8). Similar to the Me_2AlCl-(2-MeTHF) reaction, the ^{27}Al NMR spectrum revealed a signal at δ 102.1 ppm, attributed to the aluminoxane **33**. The observation of methane (^{1}H NMR δ 0.17 ppm) and methane-*d* (^{1}H NMR 1:1:1 triplet at δ 0.15 ppm) was attributed to Friedel-Crafts reaction with toluene-d_8.

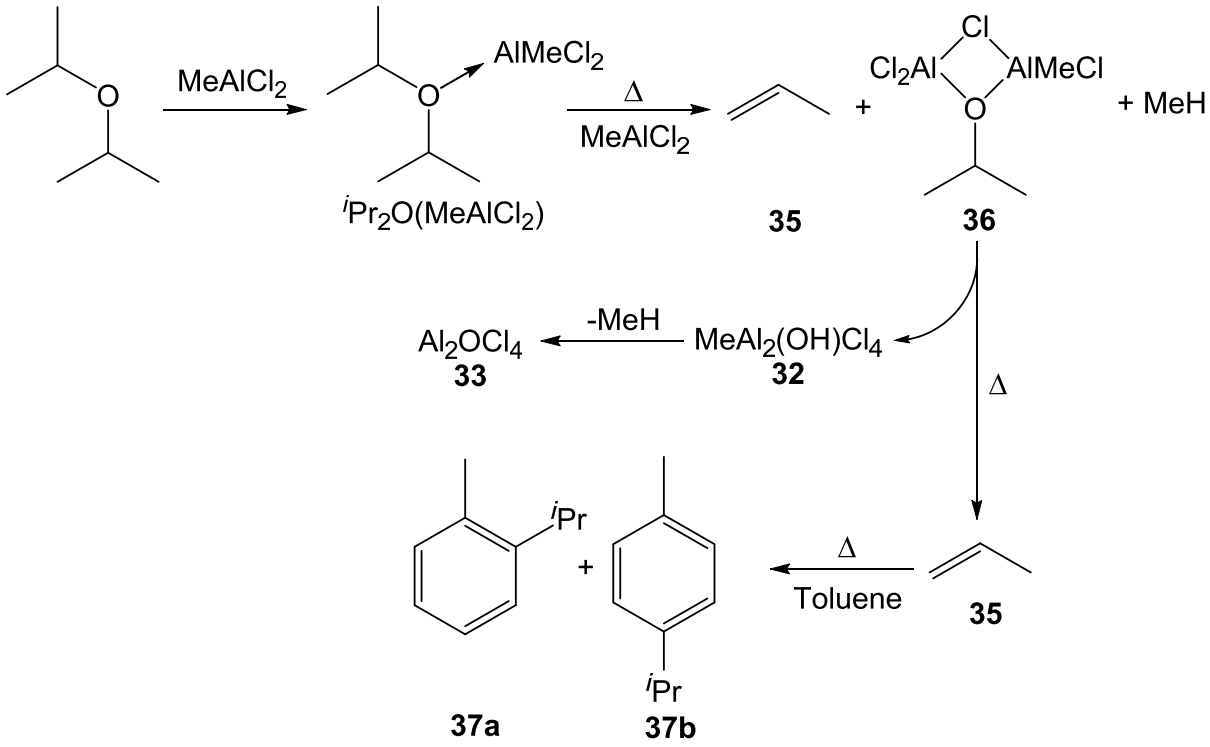

Scheme 9.8: The reaction of $^{i}Pr_2O$ with 2 equivalents of $MeAlCl_2$.

9.5 Reactivity of FVC 46D with Methylaluminium Reagents

Having established that certain types of ether are susceptible to degradation by the action of organoaluminiums, attention turned to investigating the reactivity of PVE FVC 46D (with its poly(ethyl vinyl ether) structure) with the same organoaluminium reagents. The addition of an excess of TMA to FVC 46D resulted in only adduct formation, with ^{1}H NMR spectroscopy revealing only minor movement in chemical shift for the broad FVC 46D signals and an AlMe signal at δ −0.37 ppm. Heating the sample resulted in no change by NMR spectroscopy. The reaction of 2 equivalents of Me_2AlCl with FVC 46D oil showed only adduct formation at room temperature, there being little change in the ^{1}H NMR spectrum compared to that of pristine FVC 46D and a broad AlMe signal at δ −0.25 ppm (Figure 9.5, bottom). However, heating the reaction mixture in a sealed J Young NMR tube to 100 °C for 24 hours resulted in the appearance of a quartet and a triplet in the ^{1}H NMR spectrum (Figure 9.5, top) at δ 3.00 and 1.02 ppm, respectively. This ^{1}H NMR spectrum also revealed sharp AlMe signals at δ 0.01, −0.11 and −0.40 ppm. These signals were assigned to $Me_3Al_2(OEt)Cl_2$ **38**, generated by the (formal) elimination of EtOH from the ether (Scheme 9.9), with a COSY experiment confirming coupling

between the signals at δ 3.00 and 1.02 ppm. The observation of an ethoxy group is consistent with analysis of FVC 46D oil in Section 5.3, where it was shown that the side groups were predominantly ethyl. The polymeric alkene was not clearly observed, suggesting either that the NMR signals were too broad due to its polymeric nature, or that it further reacted to form a different species.

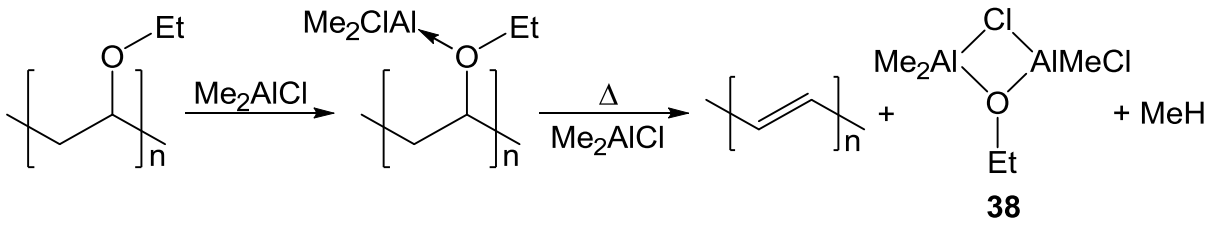

38

Scheme 9.9: The proposed reaction between FVC 46D oil and Me_2AlCl.

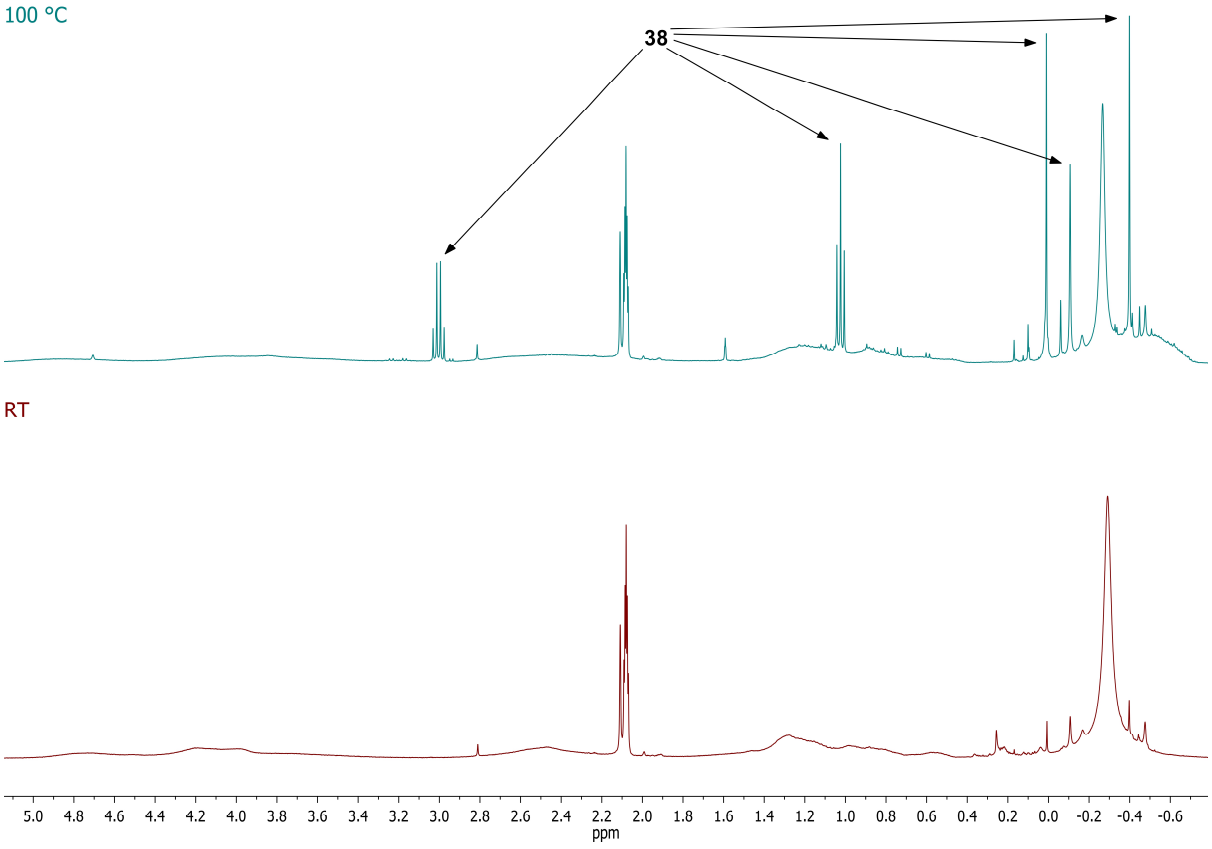

Figure 9.5: ^{1}H NMR spectra of the 2:1 combination of Me_2AlCl with FVC 46D, heated to the stated temperature for 24 hours in toluene (δ 2.11 ppm). The solvent is toluene-d_8.

Similarly, the reaction of FVC 46D oil with 2 equivalents of $MeAlCl_2$ produced only adduct formation at room temperature, as shown by ^{1}H NMR spectroscopy (Figure 9.6, bottom). Heating the reaction mixture in a sealed J Young NMR tube to 100 °C for 24 hours resulted in the appearance of sharp quartets, at δ 2.45 and 2.40 ppm, along with sharp triplets, at δ 1.11 and 1.05 ppm, in the ^{1}H NMR spectrum (Figure 9.6, top).

However, unlike reactions of Me_2AlCl with FVC 46D, these peaks appeared not to originate from ethoxide moieties, but from ethyl groups bonded to an aromatic ring (of toluene-d_8, the NMR solvent); an assignment made through a HMBC experiment. The appearance of these ethyl groups could be explained by the elimination of ethene from an AlOEt moiety and rapid *in situ* Friedel-Crafts addition of this alkene to the aromatic NMR solvent, yielding **40a** and **40b**. In addition to the signals from ethyl groups, new signals appeared at δ 1.09 and 0.85 ppm. While the exact nature of this product is not known, the aforementioned signals could tentatively be assigned to polyethene, arising from the *in situ* Lewis acid-promoted polymerisation of ethene. The ^{1}H NMR spectrum also revealed the absence of AlMe groups and, concordant with this, the presence of methane (δ 0.17 ppm) and methane-*d* (1:1:1 triplet at δ 0.15 ppm). The methane-*d* was presumably from Friedel-Crafts reaction of toluene-d_8. These data suggested essentially the same reactivity as seen for the Me_2AlCl reactions (Scheme 9.9), but with the formation of $MeAl_2(OEt)Cl_4$ **39** instead of **38** (Scheme 9.10). The formation of **33** was confirmed by ^{27}Al NMR spectroscopy, with a signal seen at δ 101.7 ppm.

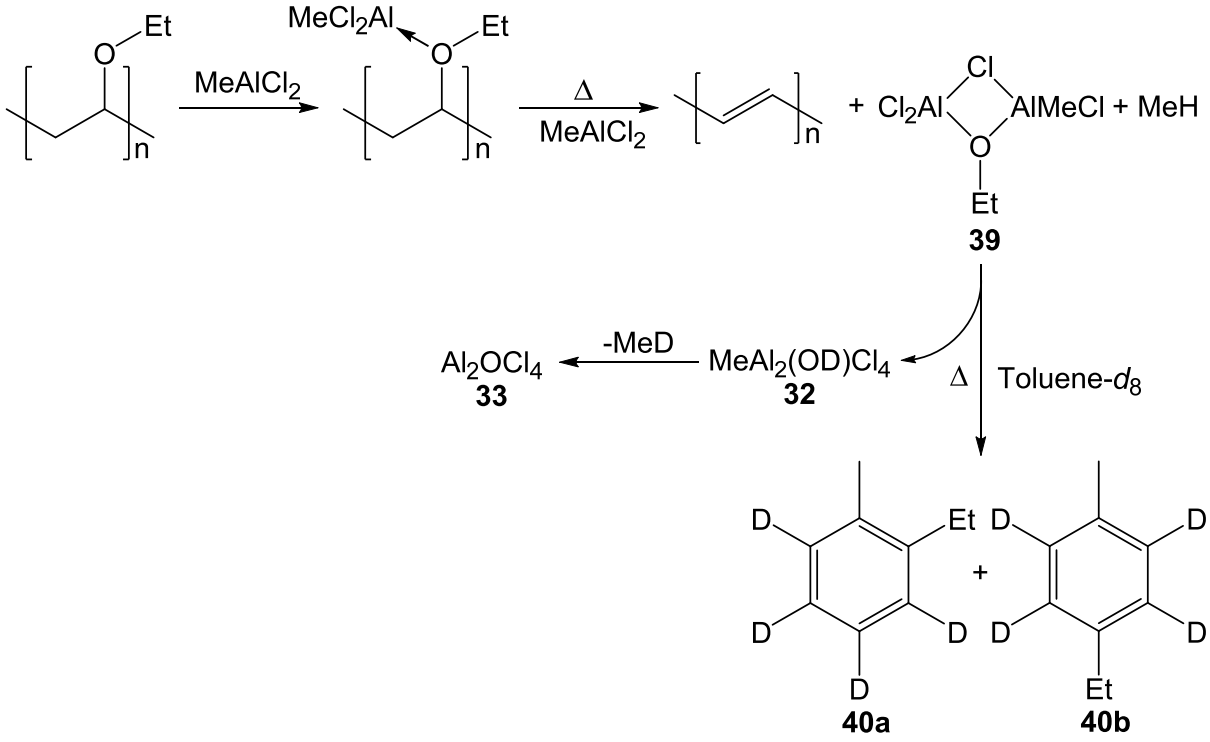

Scheme 9.10: The proposed reaction between FVC 46D oil and $MeAlCl_2$.

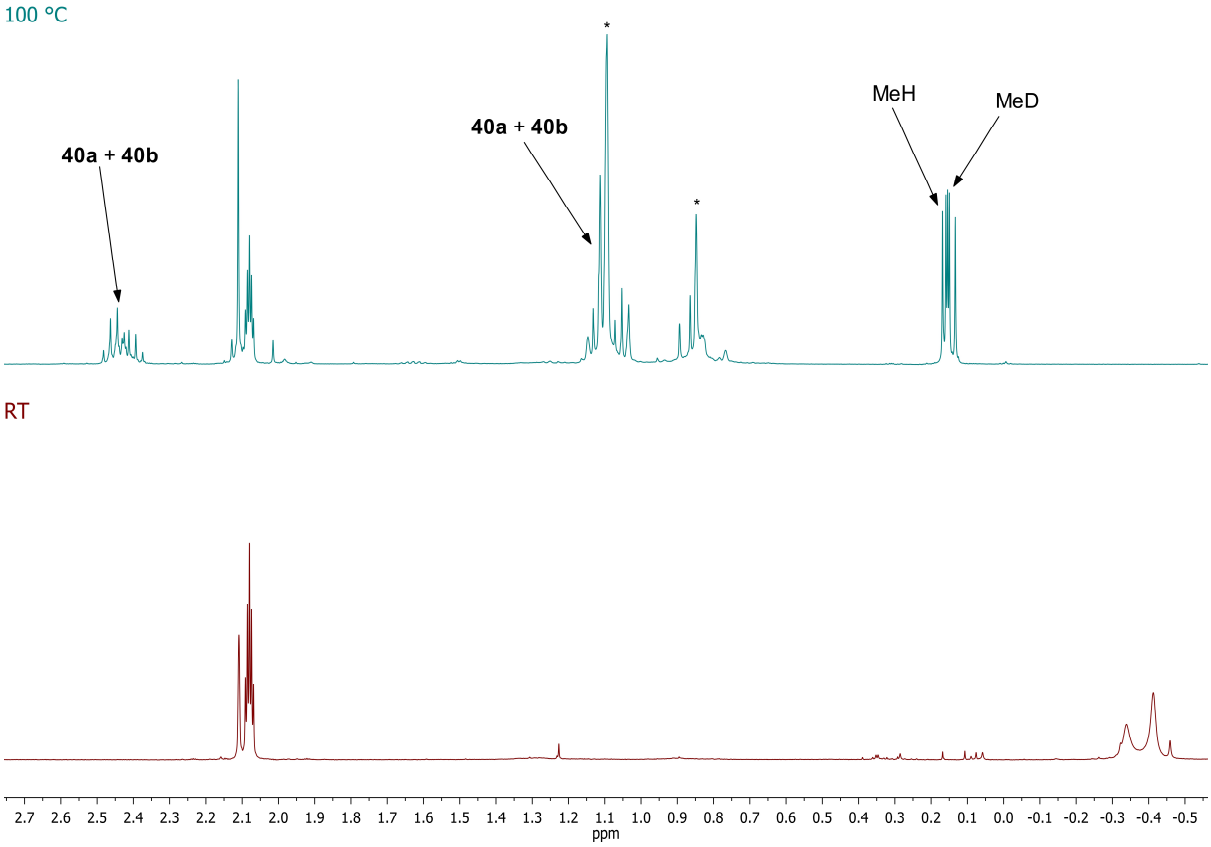

Figure 9.6: ^{1}H NMR spectra of the 2:1 combination of $MeAlCl_2$ with FVC 46D, heated to the stated temperature for 24 hours in toluene (δ 2.11 ppm). The peaks marked with * are assigned to polyethene. The peak at δ 0.13 ppm is due to Si grease. The solvent is toluene-d_8.

9.6 Summary

Combination of certain organoaluminiums and ethers resulted in ether cleavage through an elimination reaction. This elimination led to the formation of methane, an alkene and an organoaluminium alkoxide. Whether this cleavage could occur was highly dependent on the ether and the methylaluminium chloride used. Cleavage was observed for MTBE with TMA, Me_2AlCl or $MeAlCl_2$, with reactivity thought to be due to the presence of a tertiary alkyl group. Ethers with a secondary alkyl group, $^{i}Pr_2O$ and 2-MeTHF, only underwent elimination with 2 equivalents of $MeAlCl_2$ at elevated temperatures. Even then, THF and Et_2O showed no reaction. The observation that ethers incorporating tertiary alkyl groups adjacent to the oxygen reacted more readily was attributed to the formation of more thermodynamically stable substituted alkenes. It was also found that using a more chloride-rich organoaluminium aided ether cleavage, due to the higher Lewis acidity conferred.

Similar reactions were attempted using organoaluminiums and refrigeration oil FVC 46D, to determine how it may interact with *in situ* formed organoaluminiums in refrigeration systems. The addition of TMA to FVC 46D resulted in adduct formation without any subsequent reaction, even at elevated temperatures. However, combinations of FVC 46D with Me_2AlCl resulted in ether cleavage at elevated temperature, accompanied by the release of methane gas. Replacing Me_2AlCl with $MeAlCl_2$ suggested initially similar reactivity to that seen with Me_2AlCl. However, the more Lewis acidic nature of $MeAlCl_2$ led to further reaction with the solvent, toluene. The reactivity observed with Me_2AlCl and $MeAlCl_2$ corroborates the analysis of the oil (see Section 5.3), with elimination to form an AlOEt moiety due to the ethyl side groups of FVC 46D. The fact that FVC 46D underwent elimination with both Me_2AlCl and $MeAlCl_2$ is important as both of these species are expected to be produced from the reaction of aluminium and chloromethane in contaminated refrigeration systems. However, these reactions required elevated temperatures, suggesting that the systems would have to be in operation for oil degradation to occur. The breakdown of the PVE oil would clearly lead to a loss of lubrication in the system, resulting in an increase in friction and therefore temperature. Coupled with the production of flammable alkenes and methane, this could result in extremely dangerous conditions.

Chapter 10
Reactivity of Aluminium-Chloromethane Mixtures with Refrigeration Oils

10.1 Introduction

It has been known for over a hundred years that the interaction of aluminium with alkyl halides can result in the formation of alkylaluminium halides. The first instance, reported by Hallwachs and Schafarick in 1859, was from the reaction of ethyl iodide with aluminium to produce $Et_3Al_2I_3$.[181] The scope of these reactions has been expanded greatly to include numerous alkyl halides.[41,182] In the majority of the reactions reported, a small amount of catalyst, such as iodine, aluminium chloride or alkylaluminium halide, is required to initiate reactions.[40,183] In this chapter, the interaction between aluminium metal and the suspected counterfeit refrigerant R-40 (chloromethane) will be investigated in the presence and absence of the refrigeration oils RL 32H and FVC 46D (see Chapter 5).

10.2 Reactivity of Aluminium with Chloromethane

The reactions between aluminium and chloromethane have been extensively studied and the conditions required for initiation of the reaction explored. Initially, only small pieces of aluminium (4 g) and chloromethane (5 bar) were combined in a Parr reactor and heated to 120 °C. After 2 hours the reactor was vented, and no signs of reaction were detected, with no change in the aluminium visually observed. Furthermore, addition of a catalytic amount of iodine (60 mg), thought to promote reaction by removal of surface aluminium oxide,[184] to the reaction still failed to promote any detectable reaction. Analysis of the chloromethane before reaction by ^{1}H NMR spectroscopy in benzene-d_6 revealed about 1% water present. In previous reports on the reaction between aluminium and alkyl halides, rigorous exclusion of water and oxygen was necessary. Consequently, it was suspected that the presence of water in the chloromethane may have led to the failure to observe any reaction. Repeating the iodine catalysed reactions with the addition of activated 3 Å

molecular sieves now indicated the production of organoaluminium species, as shown by the release of a white smoke when the reactor was briefly vented. The product was removed from the reactor by vacuum distillation to give a clear liquid. The liquid was analysed by NMR spectroscopy, with the ^{27}Al NMR spectrum revealing signals at δ 176.8 and 134.0 ppm (Figure 10.1). These correspond to Me_2AlCl and $MeAlCl_2$, and match well with literature values for methylaluminium sesquichloride (δ 177 and 135 ppm).[185] In solution there is an equilibrium between the sesquichloride, $Me_3Al_2Cl_3$, and the homodimers, $(Me_2AlCl)_2$ and $(MeAlCl_2)_2$ (Scheme 10.1). This material was extremely pyrophoric and was handled with great care. Attempts to repeat the reaction in the absence of a catalytic amount of iodine proved unsuccessful.

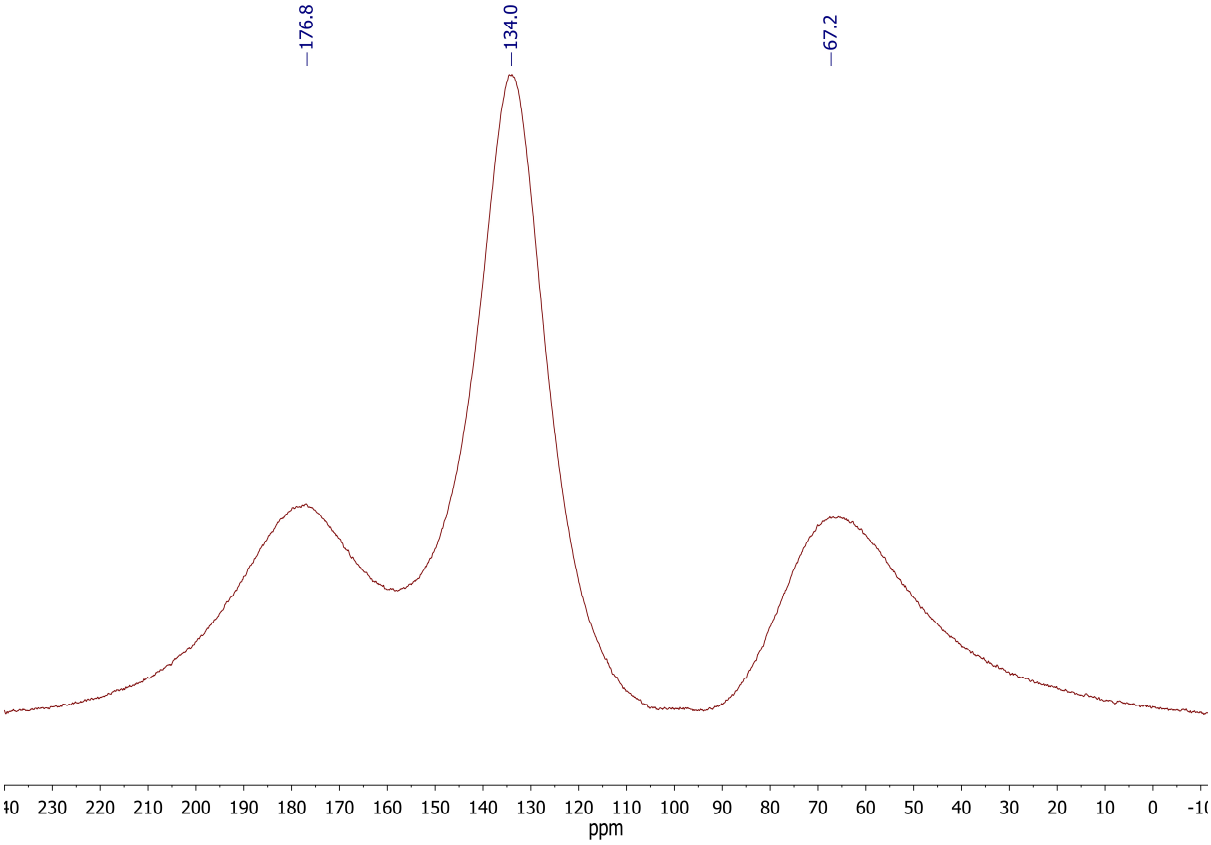

Figure 10.1: ^{27}Al NMR spectrum of the product from the reaction between aluminium and chloromethane, catalysed by iodine. The peak at δ 67.2 ppm is a background signal due to the NMR instrument. The solvent is benzene-d_6.

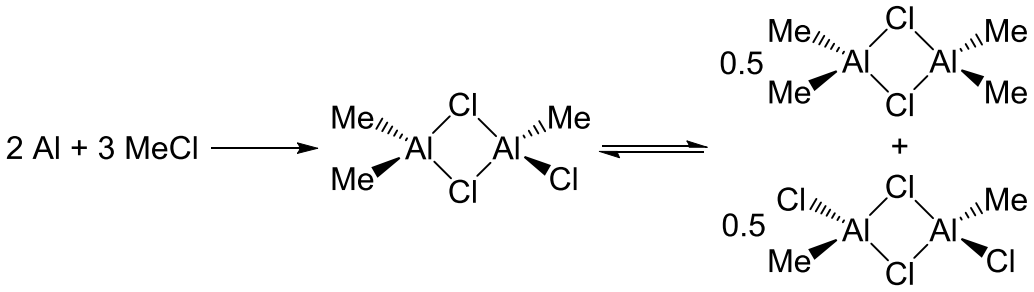

Scheme 10.1: The reaction between aluminium and chloromethane to produce methylaluminium sesquichloride.

10.3 Reactivity of Aluminium-Chloromethane Mixtures with RL 32H

The iodine catalysed reaction was repeated with the refrigeration oil RL 32H (1.26 g) also added to the reactor. After heating the reactor to 120 °C for 2 hours, the products were distilled under vacuum to give a clear liquid. A white solid remained in the reaction vessel, which proved insoluble in hydrocarbon solvents and vigorously reactive with water. The ^{27}Al NMR spectrum of the distilled product (Figure 10.2) showed a significant difference to that of the reaction without RL 32H. The signal at δ 176.8 ppm, due to Me_2AlCl, was not present, suggesting that this species had reacted with RL 32H. The signal at δ 135.1 ppm, due to $MeAlCl_2$, was still present and was accompanied by a new signal, at δ 100.2 ppm. Comparing this to the Me_2AlCl-monoester reactions (see Section 6.3) led to the view that the δ 100.2 ppm signal originated from an aluminoxane with the formula $Me_2Al_2OCl_2$ **9**. This ^{27}Al NMR signal corresponds well with that of 4-coordinate aluminium, which might be expected from the aggregation of **9**. From previous reactions between tetraesters and organoaluminiums (see Chapter 7) it was expected that addition of Me_2AlCl to the tetraesters would result in the formation of dimethylated **4**^{R}(Me_2AlCl) and **4**^{R}($MeAlCl_2$). The thermal elimination undergone by **4**^{R}($MeAlCl_2$) presumably led to the formation of **9**, alkenes and methane.

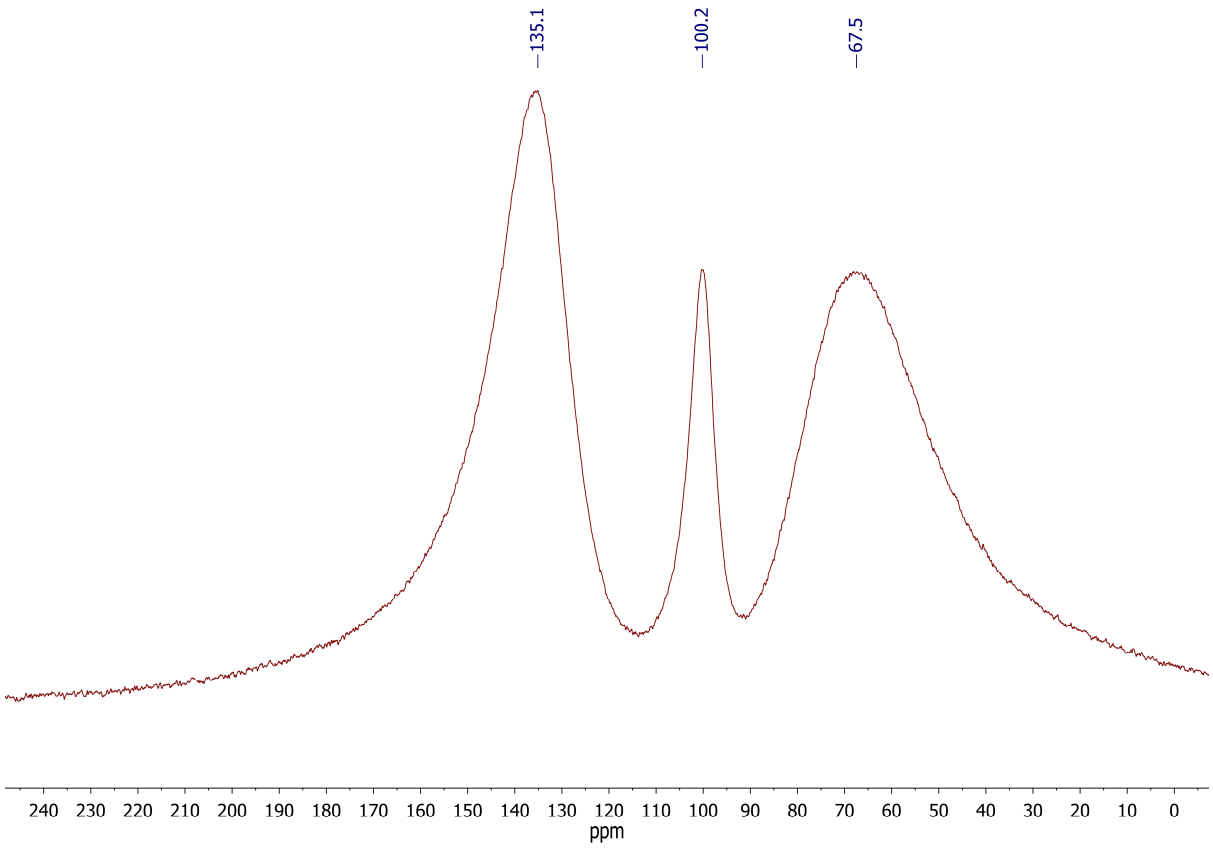

Figure 10.2: ^{27}Al NMR spectrum of the distilled product from the reaction between aluminium, chloromethane and RL 32H, catalysed by iodine. The peak at δ 67.5 ppm is a background signal due to the NMR instrument. The solvent is benzene-d_6.

The ^{1}H NMR spectrum of this liquid (Figure 10.3) revealed a sharp peak at δ −0.46 ppm, attributable to AlMe hydrogens (cf. δ −0.42 ppm for $MeAlCl_2$). There was also a very broad signal in the δ 1.7-0.5 ppm region, which could be assigned to alkene polymerisation products (whose formation was thought to be promoted by Lewis acids such as $MeAlCl_2$). To confirm this polymerisation can occur in the current system, an alkene was heated in the presence of methylaluminium chlorides. The alkene hex-1-ene was chosen as this should have a structure similar to that formed from the reaction of RL 32H with $Me_{1.5}AlCl_{1.5}$. Hex-1-ene and Me_2AlCl were heated to reflux in heptane for 2 hours, with ^{1}H NMR spectroscopy revealing no polymerisation of hex-1-ene. Repeating the reaction, but with $MeAlCl_2$ instead of Me_2AlCl resulted in complete reaction of the alkene and spectroscopy revealed polymer signals similar to those shown in Figure 10.3. This suggested that it is $MeAlCl_2$ that is catalysing the polymerisation in the RL 32H reactions.

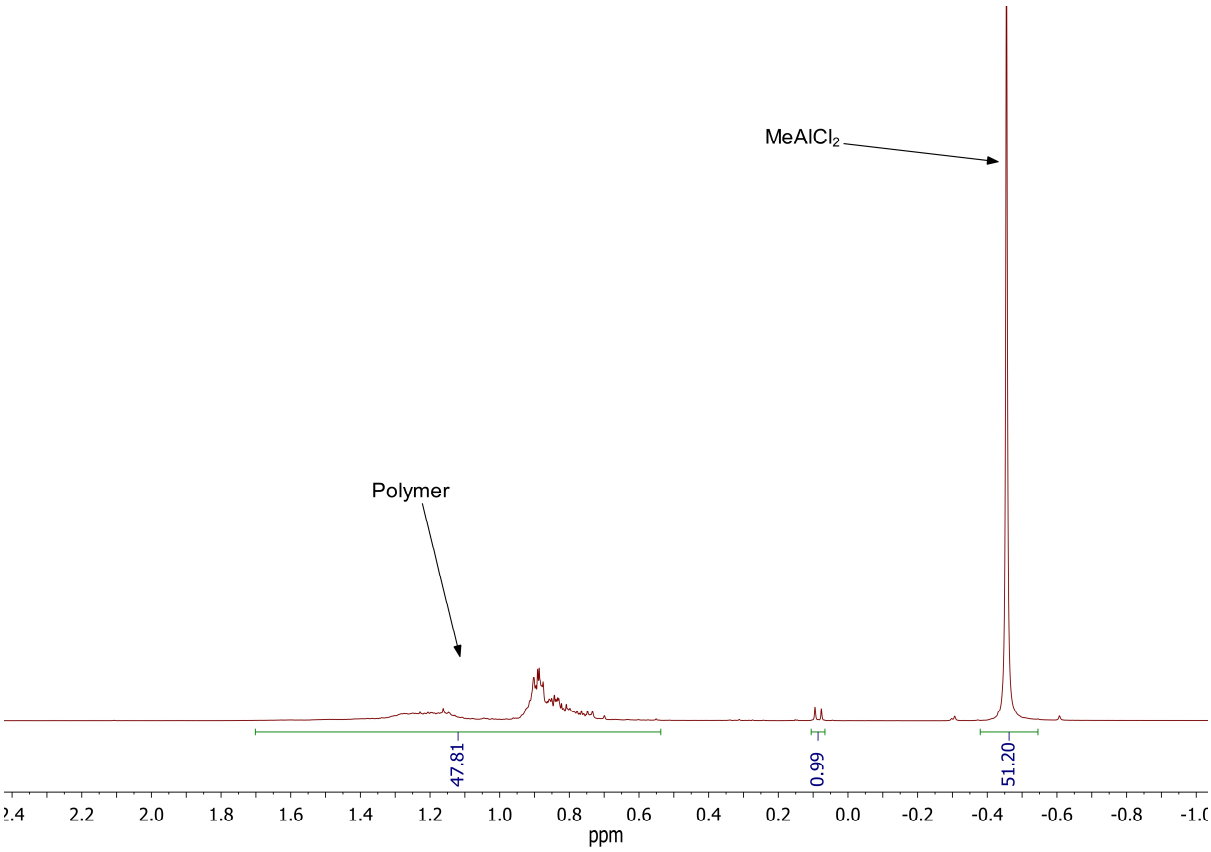

Figure 10.3: ^{1}H NMR spectrum of the distilled product from the reaction between aluminium, chloromethane and RL 32H, catalysed by iodine. The solvent is benzene-d_6.

The overall scheme of the reaction is shown below (Scheme 10.2). Initial reaction of the polyolester with Me_2AlCl results in the formation of a dialuminium alkoxide, **4**^{R}(Me_2AlCl), and a tetraaluminium species, **20**. These species then undergo thermal exchange to form **4**^{R}($MeAlCl_2$) and **21**. The insoluble solid that remained in the reaction vessel is assigned as the tetraaluminium product **21**. Formation of an organic polymer is explained by the dialuminium alkoxide undergoing elimination (as shown in Section 6.6), producing an alkene, methane and the aluminoxane **9**. The alkene can then react to form a polymer, with $MeAlCl_2$ acting as a catalyst.

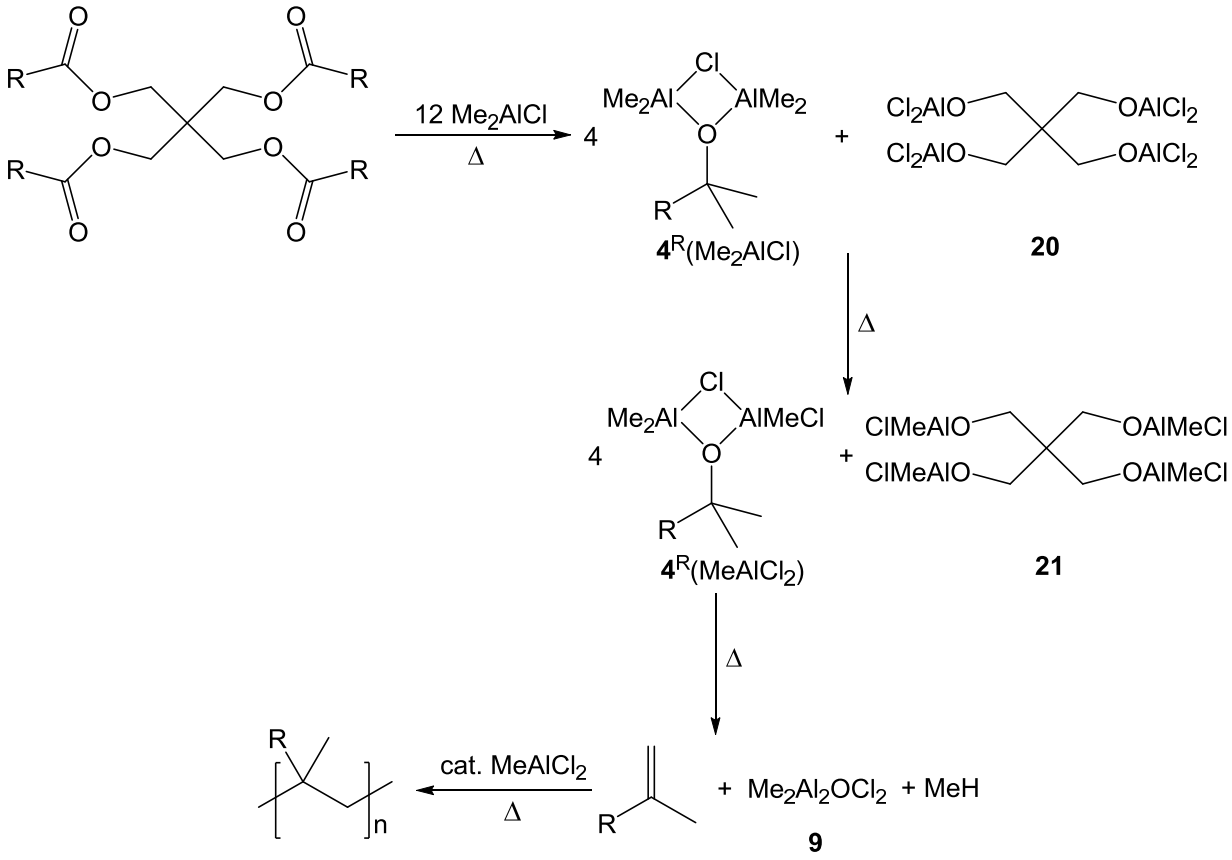

Scheme 10.2: The proposed reaction of the polyolester RL 32H with Me_2AlCl and $MeAlCl_2$, produced from the reaction of aluminium and chloromethane.

10.4 Reactivity of Aluminium-Chloromethane Mixtures with FVC 46D

Moving to polyvinyl ether-based lubricants, the above reaction was repeated, but replacing the RL 32H refrigeration oil with FVC 46D oil. This resulted in significantly different reactivity. After heating to 120 °C for 2 hours no product could be distilled from the reactor. Opening the reactor revealed the formation of a black solid, which was partially soluble in THF. Extraction in THF and analysis by NMR spectroscopy suggested the formation of $AlCl_3(THF)_2$. The observation of a sharp ^{27}Al NMR signal at δ 74.5 ppm was characteristic of 5-coordinate aluminium. In addition, ^{1}H NMR spectroscopy revealed signals, at δ 3.87 and 1.17 ppm, that could be assigned to aluminium-bound THF. The proposed presence of $AlCl_3(THF)_2$ was supported by elemental analysis. The possible observation of $AlCl_3(THF)_2$ was presumed to suggest that $AlCl_3$ was being produced in the reaction. As the reaction between chloromethane and aluminium produced an equimolar

mixture of Me_2AlCl and $MeAlCl_2$, it followed that reaction with FVC 46D had resulted in consumption of all of the AlMe groups. From the reactivity observed with ethers (see Chapter 9), it was expected that the ether functionality of FVC 46D would undergo elimination, producing alkenes, organoaluminium alkoxides and methane. Initial adduct formation was followed by elimination of **39** and the eventual production of **33**, ethene, methane and a polymeric alkene (Scheme 10.3). The black solid now observed after reaction can be tentatively attributed to the polymeric alkene undergoing cross-linking, catalysed by $MeAlCl_2$, to form cross-linked polyethylene. The formation of $AlCl_3$ was presumed to be from the thermal decomposition of **33**, or its decomposition in the presence of THF.

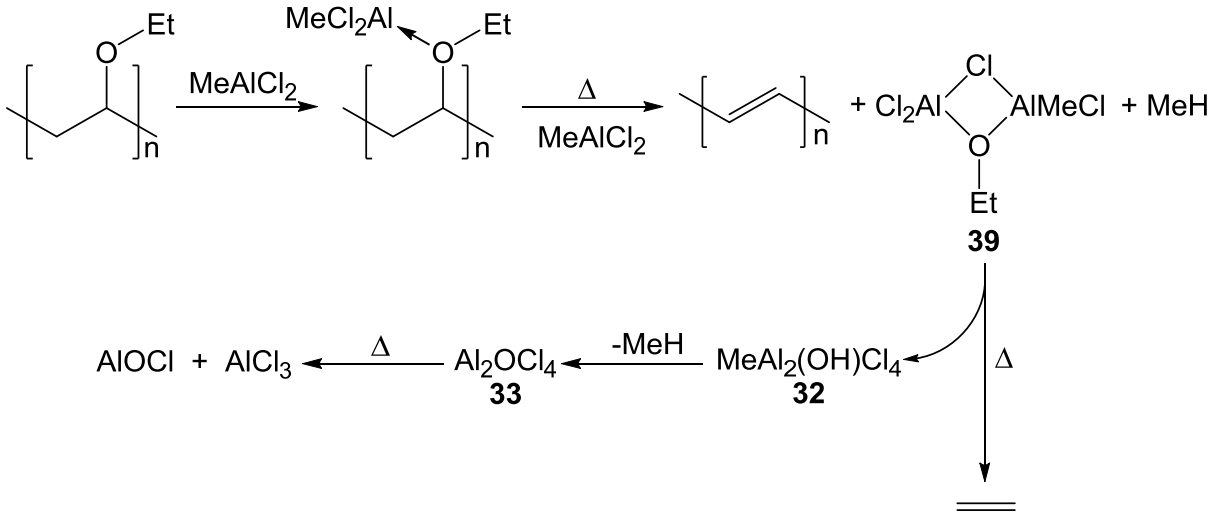

Scheme 10.3: The proposed reaction of the polyvinyl ether FVC 46D with Me_2AlCl and $MeAlCl_2$, produced from the reaction of aluminium and chloromethane.

10.5 Summary

For reaction to occur between aluminium and chloromethane particular conditions were required. The absence of water and the presence of an initiator (iodine in these reactions) resulted in the formation of Me_2AlCl and $MeAlCl_2$. These conditions resemble those that may be present in industrial systems. These systems are free of water, as the refrigerant and oil are passed through a dryer in the refrigeration cycle, and initiation of the reaction can occur through exposure of oxide-free aluminium from friction (cf. iodine exposed oxide-free aluminium in these reactions). Taken together, these points make it perfectly plausible that methylaluminium chlorides could be produced within industrial refrigeration systems contaminated by chloromethane.

The presence of refrigeration oil RL 32H in the reaction mixture did not prevent the formation of methylaluminium chlorides. Instead, RL 32H reacted with the *in situ* formed organoaluminiums, resulting in the removal of Me_2AlCl. This reactivity could be explained by RL 32H having formed the dimethylated species **4**^{R}($MeAlCl_2$), which could undergo a thermal elimination reaction to form alkenes and methane. However, in these reactions between RL 32H and *in situ* formed organoaluminiums the resulting alkenes could not be observed due to their polymerisation, catalysed by $MeAlCl_2$. This overall reactivity seen for RL 32H is concerning with regards to contaminated refrigeration systems. The degradation of the oil results in species that are unable to offer the same lubricity, therefore resulting in an increase in friction and temperature within the system. Additionally, these newly formed species create additional hazards. This is epitomised by methane production, which when coupled with the increased temperatures from friction, could lead to potentially explosive conditions.

Similarly, the addition of refrigeration oil FVC 46D to the aluminium-chloromethane reactions did not inhibit the formation of organoaluminiums. While Me_2AlCl and $MeAlCl_2$ were not directly detected, the observation of a black solid after reaction clearly showed that the oil had undergone significant decomposition. The formation of $AlCl_3$ was suggested by the observation of $AlCl_3(THF)_2$ after THF addition, but the composition of the other species in the reaction mixture was not determined. Nevertheless, the fact that the oil had decomposed is important as it can clearly no longer act as a lubricant. Whilst no pyrophoric behaviour was detected, these reactions would still result in failure in industrial refrigeration systems as the decomposed oil can no longer lubricate the system.

Chapter 11
Conclusions

Many marine container refrigeration systems around the world have demonstrated contamination and several have exploded in recent years, with these incidents thought to be caused by the illicit introduction of chloromethane. The chloromethane, added as a counterfeit refrigerant, was thought to have reacted with aluminium components in the refrigeration systems, resulting in the formation of organoaluminiums, which then readily reacted with other components in the refrigeration system. Therefore, the work in this thesis has focused on the generation of organoaluminium reagents from the reaction of aluminium and chloromethane, and the reaction of these organoaluminiums with refrigeration oils. In this chapter, the conclusions of this project will be presented.

Initial studies were focused on determining the composition of two refrigeration oils used in industrial refrigeration systems; RL 32H and FVC 46D. Through the use of multiple analytical techniques RL 32H was revealed to be a POE, with a mixture of C_3H_7 and C_5H_{11} groups, while FVC 46D was shown to predominantly be poly(ethyl vinyl ether). In addition, both oils were shown to contain other minor components. These minor components were observed directly for FVC 46D with aromatic signals present in the ^{1}H NMR spectrum. Elemental analysis of RL 32H also suggested the presence of minor components.

Attempts were next made to understand how these refrigeration oils would react with organoaluminiums produced from the reaction of aluminium with chloromethane. This was achieved by reacting models for the refrigeration oils with organoaluminiums. The oil RL 32H was initially modelled using the simple monoesters methyl propionate **1**^{Et} and methyl phenylacetate **1**^{Bn}. The reaction of **1**^{R} (R = Et, Bn) with 1 equivalent of TMA resulted in adduct formation, **1**^{R}(TMA). The addition of further equivalents of TMA resulted in addition to the ester and the formation of $Me_2AlOCRMe_2$(TMA) **4**^{R}(TMA) and Me_2AlOMe **3**. Full ester cleavage, and hence 'refrigeration oil' decomposition, was observed for the use of 3 equivalents of TMA per monoester. Heating mixtures of **4**^{R}(TMA) and **3** resulted in thermal exchange to form **4**^{R}(**3**) and the release of TMA. This

released TMA was then able to react with remaining monoester, resulting in full ester cleavage requiring 2 equivalents of TMA and therefore fewer equivalents of organoaluminium required for oil decomposition at elevated temperatures. This thermal exchange was thermodynamically favoured due to the formation of an Al_2O_2 metallacycle and the release of TMA. Reactions between Me_2AlCl and **1**^{Bn} predominantly resulted in adduct formation, giving **1**^{Bn}(Me_2AlCl) at low temperatures, due to the lower nucleophilicity of Me_2AlCl compared to TMA. However, at elevated temperatures the dimethylated species **4**^{Bn}(Me_2AlCl) and **4**^{Bn}($MeAlCl_2$) were observed. Above 60 °C, alkenes $PhCH{=}CMe_2$ **7a** and $BnC(=CH_2)Me$ **7b** were observed, along with the formation of methane. This methane production was shown to occur due to thermal elimination from **4**^{Bn}($MeAlCl_2$). The fact that thermal elimination was observed for **4**^{Bn}($MeAlCl_2$) but not for **4**^{Bn}(TMA) or **4**^{Bn}(Me_2AlCl) was attributed to the greater number of chloride ligands present, resulting in increased Lewis acidity of the aluminium centre. Reactions between $Me_{1.5}AlCl_{1.5}$ and **1**^{Bn} showed similar reactivity to that in the Me_2AlCl-**1**^{Bn} system, but **4**^{Bn}(Me_2AlCl) and **4**^{Bn}($MeAlCl_2$) were not directly observed due to a faster elimination reaction taking place as $Me_{1.5}AlCl_{1.5}$ is a stronger Lewis acid than Me_2AlCl. Reacting **1**^{Bn} with $MeAlCl_2$ resulted in only adduct formation due to the low nucleophilicity of $MeAlCl_2$. This cleavage of monoesters by TMA, Me_2AlCl and $Me_{1.5}AlCl_{1.5}$ is clearly a concern when applied to refrigeration systems as the reaction products cannot provide the same lubrication or refrigerant distribution as the pristine refrigeration oil. Also, the production of alkenes and methane is potentially hazardous due to their flammable nature and volatility.

Once the reactions between organoaluminiums and monoesters were understood, reactions between organoaluminiums and tetraesters, these organics more closely mimicking RL 32H, were investigated. Two tetraesters, **14**^{Pent} and **14**^{Bn}, were synthesised to model these reactions. Similar to the monoester reactions, cleavage of the tetraesters by nucleophilic addition was observed using TMA or Me_2AlCl at room temperature and with $Me_{1.5}AlCl_{1.5}$ at raised temperatures, due to it being a weaker nucleophile. Reactions using Me_2AlCl or $Me_{1.5}AlCl_{1.5}$ also resulted in the formation of alkenes **7a** and **7b**, and methane. However, in contrast to the monoester reactions, where **3** was formed, a tetrolate unit was now produced. For example, reactions between TMA and **14**^{R} (R = Pent, Bn) resulted in the formation of $C(CH_2OAlMe_2)_4$ **15**. This was thought to exist as a polymeric species with adduct formation of CH_2OAlMe_2 units leading to bridging of the tetrolates, as suggested

by broad signals in the ^{1}H NMR spectrum. However, heating TMA-**14**^{Bn} reaction mixtures resulted in adduct formation between the central tetrolate core and dimethylation product **4**^{Bn} to form the molecular species **16**^{Bn}(**4**^{Bn}), **17**^{Bn}(**4**^{Bn})$_2$, **18**^{Bn}(**4**^{Bn})$_3$ and **15**(**4**^{Bn})$_4$, all of which were based on Al_2O_2 metallacycles. The structures of these species were determined by NMR spectroscopy and, in the case of **17**^{Bn}(**4**^{Bn})$_2$, X-ray crystallography. It was also found that **15**(**4**^{Bn})$_4$ underwent thermal elimination to form **19**(**4**^{Bn})$_2$, (**4**^{Bn})$_2$ and **4**^{Bn}(TMA). Crystallography revealed that **19**(**4**^{Bn})$_2$ contained an Al_4O_6 Mitsubishi-type core. The thermal elimination was thought to have occurred due to the formation of the thermodynamically favourable Al_4O_6 core and a reduction in steric crowding. Reactions between organoaluminiums and RL 32H revealed similar reactivity to that shown by the model tetraesters. However, complete assignment of the reaction products proved difficult due to the multiple alkyl groups present in RL 32H, resulting in three different **4**^{R}(TMA)-type species observed when reacted with TMA. The reaction of Me_2AlCl or $Me_{1.5}AlCl_{1.5}$ with RL 32H resulted in the observation of multiple alkene signals and methane from thermal elimination. Overall, the reactions of tetraesters with organoaluminiums revealed very similar reactivity to that seen with monoesters. Ester cleavage of the POE oil would obviously be a serious problem in real-world systems and reactions with RL 32H clearly suggest that this is possible. The breakdown of RL 32H would lead to a loss of lubrication and a build up of alkenes and methane, a potentially dangerous combination.

In Chapter 8, attempts were made to further understand the formation of the molecular species seen to result from heating of the TMA-**14**^{Bn} reaction mixtures. This involved reacting a diol, a triol and a tetrol with organoaluminiums to model possible aggregation. Reactions with the diol tended to produce a trialuminium structure-type, as shown by **22**, **24**(THF)$_2$ and **24**. In contrast, reactions with the triol resulted in the formation of tetraaluminium Mitsubishi molecules **25** and **27**(THF)$_4$, whose structures were similar to that observed for **19**(**4**^{Bn})$_2$. Reactions of organoaluminiums with the tetrol resulted in intractable solids, suggesting similar behaviour to that seen in the tetraester reactions, where species such as **15** were formed. In the TMA-**14**^{Bn} reactions that were heated to reflux, only **19**(**4**^{Bn})$_2$ formed the type of structure observed from the reactions of diols or triols with organoaluminiums. The remaining species only formed adducts with **4**^{Bn}. The reason for this was thought to be the steric bulk of the Al_2O_2 metallacycles that resulted from adduct formation. The species **16**^{Bn}(**4**^{Bn}), **17**^{Bn}(**4**^{Bn})$_2$ and **18**^{Bn}(**4**^{Bn})$_3$ have only one, two and three Al_2O_2 metallacycles, respectively, so can rearrange to reduce steric strain.

However, **15**(**4**^{Bn})$_4$ has four Al_2O_2 metallacycles so is more sterically crowded. Therefore, it was proposed that **15**(**4**^{Bn})$_4$ underwent a thermal elimination to produce **19**(**4**^{Bn})$_2$.

In Chapter 9, reactions of organoaluminiums with ethers were attempted, with the aim of modelling reactivity between organoaluminiums and the PVE FVC 46D. The ethers Et_2O, $^{i}Pr_2O$, THF, 2-MeTHF and MTBE were introduced to TMA, Me_2AlCl and $MeAlCl_2$. In all of the combinations adduct formation occurred initially. However, MTBE then underwent an elimination reaction with all of the organoaluminium species tested to form in each case an organoaluminium alkoxide, an alkene and methane. In contrast, the ethers $^{i}Pr_2O$ and 2-MeTHF only experienced elimination reactions with 2 equivalents of $MeAlCl_2$ at elevated temperatures. The ethers Et_2O and THF only evidenced adduct formation under all conditions tested. These observations suggested that having a tertiary alkyl group adjacent to the oxygen aided elimination, and this was thought to be due to the formation of thermodynamically stable substituted alkenes. Using more chloride-rich organoaluminiums also favoured elimination, due to increased Lewis acidity. Similar reactions were attempted using organoaluminiums and the refrigeration oil FVC 46D. No elimination reaction was observed with TMA, but the use of either Me_2AlCl or $MeAlCl_2$ led to elimination at elevated temperatures. The fact that FVC 46D underwent reaction with both Me_2AlCl and $MeAlCl_2$ is important, as these species are the products of the reaction of aluminium and chloromethane, and are therefore expected to be formed in contaminated refrigeration systems. The breakdown of the PVE oil to organoaluminium alkoxides, alkenes and methane represents a potentially big problem with regards to industrial refrigeration systems, due to the loss of lubrication and production of volatile and flammable species. However, the observation that elimination with FVC 46D only occurred at elevated temperatures may indicate that refrigeration systems would have to be in operation to undergo oil decomposition.

Finally, in Chapter 10, reactions between aluminium and chloromethane were investigated. As expected, the reaction resulted in the formation of Me_2AlCl and $MeAlCl_2$. For reaction to occur, molecular sieves and a catalytic amount of iodine were required. The requirement for iodine was attributed to the need to remove the passivating aluminium oxide layer that coats the metal in order to expose reactive aluminium. Next, the same reaction was repeated with RL 32H also in the reaction vessel. The reaction between aluminium and chloromethane still proceeded, with degradation of the oil observed. The presence of $MeAlCl_2$ in the reaction products suggested that RL 32H had

preferentially reacted with Me_2AlCl. It was considered that the oil had undergone similar transformations to those seen for the tetraesters in Chapter 7, leading to the eventual formation of alkenes from the thermal elimination of $\mathbf{4}^{Bn}(MeAlCl_2)$. However, in the current reaction these alkenes had undergone polymerisation, catalysed by $MeAlCl_2$. Similarly, replacing RL 32H with FVC 46D also resulted in oil degradation. Neither Me_2AlCl nor $MeAlCl_2$ were directly observed amongst the reaction products. However, the formation of $AlCl_3$ was indicated by the detectable presence of $AlCl_3(THF)_2$, observed after the addition of THF to the reaction mixture after reaction. The remaining products formed an intractable black solid, which was attributed to decomposition of alkenes, formed from thermal elimination of the PVE. The reactions of organoaluminiums with both types of oil clearly resulted in oil decomposition. In industrial refrigeration this would evidently be a serious problem as the loss of the oil would decrease lubrication and increase friction. This increased friction could lead to corrosion of components in the compressors, exposure of oxide-free aluminium and an increase in temperatures. In combination with the production of methane, these reactions provide extremely dangerous conditions, which are compatible with the explosions of refrigeration containers observed in real-world situations.

Chapter 12

Future Work

The work described in this thesis has explored the circumstances under which organoaluminiums can be generated, and then undergo reactions, within industrial refrigeration systems when chloromethane is introduced. This focused on reactions with POE and PVE lubricating oils and revealed that both types of oil underwent decomposition in the presence of organoaluminiums. As well as the problem intrinsic to oil degradation, reaction of both oils resulted in the formation of methane and alkenes. The production of methane and high temperatures, from the loss of lubricating oil, have been suggested to be the cause of several explosions of industrial refrigeration units observed in the field. However, there are a number of areas of this work still to be investigated. There are still numerous refrigeration containers quarantined worldwide, due to contamination by chloromethane, which fail to show evidence of the kind of processes described above having occurred. This suggests that the conditions required for initiation of the aluminium-chloromethane reaction are not fully understood. Also, as previously discussed, the refrigerant R-134a is being phased out, due to its high GWP, and being replaced by R-1234yf. However, the introduction of R-1234yf may also have major consequences for the transportation industry.

12.1 Further Investigations into the Reactivity of Aluminium-Chloromethane Mixtures with Refrigeration Oils

In Chapter 10 it was shown that aluminium and chloromethane underwent reaction (in the presence of molecular sieves and a catalytic amount of iodine) to produce methylaluminium sesquichloride. Repeating this reaction in the presence of the refrigeration oils RL 32H or FVC 46D revealed that both oils underwent decomposition after heating to 120 °C for 2 hours. However, the temperature dependence of these reactions was not fully investigated. Therefore, reactions should be attempted over a range of temperatures and timescales. This will help us to further understand what conditions

are required for organoaluminium formation. The conditions will also influence reactions between the *in situ* formed organoaluminiums and the refrigeration oils, potentially resulting in new reaction pathways and mechanisms to give different products. This will be useful for industrial refrigeration systems as different chemical species may be present depending on whether the refrigeration unit has been in operation, and therefore experiencing higher temperatures, or has been in storage.

12.2 Investigating the Role of Oxide-Free Aluminium in Organoaluminium Formation

In spite of the longstanding problems of refrigeration unit contamination with chloromethane, the conditions required for the reaction between chloromethane and aluminium are still not completely understood. In the experiments described within this thesis, a catalyst (iodine) was required to *reliably* initiate organoaluminium formation, presumably by removing the oxide layer that forms spontaneously on aluminium surfaces and exposing reactive sites. In refrigeration systems, particularly ones where the oil is compromised, friction may wear down the oxide layer and expose aluminium. This exposed aluminium may be able to initiate organoaluminium formation, without requiring a chemical catalyst. To further investigate this, oxide-free aluminium (so-called Rieke aluminium) will be produced by reacting aluminium chloride with potassium metal to produce aluminium and potassium chloride under an atmosphere of dry nitrogen (Scheme 12.1).[186,187] Rieke aluminium is more reactive than conventional aluminium as it is oxide-free and made of finely divided particles (giving it a relatively large surface-to-volume ratio). This will act as a model for aluminium in industrial refrigeration units that is rendered oxide-free e.g. through friction. Investigation of the resulting reaction between the oxide-free aluminium and chloromethane with and without catalyst will greatly advance the understanding of reaction initiation and allow for improvements to be made in the safe operation of industrial components and processes. This could be achieved by reducing friction in the refrigeration system by using better anti-wear additives.

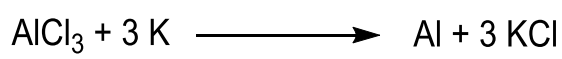

Scheme 12.1: The reduction of aluminium chloride by potassium to produce Rieke aluminium.[186,187]

12.3 Reactions with Aluminium Alloys and other Metals

In this thesis, reactivity between aluminium and chloromethane has only been investigated with aluminium metal. In industrial systems the compressor components are made of aluminium alloyed with a wide range of metals, including copper, iron, zinc and silicon. These metals offer the potential for alternative reactivity with chloromethane and the possibility of synergic effects whereby combining metals yields new reactivity not available to either metal individually. The direct preparation of dialkylaluminium halides has previously been achieved by reacting aluminium-magnesium alloy with alkyl halides,[182] or from the reduction of alkylaluminium dihalides with an active metal such as magnesium (Scheme 12.2).[38] Once reactions between aluminium metal and chloromethane are fully understood, further reactions between aluminium alloys and chloromethane should be investigated systematically to understand the effect that the alloying metals have on organoaluminium formation.

$$(2\ Al + Mg) + 4\ RX \longrightarrow 2R_2AlX + MgX_2$$

$$4\ RAlX_2 + 3\ Mg \longrightarrow 2\ R_2AlX + 2\ Al + 3\ MgX_2$$

Scheme 12.2: The reaction of aluminium-magnesium alloy with alkyl halides and the reduction of alkylaluminium dihalides with magnesium (X = halide).[38,182]

In addition to aluminium alloys, closed refrigeration systems also contain large amount of copper and steel components. It is currently unknown whether these components could contribute to or interfere with the production of organoaluminiums or alter the reactivity of these organoaluminiums with refrigeration oil. Initial reactions using chloromethane, aluminium and copper or steel should be investigated. This will lead to a better understanding of how components in the refrigeration system influence organoaluminium formation and allow for improvements in safety.

12.4 Further Studies into the Reactivity of Refrigeration Oils

The scope of refrigeration oils studied in this thesis has been limited to POEs and PVEs. Other lubricating oils in use include PAOs (polyalphaolefins) and PAGs (Figure 12.1).

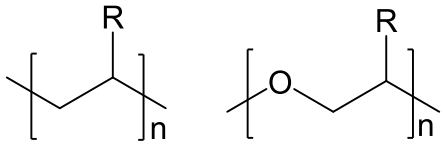

Figure 12.1: General structures for PAOs (left) and PAGs (right).

Initially, structural analysis of these refrigeration oils should be undertaken to provide an essential understanding of how they may behave towards *in situ* formed organoaluminium species. Understanding the ability of these oils to react (or not) is extremely important as they offer a potential method by which to passivate organoaluminiums and prevent a large build-up of these corrosive, flammable and highly reactive species. It is expected that PAOs would be inert with respect to organoaluminiums due to the lack of chemical functionality, resulting in unreacted methylaluminium chlorides. However, PAGs have the potential to react with organoaluminiums in a similar fashion to that seen with PVEs (see Chapter 9). Deprotonation of the PAG could lead to formation of an aluminium enolate and methane (Scheme 12.3).

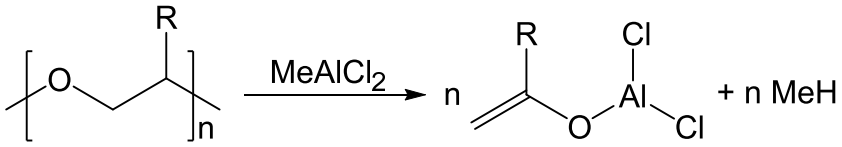

Scheme 12.3: The proposed reaction of a PAG with $MeAlCl_2$.

12.5 Refrigeration Oil Additive Analysis

A literature search revealed that additives such as amines, phosphates and alcohols are used to enhance the anti-wear and anti-oxidant properties of currently used lubricant oils (see Section 1.3.3). Analysis of refrigeration oils (see Chapter 5) has shown that these additives are only present in small amounts (<1%). However, their ability to promote or hinder the formation and reaction of organoaluminiums in refrigeration systems is completely unexplored. Initially, identification of these additives should be attempted using high resolution mass spectrometry. Once the nature and structure of the additives has been elucidated, investigation of whether these agents may serve (individually or in combination) as catalysts or to initiate reactions, such as those that produce organoaluminiums, should be undertaken.

12.6 Investigating the Reactivity of Organoaluminiums with New Refrigerants

The need to use refrigerants with lower GWP has led to the phasing out of R-134a, with R-1234yf proposed as a replacement. While R-1234yf is not expected to react with aluminium (as seen with R-40), the higher price of R-1234yf (currently £92.4 per kg, compared to £34.7 per kg for R-134a) is highly likely to lead to the use of cheaper fraudulent refrigerants (such as R-40), potentially exacerbating an already serious problem. Moreover, the reactions of R-40 with aluminium will result in organoaluminiums that have the potential to react with R-1234yf. Whilst reactivity toward Al(III) reagents has yet to be explored, recent literature has shown that Al(I) species react with R-1234yf, by oxidative addition of the C–F bond (Scheme 12.4).[49]

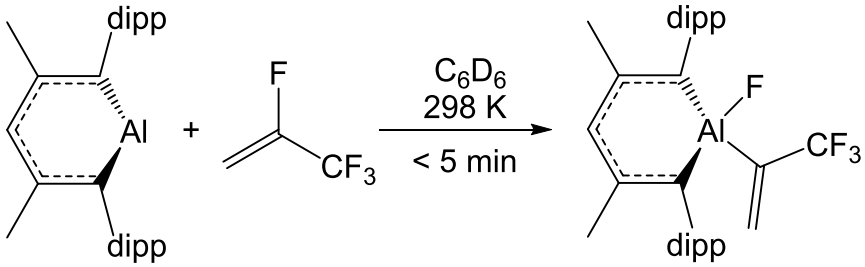

Scheme 12.4: The oxidative addition of a C–F bond of R-1234yf to an Al(I) species.[49]

Recent work has also revealed addition-elimination reactions of R-1234yf with sodium alkoxides, with substitution of the olefinic fluoride observed at room temperature (Scheme 12.5, top).[188] In industrial refrigeration units, the organoaluminiums arising from chloromethane contamination could act as nucleophiles, potentially resulting in similar reactivity. This could result in the exchange of fluoride for methyl (Scheme 12.5, bottom). The methylated product (2-(trifluoromethyl)propene) has a much higher boiling point (−6.0 °C) compared to R-1234yf (−28.3 °C).[189,190] This difference in boiling point could potentially result in problems within the refrigeration system as heat cannot be exchanged as easily without a change in state. This may result in overheating of the system. Therefore, the reactivity of R-1234yf with organoaluminiums should be investigated, to determine whether R-1234yf would degrade. This would initially involve reactions between organoaluminiums and simple fluorinated alkenes (e.g. fluoroethene) as models for R-1234yf. Once the model reactions have been understood reactions will be then be attempted with the refrigerant R-1234yf.

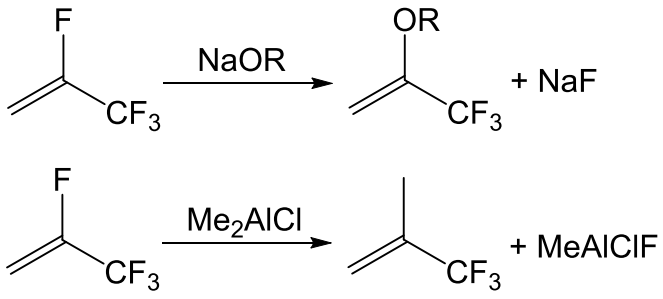

Scheme 12.5: The observed reaction between R-1234yf and sodium alkoxide (top)[188] and the proposed reaction of R-1234yf with Me_2AlCl (bottom).

Additionally, R-1234yf may react with organoaluminiums by carboalumination of the alkene. The polarity of the alkene should aid carboalumination, with the electron withdrawing groups resulting in addition of the methyl to the terminal position (Scheme 12.6). This work showed that non-fluorinated alkenes can react with organoaluminiums, with isomerisation and polymerisation observed (see Section 10.2). It is possible that R-1234yf may also undergo a polymerisation reaction, aided by the polarity of the alkene (Scheme 12.6). Polymerisation of the refrigerant would be a significant problem, as this species would no longer be able to act as refrigerant. Future work would investigate these possibilities using fluorinated alkenes, to model reactions with R-1234yf.

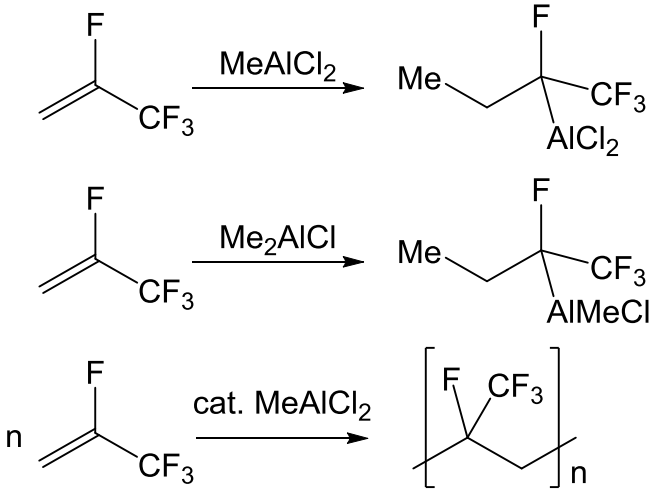

Scheme 12.6: The potential reactivity of R-1234yf with $MeAlCl_2$ and Me_2AlCl.

As noted, the increased price of R-1234yf relative to current refrigerants is likely to lead to an increase in the use of counterfeit refrigerants. A search of possible cheaper replacement refrigerants with similar properties to R-1234yf could indicate possible future contaminants. These compounds could then be screened for reactivity with aluminium and organoaluminium compounds. This work would have direct practical benefits to refrigeration safety and may help with future-proofing new technologies.

12.7 Organoaluminium Detection

Currently, a flame halide detector is used to determine whether chlorinated refrigerants are present in refrigeration systems. However, this method would be dangerously inappropriate for a system in which organoaluminiums or methane had been produced. A test for the presence of organoaluminium compounds should therefore be developed to quickly, easily and reliably identify potentially dangerous units. This could be achieved using a chemical that reacts with organoaluminiums to produce a new and differently coloured chemical. An example of such a test might be one based on the action of fluorenone, a yellow solid, whose colour alters upon complexation by an organoaluminium or its addition across the ketone bond. The addition of TMA to a toluene solution of fluorenone resulted in addition to the ketone and the formation a colourless solution (Scheme 12.7).[102] Meanwhile, in the presence of $AlCl_3$, a toluene solution of fluorenone gave a red colour, due to adduct formation (Scheme 12.7).[191] This could yield a simple field test with a small aliquot of the refrigerant inserted into a solution of fluorenone easily showing whether organoaluminiums are present. It should also allow for an understanding of the organoaluminium species present in the unit. Chloride-rich organoaluminiums, such as $MeAlCl_2$, would be expected to only form adducts and a red colour. Whereas, methyl-rich organoaluminiums, such as TMA or Me_2AlCl, would result in addition to the ketone and a colourless solution.

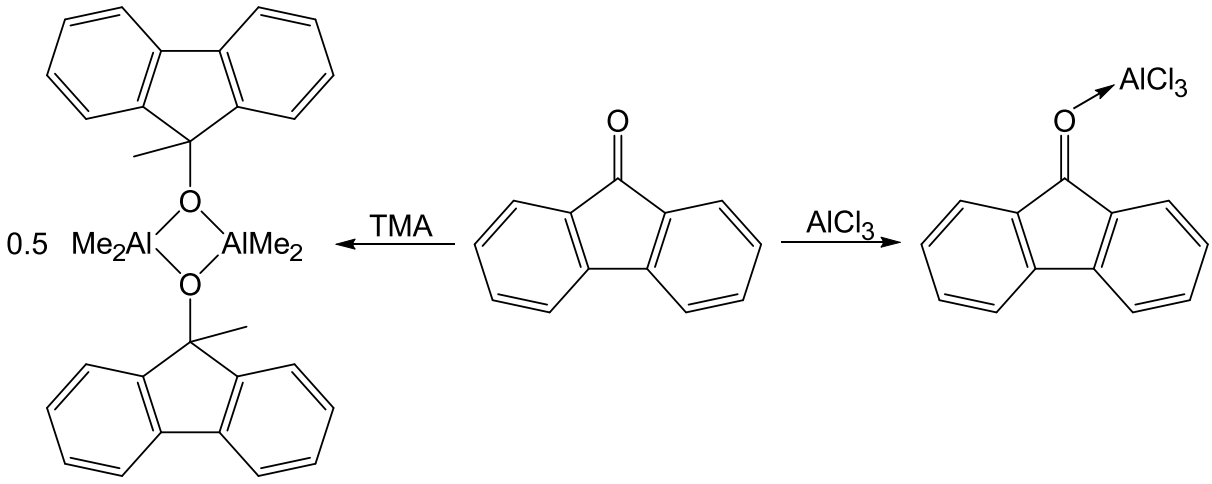

Scheme 12.7: The reaction of fluorenone with TMA and $AlCl_3$.[102,191]

References

1 *Issue Paper: Refrigerated Container (Reefer) Explosion*, 2011.

2 *AHRI White Paper: Reports of R -134a Contaminated with R -40 and Other Refrigerants*, 2013.

3 A. E. H. Wheatley, P. J. Harford and A. J. Peel, *Investigation of the composition and reactivity of counterfeit refrigerant, Reports 2 & 3*, 2012.

4 A. R. Chandra, *Refrigeration and Air Conditioning*, PHI Learning Pvt. Ltd., 2010.

5 M. J. Molina and F. S. Rowland, *Nature*, 1974, **249**, 810–812.

6 *Handbook for the Montreal Protocol on Substances that Deplete the Ozone Layer, 10th ed., UNEP*, 2016.

7 UN, *Kyoto Protocol to the United Nations Framework Convention on Climate Change, United Nations Framework Convention on Climate Change*, 1998, vol. 7.

8 D. M. Lemal, *J. Org. Chem.*, 2004, **69**, 1–11.

9 A. A. Lapkin, M. Peters, L. Greiner, S. Chemat, K. Leonhard, M. A. Liauw and W. Leitner, *Green Chem.*, 2010, **12**, 241–251.

10 *Montreal Protocol on Subtances that Deplete the Ozone Layer, 2006 Report*, .

11 European Parliament, *Off. J. Eur. Union*, 2006, **161**, 12–18.

12 European Parliament, *Off. J. Eur. Union*, 2014, **57**, 195–230.

13 T. J. Leck, *Evaluation of HFO-1234yf as a Potential Replacement for R-134a in Refrigeration Applications*, 2009.

14 *Report of the Twenty Eighth Meeting of the Parties to the Montreal Protocol on Substances that Deplete the Ozone Layer*, 2016.

15 D. Sánchez, R. Cabello, R. Llopis, I. Arauzo, J. Catalán-Gil and E. Torrella, *Int. J. Refrig.*, 2017, **74**, 267–280.

16 O. J. Nielsen, M. S. Javadi, M. P. Sulbaek Andersen, M. D. Hurley, T. J. Wallington and R. Singh, *Chem. Phys. Lett.*, 2007, **439**, 18–22.

17 C. Hetzner, *Coolant safety row puts the heat on Europe's carmakers, Reuters*, 2012.

18 M. T. Holbrook, *Kirk-Othmer Encyclopedia of Chemical Technology*, Kirk-Othmer Encyclopedia of Chemical Technology, Hoboken, NJ, USA, 2001, vol. 16.

19 F. Beilstein, *Berichte der Dtsch. Chem. Gesellschaft*, 1872, **5**, 620–621.

20 D. F. Hayman, *Ind. Eng. Chem. Anal. Ed.*, 1939, **11**, 470–470.

21 *CRT Guide to Sample Taking and Flame Testing*, 2013.

22 J.-C. Remigy, E. Nakache and P. D. Brechot, *J. Synth. Lubr.*, 1997, **14**, 237–247.

23 N. E. Schnur, *Blended Polyol Ester Lubricants for Refrigerant Heat Transfer Fluids*, US 5976399, 1999.

24 S. T. Jolley, *Liquid Compositions Containing Carboxylic Esters*, 9012849, 1990.

25 E. Beran, *Tribol. Int.*, 2010, **43**, 2372–2377.

26 E. L. Niedzielski, *Ind. Eng. Chem. Prod. Res. Dev.*, 1976, **15**, 54–58.

27 M. McHenry, D. Carr and T. Schaefer, *Poly(neopentyl polyol) ester based coolants and improved additive package*, US5895778A, 1997.

28 E. Vrahopoulou, R. Schlosberg and D. Turner, *Polyol ester distillate fuels additive*, US5993498A, 1998.

29 R. Alexander, P. G. Kralert and R. I. Kagi, *Org. Geochem.*, 1992, **19**, 133–140.

30 Q. Ashton Acton, *Vinyl Compounds-Advances in Research and Application*, ScholarlyMedia LLC, 2013.

31 E. I. Marukovich and V. J. Stetsenko, *ITM NAS Belarus*, 2011, **2**, 51–53.

32 R. C. Cavestri, *Proc.Int.Refrig.Conf.Purdue, 6th, Publ Purdue Univ.*, 1996, 169–174.

33 R. C. Cavestri, *Compatibility of Lubricant Additives With Hfc Refrigerants and Synthetic Lubricants*, 1997.

34 J.-S. Tsaih, H.-H. Tang, J.-T. Hung, T. Tsai and H.-L. Huang, *Novel refrigeration oil*, EP3072952A1, 2016.

35 H. Yoon, T. Sheiretov and C. Cusano, *Wear*, 1998, **218**, 54–65.

36 J. D. Scott and R. A. Steven, *Chemical Process*, US5243105, 1993.

37 E. Hamilton, *Examination of the Reaction of R40 with Refrigeration System Materials:*

R134a, POE Oil, Al1100, Al380, and Fe, Cu, Zeolite Silicate and Alumina Metal Catalysts (Ashrae 1665-RP), 2014.

38 J. R. Zietz, G. C. Robinson and K. L. Lindsay, in *Comprehensive Organometallic Chemistry*, Elsevier, 2006, vol. 7, pp. 365–464.

39 V. F. Hnizda and C. A. Kraus, *J. Am. Chem. Soc.*, 1938, **60**, 2276–2276.

40 H. Adkins and C. Scanley, *J. Am. Chem. Soc.*, 1951, **73**, 2854–2856.

41 D. P. Cutler, *J. Hazard. Mater.*, 1987, **17**, 99–108.

42 P. Smith, *Production of Aluminium Alkyls*, US2863894, 1958.

43 S. Pasynkiewicz and M. BolesŁawski, *J. Organomet. Chem.*, 1970, **25**, 29–32.

44 M. J. Krause, F. Orlandi, A. T. Saurage and J. R. Zietz Jr., *Ullmann's Encyclopedia of Industrial Chemistry, Aluminium Compounds, Organic*, 2000.

45 K. Ziegler, H.-G. Gellert, H. Lehmkuhl, W. Pfohl and K. Zosel, *Justus Liebigs Ann. Chem.*, 1960, **629**, 1–13.

46 C. Elschenbroich, *Organometallics*, Wiley-VCH, 2006.

47 C. Dohmeier, C. Robl, M. Tacke and H. Schnöckel, *Angew. Chemie Int. Ed. English*, 1991, **30**, 564–565.

48 W. Uhl, *Zeitschrift fur Naturforsch. B*, 1988, **43**, 1113–1118.

49 C. Bakewell, A. J. P. White and M. R. Crimmin, *Angew. Chemie Int. Ed.*, 2018, **57**, 6638–6642.

50 C.-R. Chen and H.-M. Gau, *Acta Crystallogr. Sect. E. Struct. Rep. Online*, 2008, **64**, 1381.

51 R. G. Vranka and E. L. Amma, *J. Am. Chem. Soc.*, 1967, **89**, 3121–3126.

52 Z. Černý, J. Fusek, O. Kříž, S. Heřmánek, M. Šolc and B. Čásenský, *J. Organomet. Chem.*, 1990, **386**, 157–165.

53 A. Tarazona, E. Koglin, F. Buda, B. B. Coussens, J. Renkema, S. van Heel and R. J. Meier, *J. Phys. Chem. B*, 1997, **101**, 4370–4378.

54 N. Muller and D. E. Pritchard, *J. Am. Chem. Soc.*, 1960, **82**, 248–249.

55 J. F. Malone and W. S. McDonald, *Chem. Commun.*, 1967, **0**, 444–445.

56 E. A. Jeffery, T. Mole and J. K. Saunders, *Aust. J. Chem.*, 1968, **21**, 137–144.

57 J. F. Malone and W. S. McDonald, *J. Chem. Soc., Dalt. Trans.*, 1972, **0**, 2649–2652.

58 G. Allegra, G. Perego and A. Immirzi, *Die Makromol. Chemie*, 1963, **61**, 69–78.

59 J. H. Rogers, A. W. Apblett, W. M. Cleaver, A. N. Tyler and A. R. Barron, *J. Chem. Soc. Dalt. Trans.*, 1992, **0**, 3179–3187.

60 E. A. Jeffery, T. Mole and J. K. Saunders, *Aust. J. Chem.*, 1968, **21**, 649–657.

61 J. J. Jerius, J. M. Hahn, M. M. Rahman, O. Mols, J. P. Oliver and W. H. Ilsley, *Organometallics*, 1986, **5**, 1812–1814.

62 S. Saito and H. Yamamoto, *Chem. Commun.*, 1997, **0**, 1585–1592.

63 M. D. Healy, D. A. Wierda and A. R. Barron, *Organometallics*, 1988, **7**, 2543–2548.

64 J. A. Francis, C. N. McMahon, S. G. Bott and A. R. Barron, *Organometallics*, 1999, **18**, 4399–4416.

65 P. K. Hon and C. E. Pfluger, *J. Coord. Chem.*, 1973, **3**, 67–76.

66 J. Lewiński, J. Zachara and I. Justyniak, *Organometallics*, 1997, **16**, 4597–4605.

67 J. Lewiński and A. E. H. Wheatley, in *Modern Organoaluminum Reagents*, 2012, vol. 48, pp. 1–58.

68 M. L. Munzarová and R. Hoffmann, *J. Am. Chem. Soc.*, 2002, **124**, 4787–4795.

69 M. Haouas, F. Taulelle and C. Martineau, *Prog. Nucl. Magn. Reson. Spectrosc.*, 2016, **94**–**95**, 11–36.

70 R. Benn and A. Rufińska, *Angew. Chemie Int. Ed. English*, 1986, **25**, 861–881.

71 D. E. O'Reilly, *J. Chem. Phys.*, 1960, **32**, 1007–1012.

72 S. Aldridge and A. J. Downs, *The group 13 metals aluminium, gallium, indium and thallium: chemical patterns and peculiarities*, Wiley, 2011.

73 D. C. Bradley, I. S. Harding, I. A. Maia and M. Motevalli, *J. Chem. Soc. Dalt. Trans.*, 1997, **0**, 2969–2980.

74 K. Gosling, G. M. McLaughlin, G. A. Sim and J. D. Smith, *J. Chem. Soc. D Chem. Commun.*, 1970, **0**, 1617–1618.

75 C. N. McMahon, S. G. Bott and A. R. Barron, *J. Chem. Soc. Dalt. Trans.*, 1997, **0**, 3129–3137.

76 H. S. Zijlstra and S. Harder, *Eur. J. Inorg. Chem.*, 2015, **2015**, 19–43.

77 S. Pasynkiewicz, *Polyhedron*, 1990, **9**, 429–453.

78 H. W. Roesky, M. G. Walawalkar and R. Murugavel, *Acc. Chem. Res.*, 2001, **34**, 201–211.

79 M. R. Mason, J. M. Smith, S. G. Bott and A. R. Barron, *J. Am. Chem. Soc.*, 1993, **115**, 4971–4984.

80 B. M. Trost, I. Fleming and M. M. Semmelhack, *Comprehensive Organic Synthesis: Addition to and substitution at C-C[pi]-Bonds*, Pergamon Press, 1992.

81 K. Ziegler, H. -G Gellert, K. Zosel, E. Holzkamp, J. Schneider, M. Söll and W. -R Kroll, *Justus Liebigs Ann. Chem.*, 1960, **629**, 121–166.

82 E. Negishi, D. E. Van Horn and T. Yoshida, *J. Am. Chem. Soc.*, 1985, **107**, 6639–6647.

83 J. J. Eisch and W. C. Kaska, *J. Am. Chem. Soc.*, 1963, **85**, 2165–2166.

84 S. Xu and E. I. Negishi, *Acc. Chem. Res.*, 2016, **49**, 2158–2168.

85 K. Ziegler, E. Holzkamp, H. Breil and H. Martin, *Angew. Chemie*, 1955, **67**, 541–547.

86 D. S. Breslow and N. R. Newburg, *J. Am. Chem. Soc.*, 1959, **81**, 81–86.

87 J. J. Eisch, A. M. Piotrowski, S. K. Brownstein, E. J. Gabe and F. L. Lee, *J. Am. Chem. Soc.*, 1985, **107**, 7219–7221.

88 A. Andresen, H. Cordes, J. Herwig, W. Kaminsky, A. Merck, R. Mottweiler, J. Pein, H. Sinn and H. Vollmer, *Angew. Chemie Int. Ed. English*, 1976, **15**, 630–632.

89 W. P. Long and D. S. Breslow, *Justus Liebigs Ann. Chem.*, 1975, **1975**, 463–469.

90 E. Y.-X. Chen and T. J. Marks, *Chem. Rev.*, 2000, **100**, 1391–1434.

91 I. Tritto, S. X. Li, M. C. Sacchi, P. Locatelli and G. Zannoni, *Macromolecules*, 1995, **28**, 5358–5362.

92 H. Sinn, W. Kaminsky, H. -J Vollmer and R. Woldt, *Angew. Chemie Int. Ed. English*,

1980, **19**, 390–392.

93 K. Ziegler, F. Krupp and K. Zosel, *Justus Liebigs Ann. Chem.*, 1960, **629**, 241–250.

94 K. Noweck and W. Grafahrend, in *Ullmann's Encyclopedia of Industrial Chemistry*, Wiley-VCH Verlag GmbH & Co. KGaA, Weinheim, Germany, 2006, vol. 14, pp. 117–141.

95 J. F. Allan, W. Clegg, M. R. J. Elsegood, K. W. Henderson, A. E. McKeown, P. H. Moran and I. M. Rakov, *J. Organomet. Chem.*, 2000, **602**, 15–23.

96 M. B. Power, S. G. Bott, D. L. Clark, J. L. Atwood and A. R. Barron, *Organometallics*, 1990, **9**, 3086–3097.

97 E. C. Dandley, C. D. Needham, P. S. Williams, A. H. Brozena, C. J. Oldham and G. N. Parsons, *J. Mater. Chem. C*, 2014, **2**, 9416–9424.

98 S. Pasynkiewicz and E. Sliwa, *J. Organomet. Chem.*, 1965, **3**, 121–128.

99 M. B. Power, S. G. Bott, J. L. Atwood and A. R. Barron, *J. Am. Chem. Soc.*, 1990, **112**, 3446–3451.

100 E. A. Jeffery and T. Mole, *Aust. J. Chem.*, 1970, **23**, 715–724.

101 A. Meisters and T. Mole, *J. Chem. Soc. Chem. Commun.*, 1972, **1972**, 595–596.

102 S. J. Obrey, S. G. Bott and A. R. Barron, *Organometallics*, 2001, **20**, 5162–5170.

103 Z. S. Sales, R. Nassar, J. J. Morris and K. W. Henderson, *J. Organomet. Chem.*, 2005, **690**, 3474–3478.

104 E. A. Jeffery and A. Meisters, *J. Organomet. Chem.*, 1974, **82**, 307–314.

105 E. C. Ashby and J. T. Laemmle, *Chem. Rev.*, 1975, **75**, 521–546.

106 E. C. Ashby and R. S. Smith, *J. Org. Chem.*, 1977, **42**, 425–427.

107 S. Miyajima and T. Inukai, *Bull. Chem. Soc. Jpn.*, 1972, **45**, 1553–1554.

108 J. A. Marshall, B. G. Shearer and S. L. Crooks, *J. Org. Chem.*, 1987, **52**, 1236–1245.

109 B. B. Snider, *Acc. Chem. Res.*, 1980, **13**, 426–432.

110 K. C. Majumdar, R. Islam and S. Alam, *Synth. Commun.*, 2008, **38**, 754–766.

111 S. Pasynkiewicz and W. Kuran, *J. Organomet. Chem.*, 1969, **16**, 43–50.

112 R. Wolovsky, N. Maoz and Z. Nir, *Synthesis (Stuttg).*, 1970, **1970**, 656–657.

113 D. Shriver and M. Drezdon, *The Manipulation of Air Sensitive Compounds*, Wiley, New York, Second Edi., 1986.

114 T. Kottke and D. Stalke, *J. Appl. Crystallogr.*, 1993, **26**, 615–619.

115 G. M. Sheldrick, *Acta Crystallogr. Sect. A Found. Crystallogr.*, 2015, **71**, 3–8.

116 G. M. Sheldrick, *Acta Crystallogr. Sect. C Struct. Chem.*, 2015, **71**, 3–8.

117 G. Socrates, *Infrared and Raman Characteristic Group Frequencies: Tables and Charts, 3rd Edition*, John Wiley & Sons, 2004.

118 T. Egawa, H. Yamasaki, K. Mogami, S. Nagao, T. Handa and K. Masato, *Lubricating oil for compression-type refrigerators containing pentafluoroethane and a polyvinyl ether*, US6261474B1, 1997.

119 K. B. Starowieyski, S. Pasynkiewicz and A. Sporzyński, *J. Organomet. Chem.*, 1976, **117**, 117–128.

120 S. Pasynkiewicz, *Pure Appl. Chem.*, 1972, **30**, 509–522.

121 S. Pasynkiewicz, L. Kozerski and B. Grabowski, *J. Organomet. Chem.*, 1967, **8**, 233–238.

122 K. Daly, R. Nomak and J. K. Snyder, *Tetrahedron Lett.*, 1997, **38**, 8611–8614.

123 M. Girardot, R. Nomak and J. Snyder, *J. Org. Chem.*, 1998, **63**, 10063–10068.

124 A. Itoh, K. Oshima, S. Sasaki, H. Yamamoto, T. Hiyama and H. Nozaki, *Tetrahedron Lett.*, 1979, **20**, 4751–4754.

125 J. Stephen Clark, A. G. Dossetter, A. J. Blake, W.-S. Li and W. G. Whittingham, *Chem. Commun.*, 1999, **0**, 749–750.

126 J. S. Clark and Y.-S. Wong, *Chem. Commun.*, 2000, **0**, 1079–1080.

127 K. B. Starowieyski, S. Pasynkiewicz, A. Sporzyński and K. Wisniewska, *J. Organomet. Chem.*, 1976, **117**, C1–C3.

128 A. V. Belyakov, A. Haaland, H. P. Verne and J. Weidlein, *Acta Chem. Scand.*, 1994, **48**, 169–171.

129 A. Cottone and M. J. Scott, *Organometallics*, 2000, **19**, 5254–5256.

130 A. Cottone and M. J. Scott, *Organometallics*, 2002, **21**, 3610–3627.

131 A. Ji, R. Son, M. G. Thorn, P. E. Fanwick and I. P. Rothwell, *Organometallics*, 2003, **22**, 2318–2324.

132 B. Cetinkaya, P. B. Hitchcock, H. A. Jasim, M. F. Lappert and H. D. Williams, *Polyhedron*, 1990, **9**, 239–243.

133 D. Ogrin, S. G. Bott and A. R. Barron, *J. Chem. Crystallogr.*, 2008, **38**, 397–401.

134 G. R. Fulmer, A. J. M. Miller, N. H. Sherden, H. E. Gottlieb, A. Nudelman, B. M. Stoltz, J. E. Bercaw and K. I. Goldberg, *Organometallics*, 2010, **29**, 2176–2179.

135 G. A. Olah, J. Kaspi and J. Bukala, *J. Org. Chem.*, 1977, **42**, 4187–4191.

136 A. Fischer, *J. Organomet. Chem.*, 1996, **525**, 291–294.

137 A. Del Grosso, R. G. Pritchard, C. A. Muryn and M. J. Ingleson, *Organometallics*, 2010, **29**, 241–249.

138 B. B. Snider, I. R. Ramazanov and U. M. Dzhemilev, *e-EROS Encycl. Reagents Org. Synth.*, 2009, 1–11.

139 Y. Nishimoto, S. A. Babu, M. Yasuda and A. Baba, *J. Org. Chem.*, 2008, **73**, 9465–9468.

140 S. Hadjikyriacou, M. Acar and R. Faust, *Macromolecules*, 2004, **37**, 7543–7547.

141 B. B. Snider, in *Encyclopedia of Reagents for Organic Synthesis*, John Wiley & Sons, Ltd, Chichester, UK, 2001.

142 P. Sobota, S. Szafert and T. Glowiak, *J. Organomet. Chem.*, 1996, **526**, 329–333.

143 J. Utko, M. Wróblewska, T. Lis and P. Sobota, *J. Organomet. Chem.*, 1993, **447**, 159–161.

144 J. Lewiński, P. Horeglad, K. Wójcik and I. Justyniak, *Organometallics*, 2005, **24**, 4588–4593.

145 C. Rennekamp, H. Wessel, H. W. Roesky, P. Muller, H. G. Schmidt, M. Noltemeyer, I. Uson and A. R. Barron, *Inorg. Chem.*, 1999, **38**, 5235–5240.

146 M.-A. Munoz-Hernandez, P. Wei, S. Liu and D. A. Atwood, *Coord. Chem. Rev.*, 2000, **210**, 1–10.

147 D. A. Atwood, J. A. Jegier, S. Liu, D. Rutherford, P. Wei and R. C. Tucker, *Organometallics*, 1999, **18**, 976–981.

148 T. Mole, *Aust. J. Chem.*, 1966, **19**, 373–379.

149 W. Ziemkowska and S. Pasynkiewicz, *J. Organomet. Chem.*, 1996, **508**, 243–248.

150 W. Ziemkowska, R. Anulewicz-Ostrowska and M. Cyrański, *Polyhedron*, 2008, **27**, 962–968.

151 S. Pasynkiewicz and W. Ziemkowska, *J. Organomet. Chem.*, 1992, **423**, 1–4.

152 W. Ziemkowska, *Inorg. Chem. Commun.*, 2001, **4**, 757–759.

153 C. N. McMahon, S. J. Obrey, A. Keys, S. G. Bott and A. R. Barron, *J. Chem. Soc. Dalt. Trans.*, 2000, **0**, 2151–2161.

154 C. N. McMahon, L. Alemany, R. L. Callender, S. G. Bott and A. R. Barron, *Chem. Mater.*, 1999, **11**, 3181–3188.

155 S. Pasynkiewicz and W. Ziemkowska, *J. Organomet. Chem.*, 1992, **437**, 99–110.

156 W. S. Rees and W. Hesse, *MRS Proc.*, 1990, **204**, 563–569.

157 H. Ai, Y. Wang, B. Li and L. Wu, *Eur. J. Inorg. Chem.*, 2014, **2014**, 2766–2772.

158 J. Zhang, J. Luo, P. Wang, B. Ding, Y. Huang, Z. Zhao, J. Zhang and Y. Wei, *Inorg. Chem.*, 2015, **54**, 2551–2559.

159 Q. Li and Y. Wei, *Chem. Commun.*, 2018, **54**, 1375–1378.

160 P. Joröchel and J. Sieler, *Zeitschrift für Krist. - Cryst. Mater.*, 1997, **212**, 884–889.

161 M. Skowrońska-Ptasińska, K. B. Starowieyski, S. Pasynkiewicz and M. Carewska, *J. Organomet. Chem.*, 1978, **160**, 403–409.

162 S. Szumacher, A. R. Kunicki, I. Madura and J. Zachara, *J. Organomet. Chem.*, 2003, **682**, 196–203.

163 K. B. Wiberg and D. E. Barth, *J. Am. Chem. Soc.*, 1969, **91**, 5124–5130.

164 B. Neumüller, *Chem. Soc. Rev.*, 2003, **32**, 50–55.

165 K. Bakthavachalam and N. D. Reddy, *Organometallics*, 2013, **32**, 3174–3184.

166 A. Konishi, H. Nakajima, H. Maruyama, S. Yoshioka, A. Baba and M. Yasuda,

Polyhedron, 2017, **125**, 130–134.

167 R. L. Burwell, *Chem. Rev.*, 1954, **54**, 615–685.

168 G. Wittig and L. Löhmann, *Justus Liebigs Ann. Chem.*, 1942, **550**, 260–268.

169 H. Gilman and B. J. Gaj, *J. Org. Chem.*, 1957, **22**, 1165–1168.

170 R. B. Bates, L. M. Kroposki and D. E. Potter, *J. Org. Chem.*, 1972, **37**, 560–562.

171 A. Maercker, *Angew. Chemie Int. Ed. English*, 1987, **26**, 972–989.

172 G. Baddeley, *J. Am. Chem. Soc.*, 1944, **0**, 330–332.

173 E. G. Paul and P. S. C. Wang, *J. Org. Chem.*, 1979, **44**, 2307–2308.

174 A. Haaland, S. Samdal, O. Stokkeland and J. Weidlein, *J. Organomet. Chem.*, 1977, **134**, 165–171.

175 G. H. Smith and F. J. Hamilton, *J. Phys. Chem.*, 1968, **72**, 3567–3572.

176 L. Hubener, H.-W. Lerner and M. Bolte, *Acta Crystallogr. Sect. E Struct. Reports Online*, 2003, **59**, 929–930.

177 I. V. Vasilenko, D. I. Shiman and S. V. Kostjuk, *Polym. Chem.*, 2014, **5**, 3855–3866.

178 R. Benn, E. Janssen, H. Lehmkuhl and A. Rufínska, *J. Organomet. Chem.*, 1987, **333**, 155–168.

179 T. Gelbrich, U. Dümichen and P. Jörchel, *Acta Crystallogr. Sect. C Cryst. Struct. Commun.*, 1999, **55**, 856–858.

180 Z. Moravec, R. Sluka, M. Necas, V. Jancik and J. Pinkas, *Inorg. Chem.*, 2009, **48**, 8106–8114.

181 W. Hallwachs and A. Schafarik, *Justus Liebigs Ann. Chem.*, 1859, **109**, 206–209.

182 A. V. Grosse and J. M. Mavity, *J. Org. Chem.*, 1940, **05**, 106–121.

183 K. Ziegler and K. Nagel, *Process for the Manufacture of Trialkylaluminium Compounds*, US2744127, 1956.

184 M. Gliński and U. Ulkowska, *Can. J. Chem.*, 2011, **89**, 1370–1374.

185 M. P. Shaver, L. E. N. Allan and V. C. Gibson, *Organometallics*, 2007, **26**, 2252–2257.

186 R. D. Rieke, in *Chemical Synthesis Using Highly Reactive Metals*, John Wiley & Sons, Inc., Hoboken, NJ, USA, 2016, pp. 425–427.

187 R. D. Rieke, *Acc. Chem. Res.*, 1977, **10**, 301–306.

188 Y. Hiraoka, T. Kawasaki-Takasuka, Y. Morizawa and T. Yamazaki, *J. Fluor. Chem.*, 2015, **179**, 71–76.

189 A. L. Horvath, *Chemosphere*, 2001, **44**, 897–905.

190 R. E. Banks, M. G. Barlow and M. Nickkho-Amiry, *J. Fluor. Chem.*, 1997, **82**, 171–174.

191 D. L. Boucher, M. A. Brown, B. R. McGarvey and D. G. Tuck, *J. Chem. Soc. Trans.*, 1999, **0**, 3445–3449.